




## PACC-FMAs 2022 Tentative Schedule of Events

<b>Sunday, July 24, 2022</b>	<b>Time</b>	<b>Location</b>
Conference registration	3:30 – 7 p.m.	Star Bay Foyer
Welcome reception	5:30 – 7 p.m.	Infinity Pool Deck
<b>Monday, July 25, 2022</b>		
Conference registration	7:30 a.m. – 5 p.m.	Star Bay Foyer
Opening ceremony and plenary session	8:30 a.m. – Noon	Star Bay 3
Coffee break	10:10 – 10:30 a.m.	Star Bay Foyer
Conference provided lunch (boxed meal)	Noon – 1:30 p.m.	Star Bay 3 Foyer
Concurrent technical sessions	1:30 – 5 p.m.	
Coffee break	3 – 3:20 p.m.	Star Bay Foyer
Poster session (all in-person posters), including reception	5:30 – 7 p.m.	Star Bay 1/2
<b>Tuesday, July 26, 2022</b>		
Conference registration	8 a.m. – 5 p.m.	Star Bay Foyer
Concurrent technical sessions	8:30 a.m. – Noon	
Coffee break	10 – 10:20 a.m.	Star Bay Foyer
Conference provided lunch (boxed meal)	Noon – 1:30 p.m.	Star Bay 3 Foyer
Concurrent technical sessions	1 – 5 p.m.	
Coffee break	3 – 3:20 p.m.	Star Bay Foyer
Networking reception	5:30 – 7 p.m.	Star Bay 1/2
Conference dinner	7 – 9 p.m.	Star Bay 1/2
<b>Wednesday, July 27, 2022</b>		
Conference registration	8 a.m. – Noon	Star Bay Foyer 

Concurrent technical sessions	8:30 a.m. – Noon	
Coffee break	10 – 10:20 a.m.	Star Bay Foyer
Conference provided lunch (boxed meal)	Noon – 1:30 p.m.	Star Bay 3 Foyer
Afternoon on own	Noon – 5 p.m.	
Optional tour: Miraflores Locks Visit and Half Day Tour (Additional registration required)	1:30 – 5:30 p.m.	
<b>Thursday, July 28, 2022</b>		
Conference registration	8 a.m. – Noon	Star Bay Foyer
Concurrent technical sessions	8:30 a.m. – Noon	
Coffee break	10 – 10:20 a.m.	Star Bay Foyer
<i>Updated July 21, 2022</i>		

Edit



## **FINAL Program Guide**

**Updated 25 July**

### **Attention In-person Poster presenters:**

**The two Poster sessions (PACC on Monday and FMAs on Tuesday) are condensed to allow all in-person Posters presented at the venue to be displayed in a common session on Monday, July 25 during the poster session and reception 5:30 – 7 p.m.**

### **To locate your presentation:**

- Use the search function to search your presentation by last name or title.

## Oral Presenters

Name	Date	Time	Room	Page Number	Name	Date	Time	Room	Page Number
<b>A</b>					<b>G</b>				
Acosta, C.	26-Jul	11:20AM	Star Bay 3 (Level B)	12	Galindo, R.R.	26-Jul	10:50AM	Venetian (Level B)	11
Aguirre, I.	26-Jul	3:30PM	Venetian (Level B)	14	Garnsey, S.	27-Jul	11:20AM	Star Bay 3 (Level B)	20
Apblett, A.	27-Jul	8:30AM	Vitri (Level M)	18	Gaustad, G.	27-Jul	11:10AM	Revolution (Level B)	19
Apblett, A.	27-Jul	9:40AM	Bellagio (Level B)	18	Geng, X.	26-Jul	2:30PM	Bellagio (Level B)	13
Arango-Ospina, M.	27-Jul	11:10AM	Millennium (Level B)	18	Gil Velasquez, D.	27-Jul	10:20AM	Venetian (Level B)	18
Araujo, E.B.	27-Jul	9:20AM	Star Bay 3 (Level B)	20	Gogotsi, Y.	25-Jul	3:20PM	Millennium (Level B)	5
Arunachalam, A.	26-Jul	4:20PM	Revolution (Level B)	12	Goldsby, J.C.	25-Jul	2:30PM	Revolution (Level B)	4
<b>B</b>					Goski, D.	25-Jul	2:20PM	Mirage (Level B)	5
Bailin, C.L.	26-Jul	11:50AM	Venetian (Level B)	11	Graeve, O.A.	26-Jul	8:30AM	Millennium (Level B)	9
Balazi, C.	26-Jul	3:10PM	Bellagio (Level B)	13	Gugar, N.	26-Jul	11:10AM	Mirage (Level B)	11
Balmori, H.	26-Jul	9:30AM	Millennium (Level B)	9	Gupta, S.	27-Jul	9:20AM	Vitri (Level M)	19
Barua, R.	26-Jul	2:20PM	Vitri (Level M)	13	Guzman-Verri, G.G.	25-Jul	1:30PM	Star Bay 3 (Level B)	6
Baudin, C.	25-Jul	1:30PM	Mirage (Level B)	5	<b>H</b>				
Benavidez, E.	25-Jul	2:00PM	Mirage (Level B)	5	Hayashi, Y.	26-Jul	11:40AM	Bellagio (Level B)	10
Benavidez, E.	25-Jul	3:20PM	Mirage (Level B)	5	He, Q.	26-Jul	11:10AM	Millennium (Level B)	10
Bergmann, F.	25-Jul	2:30PM	Vitri (Level M)	4	Hegedüs, N.	25-Jul	4:00PM	Revolution (Level B)	4
Bernard, S.	26-Jul	8:30AM	Bellagio (Level B)	10	Henkin, J.	26-Jul	3:10PM	Venetian (Level B)	14
Betancur-Granados, N.	26-Jul	2:50PM	Mirage (Level B)	14	Herrera-Perez, G.M.	26-Jul	9:00AM	Millennium (Level B)	9
Betancur-Granados, N.	27-Jul	9:30AM	Venetian (Level B)	18	Hotza, D.	26-Jul	10:50AM	Millennium (Level B)	10
Bhattarai, M.	26-Jul	4:00PM	Mirage (Level B)	14	Hotza, D.	26-Jul	2:20PM	Millennium (Level B)	13
Bisulca, C.	26-Jul	11:10AM	Venetian (Level B)	11	Hreniak, D.	25-Jul	3:40PM	Venetian (Level B)	5
Boccaccini, A.R.	27-Jul	9:00AM	Millennium (Level B)	17	Huerta, E.H.	26-Jul	8:50AM	Venetian (Level B)	10
Bonadio, T.G.	27-Jul	9:40AM	Star Bay 3 (Level B)	20	<b>I</b>				
Bram, M.	26-Jul	10:20AM	Millennium (Level B)	10	Ihrig, M.	26-Jul	9:40AM	Vitri (Level M)	9
Braun, M.	25-Jul	2:00PM	Revolution (Level B)	4	Iizuka, F.	26-Jul	2:30PM	Venetian (Level B)	14
Brazhkin, V.	25-Jul	3:50PM	Millennium (Level B)	5	Iñáñez, J.G.	26-Jul	1:50PM	Venetian (Level B)	14
Butt, D.P.	25-Jul	10:30AM	Star Bay 3 (Level B)	4	<b>J</b>				
<b>C</b>					Jackson, M.D.	26-Jul	8:30AM	Venetian (Level B)	10
Camacho Montes, H.	26-Jul	2:00PM	Millennium (Level B)	13	Jacobsohn, L.G.	25-Jul	3:20PM	Venetian (Level B)	5
Cardoza, A.	27-Jul	8:30AM	Venetian (Level B)	18	Jain, H.	27-Jul	10:30AM	Revolution (Level B)	19
Carvajal Contreras, D.R.	26-Jul	9:50AM	Venetian (Level B)	10	Jain, H.	27-Jul	10:50AM	Revolution (Level B)	19
Castro, R.	25-Jul	1:30PM	Millennium (Level B)	4	Jana, S.S.	27-Jul	9:00AM	Star Bay 3 (Level B)	20
Chen, A.	26-Jul	2:00PM	Star Bay 3 (Level B)	15	Jiang, J.	27-Jul	10:20AM	Mirage (Level B)	19
Chen, C.	27-Jul	8:30AM	Mirage (Level B)	19	<b>K</b>				
Chen, X.	26-Jul	2:00PM	Mirage (Level B)	14	Katiyar, R.	26-Jul	2:30PM	Mirage (Level B)	14
Cheng, Z.	26-Jul	9:20AM	Star Bay 3 (Level B)	12	Katiyar, R.	27-Jul	8:30AM	Star Bay 3 (Level B)	20
Cheng, Z.	27-Jul	10:50AM	Mirage (Level B)	19	Kawano, N.	25-Jul	2:20PM	Venetian (Level B)	5
Cho, Y.	25-Jul	2:10PM	Vitri (Level M)	4	Kisailus, D.	27-Jul	8:30AM	Millennium (Level B)	17
Chodisetti, S.	26-Jul	10:40AM	Vitri (Level M)	9	Kovalenko, O.	26-Jul	11:30AM	Mirage (Level B)	11
Colorado L., H.A.	27-Jul	8:30AM	Revolution (Level B)	19	Kumar, P.	26-Jul	9:40AM	Mirage (Level B)	11
Colorado L., H.A.	27-Jul	9:40AM	Vitri (Level M)	19	Kuo, L.	26-Jul	1:30PM	Revolution (Level B)	12
Cótica, L.F.	25-Jul	2:00PM	Star Bay 3 (Level B)	6	Kurosawa, S.	25-Jul	2:40PM	Venetian (Level B)	5
<b>D</b>					<b>L</b>				
De Obaldía, E.	26-Jul	10:20AM	Vitri (Level M)	9	Lin, H.	25-Jul	1:30PM	Revolution (Level B)	4
Dey, M.	26-Jul	4:20PM	Vitri (Level M)	14	Lin, Y.	28-Jul	8:30AM	Star Bay 3 (Level B)	20
Dey, S.	26-Jul	2:20PM	Revolution (Level B)	12	Lipke, D.	26-Jul	3:50PM	Revolution (Level B)	12
Dias, G.S.	27-Jul	9:40AM	Mirage (Level B)	19	Lipke, D.	27-Jul	9:30AM	Revolution (Level B)	19
Dias, G.S.	27-Jul	11:00AM	Star Bay 3 (Level B)	20	Littlewood, P.	25-Jul	9:30AM	Star Bay 3 (Level B)	4
Dipon, W.	28-Jul	9:00AM	Star Bay 3 (Level B)	20	Liu, C.	25-Jul	1:30PM	Venetian (Level B)	5
Duong, M.	28-Jul	9:40AM	Star Bay 3 (Level B)	20	Lopez-Bezanilla, A.	25-Jul	3:30PM	Star Bay 3 (Level B)	6
Dutra Zanotto, E.	25-Jul	8:50AM	Star Bay 3 (Level B)	4	Lu, K.	25-Jul	2:00PM	Millennium (Level B)	5
<b>E</b>					Lu, K.	26-Jul	1:30PM	Vitri (Level M)	13
Eiras, J.A.	26-Jul	10:20AM	Star Bay 3 (Level B)	12	<b>M</b>				
Eleuterio, R.V.	27-Jul	9:00AM	Venetian (Level B)	18	Mahapatra, M.	25-Jul	3:40PM	Mirage (Level B)	5
Estrada, F.R.	25-Jul	4:00PM	Star Bay 3 (Level B)	6	Mait, S.	26-Jul	9:40AM	Millennium (Level B)	9
<b>F</b>					Maiti, T.	26-Jul	1:30PM	Mirage (Level B)	14
Ferreira, E.	25-Jul	4:00PM	Venetian (Level B)	5	Mandal, K.	26-Jul	10:50AM	Mirage (Level B)	11
Fiorilli, S.	26-Jul	11:20AM	Revolution (Level B)	9	Mandal, K.	26-Jul	11:50AM	Mirage (Level B)	11
Flynn, P.	28-Jul	10:20AM	Star Bay 3 (Level B)	20	Manuspiya, H.	26-Jul	8:30AM	Mirage (Level B)	11
Freitas, V.F.	25-Jul	2:50PM	Star Bay 3 (Level B)	6	Markocsan, N.	27-Jul	10:50AM	Millennium (Level B)	18
Freitas, V.F.	27-Jul	11:30AM	Mirage (Level B)	20	Mars, E.M.	26-Jul	3:50PM	Venetian (Level B)	14
Fukushima, M.	27-Jul	9:00AM	Vitri (Level M)	18	Mathur, S.	25-Jul	1:30PM	Bellagio (Level B)	6
Furuya, Y.	25-Jul	1:30PM	Vitri (Level M)	4					

# Presenting Author List

## Oral Presenters

Name	Date	Time	Room	Page Number	Name	Date	Time	Room	Page Number
Mayo, C.J.	26-Jul	9:20AM	Mirage (Level B)	11	Shimamura, K.	26-Jul	10:40AM	Bellagio (Level B)	10
McGath, M.K.	26-Jul	11:30AM	Venetian (Level B)	11	Shvartsman, V.V.	27-Jul	11:50AM	Mirage (Level B)	20
Mehta, A.	26-Jul	4:40PM	Mirage (Level B)	15	Singh, N.B.	26-Jul	10:20AM	Mirage (Level B)	11
Michaelis, A.	26-Jul	10:50AM	Revolution (Level B)	9	Singh, N.B.	26-Jul	4:20PM	Star Bay 3 (Level B)	15
Misture, S.T.	25-Jul	2:30PM	Millennium (Level B)	5	Singh, R.N.	26-Jul	9:00AM	Mirage (Level B)	11
Muccillo, E.N.	27-Jul	8:50AM	Revolution (Level B)	19	Smeacetto, F.	26-Jul	10:20AM	Revolution (Level B)	9
Muccillo, R.	26-Jul	1:30PM	Bellagio (Level B)	13	Smith, G.D.	26-Jul	10:30AM	Venetian (Level B)	11
Mulinari, J.	26-Jul	2:50PM	Vitri (Level M)	13	Somani, N.	26-Jul	4:20PM	Mirage (Level B)	14
<b>N</b>					Srinivasan, G.	26-Jul	4:40PM	Star Bay 3 (Level B)	15
Nalandhiran, P.	25-Jul	3:40PM	Revolution (Level B)	4	Suvorov, D.	26-Jul	1:30PM	Star Bay 3 (Level B)	15
Narayan, R.	27-Jul	11:30AM	Millennium (Level B)	18	Suzuki, T.S.	26-Jul	2:00PM	Bellagio (Level B)	13
Nejatpour, M.	26-Jul	8:30AM	Vitri (Level M)	9	<b>T</b>				
Nieto, A.	26-Jul	2:00PM	Vitri (Level M)	13	Tanemura, M.	26-Jul	11:10AM	Bellagio (Level B)	10
Ning, K.	25-Jul	4:40PM	Star Bay 3 (Level B)	6	Teixeira, M.H.	26-Jul	2:40PM	Millennium (Level B)	13
Nino, J.C.	26-Jul	3:20PM	Revolution (Level B)	12	Tidrow, S.	26-Jul	10:50AM	Star Bay 3 (Level B)	12
Nudd, S.	25-Jul	4:20PM	Star Bay 3 (Level B)	6	Tokoro, C.	27-Jul	8:30AM	Bellagio (Level B)	18
<b>O</b>					Trippy, M.	25-Jul	2:30PM	Star Bay 3 (Level B)	6
Ohji, T.	26-Jul	4:10PM	Bellagio (Level B)	13	Tsuchiya, T.	25-Jul	3:50PM	Bellagio (Level B)	6
Ohji, T.	27-Jul	9:10AM	Revolution (Level B)	19	<b>V</b>				
Ohji, T.	27-Jul	11:20AM	Bellagio (Level B)	18	Vakharia, V.	25-Jul	4:10PM	Millennium (Level B)	5
Olevsky, E.	26-Jul	1:30PM	Millennium (Level B)	12	Veenhuizen, K.J.	26-Jul	12:00PM	Star Bay 3 (Level B)	12
Oliveira, R.C.	27-Jul	10:40AM	Star Bay 3 (Level B)	20	Velásquez, X.A.	26-Jul	9:00AM	Vitri (Level M)	9
Osada, M.	25-Jul	2:00PM	Bellagio (Level B)	6	VICENZI, E.P.	26-Jul	1:30PM	Venetian (Level B)	14
<b>P</b>					Volnistem, E.a.	28-Jul	9:20AM	Star Bay 3 (Level B)	20
Pabst, W.	26-Jul	11:30AM	Millennium (Level B)	10	<b>W</b>				
Parsi, J.	28-Jul	10:40AM	Star Bay 3 (Level B)	20	Wang, H.	25-Jul	2:30PM	Bellagio (Level B)	6
Pellegrino, V.	26-Jul	11:40AM	Star Bay 3 (Level B)	12	Wang, W.	26-Jul	3:40PM	Bellagio (Level B)	13
Peng, F.	26-Jul	3:20PM	Millennium (Level B)	13	Wauters, V.	26-Jul	4:30PM	Venetian (Level B)	14
Pradhan, D.K.	26-Jul	2:50PM	Star Bay 3 (Level B)	15	Weber, F.E.	27-Jul	10:20AM	Millennium (Level B)	18
Prakash, C.	26-Jul	9:40AM	Star Bay 3 (Level B)	12	Wie-Addo, G.	27-Jul	9:20AM	Bellagio (Level B)	18
Prakash, C.	27-Jul	9:00AM	Mirage (Level B)	19	Wiff, J.	25-Jul	4:20PM	Bellagio (Level B)	6
Priya, S.	25-Jul	1:50PM	Vitri (Level M)	4	Wolf, S.E.	27-Jul	9:30AM	Millennium (Level B)	17
Prokhorenko, O.	25-Jul	2:00PM	Venetian (Level B)	5	Wu, J.	26-Jul	9:00AM	Star Bay 3 (Level B)	11
<b>R</b>					<b>X</b>				
Ramirez-Rico, J.	26-Jul	3:30PM	Vitri (Level M)	13	Xu, T.	26-Jul	3:30PM	Mirage (Level B)	14
Reedy, C.L.	26-Jul	4:10PM	Venetian (Level B)	14	Xu, T.	27-Jul	9:20AM	Mirage (Level B)	19
Reimanis, I.	27-Jul	9:50AM	Revolution (Level B)	19	Xu, T.	27-Jul	10:20AM	Star Bay 3 (Level B)	20
Rendon, J.	26-Jul	2:40PM	Revolution (Level B)	12	<b>Y</b>				
Resio, L.C.	25-Jul	2:40PM	Mirage (Level B)	5	Yang, Y.	26-Jul	9:20AM	Vitri (Level M)	9
Riedel, R.	26-Jul	9:00AM	Bellagio (Level B)	10	Ye, R.	26-Jul	10:20AM	Bellagio (Level B)	10
Rosas, B.Y.	25-Jul	3:20PM	Revolution (Level B)	4	Yin, S.	25-Jul	3:20PM	Bellagio (Level B)	6
Roy, P.	27-Jul	11:10AM	Mirage (Level B)	19	Young, B.D.	26-Jul	2:30PM	Star Bay 3 (Level B)	15
<b>S</b>					<b>Z</b>				
Salazar, L.C.	26-Jul	2:10PM	Venetian (Level B)	14	Zabotto, F.L.	26-Jul	4:00PM	Star Bay 3 (Level B)	15
Salgado-Ceballos, C.	26-Jul	9:20AM	Venetian (Level B)	10	Zakotnik, M.	27-Jul	9:00AM	Bellagio (Level B)	18
Salvini, V.R.	27-Jul	10:30AM	Bellagio (Level B)	18	Zhang, J.	26-Jul	4:00PM	Vitri (Level M)	13
Salvini, V.R.	27-Jul	11:00AM	Bellagio (Level B)	18	Zhitomirsky, I.	26-Jul	9:30AM	Bellagio (Level B)	10
Santos, I.A.	26-Jul	3:30PM	Star Bay 3 (Level B)	15	Zuluaga-Gomez, C.C.	26-Jul	2:00PM	Revolution (Level B)	12
Saxena, A.	26-Jul	8:30AM	Star Bay 3 (Level B)	11					
Sharma, S.	25-Jul	2:50PM	Vitri (Level M)	4					

## Poster Presenters

Name	Date	Time	Room	Page Number	Name	Date	Time	Room	Page Number
<b>A</b>									
Aepuru, R.	25-Jul	5:30PM	Star Bay 1/2	7	Martínez-Aguilar, E.	25-Jul	5:30PM	Star Bay 1/2	7
Aparecido dos Santos Mariano, M.	26-Jul	5:30PM	Star Bay 1/2	17	Miranda, H.S.	26-Jul	5:30PM	Star Bay 1/2	17
Aredes, R.G.	25-Jul	5:30PM	Star Bay 1/2	7	Moreira, C.P.	26-Jul	5:30PM	Star Bay 1/2	15
Aslla Quispe, A.	26-Jul	5:30PM	Star Bay 1/2	17	Mujib, S.	25-Jul	5:30PM	Star Bay 1/2	7
					Muñoz Pulido, K.	25-Jul	5:30PM	Star Bay 1/2	8
<b>B</b>									
Banerjee, R.	26-Jul	5:30PM	Star Bay 1/2	17	Nascimento, A.	26-Jul	5:30PM	Star Bay 1/2	17
Betancur-Granados, N.	25-Jul	5:30PM	Star Bay 1/2	8	Ning, K.	26-Jul	5:30PM	Star Bay 1/2	15
<b>C</b>									
Camacho Montes, H.	25-Jul	5:30PM	Star Bay 1/2	8	Oliveira, A.L.	26-Jul	5:30PM	Star Bay 1/2	16
Carvalho, R.A.	26-Jul	5:30PM	Star Bay 1/2	17	Oliveira, O.G.	25-Jul	5:30PM	Star Bay 1/2	8
Catellani, I.B.	25-Jul	5:30PM	Star Bay 1/2	7	Oliveira, R.C.	26-Jul	5:30PM	Star Bay 1/2	16
Chen, Y.	26-Jul	5:30PM	Star Bay 1/2	17	Olivera Castillo, A.F.	25-Jul	5:30PM	Star Bay 1/2	7
Ching, E.A.	26-Jul	5:30PM	Star Bay 1/2	16	Olmos, B.	25-Jul	5:30PM	Star Bay 1/2	8
Chotiradsirikun, S.	26-Jul	5:30PM	Star Bay 1/2	15	<b>P</b>				
Choudhary, R.	26-Jul	5:30PM	Star Bay 1/2	15	Pabst, W.	25-Jul	5:30PM	Star Bay 1/2	8
Correr, G.I.	26-Jul	5:30PM	Star Bay 1/2	16	Pabst, W.	26-Jul	5:30PM	Star Bay 1/2	17
<b>D</b>					Pandey, R.	26-Jul	5:30PM	Star Bay 1/2	16
DAVILA ESPINOSA, L.F.	26-Jul	5:30PM	Star Bay 1/2	16	Paramee, S.	26-Jul	5:30PM	Star Bay 1/2	16
de los Santos Guerra, J.	26-Jul	5:30PM	Star Bay 1/2	15, 16, 17	Parida, A.	26-Jul	5:30PM	Star Bay 1/2	15
Delgado, J.C.	25-Jul	5:30PM	Star Bay 1/2	8	Pérez Molina, J.J.	25-Jul	5:30PM	Star Bay 1/2	8
Di Marco, M.	26-Jul	5:30PM	Star Bay 1/2	17	Posada Henao, O.F.	25-Jul	5:30PM	Star Bay 1/2	7
Difeo, M.C.	25-Jul	5:30PM	Star Bay 1/2	6, 7	Prakash, C.	26-Jul	5:30PM	Star Bay 1/2	15
DIXIT, P.	26-Jul	5:30PM	Star Bay 1/2	17	<b>R</b>				
<b>E</b>					Rebellón, H.	25-Jul	5:30PM	Star Bay 1/2	7
Espinoza Ochoa, I.M.	25-Jul	5:30PM	Star Bay 1/2	8	Restrepo Tobón, S.	25-Jul	5:30PM	Star Bay 1/2	6
<b>G</b>					Roa-Rojas, J.	26-Jul	5:30PM	Star Bay 1/2	16
Gamboia, B.	26-Jul	5:30PM	Star Bay 1/2	16	Rodrigues, A.V.	26-Jul	5:30PM	Star Bay 1/2	16
Gil Rebaza, A.V.	25-Jul	5:30PM	Star Bay 1/2	7	Rosso, J.M.	25-Jul	5:30PM	Star Bay 1/2	7
Gregorova, E.	25-Jul	5:30PM	Star Bay 1/2	8	<b>S</b>				
Guilherme Flávio Domelas, R.	26-Jul	5:30PM	Star Bay 1/2	16	Salazar González, W.	25-Jul	5:30PM	Star Bay 1/2	7
Gutiérrez-Campos, D.	25-Jul	5:30PM	Star Bay 1/2	8	Shpotyuk, Y.	25-Jul	5:30PM	Star Bay 1/2	8
<b>H</b>					Singh, V.	25-Jul	5:30PM	Star Bay 1/2	7
Hathenher Toledo Rosa, T.	26-Jul	5:30PM	Star Bay 1/2	17	Swain, S.	26-Jul	5:30PM	Star Bay 1/2	15
Hmok, H.	25-Jul	5:30PM	Star Bay 1/2	7	<b>T</b>				
Hossain, S.	26-Jul	5:30PM	Star Bay 1/2	16	Téllez Arias, M.G.	25-Jul	5:30PM	Star Bay 1/2	8
Hung Hung, Y.X.	25-Jul	5:30PM	Star Bay 1/2	8	THANDAPANI, P.	25-Jul	5:30PM	Star Bay 1/2	7
<b>I</b>					Thangaraj, P.	25-Jul	5:30PM	Star Bay 1/2	7
Imhoff, L.	26-Jul	5:30PM	Star Bay 1/2	16	Thirumurugan, A.	25-Jul	5:30PM	Star Bay 1/2	7
<b>J</b>					Trachenko, K.	25-Jul	5:30PM	Star Bay 1/2	8
Jana, S.S.	26-Jul	5:30PM	Star Bay 1/2	17	<b>V</b>				
<b>K</b>					Vacchi, M.	25-Jul	5:30PM	Star Bay 1/2	8
Kaou, M.H.	25-Jul	5:30PM	Star Bay 1/2	8	Vega Siverio, A.	25-Jul	5:30PM	Star Bay 1/2	8
Kar, B.	26-Jul	5:30PM	Star Bay 1/2	15	Villaquiran Raigoza, C.F.	26-Jul	5:30PM	Star Bay 1/2	16
<b>L</b>					Volnistem, E.a.	26-Jul	5:30PM	Star Bay 1/2	16
Lima, E.C.	26-Jul	5:30PM	Star Bay 1/2	17	<b>X</b>				
Lokanathan, M.	25-Jul	5:30PM	Star Bay 1/2	7	Xiaomin, J.	26-Jul	5:30PM	Star Bay 1/2	17
<b>M</b>					<b>Y</b>				
Machado, H.N.	26-Jul	5:30PM	Star Bay 1/2	16	Yang, A.	25-Jul	5:30PM	Star Bay 1/2	7
Macková, L.	26-Jul	5:30PM	Star Bay 1/2	16	Yusslee, E.F.	25-Jul	5:30PM	Star Bay 1/2	8
Mahapatra, M.	25-Jul	5:30PM	Star Bay 1/2	8	<b>Z</b>				
Manzani, D.	25-Jul	5:30PM	Star Bay 1/2	8	Zabala, S.A.	26-Jul	5:30PM	Star Bay 1/2	17

## Monday, July 25, 2022

### Plenary Session

Room: Star Bay 3 (Level B)

Session Chairs: Sylvia Johnson, NASA-Ames Research Center (ret.); Amar Bhalla, University of Texas, San Antonio; Mrityunjay Singh, Ohio Aerospace

**8:30 AM**

#### Opening Remarks

**8:50 AM**

#### (PLEN-001-2022) R & D on vitreous materials in the Americas: Current efforts and a look to the future

E. Dutra Zanotto\*<sup>1</sup>

1. Federal University of Sao Carlos, Materials Engineering, Brazil

**9:30 AM**

#### (PLEN-002-2022) Materials for energy and sustainability

P. Littlewood\*<sup>1</sup>

1. Faraday Institution, United Kingdom

**10:10 AM**

#### Break

**10:30 AM**

#### (PLEN-003-2022) The Science of Art: Metaphors on the Value of Diversity

D. P. Butt\*<sup>1</sup>

1. University of Utah, Materials Science and Engineering, USA

## PACC1: Ceramics for Energy and Environment

### Semiconductors and Similar Topics

Room: Revolution (Level B)

Session Chairs: Henry Colorado L., Universidad de Antioquia; Udayabhaskar Rednam, University of Atacama

**1:30 PM - WITHDRAWN**

#### (PACC-S1-001-2022) Advanced Si-based Ceramics for Carbon-free Energy Technologies (Invited)

H. Lin\*<sup>1</sup>

1. Guangdong University of Technology, School of Electronic and Mechanical Engineering, China

**2:00 PM**

#### (PACC-S1-002-2022) Semiconducting perovskite Ba<sub>2</sub>CuWO<sub>6</sub> for photovoltaics (Invited)

M. Braun\*<sup>1</sup>; S. Wagner<sup>1</sup>; M. Hinterstein<sup>1</sup>; A. Colsmann<sup>2</sup>; M. Hoffmann<sup>1</sup>

1. Karlsruhe Institute of Technology, Institute for Applied Materials - Ceramic Materials and Technologies, Germany
2. Karlsruhe Institute of Technology, Light Technology Institute, Germany

**2:30 PM - WITHDRAWN**

#### (PACC-S1-003-2022) Assessment of Silicon Germanium Proprieties for Direct Energy Conversion Using Density Functional Theory (Invited)

J. C. Goldsby\*<sup>1</sup>

1. NASA Glenn Research Center, Chemistry and Physics, USA

**3:00 PM**

#### Break

**3:20 PM**

#### (PACC-S1-004-2022) Studies of optical, dielectric, ferroelectric and structural phase transitions in [KNbO<sub>3</sub>]<sub>0.9</sub>[BaNb<sub>1/2</sub>Ni<sub>1/2</sub>O<sub>3-δ</sub>]<sub>0.1</sub> ceramics

B. Y. Rosas<sup>1</sup>; A. A. Instan<sup>1</sup>; K. K. Mishra<sup>1</sup>; S. N. Achary<sup>1</sup>; R. Katiyar\*<sup>1</sup>

1. University of Puerto Rico, Physics, USA

**3:40 PM**

#### (PACC-S1-005-2022) Natural solar light assisted photocatalytic oxidation of endocrine disrupting chemicals using rGO-black TiO<sub>2</sub> nanostructures with exposed {001} facets

P. Nalandhiran\*<sup>1</sup>; S. Panneer selvam<sup>2</sup>; M. Viswanathan<sup>3</sup>

1. Universidad Técnica Federico Santa María, Department of Chemistry, Chile
2. Vellore Institute of Technology (VIT) University, Department of Chemistry, School of Advanced Sciences, India
3. Universidad de Concepción, Department of Materials Engineering, Chile

**4:00 PM**

#### (PACC-S1-006-2022) Examination of the Hydrogen Incorporation into Radio Frequency-Sputtered Hydrogenated SiNx Thin Films

N. Hegedüs\*<sup>1</sup>; C. Balazsi<sup>1</sup>; K. Balázs<sup>1</sup>

1. ELKH Centre for Energy Research, Hungary

## PACC2: Advanced Ceramics and Composites

### Coatings and Thin Films; Electroceramics

Room: Vitri (Level M)

Session Chair: Mangalaraja Ramalinga Viswanathan, Universidad Adolfo Ibáñez

**1:30 PM**

#### (PACC-S2-001-2022) Consolidation Behavior of Alumina Particles in Aerosol Deposition Method

Y. Furuya\*<sup>1</sup>; M. Hasegawa<sup>1</sup>

1. Yokohama National University, Japan

**1:50 PM**

#### (PACC-S2-002-2022) Structural, multiferroic, optical, and magnetoelectric properties of Zr and Dy doped BiFeO<sub>3</sub> thin films

S. Priya\*<sup>2</sup>; D. Geetha<sup>2</sup>; S. Sharma<sup>1</sup>; J. SIQUEIROS<sup>1</sup>

1. UNIVERSIDAD NACIONAL AUTÓNOMA DE MÉXICO, CENTRO DE NANOCIENCIAS Y NANOTECNOLOGÍA, Mexico
2. Madras Institute of Technology, Department of Physics, India

**2:10 PM**

#### (PACC-S2-003-2022) Machine learning of gold nanoparticle/polymer hybrid films

Y. Cho<sup>1,2</sup>; K. Lu<sup>1</sup>; H. Chaney<sup>1</sup>

1. Virginia Tech, USA
2. Suncheon National University, Korea

**2:30 PM - WITHDRAWN**

#### (PACC-S2-004-2022) Polar vortices in microwave electronics

F. Bergmann\*<sup>1</sup>; B. Bosworth<sup>1</sup>; E. Marks<sup>2</sup>; A. Hagerstrom<sup>1</sup>; S. Das<sup>2</sup>; R. Ramesh<sup>1</sup>; N. Orloff<sup>2</sup>

1. NIST, CTL, USA
2. NIST, Communications Technology Laboratory, USA
3. UC Berkeley, MSE/Physics, USA

**2:50 PM**

#### (PACC-S2-005-2022) Physical properties of Ba, Na, Ti doped BiFeO<sub>3</sub> solid solutions prepared by solid state reaction method

S. Sharma\*<sup>1</sup>; O. Raymond<sup>1</sup>; J. SIQUEIROS<sup>1</sup>

1. UNIVERSIDAD NACIONAL AUTÓNOMA DE MÉXICO, CENTRO DE NANOCIENCIAS Y NANOTECNOLOGÍA, Mexico

## PACC3: Densification and Microstructural Evolution in Ceramics During Sintering

### Sintering I

Room: Millennium (Level B)

Session Chair: Dachamir Hotza, Federal University of Santa Catarina

**1:30 PM**

#### (PACC-S3-001-2022) Grain growth control in ceramics: An experimental thermo-kinetic analysis (Invited)

R. Castro\*<sup>1</sup>

1. University of California, Davis, Material Science & Engineering, USA

**2:00 PM****(PACC-S3-002-2022) Sintering behaviors of micron-sized features (Invited)**K. Lu\*<sup>1</sup>

1. Virginia Tech, USA

**2:30 PM****(PACC-S3-003-2022) In-situ SEM Study of Microstructure Evolution During Sintering and Selective Reduction of Metal Nanoparticles from Spinel Oxides (Invited)**S. T. Mixture\*<sup>1</sup>; A. Ladonis<sup>1</sup>

1. Alfred University, MSE, USA

**3:00 PM****Break****3:20 PM****(PACC-S3-004-2022) Microstructural evolution of carbide MXenes and their Composites at high-temperatures (Invited)**M. Anayee<sup>1</sup>; Y. Gogotsi\*<sup>1</sup>

1. Drexel University, USA

**3:50 PM - WITHDRAWN****(PACC-S3-005-2022) Superductile hardmetals and tools based on these materials under ultrahigh isostatic pressure**V. Brazhkin\*<sup>1</sup>

1. Institute for High Pressure Physics RAS, Russian Federation

**4:10 PM****(PACC-S3-006-2022) Processing of High Entropy Metal Carbides: A New Class of Ultrahigh Temperature, Irradiation Resistant Ceramics**V. Vakharia\*<sup>1</sup>; L. Zhang<sup>1</sup>; E. Rodas-Lima<sup>1</sup>; C. Park<sup>2</sup>; E. Torresani<sup>2</sup>; E. Olevisky<sup>2</sup>; O. A. Graeve<sup>1</sup>

1. University of California, San Diego, Mechanical and Aerospace Engineering, USA
2. San Diego State University, College of Engineering, USA

**PACC6: Refractories in The Americas****Refractories**

Room: Mirage (Level B)

Session Chair: Dana Goski, Allied Mineral Products

**1:30 PM****(PACC-S6-001-2022) Recycling of spent catalysts from Fluid Catalytic Cracking (FCC) as refractory feedstock (Invited) C.**L. Alcaraz<sup>1,2</sup>, E. Retsrepo<sup>1,3</sup>, F. Lopez<sup>2</sup>, F. Vargas<sup>3</sup>, Baudin\*<sup>1</sup>,

1. Instituto de Cerámica y Vidrio, CSIC, Ceramics, Spain
2. Centro Nacional de Investigaciones Metalúrgicas (CENIM-CSIC), Spain
3. Universidad de Antioquia, GIPMME-GIMACYR, Colombia

**2:00 PM****(PACC-S6-002-2022) Characterization of MgO-C bricks with different fused magnesia aggregates**E. Benavidez\*<sup>1</sup>; Y. Lagorio<sup>1</sup>

1. Universidad Tecnológica Nacional (Argentina), Metalurgia, Argentina

**2:20 PM****(PACC-S6-003-2022) Lessons from Failure Analyses in Challenging Refractory Application Environments**D. Goski\*<sup>1</sup>; T. Marth<sup>1</sup>

1. Allied Mineral Products, USA

**2:40 PM****(PACC-S6-004-2022) The use of steelmaking slag as protection for oxidation of MgO-C refractories**M. Moline<sup>1</sup>, W. Calvo<sup>1</sup>, S. Gass<sup>1</sup>, D. Gutierrez-Campos\*<sup>3</sup>, P. Galliano<sup>2</sup>, A. G. Tomba Martínez<sup>1</sup>;

1. INTEMA, División Cerámicos, Argentina
2. Universidad Nacional del Centro de la Provincia de Buenos Aires, Argentina
3. Universidad Simón Bolívar, Departamento de Ciencia de los Materiales, Venezuela, Bolivarian Republic of

**3:00 PM****Break****3:20 PM****(PACC-S6-005-2022) Structural evolution of a Al<sub>2</sub>O<sub>3</sub>-MgO×Al<sub>2</sub>O<sub>3</sub> castable in the range 1000-1600°C**E. Benavidez\*<sup>1</sup>; E. BRANDALEZE<sup>1</sup>

1. Universidad Tecnológica Nacional (Argentina), Metalurgia, Argentina

**3:40 PM****(PACC-S6-006-2022) Thermochemical Stability of Refractories in Hydrogen Atmosphere**M. Mahapatra\*<sup>1</sup>; J. G. Hemrick<sup>2</sup>

1. University of Alabama at Birmingham, USA
2. Oak Ridge National Laboratory, USA

**PACC7: Science and Technology of Glasses, Glass Ceramics, and Optical Materials****Glasses, Glass-ceramics, and Optical Materials**

Room: Venetian (Level B)

**1:30 PM - WITHDRAWN****(PACC-S7-001-2022) Controlled Precipitation of Cesium Lead Halide Perovskite Nanocrystals in glasses and their Applications (Invited)**C. Liu\*<sup>1</sup>; Y. Ye<sup>1</sup>; Y. Hu<sup>1</sup>; Y. Zhou<sup>1</sup>

1. Wuhan University of Technology, State Key Laboratory of Silicate Materials for Architectures, China

**2:00 PM****(PACC-S7-002-2022) Practical steps toward low-CO<sub>2</sub> environment**O. Prokhorenko\*<sup>1</sup>

1. L.G.P. International, USA

**2:20 PM****(PACC-S7-003-2022) Dosimetric properties of a rare-earth ion doped CaF<sub>2</sub> translucent ceramics fabricated by spark plasma sintering method**N. Kawano\*<sup>1</sup>; D. Nakauchi<sup>2</sup>; F. Nakamura<sup>2</sup>; T. Yanagida<sup>2</sup>

1. Akita University, Japan
2. Nara Institute of Science and Technology, Japan

**2:40 PM****(PACC-S7-004-2022) Optical and Defect Properties of Large-size Gd<sub>3</sub>(Ga,Al)<sub>5</sub>O<sub>12</sub> Transparent Ceramics**S. Kurosawa\*<sup>1</sup>; H. Sone<sup>2</sup>; H. Ujile<sup>2</sup>; A. Yamaji<sup>1</sup>

1. Tohoku University, Japan
2. Industrial Technology Institute, Miyagi Prefectural Government, Japan

**3:00 PM****Break****3:20 PM****(PACC-S7-005-2022) Thermoluminescence of Mg and Zn Aluminate Spinel**R. L. Conner<sup>1</sup>; L. G. Jacobsohn\*<sup>1</sup>

1. Clemson University, Materials Science and Engineering, USA

**3:40 PM - WITHDRAWN****(PACC-S7-006-2022) Energy traps redistribution in RE<sup>3+</sup> and Cr<sup>3+</sup> co-doped A<sub>3</sub>B<sub>2</sub>C<sub>3</sub>O<sub>12</sub>-type garnet persistent luminescence ceramics**V. Boiko<sup>1</sup>; Z. Dai<sup>2</sup>; M. Stefanski<sup>1</sup>; M. Saladino<sup>3</sup>; J. Li<sup>2</sup>; D. Hreniak\*<sup>1</sup>

1. Institute of Low Temperature and Structure Research, Division of Optical Spectroscopy, Poland
2. Shanghai Institute of Ceramics, Chinese Academy of Sciences, Transparent Ceramics Research Center, China
3. University of Palermo, STEBICEF Department, Italy

**4:00 PM****(PACC-S7-007-2022) Study of the kinetics of glass dissolution in the K<sub>2</sub>O-MgO-CaO-P<sub>2</sub>O<sub>5</sub> system**V. Cesarino<sup>1</sup>; D. Manzani<sup>2</sup>; E. Ferreira\*<sup>1</sup>

1. EESC, University of São Paulo, Brazil
2. São Carlos Institute of Chemistry, University of São Paulo, Brazil



## PACC8: Novel, Green, and Strategic Processing and Manufacturing Technologies

### Novel, Green, and Strategic Processing I

Room: Bellagio (Level B)

Session Chair: Tatsuki Ohji, National Institute of Advanced Industrial Science and Technology (AIST)

#### 1:30 PM

**(PACC-S8-007-2022) Low temperature in situ modification of silicon (carboxy)nitride ceramics by earth-abundant transition metals as promising (electro)catalysts displaying high specific surface areas for clean hydrogen production (Invited)**

M. Mallmann<sup>1</sup>; R. Morais Ferreira<sup>1</sup>; R. Nishihara<sup>1</sup>; Y. Iwamoto<sup>3</sup>; R. Machado<sup>4</sup>; S. Celerier<sup>2</sup>; A. Habrioux<sup>2</sup>; S. Bernard<sup>\*1</sup>

1. CNRS, IRCER, France
2. Institut de Chimie des Milieux et Matériaux de Poitiers IC2MP UMR7285, France
3. Nagoya Institute of Technology, Japan
4. Federal University of Santa Catarina, Brazil

#### 2:00 PM

**(PACC-S8-002-2022) 2D Nanosheet Architectonics for Hybrid Manufacturing (Invited)**

M. Osada<sup>\*1</sup>

1. Nagoya University, IMASS, Japan

#### 2:30 PM

**(PACC-S8-003-2022) Development of Aqueous Gel-casting Forming Techniques for Novel Spinel Transparent Ceramics (Invited)**

H. Wang<sup>\*1</sup>; X. Zong<sup>1</sup>; H. Zhang<sup>1</sup>; Z. Liu<sup>1</sup>; L. Ren<sup>1</sup>; B. Tu<sup>2</sup>; W. Wang<sup>1</sup>; Z. Fu<sup>2</sup>

1. Wuhan University of Technology, China
2. Wuhan University of Technology, State Key Lab of Advanced Technology for Materials Synthesis and Processing, China

#### 3:00 PM

##### Break

#### 3:20 PM

**(PACC-S8-004-2022) Thermochromic and Photocatalytic Activities of Anion Doped-VO<sub>2</sub>/Nb-TiO<sub>2</sub> Multifunctional Coating Films (Invited)**

S. Yin<sup>\*1</sup>; A. Riapanitra<sup>1</sup>; T. Hasegawa<sup>1</sup>

1. IMRAM, Tohoku University, Japan

#### 3:50 PM

**(PACC-S8-005-2022) Development of the Flexible Ceramics Films and Remanufacturing Process (Invited)**

T. Tsuchiya<sup>\*1</sup>; T. Nakajima<sup>1</sup>; Y. Kitanaka<sup>1</sup>; I. Yamaguchi<sup>1</sup>; J. Nomoto<sup>1</sup>; Y. Uzawa<sup>1</sup>

1. National Institute of Advanced Industrial Science and Technology (AIST), Advanced Manufacturing Research Institute, Japan

#### 4:20 PM

**(PACC-S8-006-2022) Electrolysis for low-carbon hydrogen production: Status, progress and industrial challenges (Invited)**

J. Wiff<sup>\*1</sup>

1. Air Liquide, Materials Science, Japan

## Ferroelectrics Meeting of Americas

### Theory and Ferroic Fundamentals

Room: Star Bay 3 (Level B)

Session Chair: Avadh Saxena, Los Alamos National Lab

#### 1:30 PM

**(FMAs-001-2022) Modulated lattice fluctuations in the vicinity of a ferroelectric quantum critical point (Invited)**

G. G. Guzman-Verri<sup>\*1</sup>; C. H. Liang<sup>2</sup>; P. Littlewood<sup>2</sup>

1. University Costa Rica, Physics, Costa Rica
2. Chicago, Physics, USA

#### 2:00 PM

**(FMAs-002-2022) First principles studies on the structural and ferroic properties of BiFeO<sub>3</sub> based compositions (Invited)**

I. B. Catellani<sup>1</sup>; O. G. Oliveira<sup>1</sup>; G. Perin<sup>1</sup>; G. S. Dias<sup>1</sup>; I. A. Santos<sup>1</sup>; L. F. Cótica<sup>\*1</sup>

1. State University of Maringa, Department of Physics, Brazil

#### 2:30 PM

**(FMAs-003-2022) Rydberg Sensors and Machine Learning Assisted Design Discovery**

M. Trippy<sup>\*1</sup>; R. Guo<sup>1</sup>; A. S. Bhalla<sup>1</sup>

1. University of Texas, San Antonio, USA

#### 2:50 PM

**(FMAs-004-2022) Geometrical Polarization Approach**

V. F. Freitas<sup>\*1</sup>; J. A. Eiras<sup>3</sup>; L. F. Cótica<sup>2</sup>; I. A. Santos<sup>2</sup>

1. Universidade Estadual do Centro-Oeste - Unicentro, Physics, Brazil
2. State University of Maringa, Physics, Brazil
3. Universidade Federal de São Carlos - UFSCAR, Physics, Brazil

#### 3:10 PM

##### Break

#### 3:30 PM

**(FMAs-005-2022) Rich behaviour of oxygen vacancies in SrTiO<sub>3</sub> (Invited)**

A. Lopez-Bezanilla<sup>\*1</sup>; P. Littlewood<sup>2</sup>

1. Los Alamos National Lab, USA
2. Chicago, Physics, USA

#### 4:00 PM

**(FMAs-006-2022) Fast acquisition XRD used to understand elastic transition in lead calcium titanate ceramics**

F. R. Estrada<sup>\*1</sup>; A. Moreno Gobbi<sup>2</sup>; D. Garcia<sup>2</sup>

1. Brazilian Center for Research in Energy and Materials, Brazilian Synchrotron Light Laboratory, Brazil
2. Federal University of São Carlos, Physics Department, Brazil
3. University of the Republic, Department of Applied Physics and Materials, Uruguay

#### 4:20 PM

**(FMAs-008-2022) Dipole Engineering at the Nanoscale: Experimental Data and Theory**

K. Ning<sup>\*1</sup>; H. Shulman<sup>1</sup>; W. A. Schulze<sup>1</sup>; S. Tidrow<sup>1</sup>

1. Alfred University, New York State College of Ceramics, School of Engineering, USA

## PACC Poster Session

Room: Star Bay 1/2

#### 5:30 PM

**(PACC-P001-2022) Composite materials development from ceramics from primary battery waste**

S. Restrepo Tobón<sup>\*1</sup>; H. A. Colorado L.<sup>1</sup>

1. Universidad de Antioquia, Colombia

**(PACC-P002-2022) Influence of ZrO<sub>2</sub> addition on dielectric and piezoelectric properties of (Bi<sub>0.5</sub>Na<sub>0.5</sub>)TiO<sub>3</sub>-BaTiO<sub>3</sub> lead-free piezoceramics**

M. C. Difeo<sup>\*1</sup>; L. Ramajo<sup>1</sup>; M. Castro<sup>1</sup>

1. INTEMA, Ceramics, Argentina

**(PACC-P003-2022) Modeling by Finite Element Method of an Ultrasonic Lead Free Piezoelectric Actuator**F. Gibbs<sup>1</sup>; L. Ramajo<sup>1</sup>; F. Rubio-Marcos<sup>2</sup>; M. Castro<sup>1</sup>; M. C. Difeo<sup>3</sup>; F. Cavalleri<sup>2</sup>

1. INTEMA, Ceramics, Argentina
2. CIMET, Ceramics, Argentina
3. Electroceramic Department, Ceramica y vidrio, Ecuador

**(PACC-P004-2022) Platinum-Based Ordered PtFeCo Ternary Alloy Electrocatalyst for Oxygen Reduction Reaction**M. Lokanathan<sup>1</sup>; R. V. Mangalaraja<sup>1</sup>; A. swamy<sup>2</sup>; C. Mercy<sup>2</sup>; S. Shaji<sup>6</sup>; R. Aepuru<sup>5</sup>; R. Udayabhaskar<sup>4</sup>; M. Gracia-Pinilla<sup>3</sup>

1. Universidad Adolfo Ibáñez, Chile
2. SRM Institute of Science and Technology, Department of Chemistry, India
3. Universidad Autónoma de Nuevo León, Facultad de Ciencias Físico-Matemáticas, Mexico
4. Institute of Scientific and Technological Research, Hybrid Nanomaterials Laboratory, Chile
5. Universidad Tecnológica Metropolitana, Departamento de Mecánica, Chile
6. Autonomous University of Nuevo León, Faculty of Mechanical and Electrical Engineering, Mexico

**(PACC-P005-2022) Thermoelectric in a kitchen heat and smoke extractor**O. F. Posada Henao<sup>1</sup>; H. A. Colorado L.<sup>1</sup>

1. Universidad de Antioquia, Colombia

**(PACC-P006-2022) Evaluation of recyclable thermoplastics for the manufacturing of wind turbines blades H-Darrieus**A. F. Olivera Castillo<sup>1</sup>; H. A. Colorado L.<sup>2</sup>; E. Chica<sup>2</sup>

1. Universidad de Antioquia, engineering, Colombia
2. Universidad de Antioquia, Colombia

**(PACC-P007-2022) Heat recovery from waste management using thermoelectrics**H. Rebellón<sup>1</sup>; H. A. Colorado L.<sup>1</sup>

1. Universidad de Antioquia, Colombia

**(PACC-P008-2022) Electrochemical Characteristics of MXene/Fe<sub>3</sub>O<sub>4</sub> Composites for Electrochemical Supercapacitor Applications**A. Thirumurugan<sup>1</sup>; U. Rednam<sup>2</sup>; M. Morel Escobar<sup>2</sup>

1. University of ATACAMA, Sede vallena, Chile
2. University of ATACAMA, Chile

**(PACC-P009-2022) Tape-casting technique enabled continuous processing of ceramic silicate-based Na<sup>+</sup> superionic conductors**A. Yang<sup>1</sup>; R. Ye<sup>1</sup>; Q. Ma<sup>1</sup>; F. Tietz<sup>2</sup>; O. Guillon<sup>1</sup> **WITHDRAWN**

1. Forschungszentrum Julich GmbH, IEK-1, Germany

**(PACC-P011-2022) Electrochemical storage capability of flexible SiOC ceramic electrodes**S. Mujib<sup>1</sup>; G. Singh<sup>1</sup>

1. Kansas State University, Mechanical & Nuclear Engineering, USA

**(PACC-P012-2022) Multifunctional Flexible Nanocomposite Based Energy Harvesters and Capacitive Pressure Sensor: Investigation of Carrier Dynamics and Performance Evaluation**R. Aepuru<sup>1</sup>; D. Vennu<sup>2</sup>; P. Aqueveque<sup>2</sup>; M. Viswanathan<sup>3</sup>

1. Universidad Tecnológica Metropolitana, Ingeniería Mecánica, Chile
2. Universidad de Concepcion, Department of Electrical Engineering, Chile
3. University of Concepcion, Materials Engineering, Chile

**(PACC-P013-2022) Multiferroic solid solution of BaTiO<sub>3</sub>-BiFeO<sub>3</sub>: Effect of grain boundaries on dielectric and photoelectric response**R. J. Boschilia<sup>2</sup>; R. G. Aredes<sup>3</sup>; Y. L. Ruiz<sup>1</sup>; E. Antonelli<sup>2</sup>

1. UFAM, materials engineering, Brazil
2. Unifesp, science and technology, Brazil

**(PACC-P014-2022) Microstructural and optical properties of nitrogen doped ZnO nanorod thin films fabricated by spin coating technique**P. Thangaraj<sup>1</sup>; M. Viswanathan<sup>2</sup>; K. B<sup>3</sup>; M. Gracia Pinilla<sup>4</sup>

1. Indian Institute of Information Technology Design and Manufacturing Kurnool, Sciences, India
2. University of Concepcion, Materials Engineering, Chile
3. National Institute of Technology Tiruchirappalli, Physics, India
4. Autonomous University of Nuevo León, Physics, Mexico

**(PACC-P015-2022) Polymer/ferrite nanocomposite films for cooling applications**P. THANDAPANI<sup>1</sup>; F. Beron<sup>2</sup>; R. Aepuru<sup>3</sup>; M. Viswanathan<sup>4</sup>; F. L. Zabotto<sup>5</sup>; J. A Jiménez<sup>6</sup>; J. C Denardin<sup>7</sup>

1. VIT-AP UNIVERSITY, Department of Physics, India
2. UNICAMP, Institute of Physics Gleb Wataghin, Brazil
3. Universidad Tecnológica Metropolitana, Department of Mechanical Engineering, Faculty of Engineering, Chile
4. University of Concepcion, Chile
5. Federal University of Sao Carlos, Physics Department, Brazil
6. CENIM-CSIC, Department of Physical Metallurgy, Spain
7. University of Santiago and CEDENNA, Department of Physics, Chile

**(PACC-P016-2022) Structural ground-state, lattice dynamic, thermodynamic and optical properties of the Ba<sub>2</sub>CaMoO<sub>6</sub> double-perovskite**C. E. Deluque Toro<sup>1</sup>; E. Villar Gonzalez<sup>1</sup>; A. V. Gil Rebaza<sup>2</sup>; D. A. Landínez Téllez<sup>2</sup>; J. Roa-Rojas<sup>2</sup>

1. Universidad del Magdalena, Colombia
2. Universidad Nacional de Colombia, Colombia
3. Universidad Nacional de La Plata, Argentina

**(PACC-P017-2022) Physical and thermo-mechanical properties of coated and non coated Magnesia-boron based refractory castable for petrochemical industry application**V. Singh<sup>1</sup>; M. Majhi<sup>1</sup>

1. IIT (BHU) VARANASI, CERAMIC ENGINEERING DEPARTMENT, India

**(PACC-P018-2022) Structural and ferroic properties of compounds based on BiFeO<sub>3</sub> by First principles study**I. B. Catellani<sup>1</sup>; O. G. Oliveira<sup>2</sup>; G. Perin<sup>1</sup>; L. F. Cótica<sup>1</sup>; I. A. Santos<sup>3</sup>

1. State University of Maringá, Physics, Brazil
2. Maringá State University, Brazil
3. State University of Maringá, Physics, Brazil

**(PACC-P019-2022) Polymer-ceramic composites**J. M. Rosso<sup>1</sup>; J. Burato<sup>1</sup>; D. M. Silva<sup>1</sup>; T. G. Bonadio<sup>2</sup>; V. F. Freitas<sup>2</sup>; G. S. Dias<sup>1</sup>; L. F. Cótica<sup>1</sup>; I. A. Santos<sup>1</sup>

1. Maringa State University, Physics, Brazil
2. Midwest State University, Physics, Brazil

**(PACC-P020-2022) Dielectric Behaviour of Ba<sub>0.25</sub>Na<sub>0.75</sub>Ti<sub>0.25</sub>Nb<sub>0.75</sub>O<sub>3</sub> System**J. M. Rosso<sup>1</sup>; D. M. Silva<sup>1</sup>; G. M. Santos<sup>1</sup>; J. Burato<sup>1</sup>; T. G. Bonadio<sup>2</sup>; V. F. Freitas<sup>2</sup>; G. S. Dias<sup>1</sup>; L. F. Cótica<sup>1</sup>; I. A. Santos<sup>1</sup>

1. Maringa State University, Physics, Brazil
2. Midwest State University, Physics, Brazil

**(PACC-P021-2022) Structure, morphology, and magnetism of SCTFO hexaferrite synthesized by Citrate's method**W. Salazar González<sup>1</sup>; J. W. Sandino del Busto<sup>1</sup>; L. C. Moreno Aldana<sup>1</sup>

1. Universidad Nacional de Colombia, Physics, Colombia

**(PACC-P022-2022) Origin of ferroelectricity in Zn<sub>1-x</sub>Mg<sub>x</sub>O by first-principles study**E. Martínez-Aguilar<sup>2</sup>; H. HMok<sup>2</sup>; J. SIQUEIROS<sup>1</sup>; R. López-Juárez<sup>2</sup>

1. UNIVERSIDAD NACIONAL AUTÓNOMA DE MÉXICO, CENTRO DE NANOCIENCIAS Y NANOTECNOLOGÍA, Mexico
2. Van Lang University, Simulation in Materials Science Research Group, Science and Technology Advanced Institute, Viet Nam
3. Universidad Nacional Autónoma de México, Unidad Morelia del Instituto de Investigaciones en Materiales, Mexico

**(PACC-P023-2022) Determination of the Polymorphic Transition Zone in KNnLiTaLa<sub>0.01</sub> by Raman Spectroscopy**Y. De Armas<sup>3</sup>; J. Portelles<sup>3</sup>; R. López-Noda<sup>4</sup>; J. Fuentes<sup>2</sup>; H. Hmok<sup>5</sup>; Z. Bedolla-Valdez<sup>4</sup>; J. SIQUEIROS<sup>1</sup>

1. UNIVERSIDAD NACIONAL AUTÓNOMA DE MÉXICO, CENTRO DE NANOCIENCIAS Y NANOTECNOLOGÍA, Mexico
2. Instituto de Cibernética, Matemática y Física, CITMA, Departamento de Física Aplicada, Cuba
3. Universidad de La Habana, Facultad de Física, Cuba
4. Instituto Tecnológico Superior de Uruapan, Mexico
5. Science and Technology Advanced Institute, Van Lang University, Simulation in Materials Science Research Group, Viet Nam

**(PACC-P024-2022) Experimental and theoretical study of ferromagnetic ordering and semiconductor response in the  $\text{La}_2\text{CoFeO}_6$  ceramic material**

K. Muñoz Pulido\*; J. Jaramillo Palacio; C. E. Deluque Toro; D. A. Landínez Téllez; J. Roa-Rojas<sup>1</sup>

1. Grupo de Física de Nuevos Materiales, Universidad Nacional de Colombia, Física, Colombia
2. Universidad del Magdalena, Colombia

**(PACC-P025-2022) Fabrication and Structural Characterization of Intermetallic Compounds of the  $\text{SrTi}_2\text{Al}_{10}$  Family**

J. C. Delgado\*; M. Cabrera; L. Huertas Pulido; D. A. Landínez Téllez; J. Roa-Rojas<sup>1</sup>

1. Grupo de Física de Nuevos Materiales, Universidad Nacional de Colombia, Física, Colombia
2. Universidade Federal de Pernambuco, Física, Brazil

**(PACC-P026-2022) Refining structural and density calculation electronic system multiferroic  $(\text{Bi}_{1-x}\text{Nd}_x)\text{FeO}_3$** 

O. G. Oliveira\*<sup>1</sup>

1. Maringá State University, Brazil

**(PACC-P027-2022) High resolution laser assisted load dilatometry focused on simultaneous axial and radial strain measurements for sintering characterization**

H. Camacho Montes\*; L. H. Montes; H. M. Loya Caraveo; A. Delgado Salido; A. García Reyes; I. M. Espinoza Ochoa; R. Bordia<sup>1</sup>

1. Universidad Autónoma de Ciudad Juárez, Physics and Mathematics, Mexico
2. Universidad Autónoma de Ciudad Juárez, Eléctrica y Computación, Mexico
3. PROQUIMAR, Mexico
4. Clemson University, Materials Science and Engineering, USA

**(PACC-P028-2022) Properties of Mullite-Ag Cermets**

M. G. Téllez Arias\*; E. Terrés; A. Reyes-Montero; L. Lartundo<sup>4</sup>

1. UNIVERSIDAD MICHOACANA DE SAN NICOLAS DE HIDALGO, FACULTAD DE INGENIERIA QUIMICA, Mexico
2. Instituto Mexicano del Petróleo, Mexico
3. Universidad Nacional Autónoma de México, Instituto de Investigaciones en Materiales, Mexico
4. Instituto Politécnico Nacional, Centro de Nanociencias y Micro y Nanotecnologías, Mexico

**(PACC-P029-2022) Lithium Aluminium Silicate ceramic glass densification during sintering**

I. M. Espinoza Ochoa\*<sup>1</sup>

1. Universidad Autónoma de Ciudad Juárez, Física y Matemáticas, Mexico

**(PACC-P030-2022) Influence of grain size on uniaxial viscosity during sintering**

A. Vega Siverio\*; H. Camacho Montes; B. M. Madrazo; I. M. Espinoza Ochoa<sup>1</sup>

1. Universidad Autónoma de Ciudad Juárez, Física y Matemáticas, Mexico
2. Universidad Autónoma de Ciudad Juárez, Physics and Mathematics, Mexico

**(PACC-P031-2022) Grain size and crystallographic texture effect on the piezoelectric coefficient  $d_{33}$  of  $\text{BaTiO}_3$  ceramics**

B. Olmos\*; O. Raymond; G. M. Herrera-Perez; H. Camacho Montes<sup>3</sup>

1. Universidad Autónoma de Ciudad Juárez, Mexico
2. CONACYT, CIMAV, Mexico
3. Universidad Autónoma de Ciudad Juárez, Physics and Mathematics, Mexico
4. Centro de Nanociencias y Nanotecnología-Universidad Nacional Autónoma de México, Mexico

**(PACC-P032-2022) Mechanism of Hydration of Belite Nanoparticles made from Flame Spray Pyrolysis**

J. J. Pérez Molina\*; D. Gil Velasquez; O. J. Restrepo; J. I. Tobón; N. Betancur-Granados<sup>2</sup>

1. Universidad Nacional de Colombia, Department of Construction, Colombia
2. Corporación Universitaria Minuto de Dios-UNIMINUTO, Department of Basic Sciences, Colombia
3. Universidad Nacional de Colombia, Department of minerals and materials, Colombia

**(PACC-P033-2022) Study of the reactivity of Alkali-activated cements added with nanoparticles of  $\text{SiO}_2$** 

I. Tabora Llano; N. Betancur-Granados; J. I. Tobón; A. A. Hoyos Montilla<sup>2</sup>

1. Corporación Universitaria Minuto de Dios - UNIMINUTO, Faculty of engineering, Colombia
2. Universidad Nacional de Colombia, School of Architecture, Colombia
3. Universidad Nacional de Colombia, Department of Materials and minerals, Colombia

**(PACC-P034-2022) Study on interfacial transition zone properties of lightweight aggregates in concrete**

D. Gonzalez\*; N. Betancur-Granados; J. I. Tobón; A. A. Hoyos Montilla<sup>2</sup>

1. Corporación Universitaria Minuto de Dios - UNIMINUTO, Faculty of engineering, Colombia
2. Universidad Nacional de Colombia, School of Architecture, Colombia
3. Universidad Nacional de Colombia, Department of Materials and minerals, Colombia

**(PACC-P035-2022) Hydrothermal Transformation of Kaolinite to Kalsilite Using Potassium Carbonate**

E. F. Yusslee\*; N. Dahon; M. Abdul Rajak; S. E. Arshad<sup>2</sup>

1. Universiti Malaysia Sabah, Pusat Persediaan Sains & Teknologi, Malaysia
2. Universiti Malaysia Sabah, Faculty of Science and Natural Resources, Malaysia

**(PACC-P036-2022) The use of steelmaking slag as protection for oxidation of MgO-C refractories**

M. N. Moliné; W. A. Calvo; S. E. Gass; D. Gutiérrez-Campos\*; P. G. Galliano; A. G. Tomba Martínez<sup>1</sup>

1. INTEMA (CONICET), Argentina
2. CINI - Tenaris REDE AR, Argentina
3. Universidad Simón Bolívar, Venezuela, Bolivarian Republic of

**(PACC-P037-2022) High-temperature Young's modulus of alumina-containing kaolin-based silicate ceramics and its evolution during sintering**

E. Gregorova\*; W. Pabst<sup>1</sup>

1. UCT Prague, Department of Glass and Ceramics, Czechia

**(PACC-P038-2022) Temperature dependence of Young's modulus of silicon carbide refractories after up to 250 firing cycles determined via impulse excitation**

W. Pabst\*; E. Gregorova<sup>1</sup>

1. University of Chemistry and Technology, Prague, Department of Glass and Ceramics, Czechia

**(PACC-P039-2022) New understanding of liquid thermodynamics, viscosity and its lower bounds**

K. Trachenko\*<sup>1</sup>

1. Queen Mary University of London, Physics, United Kingdom

**(PACC-P040-2022) Rare-Earth-doped Chalcogenide Glasses: On the Path from Passive to Active Applications**

Y. Shpotyuk\*; B. Mahlovanyi; C. Bousard-Pledel; R. Golovchak; J. Cebulski; O. Shpotyuk; B. Bureau<sup>2</sup>

1. University of Rzeszow, Poland
2. University of Rennes, France
3. Austin Peay State University, Physics and Astronomy, USA
4. Jan Dlugosz University in Czeszochowa, Poland
5. University of Rennes 1, Institute of Chemical Sciences, France

**(PACC-P041-2022) Electrical conductivity of vanado-tellurite glass-ceramics doped with  $\text{CuO}$ ,  $\text{Cu}_2\text{O}$ ,  $\text{FeO}$  and  $\text{Fe}_2\text{O}_3$** 

M. Vacchi\*; M. Affatigato; E. I. Cedillo-González; C. Siligardi<sup>1</sup>

1. Università degli studi di Modena e Reggio Emilia, Italy
2. Coe College, Physics Department, USA

**(PACC-P042-2022) SERS using sodium-titanium phosphate glasses containing Ag-NP for photocatalysis application**

D. Manzani\*; T. I. Rubio<sup>1</sup>

1. University of São Paulo, São Carlos Institute of Chemistry, Brazil

**(PACC-P043-2022) Hierarchical porous ceramics developed by using a Si-based preceramic polymer**

C. S. Certuche Arenas; J. O. Bolaños Rivera; Y. X. Hung Hung\*; M. L. Sandoval; M. H. Talou; M. A. Camerucci<sup>1</sup>

1. INTEMA - CONICET, Argentina

**(PACC-P044-2022) Porous ceramic structures obtained by using novel polymer-ceramic systems via additive manufacturing technologies**

Y. X. Hung Hung\*; D. Gutiérrez-Campos; M. L. Sandoval; M. A. Camerucci; M. H. Talou<sup>1</sup>

1. INTEMA - CONICET, Argentina
2. Universidad Simón Bolívar, Ciencias de los Materiales, Venezuela, Bolivarian Republic of

**(PACC-P045-2022) The effective role of  $\text{CaO/SiO}_2$  ratio on the binary system based on  $\text{CaO-SiO}_2$** 

M. H. Kaou\*; H. R. Ben Zine; C. Balazsi; K. Balazsi<sup>2</sup>

1. Óbuda University, Doctoral School on Materials Sciences and Technologies, Hungary
2. Institute of Technical Physics and Materials Science, Centre for Energy Research, ELKH, Hungary

**(PACC-P046-2022) Glass for Environmental Sustainability – An Overview**

M. Mahapatra\*; S. Gupta<sup>2</sup>

1. University of Alabama at Birmingham, Materials Science and Engineering, USA
2. University of North Dakota, Mechanical Engineering, USA

## Tuesday, July 26, 2022

### PACC2: Advanced Ceramics and Composites

#### Advanced Ceramics; Novel Synthesis; Structural Ceramics and Composites

Room: Vitri (Level M)

Session Chair: Mangalaraja Ramalinga Viswanathan, Universidad Adolfo Ibáñez

**8:30 AM**

#### (PACC-S2-006-2022) Bidisperse magneto-rheological fluids consisting of functional SPIONs added to commercial MRF (Invited)

M. Nejatpour\*<sup>1</sup>

1. sabanci University, Material science engineering, Turkey

**9:00 AM**

#### (PACC-S2-007-2022) Tb<sub>2</sub>CoFeO<sub>6</sub> ferromagnetic semiconductor: An experimental and theoretical correlation of physical properties

X. A. Velásquez\*<sup>1</sup>; V. Estrada Contreras<sup>1</sup>; C. E. Deluque Toro<sup>2</sup>; D. A. Landínez Téllez<sup>1</sup>; J. Roa-Rojas<sup>3</sup>

1. Grupo de Física de Nuevos Materiales, Universidad Nacional de Colombia, Física, Colombia
2. Universidad del Magdalena, Colombia
3. Universidad Nacional de Colombia, Physics, Colombia

**9:20 AM**

#### (PACC-S2-008-2022) Progress and challenges towards additive manufacturing of ceramic

Y. Yang\*<sup>1</sup>

1. Shanghai Institute of Ceramics, Chinese Academy of Sciences, China

**9:40 AM**

#### (PACC-S2-009-2022) Garnet-based All-Solid-State Li Batteries by advanced sintering

M. Ihrig\*<sup>1</sup>; A. M. Laptev<sup>1</sup>; T. Mishra<sup>2</sup>; M. Finsterbusch<sup>3</sup>; O. Guillon<sup>4</sup>

1. Forschungszentrum Juelich, IEK-1, Germany
2. Institute of Energy and Climate Research IEK-1: Materials Synthesis and Processing, Forschungszentrum Jülich GmbH, Germany
3. Forschungszentrum Juelich, IEK-1, Germany
4. Forschungszentrum Juelich, IEK-1, Germany

**10:00 AM**

Break

**10:20 AM**

#### (PACC-S2-010-2022) High Reliable High-K Dielectric Oxide-Based Nanolaminates for Next Generation Logic Analog and Memory Semiconductor Devices

E. De Obaldía\*<sup>1</sup>; Y. Chen<sup>2</sup>; o. auciello<sup>3</sup>

1. Universidad Tecnológica de Panamá, Facultad de Ciencias y Tecnología, Panama
2. MicroSol Technologies Inc, USA
3. University of Texas at Dallas, Material Science Engineering, USA

**10:40 AM**

#### (PACC-S2-011-2022) Spark plasma sintered triplet composites of SiC, TiB<sub>2</sub> and ZrN

S. Chodisetti\*<sup>1</sup>; V. B<sup>1</sup>

1. Indian Institute of Technology Roorkee, Department of Metallurgical and Materials ENgineering, India

### PACC1: Ceramics for Energy and Environment

#### Fuel, Oxide Cells and Similar Topics

Room: Revolution (Level B)

Session Chair: Henry Colorado L., Universidad de Antioquia

**10:20 AM**

#### (PACC-S1-007-2022) Glasses and ceramics as joining and coating materials for energy conversion: Issues and perspectives (Invited)

F. Smeacetto\*<sup>1</sup>; M. Salvo<sup>2</sup>; M. Ferraris<sup>3</sup>

1. Politecnico di Torino, Applied Science and Technology, Italy
2. Politecnico di Torino, Italy
3. Politecnico di Torino, Department of Applied Science and Technology, Italy

**10:50 AM**

#### (PACC-S1-008-2022) Advanced Ceramics for Energy Systems and Environmental Technology (Invited)

A. Michaelis\*<sup>1</sup>

1. Fraunhofer IKTS, Germany

**11:20 AM**

#### (PACC-S1-009-2022) Optimized Strategies for the Recovery of Critical Raw Materials from end-of-life Solid Oxide Cells

S. Fiorilli\*<sup>1</sup>; S. Saffirio<sup>1</sup>; S. Fiore<sup>2</sup>; M. Santarelli<sup>2</sup>; I. Schiavi<sup>3</sup>; S. Pylypko<sup>4</sup>; F. Smeacetto<sup>5</sup>

1. Politecnico di Torino, Applied Science and Technology, Italy
2. Politecnico di Torino, Energy, Italy
3. Environment Park S.p.A., Italy
4. Elcogen AS, Estonia
5. Politecnico di Torino, Applied Science and Technology, Italy
6. Politecnico di Torino, Environment, Italy

### PACC3: Densification and Microstructural Evolution in Ceramics During Sintering

#### Sintering II

Room: Millennium (Level B)

Session Chair: Hector Camacho Montes, Universidad Autonoma de Ciudad Juarez

**8:30 AM**

#### (PACC-S3-007-2022) Supercompatibility in Ceramic Micropillars of LaNbO<sub>4</sub> (Invited)

O. A. Graeve\*<sup>1</sup>; H. Hosseini-Toudeshki<sup>1</sup>

1. University of California, San Diego, Mechanical and Aerospace Engineering, USA

**9:00 AM**

#### (PACC-S3-008-2022) Structural and microstructural evolution of BCZT perovskite doped with vanadium

G. M. Herrera-Perez\*<sup>1</sup>; R. Borja-Urby<sup>2</sup>; C. Ornelas-Gutierrez<sup>2</sup>; A. Reyes-Rojas<sup>3</sup>; F. Paraguay-Delgado<sup>3</sup>; L. Fuentes-Cobas<sup>6</sup>

1. CONACYT, Mexico
2. CNMN-IPN, Mexico
3. Nanotech-CIMAV, Mexico
4. CIMAV, Mexico
5. CIMAV, Mexico
6. CIMAV, Mexico

**9:20 AM**

#### (PACC-S3-009-2022) Transparent magnesium aluminate spinel obtained by spark plasma sintering of sol-gel powders

H. Balmori\*<sup>1</sup>; L. Zarazua<sup>1</sup>; L. Tellez-Jurado<sup>1</sup>

1. National Polytechnic Institute, Metallurgical Eng., Mexico

**9:40 AM**

#### (PACC-S3-010-2022) Densification behavior of Yb<sub>2</sub>O<sub>3</sub> with an addition of TiO<sub>2</sub>

S. Maiti\*<sup>1</sup>; Q. Li<sup>1</sup>; F. Peng<sup>1</sup>; R. Bordia<sup>1</sup>

1. Clemson University, Materials Science and Engineering, USA

**10:00 AM**

Break

**10:20 AM****(PACC-S3-011-2022) Advanced processing of oxide ceramics for energy applications by cold sintering (Invited)**M. Bram<sup>\*3</sup>; K. Nur<sup>1</sup>; M. Kindelmann<sup>1</sup>; O. Guillon<sup>2</sup>

1. Forschungszentrum Juelich, Institute IEK-1, Germany
2. Forschungszentrum Juelich, IEK-1, Germany
3. Forschungszentrum Juelich, Institute IEK-1, Germany

**10:50 AM****(PACC-S3-012-2022) Fast Firing of Porcelain Stoneware Tiles in 20 Minutes Cold-to-Cold**C. Conceição<sup>1</sup>; D. E. Garcia<sup>1</sup>; A. De Noni Junior<sup>1</sup>; D. Hotza<sup>\*1</sup>

1. Federal University of Santa Catarina, Brazil

**11:10 AM****(PACC-S3-013-2022) Microstructure and mechanical properties of B<sub>4</sub>C-TiB<sub>2</sub> ceramic composites prepared via a two-step method**Q. He<sup>\*1</sup>; W. Guo<sup>1</sup>; W. Wang<sup>1</sup>

1. Wuhan University of Technology, China

**11:30 AM****(PACC-S3-014-2022) Temperature-dependent impulse excitation as a tool for monitoring phase transitions and microstructural changes in ceramics**W. Pabst<sup>\*1</sup>; E. Gregorova<sup>1</sup>; P. Simonova<sup>1</sup>

1. University of Chemistry and Technology, Prague, Department of Glass and Ceramics, Czechia

**PACC8: Novel, Green, and Strategic Processing and Manufacturing Technologies****Novel, Green, and Strategic Processing II**

Room: Bellagio (Level B)

Session Chair: Tatsuki Ohji, National Institute of Advanced Industrial Science and Technology (AIST)

**8:30 AM****(PACC-S8-001-2022) Efficient Water Splitting on Hematite Thin Films – A Pathway to Solar Hydrogen (Invited)**S. Mathur<sup>\*1</sup>

1. Institute of Inorganic Chemistry, University of Cologne
- 2.

**9:00 AM****(PACC-S8-008-2022) Silicon-Based Anode Materials for Advanced Lithium and Sodium Ion Batteries (Invited)**R. Riedel<sup>\*1</sup>; M. Graczyk-Zajac<sup>2</sup>

1. TU Darmstadt, Materials Science, Germany
2. EnBW, Germany

**9:30 AM****(PACC-S8-009-2022) Colloidal methods for fabrication of supercapacitor electrodes with high active mass (Invited)**I. Zhitomirsky<sup>\*1</sup>

1. McMaster University, Canada

**10:00 AM****Break****10:20 AM****(PACC-S8-010-2022) Aqueous Processing of Garnet-Type Li-Ion Conductors Enabled by Reversible Li<sup>+</sup>/H<sup>+</sup> Exchange**R. Ye<sup>\*1</sup>; M. Finsterbusch<sup>2</sup>; E. Figgemeier<sup>2</sup>

1. Forschungszentrum Juelich Institut für Energie- und Klimaforschung, Materials Synthesis and Processing (IEK-1), Germany
2. Forschungszentrum Juelich, IEK-1, Germany
3. Institute for Power Electronics and Electrical Drives (ISEA), RWTH Aachen University, Germany

**10:40 AM****(PACC-S8-011-2022) Novel single crystalline materials, growth and characteristics (Invited)**K. Shimamura<sup>\*1</sup>; E. G. Villora<sup>2</sup>; D. Yuan<sup>2</sup>; L. Vaschalde<sup>2</sup>

1. National Institute for Materials Science, Japan
2. National Institute for Materials Science (NIMS), Japan

**11:10 AM****(PACC-S8-012-2022) Green synthesis of metal-carbon nanocomposites for energy- and bio-related applications (Invited)**W. Lin<sup>1</sup>; S. Ozeki<sup>1</sup>; T. Akiyama<sup>2</sup>; S. Sharma<sup>1</sup>; S. Elnobi<sup>1</sup>; Y. Yaakob<sup>3</sup>; M. Yusop<sup>4</sup>; Y. Yang<sup>5</sup>; M. Tanemura<sup>\*1</sup>

1. Nagoya Institute of Technology, Department of Physical Science and Engineering, Japan
2. F.C.C. Co.,Ltd, Japan
3. Universiti Putra Malaysia, Department of Physics, Faculty of Science, Malaysia
4. Universiti Teknologi Malaysia, Department of Materials, Faculty of Mechanical Engineering, Malaysia
5. Shanghai Institute of Ceramics, Chinese Academy of Sciences, China

**11:40 AM****(PACC-S8-013-2022) Fabrication of Nanomaterial processing for SDGs (Invited)**Y. Hayashi<sup>\*1</sup>

1. Tohoku University, School of Engineering, Japan

**PACC11: Materials Approach to Art, Architecture, and Archaeology in the Americas****Petrography & Technology**

Room: Venetian (Level B)

Session Chair: Christina Bisulca, Detroit Institute of Arts

**8:30 AM****(PACC-S11-001-2022) Anna O. Shephard (1903–1973): Materials Science Methods in Archaeological Ceramic Analysis**M. D. Jackson<sup>\*1</sup>; C. Bisulca<sup>2</sup>

1. University of Utah, Geology and Geophysics, USA
2. Detroit Institute of Arts, USA

**8:50 AM - WITHDRAWN****(PACC-S11-002-2022) Conventional Microscopy and Thin Section Petrography in the Reduction of Ceramic Typological Variability at the Olmec Site of Los Soldados, Mexico (Invited)**E. H. Huerta<sup>\*1</sup>

1. UC Davis/CSU Fullerton, Anthropology, USA

**9:20 AM****(PACC-S11-003-2022) Early Formative ceramic production in western Mesoamerica: First results of the technological study of Capacha pottery (Invited)**C. Salgado-Ceballos<sup>\*1</sup>

1. Universidad de Guadalajara, Departamento de Estudios Mesoamericanos y Mexicanos, Mexico

**9:50 AM****(PACC-S11-004-2022) Early ceramic technology from La Isleta del Pozon and Puerto Hormiga (Colombia)**D. R. Carvajal Contreras<sup>\*1</sup>

1. Universidad Externado, Archaeology, Colombia

**10:10 AM****Break**

**Organics**

Room: Venetian (Level B)

Session Chair: Fumie Iizuka, University of California Merced

**10:30 AM****(PACC-S11-005-2022) The Common Thread: Authenticating a Nazca tunic using combined dye analysis by LCMS and radiocarbon dating on a single fiber**G. D. Smith<sup>\*</sup>; V. J. Chen<sup>1</sup>; A. Holden<sup>1</sup>; L. Hendriks<sup>2</sup>; N. Haghipour<sup>3</sup>

1. Indianapolis Museum of Art at Newfields, Conservation Science Lab, USA
2. Haute Ecole d'Ingénierie et d'Architecture, Switzerland
3. ETH-Zurich, Laboratory of Ion Beam Physics, Switzerland

**10:50 AM****(PACC-S11-006-2022) Physical Characterization of Prehispanic Ceramic Technologies in the Upper Basin of the Ariari River (Colombia)**R. R. Galindo<sup>\*</sup>; L. Laura<sup>3</sup>; M. Lopez<sup>2</sup>; D. Contreras<sup>4</sup>; V. Benavides<sup>5</sup>; J. Jaramillo<sup>3</sup>; S. Fajardo<sup>6</sup>

1. Universidad del Magdalena, Antropología, Colombia
2. Universidad de los Andes, Colombia
3. Independiente, Colombia
4. Servicio Geológico Colombiano, Colombia
5. Gmas Lab, Colombia
6. TU-Delft, Faculty of Mechanical, Maritime and Materials Engineering (3mE), Netherlands

**11:10 AM****(PACC-S11-007-2022) Phenolic Plant Exudates in the Archaeology of the American Southwest**C. Bisulca<sup>\*</sup>; J. B. Lambert<sup>2</sup>; J. A. Santiago-Blay<sup>3</sup>

1. Detroit Institute of Arts, USA
2. Trinity University, Department of Chemistry, USA
3. National Museum of Natural History, Department of Paleobiology, USA

**11:30 AM****(PACC-S11-008-2022) 19<sup>th</sup> Century Rubber Manufacture in the United States: Analysis of Objects from the USS Monitor Wreck**M. K. McGath<sup>\*</sup>; L. King<sup>1</sup>; L. Haines<sup>1</sup>; H. Fleming<sup>2</sup>

1. The Mariners' Museum and Park, Batten Conservation Complex, USA
2. Henry M. Jackson Foundation supporting supporting Defense POW/MIA Accounting Agency, USA

**11:50 AM****(PACC-S11-009-2022) Vis-NIR Reflectance Spectroscopy of Plastics in Contemporary Art**C. L. Bailin<sup>\*</sup>; E. Homberger<sup>1</sup>; C. Bisulca<sup>1</sup>

1. Detroit Institute of Arts, USA

**Ferroelectrics Meeting of Americas****Dielectrics/Composites/Growth I**

Room: Mirage (Level B)

Session Chair: Jei-Chao, University of Texas, Dallas

**8:30 AM****(FMAs-009-2022) Potentials of Biodegradable composite for Energy Storage Devices : Flexible Dielectric Film derived by PLA/PBAT Blends and Porous Clay Heterostructures (Invited)**H. Manuspiya<sup>\*</sup>

1. Chulalongkorn University, Petroleum and petrochemical college, Thailand

**9:00 AM****(FMAs-010-2022) Perspective on Dielectric Properties of Calcium Copper Titanate Ceramics (Invited)**R. N. Singh<sup>\*</sup>

1. Oklahoma State University, School of Materials Science and Engineering, USA

**9:20 AM - WITHDRAWN****(FMAs-011-2022) Nanoscale Dipole Engineering of BaTiO<sub>3</sub> Using La<sup>3+</sup>-Ta<sup>5+</sup> Dipoles**C. J. Mayo<sup>\*</sup>; V. Pellegrino<sup>2</sup>; K. Ning<sup>3</sup>; S. Tidrow<sup>4</sup>

1. Alfred University, Materials Science and Biomaterials Engineering, USA
2. Alfred University, USA
3. Alfred University, New York State College of Ceramics, School of Engineering, USA
4. Alfred University, USA

**9:40 AM****(FMAs-012-2022) Structural, Dielectric and Ferroelectric Behaviour of BaTiO<sub>3</sub>-PbZrO<sub>3</sub>-SmFeO<sub>3</sub> Solid Solution**P. Kumar<sup>\*</sup>; K. \_<sup>1</sup>

1. DIT University, Department of Physics, School of Physical Sciences, India

**10:00 AM****Break****10:20 AM****(FMAs-013-2022) Morphological evolution and transition at nanoscale in multifunctional ceramic materials (Invited)**N. B. Singh<sup>\*</sup>; C. H. Su<sup>2</sup>; F. choa<sup>1</sup>; B. R. Arnold<sup>1</sup>; B. Cullum<sup>1</sup>; K. Mandal<sup>3</sup>

1. University of Maryland Baltimore County, Chemistry and Biochemistry, USA
2. NASA Marshall Space Flight Center, EM, USA
3. Indian Institute of Technology (BHU), Chemistry, India

**10:50 AM****(FMAs-014-2022) Preparation and characterizations of Bi<sub>0.617</sub>Y<sub>0.05</sub>Cu<sub>3</sub>Ti<sub>4</sub>O<sub>12</sub> ceramic**K. Mandal<sup>1</sup>, D. Prajapati<sup>\*</sup>

1. Indian Institute of Technology (BHU), Chemistry, India

**11:10 AM****(FMAs-015-2022) Effect of DC Poling on Dielectric Properties of Lead-Free Ferroelectric Ceramics**N. Gugar<sup>\*</sup>; P. Kumar<sup>2</sup>; C. Prakash<sup>3</sup>

1. DIT University, India
2. DIT University, Physics, India
3. Maharaja Agrasen Institute of Technology, Applied Sciences, India

**11:20 AM****(FMAs-007-2022) Nanoscale Engineering of Barium Titanate Using Aluminium (III) – Tantalum (V) Dipole Pairs**S. Nudd<sup>\*</sup>; V. Pellegrino<sup>2</sup>; K. Ning<sup>3</sup>; S. Tidrow<sup>2</sup>

1. Alfred University, New York State College of Ceramics, USA
2. Alfred University, USA
3. Alfred University, New York State College of Ceramics, School of Engineering, USA

**11:50 AM****(FMAs-017-2022) Dielectric and electrical properties of Zn doped and undoped Bi<sub>2/3</sub>Cu<sub>3</sub>Ti<sub>4</sub>O<sub>12</sub> ceramic (Invited)**K. Mandal<sup>1</sup>, V. Shankar Rai<sup>1</sup>, N.B. Singh<sup>2\*</sup>

1. Indian Institute of Technology (BHU), Chemistry, India
2. University of Maryland Baltimore County, USA

**Ferroc Domains and Modeling**

Room: Star Bay 3 (Level B)

Session Chair: Ruyan Guo, University of Texas, San Antonio

**8:30 AM****(FMAs-018-2022) Topological Defects in Ferroelectrics and Functional Materials (Invited)**A. Saxena<sup>\*</sup>

1. Los Alamos National Lab, USA

**9:00 AM****(FMAs-019-2022) Switchable negative capacitance in ultrathin ferroelectric/dielectric bilayer capacitors (Invited)**J. Wu<sup>\*</sup>

1. University of Kansas, USA

**9:20 AM****(FMAs-020-2022) Creating Giant Permittivity in BaTiO<sub>3</sub> Ceramics Using Defect**Z. Cheng\*<sup>1</sup>

1. Auburn University, Materials Engineering, USA

**9:40 AM - WITHDRAWN****(FMAs-021-2022) Frequency & temperature-dependent dielectric and ferroelectric properties of Mg-substituted BST ceramics**C. Prakash\*<sup>1</sup>

1. Maharaja Agrasen Institute of Technology, Applied Sciences, India

**10:00 AM****Break****10:20 AM****(FMAs-022-2022) On the DC nonlinear dielectric permittivity and its correlation with the macroscopic polarization state in ferroelectrics (Invited)**J. A. Eiras\*<sup>1</sup>; A. M. Gonçalves<sup>1</sup>; E. B. Araujo<sup>2</sup>; R. Placeres-Jiménez<sup>1</sup>

1. Federal University of Sao Carlos, Physics, Brazil
2. São State University, Physics, Brazil

**10:50 AM****(FMAs-023-2022) Halide Perovskites: NSMM versus Goldschmidt's Tolerance Factor Formalism (Invited)**S. Tidrow\*<sup>1</sup>

1. Alfred University, USA

**11:20 AM****(FMAs-024-2022) Sensitivity analysis on the application of direct piezo-electric effect to predict the influence of variations in the material properties**C. Acosta\*<sup>1</sup>; J. de los Santos Guerra<sup>2</sup>; A. S. Bhalla<sup>1</sup>; R. Guo<sup>1</sup>

1. University of Texas, San Antonio, USA
2. Federal University of Uberlandia, Institute of Physics, Brazil

**11:40 AM****(FMAs-025-2022) Nanoscale Dipole Engineering of Barium Titanate Using Yttrium (III) - Tantalum (V) Dipoles**V. Pellegrino\*<sup>1</sup>; K. Ning<sup>1</sup>; S. Tidrow<sup>1</sup>

1. Alfred University, New York State College of Ceramics, School of Engineering, USA

**12:00 PM****(FMAs-026-2022) Domain engineering of ferroelectric single crystal architecture in glass for integrated optics applications**K. J. Veenhuizen<sup>1</sup>; S. McAnany<sup>2</sup>; R. Vasudevan<sup>3</sup>; D. Nolan<sup>3</sup>; B. Aitken<sup>3</sup>; S. Jesse<sup>4</sup>; V. Dierolf<sup>4</sup>; H. Jain\*<sup>5</sup>

1. Lebanon Valley College, Physics, USA
2. II-VI M Cubed, USA
3. Corning Incorporated, USA
4. Lehigh University, Physics, USA
5. Lehigh University, International Materials Institute for New Functionality in Glass, USA
6. Oak Ridge National Lab, USA

**PACC1: Ceramics for Energy and Environment****Batteries and Various Topics**

Room: Revolution (Level B)

Session Chair: Henry Colorado L., Universidad de Antioquia

**1:30 PM****(PACC-S1-011-2022) A first-principles study of the origin of structural changes in Li<sub>x</sub>Ni<sub>1/3</sub>Co<sub>1/3</sub>Mn<sub>1/3</sub>O<sub>2</sub> and Li<sub>x</sub>Ni<sub>0.8</sub>Co<sub>0.1</sub>Mn<sub>0.1</sub>O<sub>2</sub> cathode materials with lithiation/delithiation (Invited)**L. Kuo\*<sup>1</sup>; O. Guillon<sup>2</sup>; P. Kaghazchi<sup>3</sup>

1. Ming Chi University of Technology, Chemical Engineering, Taiwan
2. Forschungszentrum Juelich, IEK-1, Germany
3. Forschungszentrum Juelich, Germany

**2:00 PM****(PACC-S1-012-2022) Ferroelectric Implanted Cathodes for Lithium Sulfur Batteries for High-Capacity Performance**C. C. Zuluaga-Gomez<sup>1</sup>; C. plaza<sup>2</sup>; G. Morell<sup>1</sup>; Y. Lin<sup>3</sup>; M. Correa<sup>4</sup>; R. Katiyar\*<sup>1</sup>

1. Universidad de Puerto Rico Recinto de Rio Piedras, Puerto Rico
2. Massachusetts Institute of Technology, USA
3. National Institute of Aerospace, USA
4. Universidad del Atlántico, Colombia

**2:20 PM****(PACC-S1-013-2022) Supplementing Rate Capability and Cycling Efficiency of Li-ion Battery Anodes using MoSe<sub>2</sub>/SiOC self-supporting Structure**S. Dey\*<sup>1</sup>; G. Singh<sup>2</sup>

1. Kansas State University, Mechanical Engineering, USA
2. Kansas State University, Mechanical and Nuclear Engineering Dept., USA

**2:40 PM****(PACC-S1-014-2022) Mitigation of Environmental Noise Through the Use of Composite Materials Containing Nanoparticles of Rice Husk**J. Rendon\*<sup>1</sup>; C. H. Giraldo<sup>3</sup>; H. A. Colorado L.<sup>2</sup>

1. Universidad de Antioquia, CComposites Laboratory, Colombia
2. Universidad de Antioquia, Colombia
3. Missouri University of Science and Technology, USA

**3:00 PM****Break****3:20 PM****(PACC-S1-015-2022) Sustainable synthesis of advanced functional ceramics for energy applications (Invited)**J. C. Nino\*<sup>1</sup>

1. University of Florida, Materials Science and Engineering, USA

**3:50 PM****(PACC-S1-016-2022) Development of Ultra-High Temperature Ceramic Additively Manufactured Compact Heat Exchangers (Invited)**N. Timme<sup>1</sup>; V. Anthony<sup>4</sup>; M. Lakusta<sup>1</sup>; G. Basler<sup>1</sup>; S. Grier<sup>1</sup>; T. Plateau<sup>4</sup>; E. Olugbade<sup>4</sup>; P. Rao<sup>1</sup>; S. Jape<sup>6</sup>; P. Davenport<sup>2</sup>; Z. Ma<sup>6</sup>; T. Held<sup>2</sup>; G. Hilmas<sup>1</sup>; W. Fahrenholtz<sup>2</sup>; J. Watts<sup>2</sup>; M. Leu<sup>1</sup>; J. Park<sup>1</sup>; D. Lipke\*<sup>1</sup>

1. Missouri University of Science & Technology, Materials Science & Engineering, USA
2. Missouri University of Science & Technology, Dept. of Materials Science and Engineering, USA
3. Missouri University of Science & Technology, Materials Science and Engineering, USA
4. Missouri University of Science & Technology, Mechanical & Aerospace Engineering, USA
5. Echogen Power Systems, USA
6. National Renewable Energy Laboratory, USA

**4:20 PM****(PACC-S1-017-2022) Electrocatalytically Active Staggered Gap-Based g-C<sub>3</sub>N<sub>4</sub>/WS<sub>2</sub> for Robust Water Splitting**A. Arunachalam\*<sup>1</sup>; M. Viswanathan<sup>1</sup>

1. Universidad de Concepcion, Materials Engineering, Chile

**PACC3: Densification and Microstructural Evolution in Ceramics During Sintering****Sintering III**

Room: Millennium (Level B)

Session Chair: Rajendra Bordia, Clemson University

**1:30 PM****(PACC-S3-015-2022) Sintering-Assisted Additive Manufacturing of Powder Components: Effect of Gravity (Invited)**E. Olevsky\*<sup>1</sup>; E. Torresani<sup>1</sup>; R. Bordia<sup>2</sup>; R. M. German<sup>1</sup>

1. San Diego State University, College of Engineering, USA
2. Clemson University, Materials Science and Engineering, USA

**2:00 PM****(PACC-S3-016-2022) Densification and shape deformation cases descriptions for sintering based on solid mechanics**

H. Camacho Montes<sup>\*1</sup>; A. Gracia Reyes<sup>2</sup>; I. M. Espinoza Ochoa<sup>3</sup>; Y. Espinosa Almeyda<sup>1</sup>; A. Vega Siverio<sup>4</sup>; B. Olmos<sup>5</sup>; R. Bordia<sup>6</sup>

1. Universidad Autonoma de Ciudad Juarez, Physics and Mathematics, Mexico
2. PROQUIMAR, Mexico
3. Universidad Autónoma de Ciudad Juárez, Física y Matemáticas, Mexico
4. Universidad Autónoma de Ciudad Juárez, Física y Matemáticas, Mexico
5. Universidad Autónoma de Ciudad Juárez, Mexico
6. Clemson University, Materials Science and Engineering, USA

**2:20 PM****(PACC-S3-017-2022) Viscous Composite Sintering of Triaxial Ceramics**

D. Hotza<sup>\*1</sup>

1. Federal University of Santa Catarina, Brazil

**2:40 PM****(PACC-S3-018-2022) Modeling of Rapid Sintering by the Discrete Element Method**

M. H. Teixeira<sup>\*1</sup>; J. R. Neto<sup>1</sup>; D. Hotza<sup>2</sup>; R. Janssen<sup>3</sup>

1. Federal University of Santa Catarina (UFSC), Graduate Program in Materials Science and Engineering, Brazil
2. Federal University of Santa Catarina (UFSC), Department of Chemical and Food Engineering, Brazil
3. TU Hamburg-Harburg, Inst. of Advanced Ceramics, Germany

**3:00 PM****Break****3:20 PM****(PACC-S3-019-2022) Machine-learning-based Microstructure-property Prediction Enabled by High-throughput Ceramic Sample-array Preparation Using Integrated Additive/Subtractive Manufacturing (Invited)**

F. Peng<sup>\*2</sup>; X. Geng<sup>2</sup>; J. Tang<sup>3</sup>; Y. Shi<sup>1</sup>; D. Li<sup>4</sup>; R. Bordia<sup>2</sup>; J. Tong<sup>2</sup>; H. Xiao<sup>3</sup>

1. Rensselaer Polytechnic Institute, USA
2. Clemson University, Materials Science and Engineering, USA
3. Clemson University, Electrical and Computer Engineering, USA
4. Advanced Manufacturing LLC, USA

**PACC8: Novel, Green, and Strategic Processing and Manufacturing Technologies****Novel, Green, and Strategic Processing III**

Room: Bellagio (Level B)

Session Chair:

**1:30 PM****(PACC-S8-014-2022) Overview of pressureless electric field-assisted sintering solid electrolytes (Invited)**

R. Muccillo<sup>\*1</sup>

1. IPEN, Brazil

**2:00 PM****(PACC-S8-015-2022) Fabrication of transparent ceramics by colloidal processing and Spark Plasma Sintering (Invited)**

T. S. Suzuki<sup>\*1</sup>; K. Morita<sup>2</sup>; J. Li<sup>2</sup>; B. Kim<sup>2</sup>

1. National Institute for Materials Science, Ceramics Processing Group, Japan
2. National Institute for Materials Science (NIMS), Japan

**2:30 PM****(PACC-S8-016-2022) Ultra-Fast Laser Fabrication of Alumina Micro-Sample Array and High-Throughput Characterization of Microstructure and Hardness**

X. Geng<sup>\*1</sup>; J. Tang<sup>3</sup>; B. Sheridan<sup>1</sup>; S. Sarkar<sup>1</sup>; J. Tong<sup>1</sup>; H. Xiao<sup>2</sup>; D. Li<sup>4</sup>; R. Bordia<sup>2</sup>; F. Peng<sup>1</sup>

1. Clemson University, Materials Science and Engineering, USA
2. Clemson University, Materials Science and Engineering, USA
3. Clemson University, Electrical and Computer Engineering, USA
4. Advanced Manufacturing LLC, USA

**2:50 PM****Break****3:10 PM****(PACC-S8-017-2022) Effect of the pressureless post-sintering on the hot isostatic pressed Al<sub>2</sub>O<sub>3</sub> prepared from the oxidized AlN powder (Invited)**

C. Balazsi<sup>\*1</sup>; K. Balazsi<sup>2</sup>

1. ELKH Centre for Energy Research, Hungary
2. Centre for Energy Research ELKH, Thin Film Physics, Hungary

**3:40 PM****(PACC-S8-018-2022) Microstructure and properties of B-rich boron carbide fabricated by hot-pressing sintering (Invited)**

W. Wang<sup>\*1</sup>; T. Tian<sup>1</sup>; A. Wang<sup>1</sup>; W. Ji<sup>1</sup>; H. Wang<sup>1</sup>; Z. Fu<sup>1</sup>

1. Wuhan University of Technology, State Key Lab of Advanced Technology for Materials Synthesis and Processing, China

**4:10 PM****(PACC-S8-019-2022) Aluminum-to-Ceramics Joining Method by Polysiloxane**

K. Kita<sup>1</sup>; T. Ohji<sup>\*1</sup>; N. Kondo<sup>1</sup>; M. Fukushima<sup>2</sup>; M. Hotta<sup>1</sup>

1. National Institute of Advanced Industrial Science and Technology (AIST), Japan
2. National Institute of Advanced Industrial Science and Technology (AIST), Japan

**PACC10: Ceramics for Sustainable Agriculture****Water Management and Waste Recycling**

Room: Vitri (Level M)

Session Chairs: Allen Ablett, Oklahoma State University; Dileep Singh, Argonne National Lab

**1:30 PM****(PACC-S10-001-2022) Synthesis and Corrosion Study of Polymer-Derived Ceramic Coatings on 304 Stainless Steel (Invited)**

K. Lu<sup>\*1</sup>; H. Choi<sup>1</sup>; W. Wang<sup>1</sup>; R. Cai<sup>1</sup>

1. Virginia Tech, USA

**2:00 PM - WITHDRAWN****(PACC-S10-002-2022) Aggressive Simulated Atmospheric Corrosion of Copper-Lignin Composites**

A. Nieto<sup>\*1</sup>; M. Dey<sup>2</sup>; S. Gupta<sup>2</sup>

1. Naval Postgraduate School, Dept. of Mechanical and Aerospace Engineering, USA
2. University of North Dakota, Mechanical Engineering, USA

**2:20 PM****(PACC-S10-003-2022) Low-temperature Polymer-assisted Additive Manufacturing of Microchanneled Magnetocaloric Structures (Invited)**

V. Sharma<sup>2</sup>; L. Balderson<sup>1</sup>; H. Zhao<sup>1</sup>; R. Barua<sup>\*1</sup>

1. Virginia Commonwealth University, Department of Mechanical & Nuclear Engineering, USA
2. Virginia Commonwealth University, Department of Mechanical Engineering, USA

**2:50 PM****(PACC-S10-004-2022) Use of  $\alpha$ -alumina membranes with immobilized lipase for oil fouling degradation**

J. Mulinari<sup>\*1</sup>; A. Ambrosi<sup>1</sup>; M. Di Luccio<sup>1</sup>; Q. Li<sup>2</sup>; J. Oliveira<sup>1</sup>; D. Hotza<sup>1</sup>

1. Federal University of Santa Catarina, Department of Chemical Engineering and Food Engineering, Brazil
2. Rice University, Civil and Environmental Engineering Department, USA

**3:10 PM****Break****3:30 PM****(PACC-S10-005-2022) Biomass and wood derived materials for structural and energy applications (Invited)**

J. Ramirez-Rico<sup>\*1</sup>

1. Universidad de Sevilla, Spain

**4:00 PM****(PACC-S10-006-2022) Design of Novel Membranes by Using Biomass for Different Types of Applications**

J. Zhang<sup>\*1</sup>; N. Ziamahmoodi<sup>1</sup>; S. McPherson<sup>1</sup>; G. Mackenzie<sup>1</sup>; S. Gupta<sup>1</sup>

1. University of North Dakota, Mechanical Engineering, USA



4:20 PM

**(PACC-S10-007-2022) A Brief Report on Sustainable Manufacturing of Ceramics - *WITHDRAWN***M. Dey\*<sup>1</sup>; J. Sabah<sup>1</sup>; E. Sofowora<sup>2</sup>; S. Gupta<sup>1</sup>

1. University of North Dakota, Mechanical Engineering, USA
2. University of North Dakota, Chemical Engineering, USA

**PACC11: Materials Approach to Art, Architecture, and Archaeology in the Americas****Sourcing**

Room: Venetian (Level B)

Session Chair: Molly McGath, The Mariners' Museum and Park

1:30 PM

**(PACC-S11-010-2022) Advanced Microanalytical Approaches to the Study of Mesoamerican Obsidian and Jade**E. P. VICENZI\*<sup>1</sup>; T. Lam<sup>1</sup>; M. Noyes<sup>2</sup>; H. Lowers<sup>3</sup>

1. Smithsonian Institution, Museum Conservation Institute, USA
2. Rochester Institute of Technology, Image Permanence Institute, USA
3. U.S. Geological Survey, Microbeam Laboratory, USA

1:50 PM

**(PACC-S11-011-2022) Pots across the Atlantic and beyond: Assessing provenance of Spanish colonial 16th-17th centuries tin-lead glazed ceramics by Non-destructive Portable X-Ray Fluorescence in the Americas**J. G. Iñáñez\*<sup>1</sup>

1. University of the Basque Country, Geography, Prehistory and Archaeology, Spain

2:10 PM

**(PACC-S11-012-2022) Sourcing the Pottery of Machu Picchu**L. C. Salazar\*<sup>1</sup>

1. Yale, Anthropology, USA

2:30 PM

**(PACC-S11-013-2022) Sourcing Pottery with LA-ICP-MS and P-XRF: Monagrillo, the Earliest Ceramics of Panama**F. Iizuka\*<sup>1</sup>

1. University of California Merced, Social Sciences, Humanities and Arts, USA

2:50 PM

**Break****Technology**

Room: Venetian (Level B)

Session Chair: Darryl Butt, University of Utah

3:10 PM

**(PACC-S11-014-2022) X-ray MicroCT Analysis: Using Nondestructive Imaging Technology Particularly for Studying Archaeological Ceramics of the Americas and Their Residues**J. Henkin\*<sup>1</sup>

1. Field Museum of Natural History, USA

3:30 PM - *WITHDRAWN***(PACC-S11-015-2022) The pottery collections from Puerto Nuevo on the southern coast of Perú: Insights into long-distance exchange networks of prestige pottery during the Middle and Late Formative of the Central Andes**I. Aguirre\*<sup>1</sup>; J. Dulanto<sup>1</sup>

1. Pontificia Universidad Católica del Perú, Humanidades, Peru

3:50 PM

**(PACC-S11-016-2022) A Concurrent Analytical Study of Two Maya Incensario Supports**E. M. Mars\*<sup>1</sup>

1. Cleveland Museum of Art, Art Conservation, USA

4:10 PM

**(PACC-S11-017-2022) High-resolution Micro-CT with 3D Image Analysis for Porosity Characterization of Bricks and Ceramics**C. L. Reedy\*<sup>1</sup>

1. University of Delaware, Center for Historic Architecture and Design, USA

4:30 PM

**(PACC-S11-018-2022) The technology of stirrup spout bottles from the North coast of Peru. Analysis by CT scan**V. Wauters\*<sup>1</sup>

1. Royal Museums of Art and History of Brussels, Free University of Brussels(ULB), Belgium

**Ferroelectrics Meeting of Americas****Dielectrics/Composites/Growth II**

Room: Mirage (Level B)

Session Chair: Carlos Acosta, University of Texas, San Antonio

1:30 PM

**(FMAs-027-2022) Strontium titanate based n-type oxide thermoelectrics for low-cost electricity generation from waste heat (Invited)**T. Maiti\*<sup>1</sup>

1. IIT Kanpur, Dept. of Materials Science & Engineering, India

2:00 PM

**(FMAs-028-2022) Some Approaches for Single Phase Room Temperature Multiferroic Materials with Strong ME Coupling (Invited)**X. Chen\*<sup>1</sup>

1. Zhengzhou University, School of Materials Science and Engineering, China

2:30 PM

**(FMAs-029-2022) Ferroelectric ordering and electrical energy storage in lead-free ferroelectric Ba<sub>1-x</sub>Sr<sub>x</sub>TiO<sub>3</sub> capacitors**I. W. Castillo<sup>1</sup>; K. K. Mishra<sup>1</sup>; R. Katiyar\*<sup>1</sup>

1. University of Puerto Rico, USA

2:50 PM

**(FMAs-030-2022) Properties of In and Ta Dipole Substituted and Doped BaTiO<sub>3</sub>**N. Betancur-Granados\*<sup>1</sup>; E. K. Merkey<sup>2</sup>; I. Chedzoy<sup>2</sup>; K. Ning<sup>2</sup>; J. I. Tobón<sup>2</sup>; O. J. Restrepo<sup>3</sup>; H. Shulman<sup>2</sup>; S. M. Pilgrim<sup>2</sup>; W. A. Schulze<sup>2</sup>; S. Tidrow<sup>2</sup>

1. Corporación Universitaria Minuto de Dios - UNIMINUTO, Faculty of engineering, Colombia
2. Alfred University, USA
3. Universidad Nacional de Colombia, Department of Materials, Colombia

3:10 PM

**Break**

3:30 PM

**(FMAs-031-2022) High Impacts Inventions on Piezoelectric Ceramic Devices in the Last Four Decades (Invited)**T. Xu\*<sup>1</sup>; B. Zhao<sup>1</sup>

1. Old Dominion University, Mechanical and Aerospace Engineering, USA

4:00 PM

**(FMAs-032-2022) Structural, Dielectric and Ferroelectric Properties of Rare Earth Doped Lead Zirconate Titanate**M. Bhattarai<sup>1</sup>; K. K. Mishra<sup>1</sup>; R. Katiyar\*<sup>1</sup>

1. University of Puerto Rico, Río Piedras Campus, Physics, USA

4:20 PM

**(FMAs-033-2022) Synthesis and Mechanical Properties of Li<sub>2</sub>CO<sub>3</sub> and Bi<sub>2</sub>O<sub>3</sub> added BaTi<sub>1-x</sub>Zr<sub>x</sub>O<sub>3</sub> (x = 0.05 and 0.10) Ceramics**K. J.; N. Somani\*<sup>1</sup>; N. Gugar<sup>1</sup>; P. Kumar<sup>1</sup>; C. Prakash<sup>2</sup>

1. DIT University, India
2. Maharaja Agrasen Institute of Technology, Applied Sciences, India

**4:40 PM****(FMAs-034-2022) Room Temperature Dielectric and Ferroelectric Properties of Barium Titanate Ceramics Substituted Simultaneously by La<sup>3+</sup> at A-site and Fe<sup>3+</sup> at B-site**A. Mehta<sup>\*1</sup>; P. Kumar<sup>2</sup>; C. Prakash<sup>3</sup>

1. DIT University, Physics, India
2. DIT University, Physics, India
3. Maharaja Agrasen Institute of Technology, Applied Sciences, India

**Ferroids and Multiferroics I**

Room: Star Bay 3 (Level B)

Session Chair: Danilo Suvorov, Jozef Stefan Institute

**1:30 PM****(FMAs-035-2022) Rough buffer layers as a tool for stabilizing the perovskite phase in PMN-PT thin films (Invited)**D. Suvorov<sup>\*1</sup>; M. Spreitzer<sup>2</sup>

1. Jozef Stefan Institute, Advanced Materials, Slovenia
2. Jozef Stefan Institute, Advanced Materials, Slovenia

**2:00 PM****(FMAs-036-2022) Rapid discovery of superior energy storage performance in lead-free ferroelectric films with slush polar states via machine learning (Invited)**A. Chen<sup>\*1</sup>

1. Los Alamos National Lab, USA

**2:30 PM****(FMAs-037-2022) Development of Ferroic and Multiferroic Nanomaterials for Hybrid 3D Deposition of Dynamically Tunable Electromagnetic Devices**B. D. Young<sup>\*1</sup>; R. Guo<sup>2</sup>; A. S. Bhalla<sup>2</sup>

1. Sandia National Laboratories, Microsystems Packaging and Polymer Processing, USA
2. University of Texas, San Antonio, USA

**2:50 PM****(FMAs-038-2022) Phase transitions and magnetoelectric coupling of epitaxial asymmetric multilayer heterostructures and superlattices (Invited)**D. K. Pradhan<sup>\*1</sup>

1. University of Tennessee, Department of Materials Science and Engineering, USA

**3:10 PM****Break****3:30 PM****(FMAs-039-2022) Structural changes and local electric/magnetic properties of strained BiFeO<sub>3</sub> nanoparticles (Invited)**E. a. Volnistem<sup>\*1</sup>; I. A. Santos<sup>\*1</sup>

1. State University of Maringa, Physics, Brazil

**4:00 PM - WITHDRAWN****(FMAs-040-2022) Magnetodielectric and Magnetoelectric Coupling in PZT/CFO Nanostructured Composites Fabricated by RF-Sputtering**F. L. Zabotto<sup>\*1</sup>; R. P. Bonini<sup>1</sup>; A. J. Gualdi<sup>1</sup>; J. A. Eiras<sup>1</sup>

1. Federal University of Sao Carlos, Physics Department, Brazil

**4:20 PM****(FMAs-041-2022) Thallium based chalcogenide rad hard multifunctional crystals**N. B. Singh<sup>\*1</sup>; C. H. Su<sup>2</sup>; F. choa<sup>3</sup>; B. R. Arnold<sup>3</sup>; B. Cullum<sup>3</sup>; L. R. Kelly<sup>3</sup>

1. University of Maryland Baltimore County, Chemistry and Biochemistry and Computer Science and Electrical Engineering, USA
2. NASA Marshall Space Flight Center, USA
3. University of Maryland Baltimore County, Chemistry and Biochemistry, USA
4. University of Maryland Baltimore County, Computer Science and Electrical Engineering, USA

**4:40 PM****(FMAs-042-2022) Magneto-Electric Effects in Coaxial Nanofibers of Hexagonal Ferrites and Ferroelectrics (Invited)**G. Srinivasan<sup>\*1</sup>; Y. Liu<sup>1</sup>

1. Oakland University, Physics, USA

**FMAs Poster Session**

Room: Star Bay 1/2

**5:30 PM****(FMAs-P047-2022) Anomalous dielectric response of Pb<sub>0.60</sub>Ca<sub>0.40</sub>TiO<sub>3</sub> under different poling conditions**C. P. Moreira<sup>\*2</sup>; F. P. Milton<sup>2</sup>; F. R. Estrada<sup>1</sup>; D. Garcia<sup>2</sup>

1. National Research Center on Energy and Materials (CNPEM), Brazil
2. Federal University of Sao Carlos, Brazil

**(FMAs-P048-2022) High Purity [In, Ta] Dipolar Pair Substituted BaTiO<sub>3</sub> Ceramics**E. K. Merkey<sup>1</sup>; I. Chedzoy<sup>1</sup>; N. Betancur-Granados<sup>1</sup>; K. Ning<sup>\*1</sup>; J. I. Tobón<sup>2</sup>; O. J. Restrepo<sup>2</sup>; H. Shulman<sup>1</sup>; W. A. Schulze<sup>1</sup>; S. Tidrow<sup>1</sup>

1. Alfred University, New York State College of Ceramics, School of Engineering, USA
2. Universidad Nacional de Colombia, Materials and Minerals Department, Colombia

**(FMAs-P049-2022) Influence of the point-defects and microstructural characteristics on the physical properties of KNbO<sub>3</sub>-based ferroelectric ceramics**M. Cristina Oliveira Silva<sup>1</sup>; A. Carvalho da Silva<sup>1</sup>; M. Aurélio de Oliveira<sup>3</sup>; Y. Mendez González<sup>2</sup>; A. Ferreira Gomes do Monte<sup>1</sup>; J. M'Peko<sup>2</sup>; A. Carlos Hernandez<sup>2</sup>; J. de los Santos Guerra<sup>\*1</sup>

1. Federal University of Uberlandia, Institute of Physics, Brazil
2. Universidad de la Habana, Facultad de Física, Cuba
3. Universidade do Estado de Minas Gerais, Brazil
4. University of Sao Paulo, Sao Carlos Physics Institute, Brazil

**(FMAs-P050-2022) A- and B-sites co-doped PLZT system for energy-storage application: A systematic study on physical properties**A. Carvalho da Silva<sup>1</sup>; M. Aurélio de Oliveira<sup>2</sup>; Y. Mendez González<sup>2</sup>; R. Guo<sup>4</sup>; A. S. Bhalla<sup>4</sup>; J. de los Santos Guerra<sup>\*1</sup>

1. Federal University of Uberlandia, Institute of Physics, Brazil
2. Universidade do Estado de Minas Gerais, Brazil
3. Universidad de la Habana, Facultad de Física - IMRE, Cuba
4. University of Texas, San Antonio, USA

**(FMAs-P051-2022) Effect of temperature and pressure on dielectric properties of nanocomposite between porous clay heterostructure (BC-PCH) and PLA/PBAT blends**S. Chotiradsirikun<sup>\*1</sup>; R. Guo<sup>2</sup>; A. S. Bhalla<sup>3</sup>; H. Manuspiya<sup>1</sup>

1. The Petroleum and Petrochemical college, Polymer Science, Thailand
2. The University of Texas at San Antonio, Department of Electrical and Computer Engineering, USA
3. University of Texas, San Antonio, USA

**(FMAs-P052-2022) Figures of merit of PLZT ferroelectric ceramics for practical applications**J. de los Santos Guerra<sup>\*1</sup>; A. Peláiz Barranco<sup>2</sup>; F. Calderón Piñar<sup>2</sup>; A. Carlos Iglesias Jaime<sup>3</sup>

1. Federal University of Uberlandia, Institute of Physics, Brazil
2. University of Havana, Faculty of Physics, Cuba
3. Universidad Tecnológica de La Habana José A. Echeverría, Departamento de Física, Cuba

**(FMAs-P053-2022) Studies on Microwave Processed (1-x) PbZr<sub>0.65</sub>Ti<sub>0.35</sub>O<sub>3</sub> - xNi<sub>0.8</sub>Zn<sub>0.2</sub>Fe<sub>2</sub>O<sub>4</sub> Magnetoelectric Composites**C. Prakash<sup>\*1</sup> **WITHDRAWN**

1. Maharaja Agrasen Institute of Technology, Applied Sciences, India

**(FMAs-P054-2022) Structural, Ferroelectric Properties of Ba<sub>0.90</sub>Sr<sub>0.10</sub>Ti<sub>1-3x/4</sub>M<sub>x</sub>O<sub>3</sub> (M = Fe<sup>3+</sup>, Cr<sup>3+</sup>) Ceramics**R. Choudhary<sup>\*1</sup>; P. Kumar<sup>1</sup>; S. Sachdev<sup>1</sup>; C. Prakash<sup>2</sup>

1. DIT University, Department of Physics, School of Physical Sciences, India
2. Maharaja Agrasen Institute of Technology, Applied Sciences, India

**(FMAs-P055-2022) Conductivity mechanism and analysis of impedance spectroscopy of barium titanate ceramics synthesized by mechanochemical method**S. Swain<sup>\*1</sup>; P. Kumar<sup>1</sup>; D. Nanda<sup>1</sup>; R. Sahu<sup>1</sup>; A. Parida<sup>1</sup>

1. National Institute of Technology, Rourkela, Physics & Astronomy, India

**(FMAs-P056-2022) Comparative Study of CCTO Ceramics Synthesized by Normal and High Energy Ball Milling**A. Parida<sup>\*1</sup>; S. Swain<sup>1</sup>; R. Sahu<sup>1</sup>; P. Kumar<sup>1</sup>

1. National Institute of Technology, Rourkela, Physics & Astronomy, India

**(FMAs-P057-2022) Study of Structural and Electrical Properties of Lead-free Bulk 0.80(Ba<sub>0.92</sub>Ca<sub>0.08</sub>Ti<sub>0.92</sub>Sn<sub>0.08</sub>O<sub>3</sub>)-0.20NiFe<sub>2</sub>O<sub>4</sub> Composite System - **WITHDRAWN****B. Kar<sup>\*1</sup>; S. Panigrahi<sup>1</sup>; P. Kumar<sup>1</sup>

1. National Institute of Technology, Physics & Astronomy, India

**(FMAs-P058-2022) Influence of Graphene Oxide on the Dielectric Properties of Polyvinylidene Difluoride**R. Pandey<sup>\*1</sup>; N. Singhal<sup>1</sup>; P. Kumar<sup>2</sup>; A. Mehta<sup>3</sup>; C. Prakash<sup>3</sup>

1. DIT University, Chemistry, India
2. DIT University, Physics, India
3. Maharaja Agrasen Institute of Technology, Applied Sciences, India
4. DIT University, Physics, India

**(FMAs-P059-2022) Effect of Ultrasonication on Nucleation of  $\gamma$ -Phase, Dielectric and Ferroelectric properties in PVDF-HFP/Metal-Organic Framework composite films**S. Paramee<sup>\*1</sup>; S. Charoensuk<sup>1</sup>; R. Guo<sup>2</sup>; A. S. Bhalla<sup>2</sup>; H. Manuspiya<sup>3</sup>

1. The Petroleum and Petrochemical College, Chulalongkorn University, Thailand
2. University of Texas, San Antonio, USA
3. Center of Excellence on Petrochemical and Materials Technology, Chulalongkorn University, Thailand

**(FMAs-P060-2022) Multi-composite Stacked Transducers for Energy Harvesting**B. Gamboa<sup>\*1</sup>; R. Guo<sup>1</sup>; A. S. Bhalla<sup>2</sup>

1. university of texas, san antonio, USA
2. University of Texas, San Antonio, USA

**(FMAs-P061-2022) Hot uniaxial forging and magnetoelectric characterization of 50PZN-PT/50CFO particulate composites from powders synthesized by one-step Pechini method**A. V. Rodrigues<sup>\*1</sup>; C. P. Castro<sup>1</sup>; F. P. Milton<sup>1</sup>; C. P. Perdomo<sup>1</sup>; R. H. kiminami<sup>1</sup>; W. Santa-Rosa<sup>1</sup>; D. García<sup>1</sup>

1. Federal University of Sao Carlos, Physics, Brazil

**(FMAs-P062-2022) Remarkably method of synthesis of single-phase and highly resistive BiFeO<sub>3</sub> compound**H. N. Machado<sup>\*1</sup>; L. F. Cótica<sup>1</sup>; G. S. Dias<sup>1</sup>; I. A. Santos<sup>2</sup>

1. State University of Maringá, Department of Physics, Brazil
2. State University of Maringá, Physics, Brazil

**(FMAs-P063-2022) Structure-properties correlations in BiFeO<sub>3</sub> ceramics obtained via cryo-milling**H. N. Machado<sup>\*1</sup>; G. S. Dias<sup>1</sup>; I. A. Santos<sup>1</sup>; L. F. Cótica<sup>1</sup>

1. State University of Maringá, Department of Physics, Brazil

**(FMAs-P064-2022) Extreme conditions route for sintering BiFeO<sub>3</sub> based ceramics**R. C. Oliveira<sup>\*1</sup>; G. S. Dias<sup>2</sup>; I. A. Santos<sup>2</sup>; J. A. Eiras<sup>3</sup>; E. a. Volnistem<sup>1</sup>; D. Garcia<sup>4</sup>

1. State University of Maringá, PFI, Brazil
2. State University of Maringá, Department of Physics, Brazil
3. State University of Maringá, Physics, Brazil
4. Federal University of São Carlos, GMF, Brazil

**(FMAs-P065-2022) Cobalt Ferrite-Barium Titanate Core-Shell Nanoparticles for Biomedical Applications**S. Hossain<sup>\*1</sup>; R. Guo<sup>1</sup>; A. S. Bhalla<sup>1</sup>

1. The University of Texas at San Antonio, Electrical Engineering, USA

**(FMAs-P066-2022) Structural, ferroelectric and magnetic properties of single phase epitaxial (1-x)Pb(Zr,Ti)O<sub>3</sub>-xPb(Fe,Nb)O<sub>3</sub> thin films**L. Imhoff<sup>\*1</sup>; S. Barolin<sup>1</sup>; M. Rengifo<sup>2</sup>; J. Caicedo Roque<sup>2</sup>; J. Santiso<sup>3</sup>; M. Aguirre<sup>2</sup>; M. Stachiotti<sup>1</sup>

1. IFIR-UNR-CONICET, Argentina
2. INMA-UNIZAR, Spain
3. ICN2, Spain

**(FMAs-P067-2022) Structural, electric and magnetic characterization of Pb(Fe,Nb)O<sub>3</sub> thin films fabricated by a practical sol-gel route**L. Imhoff<sup>\*1</sup>; S. Barolin<sup>1</sup>; N. Pellegrini<sup>1</sup>; M. Aguirre<sup>2</sup>; M. Stachiotti<sup>1</sup>

1. IFIR-UNR-CONICET, Argentina
2. INMA-UNIZAR, Spain

**(FMAs-P068-2022) Raman investigations of pressure induced phase transitions in La doped BiFeO<sub>3</sub>-PbTiO<sub>3</sub> polycrystals**L. Macková<sup>\*1</sup>; E. a. Volnistem<sup>1</sup>; F. L. Hegeto<sup>1</sup>; H. d. Deróide<sup>1</sup>; O. A. Protzek<sup>1</sup>; A. M. Farias<sup>2</sup>; R. F. Muniz<sup>2</sup>; V. F. Freitas<sup>2</sup>; G. S. Dias<sup>1</sup>; A. M. Neto<sup>1</sup>; I. A. Santos<sup>1</sup>

1. State University of Maringá, Department of Physics, Brazil
2. Universidade Estadual do Centro-Oeste - Unicentro, Physics, Brazil
3. Universidade Tecnológica Federal do Paraná, Campus Guarapuava, Brazil
4. State University of Maringá, Department of Science, Brazil

**(FMAs-P069-2022) Variation of infrared absorption and Raman spectra of mullite-type Bi<sub>2</sub>(Fe<sub>x</sub>Ga<sub>1-x</sub>)<sub>4</sub>O<sub>9</sub>**L. Macková<sup>\*1</sup>; R. T. Santiago<sup>2</sup>; K. L. da Silva<sup>1</sup>; M. Fabian<sup>2</sup>; L. F. Cótica<sup>1</sup>; I. A. Santos<sup>1</sup>

1. State University of Maringá, Department of Physics, Brazil
2. Slovak Academy of Sciences, Institute of Geotechnics, Slovakia

**(FMAs-P070-2022) Low temperature ferroelectric Berry phase in the Eu<sub>0.5</sub>Bi<sub>0.5</sub>FeO<sub>3</sub> ferromagnetic semiconductor**J. Roa-Rojas<sup>\*1</sup>; J. A. Jairo Roa-Rojas<sup>2</sup>; C. E. Deluque Toro<sup>3</sup>; A. V. Gil Rebaza<sup>4</sup>; D. A. Landínez Téllez<sup>1</sup>

1. Universidad Nacional de Colombia, Physics, Colombia
2. Grupo de Física de Nuevos Materiales, Universidad Nacional de Colombia, Physics, Colombia
3. Grupo de Nuevos Materiales, Universidad del Magdalena, Ingeniería, Colombia
4. Universidad Nacional de La Plata, Physics, Argentina

**(FMAs-P071-2022) Microstructural and dielectric properties of (1-x)BaTiO<sub>3</sub>-(x)CoFe<sub>2</sub>O<sub>4</sub> fibers grown by LHPG technique**A. L. Oliveira<sup>\*2</sup>; F. P. Milton<sup>2</sup>; D. Fukano Viana<sup>2</sup>; M. R. Andreetta<sup>1</sup>; D. Garcia<sup>2</sup>

1. Federal University of Sao Carlos, Department of Materials Engineering, Brazil
2. Federal University of Sao Carlos, Physics Department, Brazil

**(FMAs-P072-2022) Structural and microstructural characterizations of Ta modified AgNbO<sub>3</sub> ferroelectric thin films**Y. Mendez González<sup>2</sup>; F. Agulló-Rueda<sup>2</sup>; J. de los Santos Guerra<sup>\*1</sup>; A. Fernández García<sup>1</sup>; V. Torres Costa<sup>3</sup>; M. Manso Silván<sup>4</sup>

1. Federal University of Uberlândia, Institute of Physics, Brazil
2. Universidad de la Habana, Facultad de Física - IMRE, Cuba
3. Instituto de Ciencia de Materiales de Madrid (ICMM), Spain
4. Universidad Autónoma de Madrid, Departamento de Física Aplicada and Instituto de Ciencia de Materiales Nicolás Cabrera, Spain

**(FMAs-P073-2022) Temperature and electric field effects on erbium PL emissions using PLMN-PT ferroelectric ceramics as host materials - *WITHDRAWN***G. I. Correr<sup>\*1</sup>; F. P. Milton<sup>1</sup>; F. A. Badillo<sup>2</sup>; D. Garcia<sup>1</sup>; M. P. de Godoy<sup>1</sup>

1. Federal University of Sao Carlos, Physics Department, Brazil
2. University of Antioquia, Colombia

**(FMAs-P074-2022) Structural and Optical Properties of BiFeO<sub>3</sub> Thin Films**E. A. Ching<sup>\*1</sup>; H. S. Miranda<sup>1</sup>; E. De Obaldía<sup>2</sup>

1. Universidad Tecnológica de Panamá, Natural Science, Panama
2. Universidad Tecnológica de Panamá, VIPE, Panama

**(FMAs-P075-2022) Optical and energy storage properties of TeO<sub>2</sub>-based ferroelectric glass-ceramics**R. Cruvinel de Oliveira<sup>1</sup>; A. Almeida Silva<sup>2</sup>; N. Oliveira Dantas<sup>2</sup>; J. de los Santos Guerra<sup>\*3</sup>

1. Instituto Federal Goiano, Brazil
2. Universidade Federal de Alagoas, Instituto de Física, Brazil
3. Federal University of Uberlândia, Institute of Physics, Brazil

**(FMAs-P076-2022) Study of the physical properties of BaTi<sub>1-x</sub>Sn<sub>x</sub>O<sub>3</sub> ferroelectric ceramics for practical applications**R. Guilherme Flávio Dornelas<sup>\*1</sup>; A. Carvalho da Silva<sup>1</sup>; J. Eduardo García garcía<sup>2</sup>; J. de los Santos Guerra<sup>1</sup>

1. Federal University of Uberlândia, Institute of Physics, Brazil
2. Universitat Politècnica de Catalunya, Department of Physics, Spain

**(FMAs-P077-2022) Structural and microstructural behavior of PLT:ER ferroelectric system**L. F. DAVILA ESPINOSA<sup>\*1</sup>; A. Herrera Carrillo<sup>1</sup>; F. A. Londoño Badillo<sup>2</sup>; H. A. Colorado L<sup>2</sup>; F. P. Uribe<sup>1</sup>

1. Universidad de Antioquia, ciencias exactas y naturales, Colombia
2. Universidad de Antioquia, Colombia

**(FMAs-P078-2022) Dielectric properties of BCZT ceramics prepared by combustion synthesis and spark plasma sintering**C. F. Villalquian Raigoza<sup>\*1</sup>; M. E. Figueroa Arteaga<sup>1</sup>; D. Garcia<sup>2</sup>; F. Zabotto<sup>2</sup>; F. P. Milton<sup>2</sup>

1. Universidad del Cauca, Física, Colombia
2. Universidade Federal de Sao Carlos, Física, Brazil

**(FMAs-P079-2022) Edge dislocation density in cryo-milled BiFeO<sub>3</sub> nanoparticles: Estimation approaches**E. a. Volnistem<sup>\*1</sup>; R. C. Oliveira<sup>1</sup>; V. F. Freitas<sup>2</sup>; G. S. Dias<sup>1</sup>; L. F. Cótica<sup>1</sup>; I. A. Santos<sup>1</sup>

1. State University of Maringá, Department of Physics, Brazil
2. Universidade Estadual do Centro-Oeste - Unicentro, Physics, Brazil

**(FMAs-P080-2022) Characterization of a-Ba<sub>1-x</sub>Fe<sub>x</sub>TiO<sub>3</sub> Thin films Prepared by Sol-Gel Technique**G. Pitti<sup>1</sup>; A. Watson<sup>1</sup>; E. De Obaldía<sup>1</sup>; E. A. Ching<sup>\*1</sup>

1. Universidad Tecnológica de Panamá, Natural Science, Panama

**(FMA-P081-2022) A Phenomenological Model for the Magnetodielectric Effect in Multiferroics**R. A. Carvalho<sup>\*1</sup>; F. L. Zabotto<sup>1</sup>

1. Federal University of Sao Carlos, Brazil

**(FMA-P082-2022) Scope of Samarium content on optical and structural properties of KNN-based ceramics - *WITHDRAWN***S. A. Zabala<sup>\*1</sup>; F. A. Badillo<sup>1</sup>; A. E. Isaza<sup>2</sup>

1. Universidad de Antioquia, Institute Physic, Colombia
2. Universidad de Antioquia, chemistry institute, Colombia

**(FMA-P083-2022) Influence of Mn and Cu on the Multiferroic Properties of co-doped BiFeO<sub>3</sub> Thin Films**H. S. Miranda<sup>\*1</sup>; E. De Obaldía<sup>1</sup>; A. Watson<sup>1</sup>; E. A. Ching<sup>1</sup>

1. Universidad Tecnológica de Panamá, Ciencias Naturales, Panama

**(FMA-P084-2022) Effect of the rare-earth doping on the structural phase transitions in AgNbO<sub>3</sub> ceramics**T. Hathenher Toledo Rosa<sup>\*1</sup>; A. Carvalho da Silva<sup>1</sup>; Y. Mendez González<sup>2</sup>; R. Guo<sup>3</sup>; A. S. Bhalla<sup>3</sup>; J. de los Santos Guerra<sup>1</sup>

1. Federal University of Uberlandia, Institute of Physics, Brazil
2. Institute of Science and Technology of Material, University of Havana, Cuba, NANOMAT, Cuba
3. University of Texas, San Antonio, USA

**(FMA-P085-2022) Synthesis, structural and optical characterizations of PVDF-based lead-free ceramic composites**E. Alexandre Falcão<sup>1</sup>; A. Carvalho da Silva<sup>2</sup>; Y. Mendez González<sup>2</sup>; R. Guo<sup>4</sup>; A. S. Bhalla<sup>3</sup>; J. de los Santos Guerra<sup>\*2</sup>

1. Universidade Federal da Grande Dourados, Faculdade de Ciências Exatas e Tecnologia, Brazil
2. Federal University of Uberlandia, Institute of Physics, Brazil
3. Universidad de la Habana, Facultad de Física - IMRE, Cuba
4. University of Texas, San Antonio, USA

**(FMA-P086-2022) Synthesis and characterization of Cu<sub>2</sub>O nanoparticle-embedded PZT thin films**M. Di Marco<sup>\*1</sup>; M. Roldán<sup>1</sup>; M. Santiago<sup>1</sup>; M. Stachiotti<sup>1</sup>

1. Instituto de Física de Rosario (IFIR), CONICET-UNR, Argentina

**(FMA-P087-2022) Optical and electrical characterization of sol-gel synthesized PZT thin films on FTO glass substrates**M. Di Marco<sup>\*1</sup>; L. Imhoff<sup>1</sup>; M. Roldán<sup>1</sup>; M. Stachiotti<sup>1</sup>

1. Instituto de Física de Rosario (IFIR), CONICET-UNR, Argentina

**(FMA-P088-2022) Improvement of dielectric properties of bioactive glasses through thermal treatment - *WITHDRAWN***A. Nascimento<sup>\*1</sup>; E. a. Volnistem<sup>1</sup>; W. R. Weinand<sup>1</sup>; F. Pedrochi<sup>2</sup>; I. A. Santos<sup>1</sup>; F. Sato<sup>1</sup>

1. State University of Maringa, Departmente of Physics, Brazil
2. Federal University of Maranhão, Departmente of Physics, Brazil

**(FMA-P089-2022) Investigation of the structural characteristics in PbTiO<sub>3</sub> ferroelectric thin films**M. Aparecido dos Santos Mariano<sup>\*1</sup>; A. De Giovanni Rodrigues<sup>2</sup>; Y. Mendez González<sup>3</sup>; E. Carvalho de Lima<sup>4</sup>; J. de los Santos Guerra<sup>1</sup>

1. Federal University of Uberlandia, Institute of Physics, Brazil
2. Federal University of São Carlos, Physics Department, Brazil
3. Institute of Science and Technology of Material, University of Havana, Cuba, NANOMAT, Cuba
4. Federal University of Tocantins, Brazil

**(FMA-P090-2022) Oxygen vacancy ordering structure and modulated anomalous magnetic properties in cobaltate thin films**Y. Chen<sup>\*1</sup>; C. Chen<sup>2</sup>; J. Ma<sup>1</sup>

1. Tsinghua University, School of Materials Science and Engineering, China
2. University of Texas, San Antonio, USA

**(FMA-P091-2022) Enhanced insulating behaviors in (PrCoO<sub>3</sub>)<sub>n</sub> / (CaCoO<sub>2.5</sub>)<sub>n</sub> Superlattices**J. Xiaomin<sup>\*1</sup>; C. Chen<sup>2</sup>; J. Ma<sup>1</sup>

1. Tsinghua University, School of Materials Science and Engineering, China
2. University of Texas, San Antonio, USA

**(FMA-P092-2022) Study of the electrocaloric response in lanthanum doped (Bi<sub>0.5</sub>Na<sub>0.5</sub>)<sub>0.92</sub>Ba<sub>0.08</sub>TiO<sub>3</sub> lead-free ceramics**Y. Mendez González<sup>2</sup>; A. Peláiz Barranco<sup>2</sup>; J. de los Santos Guerra<sup>\*1</sup>

1. Federal University of Uberlandia, Institute of Physics, Brazil
2. Universidad de la Habana, Facultad de Física, Cuba

**(FMA-P093-2022) High entropy perovskite: An ultra-low thermal conductivity thermoelectric material**R. Banerjee<sup>\*1</sup>; T. Maiti<sup>1</sup>

1. IIT Kanpur, MSE, India

**(FMA-P094-2022) Reinforcement of MXene in perovskite oxides for thermoelectric power generation**P. DIXIT<sup>\*1</sup>; T. Maiti<sup>1</sup>

1. IIT Kanpur, Materials Science and Engineering, India

**(FMA-P095-2022) High performance (ZT>1) n-type oxide thermoelectric composites from earth abundant materials**S. S. Jana<sup>\*1</sup>; M. Acharya<sup>1</sup>; T. Maiti<sup>2</sup>

1. IIT Kanpur, Material Science and Engineering, India
2. IIT Kanpur, Dept. of Materials Science & Engineering, India

**(FMA-P096-2022) Monitoring the ferroelectric phase transition of barium titanate ceramics via impulse excitation**W. Pabst<sup>\*1</sup>; E. Gregorova<sup>1</sup>; P. Simonova<sup>1</sup>

1. University of Chemistry and Technology, Prague, Department of Glass and Ceramics, Czechia

**(FMA-P097-2022) Evaluation of a macroscopic statistical model for the bias electric field dependence of the diffuse phase transition of relaxor ceramics**E. C. Lima<sup>\*3</sup>; J. de los Santos Guerra<sup>2</sup>; E. B. Araujo<sup>1</sup>

1. São Paulo State University, Physics and Chemistry, Brazil
2. Federal University of Uberlandia, Institute of Physics, Brazil
3. Federal University of Tocantins, Physics, Brazil

**(FMA-P098-2022) Designing High Entropy Perovskite (Na<sub>0.2</sub>Bi<sub>0.2</sub>Ba<sub>0.2</sub>Sr<sub>0.2</sub>Ca<sub>0.2</sub>)TiO<sub>3</sub> for lead free Relaxor Ferroelectrics**S. S. Jana<sup>\*1</sup>; V. P. Singh<sup>2</sup>; A. Dwivedi<sup>3</sup>; T. Maiti<sup>2</sup>

1. IIT Kanpur, Dept. Material Science and Engineering, India
2. IIT Kanpur, Dept. of Materials Science & Engineering, India
3. IIT BHU, Department of Ceramic Engineering, India

**(FMA-P100-2022) Ab initio study of samarium doped barium titanate**A. Aslla Quispe<sup>\*1</sup>; G. Cruz Yupanqui<sup>2</sup>; R. Hiroki Miwa<sup>3</sup>; J. de los Santos Guerra<sup>3</sup>

1. Universidad Nacional Intercultural de Quillabamba, Peru
2. Universidad Nacional Tecnológica de Lima Sur, Peru
3. Federal University of Uberlandia, Institute of Physics, Brazil

## Wednesday, July 27, 2022

**PACC4: Bioceramics and Biocomposites****Bioceramics and Biocomposites**

Room: Millennium (Level B)

**8:30 AM****(PACC-S4-001-2022) Biologically Derived Architectures for Next Generation Advanced Materials (Invited)**D. Kisailus<sup>\*1</sup>

1. University of California at Irvine, Materials Science and Engineering, USA

**9:00 AM****(PACC-S4-002-2022) Bioactive glass based scaffolds incorporating phytotherapeutics for bone regeneration (Invited)**A. R. Boccaccini<sup>\*1</sup>

1. University of Erlangen-Nuremberg, Institute of Biomaterials, Germany

**9:30 AM****(PACC-S4-003-2022) Unforeseen molecular mechanisms govern the formation, stabilization, and additive-incorporation behavior of amorphous calcium carbonate: Implications for biomineralization and biomaterial design (Invited)**S. E. Wolf<sup>\*1</sup>

1. Friedrich-Alexander-University Erlangen-Neurnberg, Department of Materials Science and Engineering, Chair of Glass and Ceramics, Germany

**10:00 AM****Break**

10:20 AM

**(PACC-S4-004-2022) Micro and nanoarchitecture of 3D printed ceramic scaffolds for osteoconduction and bone augmentation (Invited)**

F. E. Weber\*<sup>1</sup>

1. University Zurich, Center for Medical Dentistry/oral Biotechnology & Bioengineering, Switzerland

10:50 AM - **WITHDRAWN**

**(PACC-S4-005-2022) Hydroxyapatite-graphene coatings produced by axial suspension plasma spraying**

N. Markocsan\*<sup>1</sup>; G. Manivasagam<sup>2</sup>

1. University West, Dept. of Engineering Science, Sweden
2. VIT University, India

11:10 AM

**(PACC-S4-006-2022) In-vitro biological effect of dissolution products from silicate bioactive glasses**

M. Arango-Ospina\*<sup>1</sup>; A. R. Boccaccini<sup>1</sup>

1. University of Erlangen-Nuremberg, Institute of Biomaterials, Germany

11:30 AM

**(PACC-S4-007-2022) Additive Manufacturing of Materials of Polymers and Polymer-Ceramic Hybrid Materials for Medical Applications (Invited)**

R. Narayan\*<sup>1</sup>

1. North Carolina State University, USA

## **PACC5: Advances in Cements, Geopolymers, and Structural Clay Construction Materials**

### **Geopolymers and Structural Clay Construction Materials**

Room: Venetian (Level B)

Session Chairs: Natalia Betancur-Granados, Corporación Universitaria Minuto de Dios; Henry Colorado L., Universidad de Antioquia

8:30 AM - **MOVED TO POSTER SESSION**

**(PACC-S5-001-2022) Use of construction and demolition waste for developing geopolymer cements (Invited)**

A. Cardoza\*<sup>1</sup>; H. A. Colorado L.<sup>1</sup>

1. Universidad de Antioquia, Colombia

9:00 AM

**(PACC-S5-002-2022) Thermal behavior of geopolymers for new catalytic applications (Invited)**

R. V. Eleuterio\*<sup>1</sup>; F. T. Albino<sup>1</sup>; L. Simão<sup>1</sup>; L. Senff<sup>1</sup>; D. Hotza<sup>1</sup>

1. Federal University of Santa Catarina, Brazil

9:30 AM

**(PACC-S5-003-2022) Manufacture of alkali-activated cements from agro-industrial waste (Invited)**

N. Betancur-Granados\*<sup>1</sup>; D. Gonzalez<sup>2</sup>; F. F. Franco Aguirre<sup>2</sup>; I. Taborda Llano<sup>2</sup>; J. J. Pérez Molina<sup>2</sup>; M. J. Florez Tirado<sup>2</sup>; N. Zapata Perez<sup>2</sup>; P. A. Giraldo Gamboa<sup>2</sup>; S. Restrepo Lopez<sup>2</sup>; J. Durango Duarte<sup>1</sup>; A. A. Hoyos Montilla<sup>2</sup>

1. Corporación Universitaria Minuto de Dios - UNIMINUTO, Faculty of engineering, Colombia
2. Universidad Nacional de Colombia, School of architecture, Colombia

10:00 AM

Break

10:20 AM

**(PACC-S5-004-2022) Potential for industrialization of belite nanoparticles manufactured by aerosol pyrolysis compared to other synthesis methods (Invited)**

D. Gil Velasquez\*<sup>1</sup>; J. J. Pérez Molina<sup>1</sup>; J. I. Tobón<sup>2</sup>; O. J. Restrepo<sup>2</sup>; N. Betancur Granados<sup>1</sup>

1. Universidad Nacional de Colombia, Architecture, Colombia
2. Universidad Nacional de Colombia, Department of minerals and materials, Colombia
3. Corporación universitaria minuto de dios UNIMINUTO, Department of Basic Sciences, Colombia

## **PACC8: Novel, Green, and Strategic Processing and Manufacturing Technologies**

### **Novel, Green, and Strategic Processing IV**

Room: Bellagio (Level B)

8:30 AM

**(PACC-S8-020-2022) High Voltage Pulsed Discharge for selective separation at the multi-materials interface (Invited)**

C. Tokoro\*<sup>1</sup>

1. Waseda University, Japan

9:00 AM

**(PACC-S8-021-2022) Sustainable Recovery, Reprocessing and Reuse of Rare-Earth Magnets in Circular Economy**

M. Zakotnik\*<sup>1</sup>

1. Urban Mining Company, USA

9:20 AM

**(PACC-S8-022-2022) Recycling Wastes Into Clay Brick Manufacturing**

G. Wie-Addo\*<sup>1</sup>; A. H. Jones<sup>1</sup>; S. Palmer<sup>2</sup>; J. Renshaw<sup>2</sup>; P. A. Bingham<sup>1</sup>

1. Sheffield Hallam University, Materials and Engineering Research Institute, United Kingdom
2. Wienerberger Ltd., United Kingdom

9:40 AM

**(PACC-S8-023-2022) Green Synthesis of Materials Via Reaction of Metal Oxides with Aqueous Reagents (Invited)**

A. Apblett\*<sup>1</sup>

1. Oklahoma State University, USA

10:10 AM

Break

10:30 AM

**(PACC-S8-024-2022) Design of insulating ceramic foams for high temperature applications (Invited)**

V. R. Salvini\*<sup>1</sup>

1. UFSCar, Materials Engineering, Brazil

11:00 AM

**(PACC-S8-025-2022) Nb<sub>2</sub>O<sub>5</sub> containing alumina foams for high temperature applications**

V. R. Salvini\*<sup>1</sup>; M. F. Santos<sup>2</sup>; E. França<sup>3</sup>; R. A. Mesquita<sup>3</sup>; m. stuart<sup>4</sup>; V. C. Pandolfelli<sup>1</sup>

1. UFSCar, Materials Engineering, Brazil
2. RED Lab, Brazil
3. CBMM, Brazil
4. St3 Consultoria, Brazil

11:20 AM

**(PACC-S8-026-2022) Novel Processing of Porous Ceramics for Unidirectional Porous Structures**

T. Ohji\*<sup>1</sup>; M. Fukushima<sup>2</sup>

1. National Institute of Advanced Industrial Science and Technology (AIST), Japan
2. National Institute of Advanced Industrial Science and Technology (AIST), Japan

## **PACC10: Ceramics for Sustainable Agriculture**

### **Soil Management**

Room: Vitri (Level M)

8:30 AM

**(PACC-S10-008-2022) Ceramics for Capture of Plant Nutrients and Their Subsequent Use as a Slow Release Fertilizer (Invited)**

A. Apblett\*<sup>1</sup>; C. Kelley<sup>1</sup>; R. Rahman<sup>1</sup>; P. Kitzel<sup>1</sup>; N. materer<sup>1</sup>; E. Kadossov<sup>2</sup>; S. Shaikh<sup>2</sup>

1. Oklahoma State University, USA
2. XploSafe, LLC, USA

9:00 AM

**(PACC-S10-009-2022) Utilization of porous ceramics for plant growth materials**

M. Fukushima\*<sup>1</sup>; T. Ohji<sup>1</sup>

1. National Institute of Advanced Industrial Science and Technology (AIST), Japan

**9:20 AM****(PACC-S10-010-2022) An Overview of Biomass as a Potential Source for Designing Functional Materials**S. Gupta\*<sup>1</sup>

1. University of North Dakota, Mechanical Engineering, USA

**9:40 AM****(PACC-S10-011-2022) Natural fibers and ceramic wastes in composites and soils**H. A. Colorado L.\*<sup>1</sup>

1. Universidad de Antioquia, Colombia

**PACC12: Special Symposium: Ceramics and Materials Education in the Americas****Education**

Room: Revolution (Level B)

Session Chairs: Sylvia Johnson, NASA-Ames Research Center (ret.)

**8:30 AM****(PACC-S12-001-2022) An interdisciplinary experience of teaching Materials Science at the Universidad de Antioquia (Invited)**H. A. Colorado L.\*<sup>1</sup>

1. Universidad de Antioquia, Colombia

**8:50 AM****(PACC-S12-002-2022) Ceramics and Materials Education in Brazil (Invited)**E. N. Muccillo\*<sup>1</sup>

1. Energy and Nuclear Research Institute, Brazil

**9:10 AM****(PACC-S12-003-2022) Ceramic Education in Japan (Invited)**T. Ohji\*<sup>1</sup>

1. National Institute of Advanced Industrial Science and Technology (AIST), Japan

**9:30 AM****(PACC-S12-004-2022) Ceramic Engineering Education at Missouri University of Science and Technology (Invited)**D. Lipke\*<sup>1</sup>; G. Hilmas<sup>1</sup>

1. Missouri University of Science & Technology, Materials Science & Engineering, USA

**9:50 AM****(PACC-S12-005-2022) Considerations of a BS in Ceramic Engineering at Colorado School of Mines (Invited)**I. Reimanis\*<sup>1</sup>; G. L. Brenneka<sup>2</sup>; B. Gorman<sup>1</sup>; A. Rockett<sup>1</sup>; V. E. Stevanovic<sup>1</sup>

1. Colorado School of Mines, USA
2. Colorado School of Mines, USA

**10:10 AM****Break****10:30 AM****(PACC-S12-006-2022) An alternative to traditional doctorate in USA: The Pasteur Partners PhD (P3) track (Invited)**H. Jain\*<sup>1</sup>; V. Dierolf<sup>2</sup>; A. Jagota<sup>1</sup>; H. L. Columba<sup>1</sup>

1. Lehigh University, USA
2. Lehigh University, Physics, USA

**10:50 AM****(PACC-S12-007-2022) North American Summer School on Photonic Materials (NASSPM): An experiment on incorporating laboratory experience in short courses (Invited)**H. Jain\*<sup>1</sup>; K. Richardson<sup>2</sup>; Y. Messaddeq<sup>3</sup>

1. Lehigh University, International Materials Institute for New Functionality in Glass, USA
2. University of Central Florida, CREOL, USA
3. Université Laval, Optic-Photonic Pavillion, Canada

**11:10 AM****(PACC-S12-008-2022) Discovering, Designing, Making, and Manufacturing Materials to 2040 (Invited)**G. Gaustad\*<sup>1</sup>; S. Tidrow<sup>2</sup>

1. NYS College of Ceramics, Alfred University, Inamori School of Engineering, USA
2. Alfred University, USA

**11:30 AM****Panel Discussion****Ferroelectrics Meeting of Americas****Applications of Ferroics**

Room: Mirage (Level B)

Session Chair: Steven Tidrow, Alfred University

**8:30 AM****(FMAs-043-2022) Defect Engineered Complex Oxide Thin Films with Anomalous Multifunctionalities (Invited)**C. Chen\*<sup>1</sup>

1. University of Texas San Antonio, Physics, USA

**9:00 AM - WITHDRAWN****(FMAs-044-2022) Novel Processing of Advanced Functional Materials (Invited)**C. Prakash\*<sup>1</sup>

1. Maharaja Agrasen Institute of Technology, Applied Sciences, India

**9:20 AM****(FMAs-045-2022) Review on Piezoelectric Footwear Power Generators**B. Zhao<sup>1</sup>; B. Poster<sup>1</sup>; A. Hatfield<sup>1</sup>; F. Qian<sup>2</sup>; L. Zuo<sup>2</sup>; T. Xu\*<sup>1</sup>

1. Old Dominion University, Mechanical and Aerospace Engineering, USA
2. Virginia Tech, Mechanical Engineering, USA
3. Penn State Behrend, Department of Mechanical Engineering Technology, USA

**9:40 AM****(FMAs-046-2022) Enhanced Photocatalytic Degradation Activity of Cryomilled BiFeO<sub>3</sub>-Fe<sub>3</sub>O<sub>4</sub> Nanocomposites**V. S. Silva<sup>1</sup>; E. a. Volnistem<sup>1</sup>; L. F. Cótica<sup>1</sup>; I. A. Santos<sup>1</sup>; G. S. Dias\*<sup>1</sup>

1. State University of Maringa, Department of Physics, Brazil

**10:00 AM****Break****10:20 AM****(FMAs-047-2022) Multifunctional epitaxial LaBaCo<sub>2</sub>O<sub>5.5+δ</sub> and PrBaCo<sub>2</sub>O<sub>5.5+δ</sub> thin films: A systematic microstructure and interface investigation (Invited)**J. Jiang\*<sup>1</sup>; C. Chen<sup>2</sup>; E. I. Meletis<sup>1</sup>

1. University of Texas, Arlington, Materials Science and Engineering, USA
2. University of Texas, San Antonio, Department of Physics and Astronomy, USA

**10:50 AM****(FMAs-048-2022) Fundamental Issues related to Characterization of Electrocaloric Effect**F. Najimi<sup>1</sup>; Z. Cheng\*<sup>1</sup>

1. Auburn University, Materials Engineering, USA

**11:10 AM****(FMAs-049-2022) Role of Defect and Power Dispersion on Ferroelectric Memristive Switching**P. Roy\*<sup>2</sup>; D. Zhang<sup>1</sup>; S. Kunwar<sup>1</sup>; J. MacManus-Driscoll<sup>3</sup>; H. Wang<sup>4</sup>; Q. Jia<sup>2</sup>; A. Chen<sup>1</sup>

1. Los Alamos National Lab, USA
2. University at Buffalo, Materials Design and Innovation, USA
3. University of Cambridge, Dept. of Materials Science, United Kingdom
4. Purdue University, School of Materials Engineering, USA

11:30 AM

**(FMAs-050-2022) BiFeO<sub>3</sub>-Based Ferroelectric Perovskites: Potential for Multifunctional Photovoltaic Applications**V. F. Freitas<sup>\*</sup>; E. A. Astrath<sup>2</sup>; L. C. Dias<sup>1</sup>; M. Mazur<sup>1</sup>; T. G. Bonadio<sup>1</sup>; D. M. Silva<sup>1</sup>; G. S. Dias<sup>4</sup>; L. F. Cótica<sup>4</sup>; I. A. Santos<sup>5</sup>

1. Universidade Estadual do Centro-Oeste - Unicentro, Physics, Brazil
2. Federal Institute of Paraná, Campus Paranavaí, Brazil
3. State university of Maringá, Physics, Brazil
4. State University of Maringá, Department of Physics, Brazil
5. State University of Maringá, Physics, Brazil

11:50 AM - **WITHDRAWN****(FMAs-051-2022) Electrocaloric effect in (Na<sub>0.5</sub>Bi<sub>0.5</sub>)TiO<sub>3</sub> - BaTiO<sub>3</sub> - Bi(Mg<sub>0.5</sub>Ti<sub>0.5</sub>)O<sub>3</sub> relaxor ceramics**V. V. Shvartsman<sup>\*</sup>; S. M. Fathabad<sup>1</sup>; D. C. Lupascu<sup>2</sup>; E. Politova<sup>2</sup>

1. University of Duisburg-Essen, Institute for Materials Science, Germany
2. Semenov Federal Research Center for Chemical Physics, Russian Academy of Sciences, Russian Federation
3. University of Duisburg-Essen, Institute for Materials Science, Germany

**Ferroids and Multiferroids II**

Room: Star Bay 3 (Level B)

Session Chair: Hathaikarn Manuspiya, Chulalongkorn University

8:30 AM

**(FMAs-056-2022) Investigations on PZT-PFN - A Room Temperature Nanoscale Multiferroic Prepared by PLD Technique (Invited)**R. Katiyar<sup>\*</sup>; K. Mishra<sup>1</sup>

1. University of Puerto Rico, USA

9:00 AM

**(FMAs-053-2022) Enhanced Thermoelectric Performance in La And Nb Co-doped SrTiO<sub>3</sub> Composite Using Graphite as a Momentum Booster**S. S. Jana<sup>\*</sup>; T. Maiti<sup>2</sup>

1. IIT Kanpur, Material Science and Engineering, India
2. IIT Kanpur, Dept. of Materials Science & Engineering, India

9:20 AM

**(FMAs-054-2022) Revisiting the origin of defects and their relationship to the electrical properties of BiFeO<sub>3</sub> thin films**E. B. Araujo<sup>\*</sup> - **WITHDRAWN**

1. São Paulo State University, Physics and Chemistry, Brazil

9:40 AM

**(FMAs-055-2022) Apatite Growth Induced by Electric Field in Bioferroelectric PVDF/BCP composite**T. G. Bonadio<sup>\*</sup>; J. M. Rosso<sup>2</sup>; G. B. Souza<sup>2</sup>; L. M. Silva<sup>2</sup>; D. M. Silva<sup>2</sup>; V. F. Freitas<sup>1</sup>; W. R. Weinand<sup>2</sup>; I. A. Santos<sup>2</sup>

1. Midwestern Parana State University, Brazil
2. State University of Maringá, Physics, Brazil

10:00 AM

Break

10:20 AM

**(FMAs-057-2022) Review on Piezoelectric Ultrasonic Motors (2015-2020) and Perspectives from Industry 4.0 (Invited)**T. Xu<sup>\*</sup>

1. Old Dominion University, Mechanical and Aerospace Engineering, USA

10:40 AM

**(FMAs-058-2022) Structural and magnetic properties of BiFeO<sub>3</sub> doped ceramics sintered under extreme conditions**R. C. Oliveira<sup>\*</sup>; G. S. Dias<sup>2</sup>; I. A. Santos<sup>2</sup>; M. Melo<sup>2</sup>; E. a. Volnistem<sup>1</sup>; S. J. Süllow<sup>4</sup>; F. J. Litteste<sup>4</sup>; D. J. Baabe<sup>5</sup>

1. State University of Maringá, PFI, Brazil
2. State University of Maringá, Department of Physics, Brazil
3. State University of Maringá, Physics, Brazil
4. Technische Universität Braunschweig, Institut für Physik der Kondensierten Materie, Germany
5. TU Braunschweig, Institut für Anorganische und Analytische Chemie, Germany

11:00 AM

**(FMAs-059-2022) Improving the photocatalytic degradation of organic dyes by the formation of BiFeO<sub>3</sub>/Fe<sub>2</sub>O<sub>3</sub> nanointerfaces**G. S. Dias<sup>\*</sup>; E. a. Volnistem<sup>1</sup>; R. D. Bini<sup>1</sup>; D. M. Silva<sup>1</sup>; J. M. Rosso<sup>1</sup>; L. F. Cótica<sup>1</sup>; I. A. Santos<sup>1</sup>

1. State University of Maringá, Department of Physics, Brazil

11:20 AM

**(FMAs-060-2022) Processing of zinc oxide using a reactive inkjet printing technique**S. Garnsey<sup>\*</sup>; A. S. Bhalla<sup>1</sup>; R. Guo<sup>1</sup>

1. University of Texas, San Antonio, USA

**Thursday, July 28, 2022****Ferroelectrics Meeting of Americas****Design, Synthesis and Fabrication**

Room: Star Bay 3 (Level B)

Session Chair:

8:30 AM

**(FMAs-061-2022) Tailoring the electromechanical coupling in stretchable inorganic thin-film electronics (Invited)**Y. Lin<sup>\*</sup>

1. University of Electronic Science and Technology of China, School of Materials and Energy, China

9:00 AM

**(FMAs-062-2022) Fabrication and evaluation of 3D printed strain gauge sensor**W. Dipon<sup>\*</sup>; S. Garnsey<sup>1</sup>; A. S. Bhalla<sup>1</sup>; R. Guo<sup>1</sup>

1. University of Texas at San Antonio, Electrical and Computer Engineering, USA

9:20 AM

**(FMAs-063-2022) Edge dislocation in BiFeO<sub>3</sub> nanoparticles: Magnetism and Mossbauer effects**E. a. Volnistem<sup>\*</sup>; R. C. Oliveira<sup>1</sup>; G. S. Dias<sup>1</sup>; M. Melo<sup>1</sup>; L. F. Cótica<sup>1</sup>; F. J. Litteste<sup>4</sup>; S. J. Süllow<sup>4</sup>; D. J. Baabe<sup>5</sup>; I. A. Santos<sup>3</sup>

1. State University of Maringá, Department of Physics, Brazil
2. State University of Maringá, Department of Physics, Brazil
3. State University of Maringá, Physics, Brazil
4. TU Braunschweig, Institut für Physik der Kondensierten Materie, Germany
5. TU Braunschweig, Institut für Anorganische und Analytische Chemie, Germany

9:40 AM

**(FMAs-064-2022) Fabrication of a pressure sensor using inkjet printed metal-organic frameworks and interdigitated electrodes**M. Duong<sup>\*</sup>; A. S. Bhalla<sup>1</sup>; R. Guo<sup>1</sup>

1. The University of Texas at San Antonio, USA

10:00 AM

Break

10:20 AM

**(FMAs-065-2022) Multi-ferritic CFO/BTO Core-shell Nanocomposite Films fabricated via Inkjet Printing for Wireless Sensing Applications**P. Flynn<sup>\*</sup>; R. Guo<sup>1</sup>; A. S. Bhalla<sup>1</sup>

1. The University of Texas at San Antonio, USA

10:40 AM

**(FMAs-066-2022) Smart Tooth to Measure Glucose Level for Diabetic Patient Using Piezoelectric**J. Parsi<sup>\*</sup>; N. Namakforoosh<sup>1</sup>; P. Morton<sup>1</sup>; A. S. Bhalla<sup>1</sup>; C. Qian<sup>1</sup>; R. Guo<sup>1</sup>

1. University of Texas, San Antonio, ECE Dept., USA

**The American Ceramic Society**

**Pan American Ceramics Congress and Ferroelectrics  
Meeting of Americas 2022**

**ABSTRACT BOOK**

**July 25–28, 2022  
Panama City, Panama**



# Introduction

---

This volume contains abstracts for 299 presentations during the Pan American Ceramics Congress and Ferroelectrics Meeting of Americas 2022 in Panama City, Panama. The abstracts are reproduced as submitted by authors, a format that provides for longer, more detailed descriptions of papers. The American Ceramic Society accepts no responsibility for the content or quality of the abstract content. Abstracts are arranged by day, then by symposium and session title. An Author Index appears at the back of this book. The Meeting Guide contains locations of sessions with times, titles and authors of papers, but not presentation abstracts.

## How to Use the Abstract Book

---

Refer to the Table of Contents to determine page numbers on which specific session abstracts begin. At the beginning of each session are headings that list session title, location and session chair. Starting times for presentations and paper numbers precede each paper title. The Author Index lists each author and the page number on which their abstract can be found.

Copyright © 2022 The American Ceramic Society ([www.ceramics.org](http://www.ceramics.org)). All rights reserved.

### MEETING REGULATIONS

The American Ceramic Society is a nonprofit scientific organization that facilitates the exchange of knowledge meetings and publication of papers for future reference. The Society owns and retains full right to control its publications and its meetings. The Society has an obligation to protect its members and meetings from intrusion by others who may wish to use the meetings for their own private promotion purpose. Literature found not to be in agreement with the Society's goals, in competition with Society services or of an offensive nature will not be displayed anywhere in the vicinity of the meeting. Promotional literature of any kind may not be displayed without the Society's permission and unless the Society provides tables for this purpose. Literature not conforming to this policy or displayed in other than designated areas will be disposed. The Society will not permit unauthorized scheduling of activities during its meeting by any person or group when those activities are conducted at its meeting place in interference with its programs and scheduled activities. The Society does not object to appropriate activities by others during its meetings if it is consulted with regard to time, place, and suitability. Any person or group wishing to conduct any activity at the time and location of the Society meeting must obtain permission from the Executive Director or Director of Meetings, giving full details regarding desired time, place and nature of activity.

**Diversity Statement:** The American Ceramic Society values diverse and inclusive participation within the field of ceramic science and engineering. ACerS strives to promote involvement and access to leadership opportunity regardless of race, ethnicity, gender, religion, age, sexual orientation, nationality, disability, appearance, geographic location, career path or academic level.

Visit the registration desk if you need access to a nursing mother's room or need further assistance. For childcare services, please check with the concierge at individual hotels for a listing of licensed and bonded child care options.

The American Ceramic Society plans to take photographs and video at the conference and reproduce them in educational, news or promotional materials,

whether in print, electronic or other media, including The American Ceramic Society's website. By participating in the conference, you grant The American Ceramic Society the right to use your name and photograph for such purposes. All postings become the property of The American Ceramic Society.

---

During oral sessions conducted during Society meetings, **unauthorized photography, videotaping and audio recording is prohibited**. Failure to comply may result in the removal of the offender from the session or from the remainder of the meeting.

---

**Registration Requirements:** Attendance at any meeting of the Society shall be limited to duly registered persons.

**Disclaimer:** Statements of fact and opinion are the responsibility of the authors alone and do not imply an opinion on the part of the officers, staff or members of The American Ceramic Society. The American Ceramic Society assumes no responsibility for the statements and opinions advanced by the contributors to its publications or by the speakers at its programs; nor does The American Ceramic Society assume any liability for losses or injuries suffered by attendees at its meetings. Registered names and trademarks, etc. used in its publications, even without specific indications thereof, are not to be considered unprotected by the law. Mention of trade names of commercial products does not constitute endorsement or recommendations for use by the publishers, editors or authors.

Final determination of the suitability of any information, procedure or products for use contemplated by any user, and the manner of that use, is the sole responsibility of the user. Expert advice should be obtained at all times when implementation is being considered, particularly where hazardous materials or processes are encountered.

Copyright © 2022. The American Ceramic Society ([www.ceramics.org](http://www.ceramics.org)). All rights reserved.

# Table of Contents

---

Plenary Session .....	7
<b>PACC1: Ceramics for Energy and Environment</b>	
Semiconductors and Similar Topics .....	7
<b>PACC2: Advanced Ceramics and Composites</b>	
Coatings and Thin Films; Electroceramics .....	9
<b>PACC3: Densification and Microstructural Evolution in Ceramics During Sintering</b>	
Sintering I.....	10
<b>PACC6: Refractories in The Americas</b>	
Refractories .....	11
<b>PACC7: Science and Technology of Glasses, Glass Ceramics, and Optical Materials</b>	
Glasses, Glass-ceramics, and Optical Materials.....	12
<b>PACC8: Novel, Green, and Strategic Processing and Manufacturing Technologies</b>	
Novel, Green, and Strategic Processing I.....	14
<b>Ferroelectrics Meeting of Americas</b>	
Theory and Ferroic Fundamentals .....	15
<b>PACC Poster Session .....</b>	<b>17</b>
<b>PACC2: Advanced Ceramics and Composites</b>	
Advanced Ceramics; Novel Synthesis; Structural Ceramics and Composites.....	26
<b>PACC1: Ceramics for Energy and Environment</b>	
Fuel, Oxide Cells and Similar Topics .....	27
<b>PACC3: Densification and Microstructural Evolution in Ceramics During Sintering</b>	
Sintering II .....	28

<b>PACC8: Novel, Green, and Strategic Processing and Manufacturing Technologies</b>	
Novel, Green, and Strategic Processing II .....	30
<b>PACC11: Materials Approach to Art, Architecture, and Archaeology in the Americas</b>	
Petrography & Technology .....	31
Organics .....	32
<b>Ferroelectrics Meeting of Americas</b>	
Dielectrics/Composites/Growth I .....	33
Ferroic Domains and Modeling .....	35
<b>PACC1: Ceramics for Energy and Environment</b>	
Batteries and Various Topics .....	37
<b>PACC3: Densification and Microstructural Evolution in Ceramics During Sintering</b>	
Sintering III .....	39
<b>PACC8: Novel, Green, and Strategic Processing and Manufacturing Technologies</b>	
Novel, Green, and Strategic Processing III .....	40
<b>PACC10: Ceramics for Sustainable Agriculture</b>	
Water Management and Waste Recycling .....	41
<b>PACC11: Materials Approach to Art, Architecture, and Archaeology in the Americas</b>	
Sourcing .....	43
Technology .....	43
<b>Ferroelectrics Meeting of Americas</b>	
Dielectrics/Composites/Growth II .....	45
Ferroics and Multiferroics I .....	46

<b>FMA's Poster Session</b> .....	48
<b>PACC4: Bioceramics and Biocomposites</b>	
Bioceramics and Biocomposites .....	59
<b>PACC5: Advances in Cements, Geopolymers, and Structural Clay Construction Materials</b>	
Geopolymers and Structural Clay Construction Materials .....	60
<b>PACC8: Novel, Green, and Strategic Processing and Manufacturing Technologies</b>	
Novel, Green, and Strategic Processing IV .....	61
<b>PACC10: Ceramics for Sustainable Agriculture</b>	
Soil Management .....	63
<b>PACC12: Special Symposium: Ceramics and Materials Education in the Americas</b>	
Education .....	63
<b>Ferroelectrics Meeting of Americas</b>	
Applications of Ferroics .....	65
Ferroics and Multiferroics II .....	67
<b>Ferroelectrics Meeting of Americas</b>	
Design, Synthesis and Fabrication .....	69



Monday, July 25, 2022

### Plenary Session

Room: Star Bay 3 (Level B)

Session Chairs: Sylvia Johnson, NASA-Ames Research Center (ret.); Amar Bhalla, University of Texas, San Antonio

8:50 AM

#### (PLEN-001-2022) R & D on vitreous materials in the Americas: Current efforts and a look to the future

E. Dutra Zanotto\*<sup>1</sup>

1. Federal University of Sao Carlos, Materials Engineering, Brazil

Glasses have been known for 6,000 years and are now one of the most ubiquitous, valuable materials to humankind. Due to their large and increasing number of domestic and high-tech applications, some authors have coined the terms “the eyes of science” to characterize their scientific importance and “glass age” as the current era. In this talk, we describe some novel, relatively unknown optical, chemical, biomedical, and mechanical applications of vitreous materials. Then we show the main active glass research groups in the Americas, their main research topics, and publication statistics. Finally, we dwell on “burning” topics and upcoming opportunities – such as the use of Artificial Intelligence, an invaluable tool for new developments in the science and technology of glasses and glass-ceramics.

9:30 AM

#### (PLEN-002-2022) Materials for energy and sustainability

P. Littlewood\*<sup>1</sup>

1. Faraday Institution, United Kingdom

The last century’s advances in information technologies have been propelled by the control of simple electronic materials (metals, insulators, and semiconductors) on increasingly small length scales, now having reached the nanoscale. Semiconductor devices are built via a top-down manufacturing process that is suitable for low volume manufacture. Nanostructured materials of many kinds will also be critical for the energy revolution, e.g. for applications including solar, electrical storage, lightweight components, water treatment, and catalysis. However these materials will need to be manufactured by the ton, or by the square kilometer, which will require us to obtain unprecedented control of functional materials synthesis and manufacture. Modelling, synthesis, and measurement will need to be combined synergistically to develop new materials at scale. There is perhaps nowhere where this change of scale is becoming more visible than in electrical energy storage. As well as changes to the physical approach to manufacturing and design, one needs changes in the institutional structure to support the changing research activities. So this talk, as well as discussing some science, will also describe some of the principles of the recently established Faraday Institution.

10:30 AM

#### (PLEN-003-2022) The Science of Art: Metaphors on the Value of Diversity

D. P. Butt\*<sup>1</sup>

1. University of Utah, Materials Science and Engineering, USA

Art binds us all as humans, connects us with our past, allows us to express the present, and perhaps anticipate or even affect our future. As scientists, we have tools to shine light on art and our cultural heritage both literally and metaphorically. The science of art and the act of making art can be a transdisciplinary, communal experience. Through diverse tools and from diverse perspectives we are, metaphorically speaking, able to expand our visible spectrum. In this lecture, I’ll attempt to weave some thoughts and ideas together based on my experiences as an artist, a professor, and researcher in an attempt to highlight the value of art in science (and vice versa)

with an underlying motivation to leverage diversity, enhance collaboration, and perhaps make two plus two equal something greater than four. Citing a few examples of collaborative research experiences involving diverse groups, and highlighting historical and modern art of the Americas, we’ll take a moment to reflect on how we can all interact more effectively together as we kick off this inaugural Pan American Ceramics Congress. Respect and gratitude to the ancestors and indigenous peoples of Naso, Guna, Bri Bri, Bokata, Ngöbe-Buglé, and Emberá-Wounaan groups whose lands we will be enjoying this week in beautiful Panama.

### PACCI: Ceramics for Energy and Environment

#### Semiconductors and Similar Topics

Room: Revolution (Level B)

Session Chairs: Henry Colorado L., Universidad de Antioquia; Udayabhaskar Rednam, University of Atacama

1:30 PM - **WITHDRAWN**

#### (PACC-S1-001-2022) Advanced Si-based Ceramics for Carbon-free Energy Technologies (Invited)

H. Lin\*<sup>1</sup>

1. Guangdong University of Technology, School of Electronic and Mechanical Engineering, China

Forecasts, based on the data analyzed and published by the U.S. DOE, indicate that the total global energy consumption will increase up to 50% by 2035. The key driving forces behind the predicted increase in worldwide demand include: industrialization and strong economic growth in emerging markets, especially in China, India, and Africa, globalization of commerce, and concerns over national energy security by reducing energy imports. It has been well recognized by the community that the use of fossil energy will continue to grow and dominate the energy market, but that in turn causes increased concerns about greenhouse gas emissions and global warming that have caused many to look negatively at long-term use of fossil fuels. Therefore, there is an imminent need for alternative energy resources such as renewable and nuclear energy to meet the worldwide fast-growing demand. This need has now created tremendous new markets for these renewable and nuclear energy technologies. However, most renewable energy technologies still cannot compete economically with fossil fuels. This lecture will review how emerging advanced Si-based ceramic technologies would help to improve manufacturing and energy generation efficiency and bring renewable energy production closer to reality. The adoption of those Si-based ceramic technologies to carbon-free energy generation will be also discussed in this presentation.

2:00 PM

#### (PACC-S1-002-2022) Semiconducting perovskite Ba<sub>2</sub>CuWO<sub>6</sub> for photovoltaics (Invited)

M. Braun\*<sup>1</sup>; S. Wagner<sup>1</sup>; M. Hinterstein<sup>1</sup>; A. Colsmann<sup>2</sup>; M. Hoffmann<sup>1</sup>

1. Karlsruhe Institute of Technology, Institute for Applied Materials - Ceramic Materials and Technologies, Germany
2. Karlsruhe Institute of Technology, Light Technology Institute, Germany

Thin film solar cells made of metal halide perovskites are attracting a lot of attention since power conversion efficiencies have increased rapidly over the past two decades. While prospective cheap and easy processing could be advantageous, problems such as toxicity and low stability will be difficult to overcome. These drawbacks fostered the research for new material combinations suitable for efficient, nontoxic and stable absorbers for thin film solar cells. Most of these properties can be found in the class of inorganic ABO<sub>3</sub>-perovskites. However, they are mainly insulating due to their wide band gap and low charge carrier mobility. In this contribution, results from

the investigation on the influence of substituting the B-site by two different cations on the properties of the  $ABO_3$ -perovskites will be presented.  $Ba_2CuWO_6$  was synthesized by solid state reaction and thin films with several hundred nanometers thickness were deposited on transparent conducting oxides by pulsed laser deposition. Important optical and electrical characteristics were analyzed taking the synthesis conditions into account and fundamental material properties were characterized by Rietveld refinement of diffraction data, UV-VIS-NIR spectroscopy, as well as SEM and EDX.

### 2:30 PM - **WITHDRAWN**

#### (PACC-S1-003-2022) Assessment of Silicon Germanium Proprieties for Direct Energy Conversion Using Density Functional Theory (Invited)

J. C. Goldsby\*<sup>1</sup>

1. NASA Glenn Research Center, Chemistry and Physics, USA

Radioisotope power systems allow for decades-long spacecraft operation, critical for a deep space mission. Silicon-Germanium (SiGe) based alloys are the traditional thermoelectric materials used in radioisotope power generation. These materials harvest energy from the decay of radioactive sources such as plutonium. Solid-state power conversion devices like thermoelectrics depend solely on their operation's temperature gradients. Computational methods offer an efficient and systematic manner to study and design SiGe heritage materials and determine new formulations. SiGe calculations were carried out to determine this study's relevant electronic and mechanical properties. Comparisons are made between predicted and experimental measurements of Seebeck coefficients. The Zacharias and Giustino approach were used to calculate the phonon-induced change of the band structure as a function of temperature. The calculations were carried out using a projector augmented wave (PAW) method using a commercial code MedeA incorporates the Vienna Ab-initio Simulation Package (VASP) as the computational engine. The calculation was based on density functional theory using the GGA-PBE exchange-correlation functional and optimized mesh. This study makes predictions and comparisons between experimental and theoretical data of electrical, structural, and crystallographic properties.

### 3:20 PM

#### (PACC-S1-004-2022) Studies of optical, dielectric, ferroelectric and structural phase transitions in $[KNbO_3]_{0.9}[BaNb_{1/2}Ni_{1/2}O_{3-\delta}]_{0.1}$ ceramics

B. Y. Rosas<sup>1</sup>; A. A. Instan<sup>1</sup>; K. K. Mishra<sup>1</sup>; S. N. Achary<sup>1</sup>; R. Katiyar\*<sup>1</sup>

1. University of Puerto Rico, Physics, USA

A robust eco-friendly (lead-free) ferroelectric perovskite of  $[KNbO_3]_{0.9}[BaNb_{1/2}Ni_{1/2}O_{3-\delta}]_{0.1}$  (KBNNO) has diverse applications in electronic and photonic devices. We report the optical, dielectric, and structural phase transitions behavior in KBNNO compound using X-ray diffraction (XRD) and Rietveld analyses, Raman, and Dielectric studies at ambient and as a function of temperature. A direct optical band gap  $E_g$  of 1.66 eV was estimated at RT from the UV-Vis reflectance spectrum analysis. Temperature-dependent magnetization studies revealed that KBNNO has a lightly tendency to the magnetization due to the low presence of nickel. XRD studies on KBNNO at elevated temperatures revealed orthorhombic to tetragonal to cubic phase transitions between (500 K-535 K) and (675 K-725 K), respectively. Temperature-dependent dielectric studies on KBNNO identified two dielectric anomalies at ~225 K, ~590 K, and ~690 K, corresponding to the rhombohedral (R) to orthorhombic (O) to tetragonal (T) and to cubic (C) phase transitions, respectively. Electrical conductivity data as a function of temperature obeys Jonscher power law. Temperature-dependent Raman spectroscopy studies over a wide range of temperatures (82 K-1025 K) inferred the R-O-T-C phase transitions at ~250 K, ~550 K, and ~675 K, respectively.

### 3:40 PM

#### (PACC-S1-005-2022) Natural solar light assisted photocatalytic oxidation of endocrine disrupting chemicals using rGO-black $TiO_2$ nanostructures with exposed {001} facets

P. Nalandhiran\*<sup>1</sup>; S. Panneer selvam<sup>2</sup>; M. Viswanathan<sup>3</sup>

1. Universidad Técnica Federico Santa María, Department of Chemistry, Chile

2. Vellore Institute of Technology (VIT) University, Department of Chemistry, School of Advanced Sciences, India

3. Universidad de Concepción, Department of Materials Engineering, Chile

Endocrine-disrupting chemicals (EDCs) in particular medicines, pesticides, detergents and industrial chemicals at very small (ng/L) concentration cause serious health and environmental effects. Considering the above facts, the present work aimed to develop a new heterogeneous photocatalyst through tailoring of bandgap, crystal facet, size and shape by simple solvothermal and solid face reaction. More specifically, anatase {001} black  $TiO_2$  nanosheets (NShts) and anatase {001} black  $TiO_2$  nanocubes (NCs) were synthesized and their surface was modified with reduced graphene oxide (rGO). The photocatalytic efficiency of synthesized photocatalysts was assessed using bisphenol-A and  $\beta$ -lactam antibiotics as the target pollutants under natural solar light irradiation. Further, the implications of chemical surface characteristics of rGO modified anatase {001} black  $TiO_2$  nanostructures was assessed before and after the photocatalytic oxidation reaction. In addition, the photocatalytic activity was compared to benchmark  $TiO_2$  (Degussa P25). The observed results suggested that rGO modified {001} black  $TiO_2$  nanostructures could be used for the effective removal of various EDCs in large wastewater treatment plants by exploiting natural solar light source.

### 4:00 PM

#### (PACC-S1-006-2022) Examination of the Hydrogen Incorporation into Radio Frequency-Sputtered Hydrogenated SiNx Thin Films

N. Hegedüs\*<sup>1</sup>; C. Balazsi<sup>1</sup>; K. Balázs<sup>1</sup>

1. ELKH Centre for Energy Research, Hungary

Silicon nitride (SiNx) and hydrogenated silicon nitride (SiNx:H) thin films have widespread applications, including passivation films for semiconductor devices in microelectronics industry or antireflective layers for solar cells. The most common deposition techniques of SiNx:H thin films are different types of chemical vapor deposition methods, such as plasma enhanced chemical vapor deposition (PE-CVD) or hot wire chemical vapor deposition (HW-CVD). Due to the hydrogen content of the precursor gases (most often silane) CVD-deposited films always contain hydrogen and its amount cannot be controlled directly during the preparation process. Therefore, sputtering methods could be interesting as alternative fabrication techniques for controlled hydrogen concentration in direct way from zero by adjusting the applied hydrogen gas flow to the chamber. In this work amorphous SiNx and SiNx:H films were deposited by radio frequency (RF) sputtering. Optical properties were investigated as a function of hydrogen concentration of the plasma. Structural investigation revealed correlation between hydrogenation process and the layer porosity. 4 at% of bounded hydrogen content was proved by Fourier Transform Infrared Spectroscopy (FTIR) while Elastic Recoil Detection Analysis indicated 6 at% hydrogen which suggests the presence of molecular hydrogen in the films.

## PACC2: Advanced Ceramics and Composites

### Coatings and Thin Films; Electroceramics

Room: Vitri (Level M)

Session Chair: Mangalaraja Ramalinga Viswanathan, Universidad Adolfo Ibáñez

1:30 PM

#### (PACC-S2-001-2022) Consolidation Behavior of Alumina Particles in Aerosol Deposition Method

Y. Furuya<sup>\*1</sup>; M. Hasegawa<sup>1</sup>

1. Yokohama National University, Japan

An aerosol deposition (AD) method can produce ceramic coatings by colliding particles with a substrate. AD coatings are generally considered to be fabricated by fracture and/or plastic deformation of the particles. It has been reported by us that texture is formed in a coating due to the plastic deformation of particles such as Al<sub>2</sub>O<sub>3</sub>, SiAlON, and Ni. An AD mechanism is not quantitatively understood because kinetic energy of the particles is unknown in real deposition conditions. In this study, the AD mechanism was considered based on the kinetic energy of the Al<sub>2</sub>O<sub>3</sub> particles in real deposition conditions. The kinetic energy of the particles was decided from the impact pressure at the collision. Deposition rate and texture development were derived from thickness and XRD measurements, respectively. The deposition rate increased and then decreased with increasing the kinetic energy of the particles. Texture, where (0001) plane was tilted about 15° from the coating plane, was observed in all the deposition conditions. With increasing the kinetic energy of the particles, the texture developed, then decreased and became constant. This suggests that the higher the kinetic energy of the particles, the ratio of the fracture to the plastic deformation of the particles increased. It is expected that both fracture and plastic deformation occurred in the particle to form the coating in all the deposition conditions.

1:50 PM

#### (PACC-S2-002-2022) Structural, multiferroic, optical, and magnetoelectric properties of Zr and Dy doped BiFeO<sub>3</sub> thin films

S. Priya<sup>\*2</sup>; D. Geetha<sup>2</sup>; S. Sharma<sup>1</sup>; J. Siqueiros<sup>1</sup>

1. Universidad Nacional Autonoma De Mexico, Centro De Nanociencias y Nanotecnologia, Mexico

2. Madras Institute of Technology, Department of Physics, India

This work is focused on the fabrication of multiferroic thin films. The influence of doping materials on the structure, optical, morphology, ferroelectric and ferromagnetic properties and magnetoelectric effect were studied comprehensively. Thin films of BiFeO<sub>3</sub> (BFO), Bi<sub>0.95</sub>Zr<sub>0.05</sub>FeO<sub>3</sub> (BZFO), and Bi<sub>0.95</sub>Dy<sub>0.05</sub>FeO<sub>3</sub> (BDFO) were coated on Pt/TiO<sub>2</sub>/TiO/SiO<sub>2</sub>/Si substrates by the spin coating method. X-ray diffraction confirms that all films possess rhombohedral structure of the R3c space group. The band gap values of BFO, BDFO, and BZFO on Pt/TiO<sub>2</sub>/TiO/SiO<sub>2</sub>/Si substrate films were 2.36, 2.3, and 2 eV, respectively. The prepared films exhibit ferromagnetic and ferroelectric nature. The remnant polarization of the BFO, BDFO, and BZFO films are 1.8, 15.2, and 53.2 μC/cm<sup>2</sup>, respectively. The remnant magnetization of BZFO is greater for BFO, than for BDFO films. The magnetoelectric effect in BZFO is larger than for doped and undoped BFO thin films. These findings suggest that BZFO thin film properties may be practical for technological applications. \*Corresponding author [jesus@cny.unam.mx](mailto:jesus@cny.unam.mx) Acknowledgements Subhash Sharma, acknowledges support from Conacyt Catedra Program through Project 352-2018. Work partially supported by PAPIIT-DGAPA-UNAM Grant IN104320. Sathiya Priya, acknowledges support from a postdoctoral scholarship from DGAPA-UNAM.

2:10 PM

#### (PACC-S2-003-2022) Machine learning of gold nanoparticle/polymer hybrid films

Y. Cho<sup>1,2</sup>; K. Lu<sup>\*1</sup>; H. Chaney<sup>1</sup>

1. Virginia Tech, USA

2. Suncheon National University, Korea

Emerging machine learning approaches have been adopted to various material systems to predict novel properties with the assistance of large datasets. For newly developed materials, however, collecting sufficient data points for machine training is not viable, which is the case for gold nanoparticle/polymer hybrid films. In this study, a data analytics framework is proposed for the gold nanoparticle/polymer hybrid films in conjunction with finite element modeling to satisfy the quality and quantity of the data points needed for establishing machine learning models. First, datasets of optical and photothermal properties were built using experimental results from literatures. Then, simulations using models with various microstructural configurations were conducted to generate the data points. Based on the datasets thus obtained, correlation analysis was performed to evaluate the relative importance of the features to the properties of the hybrid films. Then, the selected highly-ranked features were utilized for the machine learning and the model performance was compared. The combined finite element modeling-machine learning approach proposed in this study offers reliable prediction of optical and photothermal properties over different combinations of gold nanoparticles and polymer matrices.

2:30 PM - **WITHDRAWN**

#### (PACC-S2-004-2022) Polar vortices in microwave electronics

F. Bergmann<sup>\*1</sup>; B. Bosworth<sup>1</sup>; E. Marks<sup>2</sup>; A. Hagerstrom<sup>1</sup>; S. Das<sup>3</sup>;

R. Ramesh<sup>3</sup>; N. Orloff<sup>2</sup>

1. NIST, CTL, USA

2. NIST, Communications Technology Laboratory, USA

3. UC Berkeley, MSE/Physics, USA

Ferroelectric PbTiO<sub>3</sub>-SrTiO<sub>3</sub> superlattice films form polar vortices under the right lattice periodicity conditions. Theorists predict that there is a peak in the real part of the permittivity versus lattice periodicity when vortices form. Some researchers suggest that this peak is due to a large negative permittivity present in the vortex core. Here, we study complex permittivity of super lattice films versus periodicity as a function of frequency to understand the frequency dependent signatures of vortex formation and how they might be indicative of negative permittivity. Our measurements show the complex permittivity from 70 kHz to 110 GHz both parallel and perpendicular to the vortex core and as a function of bias voltage. If true, such a remarkable property could enable new microwave devices including parametric amplifiers and non-reciprocal devices like circulators.

2:50 PM

#### (PACC-S2-005-2022) Physical properties of Ba, Na, Ti doped BiFeO<sub>3</sub> solid solutions prepared by solid state reaction method

S. Sharma<sup>\*1</sup>; O. Raymond<sup>1</sup>; J. Siqueiros<sup>1</sup>

Universidad Nacional Autonoma De Mexico, Centro De

Nanociencias y Nanotecnologia, Mexico

The crystal structure and the dielectric and ferroelectric properties are studied in detail for (1-x) BiFeO<sub>3</sub> - x (Ba<sub>0.5</sub>Na<sub>0.5</sub>)TiO<sub>3</sub> or BFO-BNT. Rietveld refinement of the X-ray diffraction data demonstrate that the system is single phase with R3c symmetry up to x = 0.09 while for x = 0.12, a small quantity of a secondary phase with P4mm symmetry appears. Scanning electron microscopy demonstrates that BNT presence promotes grain growth resulting in larger grains. Raman spectroscopy shows that, with increasing x, some of the A and E Raman modes slightly reduce their intensity while shifting in frequency, evincing the structural changes caused by the Ba, Na, and Ti incorporation into the BFO lattice. The X-ray photoelectron spectroscopy study confirms the successful substitution



and gradual structural distortion in the samples. The improvement in dielectric properties with increasing BNT concentration can be attributed to stable dipole moment formation. Compared with pure BFO ceramics, doped BFO samples exhibit remarkably enhanced ferroelectric properties. Acknowledgements Subhash Sharma, acknowledges support from Conacyt Catedra Program through Project 352-2018. This work was partially supported by PAPIIT-DGAPA-UNAM Grants IT100521 and IN104320. The authors thank R. Campos and P. Casillas for their technical assistance.

### **PACC3: Densification and Microstructural Evolution in Ceramics During Sintering**

#### **Sintering I**

Room: Millennium (Level B)

Session Chair: Dachamir Hotza, Federal University of Santa Catarina

**1:30 PM**

#### **(PACC-S3-001-2022) Grain growth control in ceramics: An experimental thermo-kinetic analysis (Invited)**

R. Castro\*<sup>1</sup>

1. University of California, Davis, Material Science & Engineering, USA

Grain growth is an omnipresent phenomenon in ceramic processing and application. The process entails the cooperative movement of atoms across grain boundaries towards the center of curvature of the interface. In this study we investigate the possibility of separating kinetics and thermodynamics of grain growth in oxide materials. Based on unique data obtained by calorimetric techniques, we are able to quantitatively separate kinetics and thermodynamic contributions to grain growth. The results indicate that the energy of the grain boundary is an essential variable for the control of grain size, and targeting lowering of this excess energy using dopants prone to segregation is an effective manner to induce highly metastable nanocrystalline ceramics. We focus the study on relevant oxide systems, such as YSZ and MgAl<sub>2</sub>O<sub>4</sub>.

**2:00 PM**

#### **(PACC-S3-002-2022) Sintering behaviors of micron-sized features (Invited)**

K. Lu\*<sup>1</sup>

1. Virginia Tech, USA

During the fabrication of micron-sized ceramic features, sintering plays a critical role in shape retention and microstructure evolution. Attributed to their sintering mechanism difference, the grains in the ZnO features have a faster growth rate than those in the bulk, while the grains in the ZrO<sub>2</sub> features have a similar growth rate to those in the bulk. ZnO has a much faster grain growth behavior, leading to ridge fidelity loss and severe ridge destruction, while ZrO<sub>2</sub> has a much slower grain growth rate, resulting in high ridge fidelity and strong resistance to ridge destruction. Because of the high evaporation tendency of ZnO, atmosphere has a significant influence on its sintering behavior and feature fidelity. Oxygen partial pressure is the deciding factor in the ridge feature evolution. The pore number in the ridges decreases with the pore size increase. Both grain boundary diffusion related flux and evaporation–condensation related diffusion flux increase with the sintering time. However, the former is five orders of magnitude lower than the latter, indicating the dominance of the grain growth process in the ridges. The decreasing dihedral angle during sintering indicates increased surface energy of pores, consistent with the 3D reconstruction results. Such understanding provides new insight into the sintering behaviors of micron-sized ridges.

**2:30 PM**

#### **(PACC-S3-003-2022) In-situ SEM Study of Microstructure Evolution During Sintering and Selective Reduction of Metal Nanoparticles from Spinel Oxides (Invited)**

S. T. Mixture\*<sup>1</sup>; A. Ladonis<sup>1</sup>

1. Alfred University, MSE, USA

In-situ techniques offer insights into reaction mechanisms that may be missed entirely when studying complex materials systems. Nickel/cobalt aluminate spinel is an interesting case study, where reducing atmospheres extract reducible cations from the MA12O<sub>4</sub> spinel starting phase. The spinel materials are chemically highly tailorable, and selectively reduced materials are useful as catalysts for fuel reforming, for example. The microstructures, however, are of critical importance. Here we present a study employing in-situ scanning electron microscopy as the primary tool for tracking the processes dynamically. The talk will show how we track first the evolution of the faceting of the particles, then sintering of particles, and finally Ni/Co exsolution and resorption – as functions of temperature and oxygen partial pressure. Reduction of the metal nanoparticles from the oxide yields surface sockets but the metal particles nonetheless may diffuse along the surface and coalesce. Using catalysis measurements, we learn that the oxide surfaces are in fact massively oxygen defective, allowing rapid near-surface mass transport and remarkable surface changes. We consider possible mechanisms that enable rapid diffusion of particles on these unique oxide surfaces.

**3:20 PM**

#### **(PACC-S3-004-2022) Microstructural evolution of carbide MXenes and their Composites at high-temperatures (Invited)**

M. Anayee<sup>1</sup>; Y. Gogotsi\*<sup>1</sup>

1. Drexel University, USA

Two-dimensional (2D) transition metal carbides and nitrides (MXenes) have attracted attention because of their electronic, electrochemical, chemical, and optical properties. However, understanding of their thermal stability and sintering behavior is still lacking. Given their compositional diversity and tunable surface chemistry, the thermal properties of MXenes vary widely. Here, we performed thermal gravimetric analysis with mass spectrometry up to 1500 °C for several carbide MXenes (Ti<sub>3</sub>C<sub>2</sub>T<sub>x</sub>, Ti<sub>2</sub>CT<sub>x</sub>, Mo<sub>2</sub>CT<sub>x</sub> and others) and showed that stability of MXenes strongly depends on their chemical composition, structure and transition metal layers. For example, the stability of Ti<sub>3</sub>C<sub>2</sub>T<sub>x</sub> can be improved by employing synthesis conditions that lead to reduced fluorine content and defects density. We also showed the structural evolution from 2D Ti<sub>3</sub>C<sub>2</sub>T<sub>x</sub> to defunctionalized Ti<sub>3</sub>C<sub>2</sub>, to thicker Ti<sub>4</sub>C<sub>3</sub> and Ti<sub>5</sub>C<sub>4</sub> fragments, to layered cubic TiC<sub>x</sub> films. Finally, we report on co-sintering of Ti<sub>3</sub>C<sub>2</sub>T<sub>x</sub> with ZnO using a cold sintering process at 300 °C, to achieve composites with 92–98% of the theoretical density, while avoiding oxidation or interdiffusion and showing homogeneous distribution of MXene along the ZnO grain boundaries. The electrical conductivity (1-2 orders) and the hardness (150%) show an increase with addition of 5 wt% MXene. Thus, MXene is a promising additive for reinforced ceramic composites.

**3:50 PM - WITHDRAWN**

#### **(PACC-S3-005-2022) Superductile hardmetals and tools based on these materials under ultrahigh isostatic pressure**

V. Brazhkin\*<sup>1</sup>

1. Institute for High Pressure Physics RAS, Russian Federation

This work was designed to study compressibility behavior of nanopowders of various materials under ultrahigh cold isostatic pressing (CIP) in pure hydrostatic conditions. The results indicate that creation of hardmetals for large-size tools by high-pressure

consolidation of nanoparticles is not a very promising approach. An alternative technique for producing hardmetals with the disperse substructure of carbide grains at ultrahigh (CIP) in pure hydrostatic conditions has been developed. The new hardmetals thus obtained have dual properties of high strength and unique superductility under compression. The large-size tools based on these alloys have commercially demonstrated a record-breaking impact resistance an order of magnitude higher than that of the currently available standard hardmetals tools.

#### 4:10 PM

##### (PACC-S3-006-2022) Processing of High Entropy Metal Carbides: A New Class of Ultrahigh Temperature, Irradiation Resistant Ceramics

V. Vakharia<sup>1</sup>; L. Zhang<sup>1</sup>; E. Rodas-Lima<sup>1</sup>; C. Park<sup>2</sup>; E. Torresani<sup>2</sup>; E. Olevisky<sup>2</sup>; O. A. Graeve<sup>1</sup>

1. University of California, San Diego, Mechanical and Aerospace Engineering, USA
2. San Diego State University, College of Engineering, USA

We have implemented a solvothermal synthesis process to synthesize high entropy metal carbides of Mo-Nb-Ta-V-W. The synthesis process is appealing because the reaction occurs at a high temperature (upwards of 2000°C), which allows the carbides to undergo reaction-driven alloying and form single phase solutions of nanopowders without the need for later thermal treatments. Our full single-phase nanopowders can also allow full densification to occur at lower sintering temperature (near 1600°C), creating a finer grain size distribution. The solvothermal synthesis technique consists of mixing metal chlorides and carbon powder in the presence of molten lithium. We have produced binary, ternary, quaternary, quinary, and senary metal carbides through systematic manipulation of elemental composition, resulting in solid solutions of (Nb-Ta)C, (Nb-Ta-W)C, and (Mo-Nb-Ta-W)C, determined from X-ray diffraction (XRD) and energy dispersive spectroscopy (EDS). Rietveld refinement was used to deconvolute the XRD data and confirm the phase compositions of the different carbides to reestablish precursor amounts and optimize the solid solution powders. Then, through a spark plasma sintering process, dense samples of compositionally complex ceramics have been produced.

## PACC6: Refractories in The Americas

### Refractories

Room: Mirage (Level B)

Session Chair: Dana Goski, Allied Mineral Products

#### 1:30 PM

##### (PACC-S6-001-2022) Recycling of spent catalysts from Fluid Catalytic Cracking (FCC) as refractory feedstock (Invited)

L. Alcaraz<sup>1,2</sup>, E. Retsrepo<sup>1,3</sup>, F. Lopez<sup>2</sup>, F. Vargas<sup>3</sup>, Baudin<sup>\*1</sup>,

1. Instituto de Cerámica y Vidrio, CSIC, Ceramics, Spain
2. Centro Nacional de Investigaciones Metalúrgicas (CENIM-CSIC), Spain
3. Universidad de Antioquia, GIPMME-GIMACYR, Colombia

In the last fifty years, the significant expansion of the industrial, commercial and agricultural sectors was accompanied by a huge increase in the production of petrochemical products and intermediates, as well as refined fuels like gasoline, diesel fuel, kerosene, jet fuel, naphtha, and gas oil. Fluid catalytic cracking (FCC) catalysts cannot be regenerated and they are fully replaced by fresh ones when their performance drops below the limits of acceptability. Apart from raw materials and energy consumption for their production, spent catalysts are mostly disposed in landfills leading to serious environmental pollution and human health problems. Most FCC catalysts consist of zeolites as active components embedded in a

silica-alumina matrix made of amorphous phases and clays. The relatively high contents of alumina and silica make the spent FCC catalysts candidates for alumina-silica refractories. Moreover, extraction of the active component lanthanum is sought due to the industrial strategic character of rare earths. In this work, the collaborative research performed on the potential of “as spent” FCC catalysts and powders obtained after La-extraction for alumina-silica refractories is presented. The work has been performed on three “as spent” catalysts with different amounts of La.

#### 2:00 PM

##### (PACC-S6-002-2022) Characterization of MgO-C bricks with different fused magnesia aggregates

E. Benavidez<sup>\*1</sup>; Y. Lagorio<sup>1</sup>

1. Universidad Tecnológica Nacional (Argentina), Metalurgia, Argentina

The influence of fused magnesia (FM) on the corrosion resistance, mechanical behavior and thermal evolution of MgO-C bricks was studied. Three qualities of electrofused magnesia were used as main raw material to form three bricks identified as A (purity 97.6 wt%), B (purity 98.2 wt%) and C (purity 98.7 wt%). Si and Al were used as antioxidants and phenolic resin was chosen as binder. Chemical resistance was evaluated through a cup test at 1600°C (2 h) using a steelmaking slag from LD converter. The mechanical evaluation was performed through compression tests at room temperature (air) and at 1400°C (argon). From the stress-strain curves different mechanical parameters were determined. Dilatometries up to 1400°C (in Ar) were performed to evaluate the thermal evolution. Microstructures were observed by optical microscopy and by SEM/EDS. The grain size of magnesia aggregates was determined. Besides, density and porosity of bricks were measured. Brick C presented a higher resistance to slag corrosion due to its highest purity and largest grain size of FM. At 1400°C, brick A presented the highest fracture strain ( $\epsilon_f$ ) and fracture energy ( $U_f$ ). Thus, the corrosion resistance increases and the fracture parameters decrease when the purity of FM grains increases.

#### 2:20 PM

##### (PACC-S6-003-2022) Lessons from Failure Analyses in Challenging Refractory Application Environments

D. Goski<sup>\*1</sup>; T. Marth<sup>1</sup>

1. Allied Mineral Products, USA

The never-ending drive for improved operational efficiency in the context of life cycle cost analysis and cradle to grave environmental stewardship are conspiring to catalyze improvements in refractory performance in a wide range of Industrial processes. Diagnosing the likely failure mechanism in order to enable process or refractory improvement recommendations can help to prevent similar events from reoccurring. A selection of representative example cases will be explored to appreciate the complex multi-variable environments of many refractory applications, with an eye toward identifying patterns of recurring contributors to failure across the varied environments. Observations will be drawn from a variety sources: laboratory testing, published literature, customized testing to simulate operating environments, and spent refractory characterization for a range of industrial applications. Alkali attack (alkali burst and/or alkali-based corrosion) is observed in many Industrial application environments, including but not limited to: hazardous waste incineration, biomass incineration, glass, cement, pulp & paper, chemical processing, petrochemical, zinc recovery. Lessons learned and unmet challenges identified will be discussed, providing the motivation for continued research and product development efforts.

### 2:40 PM

#### (PACC-S6-004-2022) The use of steelmaking slag as protection for oxidation of MgO-C refractories

M. Moline<sup>1</sup>, W. Calvo<sup>1</sup>, S. Gass<sup>1</sup>, D. Gutierrez-Campos<sup>\*3</sup>, P. Galliano<sup>2</sup>, A. G. Tomba Martínez<sup>1</sup>

1. INTEMA, División Cerámicos, Argentina
2. Universidad Nacional del Centro de la Provincia de Buenos Aires, Laboratorio de micropartículas, Argentina
3. Universidad Simón Bolívar, Departamento de Ciencia de los Materiales, Venezuela, Bolivarian Republic of

MgO-C is one of the most important refractories for steelmaking ladles. Carbon is a key component which allows the refractory to have high resistance to thermal shock and to slag attack. However, it oxidizes in air; this risk is currently found during the pre-heating of the ladle (at the beginning and between production cycles). During the operation, the liquid steel is evacuated through ladle bottom leaving a slag layer adhered to the working lining which serves as protection against oxidation of refractories' carbon. Nevertheless, this layer could suffer degradation by ambient humidity which affects its role as an oxygen diffusion barrier. This work analyzes how the refractory composition (graphite content, type of binder) and the slag degradation affect the oxidation resistance of MgO-C materials. For testing, a slag layer was generated over one of the plane surface of the refractory cylinder (25x25 mm) by treatment at 1400°C (graphite bed). Only this face was exposed to air (unidirectional test) at 1000°C (2 h). Variations in weight, depth of decarburized layer and graphite content were used as oxidation indicators. To evaluate the effect of slag weathering, tests were carried out after 2 and 10 weeks from the sample conditioning.

### 3:20 PM

#### (PACC-S6-005-2022) Structural evolution of a $Al_2O_3$ -MgO $\times$ $Al_2O_3$ castable in the range 1000-1600°C

E. Benavidez<sup>\*1</sup>; E. Brandalez<sup>1</sup>

1. Universidad Tecnológica Nacional (Argentina), Metalurgia, Argentina

Thermal and structural characteristics of an alumina-spinel castable (containing 2.5 wt.% CaO) was studied. The specimens were cast (8.0 wt.% water), cured in air at ambient temperature (48 h), then dried at 100°C (24 h) and pre-firing at 500°C (3 h). Thermal behavior was analyzed by dilatometries at constant heating rate (5°C/min) up to 1600°C, and at constant temperature (range: 1000-1500°C). Crystallographic phases were determined by XRD and microstructures were analyzed by SEM/EDS. Specimens heat treated at 1000°C and 1200°C showed  $Al_2O_3$  (A) and  $MgAl_2O_4$  (MA) as main phases. Between 1200-1300°C, the  $2Al_2O_3 \times CaO$  ( $CA_2$ ) formation is promoted. Calcium hexaluminate  $6Al_2O_3 \times CaO$  ( $CA_6$ ) is detected from 1400°C. The presence of  $CA_6$  increases at 1500°C and 1600°C. From dilatometric curve, in the range 1000-1600°C, expansion and shrinkage alternative zones were observed. This behavior is associated to (i) the  $CA_2$  and  $CA_6$  formation, and (ii) the sintering/densification of ceramic grains with probable liquid assistance. Thus, considering the temperature profile, generated in service, through this material, both the formation of  $CA_2$  and  $CA_6$  and the sintering evolution during the first hours, lead to volumetric contractions and expansions in different zones. These volumetric changes generate mechanical stresses that can cause faults in the material.

### 3:40 PM

#### (PACC-S6-006-2022) Thermochemical Stability of Refractories in Hydrogen Atmosphere

M. Mahapatra<sup>\*1</sup>; J. G. Hemrick<sup>2</sup>

1. University of Alabama at Birmingham, USA
2. Oak Ridge National Laboratory, USA

Direct reduction (DR) of iron oxide by hydrogen and use of alternative fuels such as natural gas and hydrogen in furnace have the potential to significantly decrease greenhouse gas emission

in steelmaking while remain energy-efficient and economically competitive. However, the thermochemical stability of the refractories in the furnace linings in hydrogen atmosphere is not well known. Also, the effect of  $H_2O$ , formed during the DR, on the stability of the refractories is not known. This study focuses on predicting the thermochemical stability of magnesia, spinel, chrome, and alumina and aluminosilicate refractories in  $H_2$  atmosphere (with/without  $H_2O$ ) based on minimization of Gibbs free energy of reactions approach.

## PACC7: Science and Technology of Glasses, Glass Ceramics, and Optical Materials

### Glasses, Glass-ceramics, and Optical Materials

Room: Venetian (Level B)

### 1:30 PM - WITHDRAWN

#### (PACC-S7-001-2022) Controlled Precipitation of Cesium Lead Halide Perovskite Nanocrystals in glasses and their Applications (Invited)

C. Liu<sup>\*1</sup>; Y. Ye<sup>1</sup>; Y. Hu<sup>1</sup>; Y. Zhou<sup>1</sup>

1. Wuhan University of Technology, State Key Laboratory of Silicate Materials for Architectures, China

Cesium lead halide perovskite nanocrystals have intriguing opto-electronic properties, and have promising applications in energy harvesting, information display and storage, etc. Glasses are chemically and thermally stable materials, and can serve as good host matrix for the cesium lead halide perovskite nanocrystals. Incorporation of cesium lead halide perovskite nanocrystals into glasses can significantly improve their stability and extend their applications. This work summarizes the recent progress on cesium lead halide perovskite nanocrystals embedded glasses, including controlled precipitation of these nanocrystals through thermal treatment, ion-exchange, and femtosecond laser irradiation. These controlled precipitation make it possible to achieve high photoluminescence quantum yields, tunable composition and photoluminescence spectral range, spatially controlled distribution in glasses. Potential applications of these cesium lead halide perovskite nanocrystals embedded glasses as light-emitting diodes, micro-LEDs, and solar concentrators will be demonstrated.

### 2:00 PM

#### (PACC-S7-002-2022) Practical steps toward low-CO<sub>2</sub> environment

O. Prokhorenko<sup>\*1</sup>

1. L.G.P. International, USA

During last decades low-CO<sub>2</sub> environment has become number 1 priority, which unites governments, manufacturers, scientists, and public organizations globally. Serious actions in the direction of low-emission world may save human civilization. Let's consider some examples, showing how selected R&D organization in close cooperation with industrial partners can promote low-emission material manufacturing, energy-saving applications, and, ultimately, alternative energy production. Material for wind-blade manufacturing. This particular development united several goals related to low-CO<sub>2</sub> initiative. First, W fiber glass developed by L.G.P. for and in close cooperation with 3B Fibreglass Company (Battice, Belgium) with wind blades production as the major application. Second, W-glass melting consumes much less energy per ton vs. such glasses as S-2 fiber glass that improves situation with CO<sub>2</sub> emission. Third, W-glass is cost effective material allowing to invest more resources in low-carbon initiatives. Low-Dk/Df L-glass developed by L.G.P. for AGY (Aiken, SC, USA) allowed making ultra-high frequency units, which made it easy to introduce 5G networks, and promoted faster development of many other energy-efficient communication technologies. Low melting, forming, annealing/tempering energy glasses

have become No 1 priority of L.G.P. work since early 90's moves thermal processes at glass manufacturing from energy-intensive zone to energy-saving one.

### 2:20 PM

#### (PACC-S7-003-2022) Dosimetric properties of a rare-earth ion doped CaF<sub>2</sub> translucent ceramics fabricated by spark plasma sintering method

N. Kawano<sup>\*1</sup>; D. Nakauchi<sup>2</sup>; F. Nakamura<sup>2</sup>; T. Yanagida<sup>2</sup>

1. Akita University, Japan
2. Nara Institute of Science and Technology, Japan

Dosimeters using phosphor materials have received research attention for estimation of accumulated radiation dose, energy and spatial distribution. Among the phosphor materials, CaF<sub>2</sub> with an impurity is one of the well-known phosphor materials for radiation dosimetric method because of high sensitivity and low effective atomic number. In this work, we synthesized CaF<sub>2</sub> translucent ceramics doped with a rare-earth ion by spark plasma sintering (SPS) method and investigated scintillation and dosimetric characteristics. The translucent ceramic synthesized by the SPS could show excellent dosimetric characteristics since a lot of anion vacancies responsible for thermally stimulated luminescence and optically stimulated luminescence might be formed in the translucent ceramic due to the synthesis in reducing atmosphere. A Dy-doped CaF<sub>2</sub> translucent ceramic showed scintillation peaks due to the 4f-4f transition of Dy<sup>3+</sup> and self-trapped exciton. Regarding thermally-stimulated luminescence, the translucent ceramic exhibited a high thermally-stimulated luminescence sensitivity, and the lowest detectable dose was 0.01 mGy. Furthermore, the translucent ceramic exhibited optically stimulated luminescence due to the 4f-4f transitions of Dy<sup>3+</sup> during 590 nm stimulation light, and the lowest detection limit was about 10 mGy.

### 2:40 PM

#### (PACC-S7-004-2022) Optical and Defect Properties of Large-size Gd<sub>3</sub>(Ga,Al)<sub>5</sub>O<sub>12</sub> Transparent Ceramics

S. Kurosawa<sup>\*1</sup>; H. Sone<sup>2</sup>; H. Ujiie<sup>2</sup>; A. Yamaji<sup>1</sup>

1. Tohoku University, Japan
2. Industrial Technology Institute, Miyagi Prefectural Government, Japan

Transparency is required for material search of optical materials such as laser or scintillator. From around 2010, transparent ceramic scintillators have been studied using Vacuum sintering process or/and Hot Isostatic Pressing (HIP). Spark Plasma Sintering (SPS) Process is much simpler and shorter sintering time than other methods, and we have investigated the scintillation properties for the transparent ceramics (i.e. Ce:SrHfO<sub>3</sub>, Nd:Lu<sub>2</sub>O<sub>3</sub>) prepared by the SPS process. Although such materials are attractive samples as gamma-ray scintillation materials due to good gamma-ray stopping power, preparation of single crystals (good transparent materials) are hard with good transmittance owing to high-melting temperatures. Thus, transparent ceramics have the advantage in material search for such materials. In this paper, we prepared Gd<sub>3</sub>(Ga,Al)<sub>5</sub>O<sub>12</sub>-based materials with a diameter of 20 mm by SPS process and compared the optical and scintillation properties for the same materials by the Czochralski growth and other techniques. Photo-luminescence (PL) and radio-luminescence peaks were located at around 550 nm excited by 420-nm photons, X-ray and 5.5 MeV alpha-rays, and this is the same results as the single crystal and ceramics by HIP. We also show other results such as transmittance, light output and defect analysis.

### 3:20 PM

#### (PACC-S7-005-2022) Thermoluminescence of Mg and Zn Aluminate Spinels

R. L. Conner<sup>1</sup>; L. G. Jacobsohn<sup>\*1</sup>

1. Clemson University, Materials Science and Engineering, USA

This work aims at investigating defects in selected spinels towards gaining insight on the effects of ion irradiation of these materials. MgAl<sub>2</sub>O<sub>4</sub> and ZnAl<sub>2</sub>O<sub>4</sub> powders were prepared by the co-precipitation method and calcined at 900 °C for 1 hr in air. Natural ('spinel' and gahnite) and artificial crystals were also investigated. Structural characterization was executed by X-ray diffraction and Raman spectroscopy. Radioluminescence (RL) under X-ray excitation from room temperature to 400 °C was recorded towards the identification of all luminescence centers present in the samples. Thermoluminescence (TL) spectroscopy measurements up to 400 °C were executed towards the identification of the recombination centers involved in the TL process. RL measurements revealed that both spinels presented a broad band peaked at ~400 nm attributed to antisites and Cr<sup>3+</sup> and Mn<sup>2+</sup> impurities. TL spectroscopy measurements revealed negligible contribution from the antisite band, with TL signal being originated mostly from Cr<sup>3+</sup> impurities. Analysis of the glow peak shape and behavior under different X-ray irradiation times revealed a complex behavior not described by either first or second order kinetics. This work was supported by the NASA South Carolina Space Grant 521383-RP-CM005.

### 3:40 PM - WITHDRAWN

#### (PACC-S7-006-2022) Energy traps redistribution in RE<sup>3+</sup> and Cr<sup>3+</sup> co-doped A<sub>3</sub>B<sub>2</sub>C<sub>3</sub>O<sub>12</sub>-type garnet persistent luminescence ceramics

V. Boiko<sup>1</sup>; Z. Dai<sup>2</sup>; M. Stefanski<sup>1</sup>; M. Saladino<sup>3</sup>; J. Li<sup>2</sup>; D. Hreniak<sup>\*1</sup>

1. Institute of Low Temperature and Structure Research, Division of Optical Spectroscopy, Poland
2. Shanghai Institute of Ceramics, Chinese Academy of Sciences, Transparent Ceramics Research Center, China
3. University of Palermo, STEBICEF Department, Italy

Persistent luminescence (PersL) materials are of interest both from a fundamental research point of view (trapping and de-trapping mechanisms) and from the point of view of applications in various fields such as sensorics or medicine. In particular, garnet type A<sub>3</sub>B<sub>2</sub>C<sub>3</sub>O<sub>12</sub> doped with rare earth ions and co-doped with transition metal ions is a promising material for research in this direction. Both the doping and the post-annealing treatment used in this work may lead to the formation of defects that can act as traps for electrons and holes and thus affect the duration of the afterglow. Therefore, the influence of each trap type and its redistribution on the PersL has been studied in detail both for starting powders and ceramics. Obtaining high quality ceramics from ready-made nanopowders is still a challenge, especially for Y<sub>3</sub>Al<sub>2</sub>Ga<sub>3</sub>O<sub>12</sub> (YAGG). The starting YAGG powders were synthesized by different wet-chemistry methods and crystallized below 1000 °C. In the next step, ceramics were fabricated by hot isostatic pressing. The microstructure of the starting powders and ceramics was characterized by XRD, TEM and SEM analyses. The optical properties were measured and analyzed by photoluminescence and thermoluminescence techniques. As a result, the intrinsic relationships between composition, microstructure, spectral properties and ceramic quality were determined.

4:00 PM

### (PACC-S7-007-2022) Study of the kinetics of glass dissolution in the $K_2O$ - $MgO$ - $CaO$ - $P_2O_5$ system

V. Cesarino<sup>1</sup>; D. Manzano<sup>2</sup>; E. Ferreira<sup>\*1</sup>

1. EESC, University of São Paulo, Brazil
2. São Carlos Institute of Chemistry, University of São Paulo, Brazil

Intensive agriculture contributes to the impoverishment of soils, and exogenous fertilization comes as a strategy for minerals regulation. However, conventional fertilization has low uptake efficiency by crops and other disadvantages related to rapid solubilization, washing, and weathering, leading to soil salinization and acidification, leaching of  $NH_4^+$ ,  $NO_3^-$ , and groundwater contamination. In this scenario, vitreous fertilizers emerge as an alternative to the controlled release of macronutrients and micronutrients, with great potential for crop specification. This work studied glass formation and solubility in the  $K_2O$ - $MgO$ - $CaO$ - $P_2O_5$  system as a medium for controlled nutrient release. Statistical planning was carried out, and we show the preliminary results for the composition 60 $P_2O_5$ .4 $MgO$ .16 $K_2O$ .20 $CaO$  % by weight. Glass with this composition was obtained by melting and quenching by splat cooling. Prismatic samples were left in an aqueous citric acid solution with constant pH equal to  $2.9 \pm 0$  at  $35 \pm 1$  °C with agitation, and the mass loss was determined as a function of time. The dissolution rate was determined for samples of different sizes, which turned out to be the same. The mass loss data fitted with great precision to an exponential model whose activation energy for dissolution was determined. The studied model thus proved to be suitable for the dissolution kinetics in the search for controlled-release glasses. Our work contributes to the determination of new high-efficiency planned action fertilizers for different crops.

## PACC8: Novel, Green, and Strategic Processing and Manufacturing Technologies

### Novel, Green, and Strategic Processing I

Room: Bellagio (Level B)

Session Chair:

1:30 PM

### (PACC-S8-007-2022) Low temperature in situ modification of silicon (carboxy)nitride ceramics by earth-abundant transition metals as promising (electro)catalysts displaying high specific surface areas for clean hydrogen production (Invited)

M. Mallmann<sup>1</sup>; R. Morais Ferreira<sup>1</sup>; R. Nishihara<sup>1</sup>; Y. Iwamoto<sup>3</sup>; R. Machado<sup>4</sup>; S. Celerier<sup>2</sup>; A. Habrioux<sup>2</sup>; S. Bernard<sup>\*1</sup>

1. CNRS, IRCER, France
2. Institut de Chimie des Milieux et Matériaux de Poitiers IC2MP UMR7285, France
3. Nagoya Institute of Technology, Japan
4. Federal University of Santa Catarina, Brazil

Technologies exploiting sustainable energy resources such as solar and wind have been the first step towards a CO<sub>2</sub> and nuclear waste free energy future resulting in a recent decline of pollutant emissions in Europe. Dihydrogen (H<sub>2</sub>) has the potential to achieve the second step and to enable transition to a clean, low-carbon energy system in line with the Paris agreement. It can be produced from lightweight inorganic hydrides by hydrolysis or by water electrolysis through hydrogen evolution reactions (HER) and oxygen evolution reactions (OER) that would be among the most efficient, environmentally friendly and decarbonized routes to H<sub>2</sub>. In both cases, significant advances have to be made in the efficiency of catalysts and electrocatalysts working in alkaline media. Some non-noble transition metal (TM)-based catalysts and electrocatalysts are highly efficient for hydride hydrolysis such as sodium borohydrides as well as for both HER and OER. In this talk, we will present our last results on the development of a precursor approach toward the design of silicon (carboxy)nitride-based ceramics in-situ modified by transition metals acting both as support and catalyst to boost the hydrolysis of sodium borohydride and the electrocatalytic OER performances.

2:00 PM

### (PACC-S8-002-2022) 2D Nanosheet Architectonics for Hybrid Manufacturing (Invited)

M. Osada<sup>\*1</sup>

1. Nagoya University, IMASS, Japan

Two-dimensional (2D) nanosheets, which possess atomic or molecular thickness, have been emerging as important new materials due to their unique properties. In this talk, we review the progress made in the synthesis, assembly, and properties of 2D oxide nanosheets, highlighting hybrid manufacturing. A variety of 2D oxide nanosheets were synthesized by delaminating appropriate layered precursors into their molecular single sheets via soft-chemical process. These oxide nanosheets have distinct differences and advantages compared with graphene because of their potential to be used as insulators, semiconductors, and even conductors, depending on their composition and structures. An attractive aspect is that 2D oxide nanosheets can be organized into various nanoarchitectures by applying solution-based assembly. We utilized oxide nanosheets as building blocks in the LEGO-like assembly, and successfully developed various functional nanodevices such as FETs, capacitors, artificial ferroelectrics, Li-ion batteries/solar cells, actuator crystals, etc. Our work is a proof-of-concept, showing that new hybrid materials/devices can be made from nanosheet architectonics.

2:30 PM

### (PACC-S8-003-2022) Development of Aqueous Gel-casting Forming Techniques for Novel Spinel Transparent Ceramics (Invited)

H. Wang<sup>\*1</sup>; X. Zong<sup>1</sup>; H. Zhang<sup>1</sup>; Z. Liu<sup>1</sup>; L. Ren<sup>1</sup>; B. Tu<sup>2</sup>; W. Wang<sup>1</sup>; Z. Fu<sup>2</sup>

1. Wuhan University of Technology, China
2. Wuhan University of Technology, State Key Lab of Advanced Technology for Materials Synthesis and Processing, China

Spinel transparent ceramics with disorder solid solution structure, e.g. aluminum oxynitride ( $\gamma$ -AlON), magnesium aluminate ( $MgO \cdot nAl_2O_3$ ), and magnesium aluminum oxynitride ( $MgAlON$ ), have already been regarded as important candidates for sapphire, due to their outstanding optical and mechanical properties. In order to fit the increasing requirements in various application fields, components with large sizes and complex shapes are highly demanded. In this work, some transparent ceramics have been prepared through aqueous gel-casting forming technique. The effects of pH value, dispersant, ball-milling time and solid loading on the rheological behavior of slurries were investigated. The influences of monomer concentration, MAM/MBAM ratio and solid volume fraction on the bending strength and relative density of green bodies were studied. Finally, slurries with high solid loading (>50vol%) and low viscosity (<500mPa·s) were prepared through all above optimized parameters. After casting and calcining, the obtained samples were densified by pressureless sintering and further hot isostatic pressing. The sintered transparent ceramics showed high in-line optical transmittance. The microstructure and properties of sintered transparent ceramics were investigated.

3:20 PM

### (PACC-S8-004-2022) Thermochromic and Photocatalytic Activities of Anion Doped-VO<sub>2</sub>/Nb-TiO<sub>2</sub> Multifunctional Coating Films (Invited)

S. Yin<sup>\*1</sup>; A. Riapanitra<sup>1</sup>; T. Hasegawa<sup>1</sup>

1. IMRAM, Tohoku University, Japan

Multifunctional composites consisting of anion doped-vanadium dioxide (A-VO<sub>2</sub>) and niobium-doped TiO<sub>2</sub> (NTO) were prepared by a simple physical mixing process. The composites exhibit higher thermochromic activity and nitrogen monoxide decomposition activity than those of pristine A-VO<sub>2</sub>/NTO. Both components were synthesized by an environmentally friendly solvothermal process. The NTO nanoparticles showed controllable particle size via solvothermal synthesized with different ethanol to acetic acid

ratios. The A-VO<sub>2</sub>/NTO showed better multifunctionality of thermochromic and photocatalytic activities, compared to that of non-doping VO<sub>2</sub>/NTO samples. In addition, the coexistence coating films of A-VO<sub>2</sub>/NTO showed better results in thermochromic and deNO<sub>x</sub> activity compared to that with double-sided structure. The best thermochromic and photocatalytic activities could be realized by fluorine doping, i.e. F-VO<sub>2</sub>/NTO composite showed such high thermochromic properties as  $\Delta T_{1500\text{nm}}$  up to 29.5 % and deNO<sub>x</sub> activity up to 40% at  $\lambda > 290$  nm under mercury lamp irradiation. The effect of different anion doping was also investigated in detail. The A-VO<sub>2</sub>/NTO composite coating films showed great potential for the application as multifunctional materials.

### 3:50 PM

#### (PACC-S8-005-2022) Development of the Flexible Ceramics Films and Remanufacturing Process (Invited)

T. Tsuchiya\*<sup>1</sup>; T. Nakajima<sup>1</sup>; Y. Kitanaka<sup>1</sup>; I. Yamaguchi<sup>1</sup>; J. Nomoto<sup>1</sup>; Y. Uzawa<sup>1</sup>

1. National Institute of Advanced Industrial Science and Technology (AIST), Advanced Manufacturing Research Institute, Japan

To construct low carbon society more and more in the world, it is necessary to develop a high performances new green device such as a solar cell, a lithium battery, a power semiconductor, and light emitting diode (LED) lighting, superconducting device and so on. In addition, for the development of IoT society, flexible device and sensor is necessary. For these purposes, we have developed the photo-induced chemical solution process such as excimer laser-assisted metal organic deposition (ELAMOD) and photo reaction of nano-particle (PRNP), and photo reaction of hybrid solution (PRHS) for the preparation of the patterned metal oxide thin film on organic, glass and single crystalline substrates. In addition, In the future, it will be indispensable to build an innovative resource recycling cycle for electronic materials and components used in various products such as solar cell panels, organic EL displays, smartphones, and lighting. Therefore, for this aim, for the construction of low-carbon society, it is essential to build a circular manufacturing with low environmental load. In this presentation, we demonstrate a preparation of epitaxial and flexible ceramics for the optical and electrical applications such as sensor, SiC power device, fuel cell and OLED and new recycling system for the components.

### 4:20 PM

#### (PACC-S8-006-2022) Electrolysis for low-carbon hydrogen production: Status, progress and industrial challenges (Invited)

J. Wiff\*<sup>1</sup>

1. Air Liquide, Materials Science, Japan

Nowadays we are facing key transformations in the global energy system, triggering multiple challenges and opportunities. Low-carbon hydrogen is at the heart of the energy transition by decarbonizing the energy production and reducing the carbon footprint of relevant chemical processes such as fertilizers, steel production, e-fuels, etc. Air Liquide, as a leader in the gas industry, is taking part of this challenge by promoting electrolysis as a suitable route for low-carbon hydrogen production. Such as the 20 MW Polymer Exchange Membrane Electrolyzer (PEMEC) production unit installed in Becancour Canada, capable of producing up to 8.2 tonnes per day of low-carbon hydrogen for industrial and mobility uses and avoiding the emission of 27,000 ton of CO<sub>2</sub> per year. Nonetheless, the successful deployment of low-carbon electrolyzer units depends strongly on the associated cost (CAPEX and OPEX) and also from the adequate development of the entire value chain. This work presents an overview of the global electrolysis technologies operating at low or high temperature, focusing on their current status, industrial opportunities and challenges along the value chain.

## Ferroelectrics Meeting of Americas

### Theory and Ferroic Fundamentals

Room: Star Bay 3 (Level B)

Session Chair: Avadh Saxena, Los Alamos National Lab

#### 1:30 PM

#### (FMAs-001-2022) Modulated lattice fluctuations in the vicinity of a ferroelectric quantum critical point (Invited)

G. G. Guzman-Verri\*<sup>1</sup>; C. H. Liang<sup>2</sup>; P. Littlewood<sup>2</sup>

1. University Costa Rica, Physics, Costa Rica
2. Chicago, Physics, USA

In this talk, we present a phenomenology of a ferroelectric phase transition whose primary order parameter (electrical polarization) is coupled to gradients of elastic strain (flexoelectricity). At the harmonic level, it is known that such couplings produce a hybridization of acoustic and optic phonon modes and can lead to phases with modulated lattice structures that precede the symmetry broken state due to level repulsion. Here, we show that at the mean field plus Gaussian approximation, the fluctuations of polarization of the parent phase tend to diverge at the onset of the transition and therefore the modulated phase is avoided. We discuss the implications of this for the perovskites KTaO<sub>3</sub> and SrTiO<sub>3</sub>, which are usually considered standard quantum paraelectrics.

#### 2:00 PM

#### (FMAs-002-2022) First principles studies on the structural and ferroic properties of BiFeO<sub>3</sub> based compositions (Invited)

I. B. Catellani<sup>1</sup>; O. G. Oliveira<sup>1</sup>; G. Perin<sup>1</sup>; G. S. Dias<sup>1</sup>; I. A. Santos<sup>1</sup>; L. F. Cótica\*<sup>1</sup>

1. State University of Maringa, Department of Physics, Brazil

During the last decades, attention has been devoted to the investigation of perovskite-type crystals that have multiferroic properties due to their applications in multifunctional devices. BiFeO<sub>3</sub> is one of the most studied magnetoelectric multiferroics, as it presents ferroelectric and magnetic orders above room temperature. It makes this material a candidate for multifunctional devices. There are drawbacks that makes difficult the practical applications of these materials, which are the low resistivity and the high coercive field. One of the approaches to improve the ferroelectric properties is the solid solutions of BiFeO<sub>3</sub> with other ferroelectrics. In this work we studied BiFeO<sub>3</sub> and the (0.6)BiFeO<sub>3</sub>-(0.4)PbTiO<sub>3</sub> solid solution. These combination is expected to have improved ferroelectric and magnetic properties when compared with BiFeO<sub>3</sub>. In this sense, density functional theory (DFT) calculations as implemented in the OpenMx software were performed. The Hubbard correction was used to obtain structural and electronic properties. The behavior of the structural, electrical and magnetic properties of the studied compositions were obtained and compared. Finally, analyzes of the electron densities were carried out, giving some insights on the origin of ferroelectricity in these materials, mainly showing electronic and structural distortions caused by lone pairs.

#### 2:30 PM

#### (FMAs-003-2022) Rydberg Sensors and Machine Learning Assisted Design Discovery

M. Trippy\*<sup>1</sup>; R. Guo<sup>1</sup>; A. S. Bhalla<sup>1</sup>

1. University of Texas, San Antonio, USA

Recent developments in Machine Learning (ML) models that purport to automate material discovery are explored, with a treatment of the logical extension of this work that we have defined as "Design Discovery". The definition of a sufficient feature set to establish an ML model requires the quantum mechanical description of

electrical and magnetic interactions that contrast Stark effects from Rydberg states, as well as other forces within the atom. This provides a feature rich environment from the standpoint of predictive design using Machine Learning models. The paper concludes with a theoretical treatment of a Rydberg sensor and its potential sensitivity to measurement of extremely small electromagnetic phenomena, with an initial treatment of potential variations of existing experiments that can be “discovered” from an appropriately defined ML design discovery model.

**2:50 PM**

### (FMAs-004-2022) Geometrical Polarization Approach

V. F. Freitas<sup>\*1</sup>; J. A. Eiras<sup>3</sup>; L. F. Cótica<sup>2</sup>; I. A. Santos<sup>2</sup>

1. Universidade Estadual do Centro-Oeste - Unicentro, Physics, Brazil
2. State University of Maringa, Physics, Brazil
3. Universidade Federal de São Carlos - UFSCAR, Physics, Brazil

The geometric polarization approach (GPA) was developed to obtain the nature of a polar unit cell structure in displacive ferroelectric and non-ferroelectric materials using a classical electric dipole calculation protocol. It is an interesting tool to identify whether a given material has a polar nature and to quantify the intensity of this polarization, as if it were ferroelectricity. The main advantage is being able to analyze the material polarization from X-ray diffraction data in materials still in the powder state, which is the first stage of development of any material. In this sense, the atomic positions and lattice parameters are obtained through Rietveld refinement and associated with the ionic nominal valences in a protocol to obtain the polarization of the material. This protocol was applied to known ferroelectric materials, with different structural symmetries, and the polarization obtained was in agreement with measurable experimental values. In fact, the results obtained from the GPA for BaTiO<sub>3</sub> at different temperatures and different structural symmetries were compared with experimental polarization measurements obtained from single crystals of BaTiO<sub>3</sub> and the results indicated very similar behaviors.

**3:30 PM**

### (FMAs-005-2022) Rich behaviour of oxygen vacancies in SrTiO<sub>3</sub> (Invited)

A. Lopez-Bezanilla<sup>\*1</sup>; P. Littlewood<sup>2</sup>

1. Los Alamos National Lab, USA
2. Chicago, Physics, USA

Titanate ceramics are widely used electronic materials that show a very rich behavior in the presence of oxygen vacancies. We report new findings in the electronic structure and magnetism of oxygen vacancies in SrTiO<sub>3</sub>. By means of first-principles calculations we show that the appearance of magnetism is not determined solely by the presence of a single-oxygen vacancy but by the density of free carriers and the relative proximity of the vacant sites. While an isolated O vacancy behaves as a non-magnetic double donor, manipulation of the doping conditions allows the stability of a single donor state with emergent local moments. Strong local lattice distortions enhance the binding of this state. Consequently we find that the free-carrier density and strain are fundamental components to obtaining trapped spin-polarized electrons in oxygen-deficient SrTiO<sub>3</sub>, which may have important implications in the design of switchable magneto-optic devices.

**4:00 PM**

### (FMAs-006-2022) Fast acquisition XRD used to understand elastic transition in lead calcium titanate ceramics

F. R. Estrada<sup>\*1</sup>; A. Moreno Gobbi<sup>3</sup>; D. Garcia<sup>2</sup>

1. Brazilian Center for Research in Energy and Materials, Brazilian Synchrotron Light Laboratory, Brazil
2. Federal University of São Carlos, Physics Department, Brazil
3. University of the Republic, Department of Applied Physics and Materials, Uruguay

In classical displacive ferroelectric PbTiO<sub>3</sub>-based materials, a symmetry transformation is expected with each ferroelectric phase transition. The room temperature symmetry of such a compound was determined as orthorhombic with octahedral tilting and deformation Pna2<sub>1</sub>. Such determination was carried out using EXPO and considering the high quality of the fast synchrotron X Ray Diffraction (XRD) pattern in Debye-Scherrer geometry. This space group agrees with the results obtained from convergent beam electron diffraction analysis using TEM. In this work, we measured the ultrasonic velocity and attenuation anomalies as a function of the temperature of the compound Pb<sub>0.55</sub>Ca<sub>0.45</sub>TiO<sub>3</sub> from 100K up to room temperature. To understand such an elastic anomaly related to the ferro-ferroelectric phase transition at 150K, synchrotron XRD patterns were measured at the same temperature range. As a result of the temperature dependence microstrain and lattice parameters, an anomaly has been observed but no symmetry transition has been observed. Therefore, we are going to discuss here the importance of the high resolution and fast XRD to understand the elastic transition phenomena as a function of temperature, spatially in lead titanate-based materials. The authors are grateful to CAPES, FAPESP and CNPq Brazilian funding agencies for financial support, and the Brazilian Synchrotron LNLS to the support.

**4:20 PM**

### (FMAs-007-2022) Nanoscale Engineering of Barium Titanate Using Aluminium (III) – Tantalum (V) Dipole Pairs

S. Nudd<sup>\*1</sup>; V. Pellegrino<sup>2</sup>; K. Ning<sup>3</sup>; S. Tidrow<sup>2</sup>

1. Alfred University, New York State College of Ceramics, USA
2. Alfred University, USA
3. Alfred University, New York State College of Ceramics, School of Engineering, USA

BaTiO<sub>3</sub> is a popular material of choice for ceramic capacitors and other electro-ceramic technologies. Using the Clausius-Mossotti relation as a basis, it's known that phase transitions in the BaTiO<sub>3</sub> structure can be induced by polarizability. Polarization and polarizability can be introduced to the perovskite structure through dipole substitutions using the method called electric-field dipole engineering at the nanoscale (*E*-DENS). By substituting dipole pairs Al<sup>3+</sup> and Ta<sup>5+</sup> for Ti<sup>4+</sup> - Ti<sup>4+</sup> in the BaTiO<sub>3</sub> structure, localized electric fields can be introduced to decrease atom polarizability per molar volume while producing strong local dipole field. The newly formed materials are anticipated to behave similar to previously reported *E*-DENS materials, where dipole pairs Ga<sup>3+</sup> - Ta<sup>5+</sup>, transformed BaTiO<sub>3</sub> from ferroelectric to diffuse phase to relaxor-like material within a solid solution range 0.0000 ≤ x ≤ 0.0500. To further investigate the interaction that *E*-DENS plays with regard to changes in material properties, compositions of Ba(Al<sup>3+</sup>,Ta<sup>5+</sup>)Ti<sub>1-2x</sub>O<sub>3</sub> with x equal to 0.0000, 0.0025, 0.0050, 0.0075, 0.0100, 0.0250 have been prepared, characterized and properties are reported.

4:40 PM

**(FMAs-008-2022) Dipole Engineering at the Nanoscale: Experimental Data and Theory**K. Ning\*<sup>1</sup>; H. Shulman<sup>1</sup>; W. A. Schulze<sup>1</sup>; S. Tidrow<sup>1</sup>

1. Alfred University, New York State College of Ceramics, School of Engineering, USA

Material properties depend upon the atoms utilized and their positions in space with respect to time. The extendable new simple material model (NSMM), discussed elsewhere, has been shown to provide temperature dependent lattice structure, lattice constant, relative permittivity, etc. of “simple” and “simply mixed” perovskites. Building upon the NSMM model, dilute dipole engineering at the nanoscale has been used to control local electric-field of materials and has resulted in dielectric materials evolving from strict ferroelectric to diffuse phase transition to relaxor-like and perhaps even strict relaxor properties depending upon the concentration and strength of the introduced engineered dipoles. In this presentation, experimental data and theory are discussed in terms of how dipole engineering at the nanoscale can be used to increase material resistivity, breakdown field strength, and overall energy product. A quick review of semi-conductor theory, including activation energy and bandgap, will be covered as an introduction to a modified model that can be used to understand experimental results of dipole engineering at the nanoscale of dielectrics, including enhanced resistivity and electric-field breakdown strength.

**PACC Poster Session**

Room: Star Bay 1/2

5:30 PM

**(PACC-P001-2022) Composite materials development from ceramics from primary battery waste**S. Restrepo Tobón\*<sup>1</sup>; H. A. Colorado L.<sup>1</sup>

1. Universidad de Antioquia, Colombia

Battery waste is a worldwide problem due to the increase in battery consumption and in the nature of the materials involved, typically classified as hazardous. Particularly the primary battery waste is a major issue in many developing countries as most of the batteries consumed are from this type for reasons including their lower costs and the available local industry of this batteries. Normally these batteries are disposed in landfills, contrary to all recommendations of recycling or a circular economy. Primary battery waste is mostly constituted for some materials easy to separate and recycle such as metal, plastic, and paper; and others more difficult to process, ceramics powders, mostly graphite, zinc oxides, and manganese oxides. This research focusses in finding alternative uses for these ceramic powders, in combination with polymer matrix. Several formulations have been fabricated, and their corresponding materials characterization has been conducted. Results show alternative composites, with potential applications as electronics and structural materials.

**(PACC-P002-2022) Influence of ZrO<sub>2</sub> addition on dielectric and piezoelectric properties of (Bi<sub>0.5</sub>Na<sub>0.5</sub>)TiO<sub>3</sub>-BaTiO<sub>3</sub> lead-free piezoceramics**M. C. Difeo\*<sup>1</sup>; L. Ramajo<sup>1</sup>; M. Castro<sup>1</sup>

1. INTEMA, Ceramics, Argentina

Piezoelectric materials based on lead zirconate titanate (PZT) are widely used in many electronic devices due to their excellent electrical properties. However, the European Union (EU) legislation restricts the use of hazardous substances and encouraged a strong effort, into the science and technology of lead-free piezoceramics, for the development of piezoelectric lead-free compositions. Bismuth sodium titanates are one of the most studied lead-free piezoceramics

families. However, the high coercive field ( $E_c \sim 73$  kV/cm), in addition to the relatively high leakage currents, hinders the complete polarization of these ceramics. Therefore, to solve the main drawbacks presented by the BNT composition, (Bi<sub>0.5</sub>Na<sub>0.5</sub>)TiO<sub>3</sub>-BaTiO<sub>3</sub> (BNT-BT) solid solutions were studied. These ceramics present a polymorphic phase transition where good piezoelectric properties are obtained and, consequently, are considered as promising candidates to replace lead-based piezoelectric materials and can also be modified by the incorporation of additives for specific applications. Taking into account the previous results reported by other researchers, different amounts of ZrO<sub>2</sub> (x = 0.0, 0.5, 1.0, 2.0 mol%) were added to the 0.94(Bi<sub>0.5</sub>Na<sub>0.5</sub>)TiO<sub>3</sub>-0.06BaTiO<sub>3</sub> polymorphic phase boundary composition synthesized by the solid-state method. Samples were sintered at 1150 °C and structural, microstructural and functionally characterized.

**(PACC-P003-2022) Modeling by Finite Element Method of an Ultrasonic Lead Free Piezoelectric Actuator**F. Gibbs<sup>1</sup>; L. Ramajo<sup>1</sup>; F. Rubio-Marcos<sup>3</sup>; M. Castro<sup>1</sup>; M. C. Difeo\*<sup>1</sup>; F. Cavallieri<sup>2</sup>

1. INTEMA, Ceramics, Argentina

2. CIMET, Ceramics, Argentina

3. Electroceramic Department, Ceramica y vidrio, Ecuador

The industry has shown interest in ultrasonic piezoelectric actuators and ultrasonic drives. Piezoelectric ultrasonic actuators make possible systems that are of simple design and are thus finding wider and wider application in micropositioning systems. Especially advantageous and cost-efficient systems can be made with ultrasonic actuators having a rectangular piezoceramic plate as a resonator and using eigenmodes associated with that shape. In this way, the most widely used piezoelectric ceramic is lead-zirconate-titanate (PZT). However, the growing awareness of environmental and health issues, related to the toxic emissions of PbO from PZT-based products, has triggered widespread scientific interest in developing novel efficient lead-free alternatives. Three main groups of lead-free perovskite ferroelectric oxides have henceforth been considered as environment-friendly alternatives to PZT piezoceramics. These include sodium-potassium niobate, sodium bismuth titanate, and modified barium titanate. Nevertheless, it is well known that excellent electro-deformation characteristics can be obtained using a piezoelectric material based on (K<sub>0.44</sub>Na<sub>0.52</sub>Li<sub>0.04</sub>)(Nb<sub>0.86</sub>Ta<sub>0.1</sub>Sb<sub>0.04</sub>) (KNL-NTS). In this work, the ultrasonic response of a KNL-NTS based piezoceramic resonator, synthesized by the solid-reaction method, was modeled by the Finite Element Method (FEM). The vibration mode and resonance frequency of the device were determined.

**(PACC-P004-2022) Platinum-Based Ordered PtFeCo Ternary Alloy Electrocatalyst for Oxygen Reduction Reaction**M. Lokanathan\*<sup>1</sup>; R. V. Mangalaraja<sup>1</sup>; A. swamy<sup>2</sup>; C. Mercy<sup>2</sup>; S. Shaji<sup>6</sup>;R. Aepuru<sup>5</sup>; R. Udayabhaskar<sup>4</sup>; M. Gracia-Pinilla<sup>3</sup>

1. Universidad Adolfo Ibáñez, Chile

2. SRM Institute of Science and Technology, Department of Chemistry, India

3. Universidad Autónoma de Nuevo León, Facultad de Ciencias Físico-Matemáticas, Mexico

4. Institute of Scientific and Technological Research, Hybrid Nanomaterials Laboratory, Chile

5. Universidad Tecnológica Metropolitana, Departamento de Mecánica, Chile

6. Autonomous University of Nuevo León, Faculty of Mechanical and Electrical Engineering, Mexico

The improved sluggish kinetics of electro reduction of oxygen (ORR) at the cathode of the polymer electrolyte membrane fuel cells (PEMFCs) was attained through PtFeCo ternary alloy electrocatalytic-nanoparticles on the high surface area carbon support prepared through high polarized ionic pool (molten) condition. The formation of majority nanoparticles with the size of 7 nm with fct structure was confirmed by the transmission electron microscopy (TEM) and the presence of super lattice peaks in the X-ray



diffraction (XRD) pattern, respectively. The scanning electron microscopy (SEM), energy dispersive spectrometry (EDS) and elemental mapping confirmed the presence of all elements in the nanoparticles. The X-ray photoelectron spectroscopy revealed that the existence of Pt, Fe and Co on the surface of the electrocatalytic-nanoparticles. Further, the electrochemical measurements revealed that the PtFeCo/C ternary alloy nanoparticles expressed  $1.2 \text{ Amg}_{\text{Pt}}^{-1}$ ,  $2.8 \text{ mAcm}^{-2}$  of mass and specific activity, respectively. These were 8 and 14 times higher mass and specific activity than the commercial Pt/C. Finally, the stability test showed that even after 30,000 potential cycles the PtFeCo/C nanoparticles retained its initial activity which confirmed the highly stable nature of the PtFeCo/C ternary alloy electrocatalyst.

### (PACC-P005-2022) Thermoelectric in a kitchen heat and smoke extractor

O. F. Posada Henao<sup>\*1</sup>; H. A. Colorado L.<sup>1</sup>

1. Universidad de Antioquia, Colombia

The growing energy demand requires new forms of extraction, recovery, and use of energy. This article presents thermoelectric cells applied to kitchen heat and smoke extractors, which reach temperatures up to  $100^\circ\text{C}$  due to cooking gases, with contribution of convection and radiation heat sources. Two different heat sources were considered, using water and oil for cooking. A high potential was found for the generation and use of heat on a small scale that contributes to circular economy in the food industry. This work was conducted during the pandemic closedowns, for students at home, thereby showing a new way for teaching and learning in a practical course.

### (PACC-P006-2022) Evaluation of recyclable thermoplastics for the manufacturing of wind turbines blades H-Darrieus

A. F. Olivera Castillo<sup>\*1</sup>; H. A. Colorado L.<sup>2</sup>; E. chica<sup>2</sup>

1. Universidad de Antioquia, engineering, Colombia

2. Universidad de Antioquia, Colombia

Wind energy is one of the most important clean energy sources. However, the manufacturing of the blades requires a rethinking considering circular economy concepts, moreover, the blades can hold solid wastes from other processes. However, the most direct adverse environmental effect is in the dismantling of the turbines wind power since thermoset materials are the most typical material for the blades. Thus, this research seeks to evaluate 4 types of thermoplastic materials (PLA, PLA with carbon fiber, PETG, PETG with carbon fiber) manufactured in a 3D printer, which were compared via mechanical, thermal, and UV exposure tests. The material that meets the best conditions will be the one used to manufacture the blades of an H-Darrieus wind turbine on a laboratory scale. The power curve will be evaluated and will be compared with a turbine manufactured with conventional materials (Epoxy and carbon fiber).

### (PACC-P007-2022) Heat recovery from waste management using thermoelectrics

H. Rebellón<sup>\*1</sup>; H. A. Colorado L.<sup>1</sup>

1. Universidad de Antioquia, Colombia

There is a continuous search of materials and methods for new and more efficient ways to save and recover the wasted heat. In all these possibilities, thermoelectrics generators can solve directly the energy waste problem. Their compact design and low maintenance are well-known advantages. However, these systems have still limitations, being their relatively low efficiency perhaps the most significant. This article reviews the thermoelectrics generators as a solution for recovering the wasted head coming from waste management, from municipal and repository sites, and biomass.

### (PACC-P008-2022) Electrochemical Characteristics of MXene/Fe<sub>3</sub>O<sub>4</sub> Composites for Electrochemical Supercapacitor Applications

A. Thirumurugan<sup>\*1</sup>; U. Rednam<sup>2</sup>; M. Morel Escobar<sup>2</sup>

1. University of ATACAMA, Sede vallenar, Chile

2. University of ATACAMA, Chile

Hybrid magnetic RGO/MXene/Fe<sub>3</sub>O<sub>4</sub> nanocomposites were developed by the chemical oxidation method without any impurities by using an optimized experimental parameters. The grain size of bare Fe<sub>3</sub>O<sub>4</sub> was found as 43 nm and it was reduced to 30 nm when it is prepared with MXene. The saturation magnetization of bare Fe<sub>3</sub>O<sub>4</sub> was observed as 89 emu/g, it was decreased to 70 emu/g for MXene nanocomposite. The reduction in the saturation magnetization is obvious due to the nonmagnetic fraction of MXene within the composite. FESEM micrograph was confirmed the sheet-like morphology of MXene and the decoration of Fe<sub>3</sub>O<sub>4</sub> was observed on the MXene layer. The developed hybrid magnetic nanocomposite was used as a negative electrode material for supercapacitor applications. The electrochemical characteristics of the magnetic nanocomposite were studied by cyclic voltammetry and galvanostatic charge/discharge analysis. The performance of the electrodes was evaluated with different electrolytes. The detailed physical and electrochemical characteristics of the hybrid magnetic nanocomposite will be discussed in detail.

### (PACC-P009-2022) Tape-casting technique enabled continuous processing of ceramic silicate-based Na<sup>+</sup> superionic conductors

A. Yang<sup>\*1</sup>; R. Ye<sup>1</sup>; Q. Ma<sup>1</sup>; F. Tietz<sup>1</sup>; O. Guillon<sup>1</sup> **WITHDRAWN**

1. Forschungszentrum Julich GmbH, IEK-1, Germany

All-solid-state sodium batteries (ASSNBs), which combine the benefits of high safety and low cost, are expected to be an alternative or complementary storage technology to lithium ion batteries. Herein, we developed an aqueous tape casting technique for the continuous fabrication of ceramic sheets made of silicate-based Na<sub>3</sub>YSi<sub>4</sub>O<sub>12</sub> (NYS) Na<sup>+</sup> ion superionic conductor for the first time. After sintering, the ceramics showed a total conductivity of  $1.0 \text{ mS cm}^{-1}$  at room-temperature, low total activation energy of 0.30 eV, and wide electrochemical window of over 8 V. The critical current density of NYS tape against Na-metal electrodes can reach  $2.2 \text{ mA cm}^{-2}$  and the galvanostatic cycling time is over 280 h under the current density of  $0.8 \text{ mA cm}^{-2}$  and capacity of  $0.8 \text{ mAh cm}^{-2}$ . The obtained tape has high crystalline purity, dense microstructure, favorable mechanical properties (hardness H of 2 GPa and elastic modulus E of 45 GPa). This work not only highlights the potential of the scarcely studied silicate-based NYS ionic conductor as a functional separator, but also presents a cost-efficient and eco-friendly continuous fabrication using the aqueous tape casting technique, thus being expected to boost the practical application of NYS as solid-state electrolyte in ASSNBs. A further step towards ASSNBs with NYS tape is also on the way.

### (PACC-P011-2022) Electrochemical storage capability of flexible SiOC ceramic electrodes

S. Mujib<sup>\*1</sup>; G. Singh<sup>1</sup>

1. Kansas State University, Mechanical & Nuclear Engineering, USA

Within this work, three little known polymer-derived ceramics (PDC)-based fibers are being studied systemically as potential high-capacity electrode materials for electrochemical energy devices. We report fabrication of precursor-derived SiOC fibermats via one-step spinning from varying composition of siloxane oligomers followed by stabilization and pyrolysis at  $800^\circ\text{C}$ . Electron microscopy, Raman, FTIR, XPS, and NMR spectroscopies reveal transformation from polymer to ceramic stages of the various SiOC ceramic fibers. The ceramic samples are few microns in diameter with free carbon phase embedded in the amorphous Si-O-C structure. Free carbon phase improves the electronic conductivity

and provides major sites for ion storage, whereas Si-O-C structure contribute to high efficiency. The self-standing electrodes in lithium-ion battery half-cells delivers a charge capacity of 866 mAh g<sup>-1</sup> electrode with a high initial coulombic efficiency of 72%. As supercapacitor electrode, SiOC fibers maintain 100% capacitance over 5000 cycles at a current density of 3 A g<sup>-1</sup>.

**(PACC-P012-2022) Multifunctional Flexible Nanocomposite Based Energy Harvesters and Capacitive Pressure Sensor: Investigation of Carrier Dynamics and Performance Evaluation**

R. Aepuru<sup>1</sup>; D. Vennu<sup>2</sup>; P. Aqueque<sup>2</sup>; M. Viswanathan<sup>3</sup>

1. Universidad Tecnológica Metropolitana, Ingeniería Mecánica, Chile
2. Universidad de Concepcion, Department of Electrical Engineering, Chile
3. University of Concepcion, Materials Engineering, Chile

The demand of flexible electronic devices led the scientific community to develop novel electroactive materials for various energy harvesting and sensing devices. Especially, monitoring the human activities using integrated sensors are dedicated to non/invasive measurements such as pressure and force are seen in wide applications. Most of the sensing mechanisms are piezoresistive, piezoelectric and capacitive type. In the contest, many inorganic nanostructures have been explored to fabricate various electromechanical devices. The basic physical process involved in these devices such as charge generation, separation, and charge flow across the electrodes will be addressed. The interaction of nanostructures and their excited charge carrier dynamics, charge separation, and fast carrier mobility are presented. Mostly, inorganic nanostructures based on ZnO, perovskites and their nanocomposites with polymers are demonstrated for energy harvesters and sensors. The characterization of the nanostructures and nanocomposites are carried out through X-ray diffraction and high-resolution transmission electron microscopy (TEM) and broadband dielectric studies. The ease of fabricating the energy harvesters and capacitive pressure sensors and the polarization mechanism will be demonstrated.

**(PACC-P013-2022) Multiferroic solid solution of BaTiO<sub>3</sub>-BiFeO<sub>3</sub>; Effect of grain boundaries on dielectric and photoelectric response**

R. J. Boschilia<sup>2</sup>; R. G. Aredes<sup>1</sup>; Y. L. Ruiz<sup>1</sup>; E. Antonelli<sup>2</sup>

1. UFAM, materials engineering, Brazil
2. Unifesp, science and technology, Brazil

Multiferroic ceramics have received much attention in recent years due to the coupling of light absorption with other properties of these materials. It has been demonstrated that interfacial characteristics of polycrystalline ceramics have a significant influence on these properties. This paper reports an experimental study of micro-structural, dielectric, and photoelectric properties of (Bi<sub>0.9</sub>Ba<sub>0.1</sub>)(Fe<sub>0.9</sub>Ti<sub>0.1</sub>)O<sub>3</sub> ceramics. The crystalline structure and phase formation were investigated by X-ray diffraction and Raman spectroscopy techniques and reflect the formation of a single-phase compound. The samples were characterized by impedance spectroscopy under the domain of temperature, frequency, and light incidence. Were observed thermal-induced dielectric anomalies that are not related to any phase transition. The impedance spectroscopy analyzed in terms of equivalent circuits allows us to conclude that the responses are related to the electrical response from grain to grain-boundary dominance. We extended this methodology of characterization to explain this material's photo-response and conclude that the changes of resistivity induced by light occur principally in interfacial regions.

**(PACC-P014-2022) Microstructural and optical properties of nitrogen doped ZnO nanorod thin films fabricated by spin coating technique**

P. Thangaraj<sup>1</sup>; M. Viswanathan<sup>2</sup>; K. B<sup>3</sup>; M. Gracia Pinilla<sup>4</sup>

1. Indian Institute of Information Technology Design and Manufacturing Kurnool, Sciences, India
2. University of Concepcion, Materials Engineering, Chile
3. National Institute of Technology Tiruchirappalli, Physics, India
4. Autonomous University of Nuevo León, Physics, Mexico

ZnO NM has been utilized in various technological fields such as optoelectronics, solar cells, energy and environmental industries. The electrical conductivity and bandgap of ZnO materials can be easily tuned upon appropriate doping elements. Among various dopants, nitrogen plays a significant role to tailor the optical and electrical properties of ZnO nanostructured materials. The present work reports the successful fabrication of nitrogen doped ZnO nanorod thin films via spin coating technique, and their microstructural and optical properties were explored. The microstructural parameters such as unit cell volume, microstrain and residual stress were considerably changed upon by successful incorporation of nitrogen dopant into ZnO lattice. The SEM images revealed that the ZnO had the hexagonal rod like structure and the diameters of nanorods were in the range of around 500 nm and their lengths were more than 2 μm. The reflectance spectrum of pure ZnO nanorods exhibited a band at 370 nm was attributed to the free excitonic absorption of ZnO and the band got shifted to higher energy upon nitrogen doping. The optical emission properties of pure and nitrogen doped ZnO nanorods were analysed using photoluminescence spectroscopy and the results revealed that the reduction on NBE emission intensity and an enhancement of visible light emissions.

**(PACC-P015-2022) Polymer/ferrite nanocomposite films for cooling applications**

P. Thandapani<sup>1</sup>; F. Beron<sup>2</sup>; R. Aepuru<sup>3</sup>; M. Viswanathan<sup>4</sup>; F. L. Zabotto<sup>5</sup>; J. A Jiménez<sup>6</sup>; J. C Denardin<sup>7</sup>

1. VIT-AP University, Department of Physics, India
2. UNICAMP, Institute of Physics Gleb Wataghin, Brazil
3. Universidad Tecnológica Metropolitana, Department of Mechanical Engineering, Faculty of Engineering, Chile
4. University of Concepcion, Chile
5. Federal University of Sao Carlos, Physics Department, Brazil
6. CENIM-CSIC, Department of Physical Metallurgy, Spain
7. University of Santiago and CEDENNA, Department of Physics, Chile

Cooling is one of the serious issues where the demand of fossil fuels is greater. Many magnetic materials have been produced as refrigerants for cooling application. However, the better performance found either at low temperature or at higher magnetic field and high product cost are the limitations. The materials with two or more functionalities can be tuned by external stimuli such as electric, magnetic, and stress fields. They would be of great advantage in the case of micro device cooling. Multiferroic polymer nanocomposites are our prime interest due to their multi-functionalities and would be suitable refrigerants. To attempt this, we developed flexible nanocomposite film using ferroelectric polymer blend Poly(methyl methacrylate)/Poly(vinylidene fluoride-co-hexafluoropropylene) (PMMA/PVDF-HFP) and nano Zn<sub>0.5</sub>Cu<sub>0.5</sub>Fe<sub>2</sub>O<sub>4</sub>. The nanocomposite shows superparamagnetic nature as similar to nano ferrite. Both nanoparticles and composite film display table-like entropy change with respect to temperature at constant field. The DS<sub>M</sub> (refrigerant capacity) at 300 K is found to be -0.69 (293 J/kg) and -0.094 (40 J/kg) J/kg/K for Zn<sub>0.5</sub>Cu<sub>0.5</sub>Fe<sub>2</sub>O<sub>4</sub> and PMMA/PVDF-HFP/Zn<sub>0.5</sub>Cu<sub>0.5</sub>Fe<sub>2</sub>O<sub>4</sub>, respectively. It showed less magnetoelectric coupling coefficient. Thus, developing composites with suitable composition would offer i-caloric materials where the electrocaloric and magnetocaloric effects are expected.

**(PACC-P016-2022) Structural ground-state, lattice dynamic, thermodynamic and optical properties of the Ba<sub>2</sub>CaMoO<sub>6</sub> double-perovskite**

C. E. Deluque Toro<sup>1</sup>; E. Villar Gonzalez<sup>1</sup>; A. V. Gil Rebaza<sup>\*3</sup>; D. A. Landínez Téllez<sup>2</sup>; J. Roa-Rojas<sup>2</sup>

1. Universidad del Magdalena, Colombia
2. Universidad Nacional de Colombia, Colombia
3. Universidad Nacional de La Plata, Argentina

Ab-initio calculations based on density functional theory have been performed to establish the ground state properties for the double perovskite type material Ba<sub>2</sub>CaMoO<sub>6</sub>. The Projector Augmented Wave Method (PAW) and the Perdew-Wang exchange and correlation functions in the Generalized Gradient Approximation allowed the structural study of this material, as well as the cell dynamics and the thermodynamic and optical properties in its transition between the tetragonal I4/m and cubic Fm3m phases. The results obtained on the structural stability reveal that the I4/m space group corresponds to the most stable phase. Likewise, the structural phase transition was obtained for a pressure of 0.067 GPa. On the other hand, the analysis of the electronic properties shows that the material presents a semiconducting behavior, with a direct band gap of 2.397 eV and 2.258 eV for the tetragonal and cubic structures, respectively. These results are in agreement with experimental values reported in the literature.

**(PACC-P017-2022) Physical and thermo-mechanical properties of coated and non coated Magnesia-boron based refractory castable for petrochemical industry application**

V. Singh<sup>\*1</sup>; M. Majhi<sup>1</sup>

1. IIT (BHU) Varanasi, Ceramic Engineering Department, India

In this research work we studied about the Physical and thermo-mechanical properties of coated and non-coated Magnesia-boron based refractory castable for petrochemical industry application. The coating of Magnesium borate (Mg<sub>2</sub>B<sub>2</sub>O<sub>5</sub>) with Nobel metal oxide is uniform and doesn't change the chemical composition of the composite. The present work is aimed to compare the effect of various coatings over the refractory properties of magnesium borate. Four coatings were studied (Cr<sub>2</sub>O<sub>3</sub>, ZnO, TiO<sub>2</sub>, and SiO<sub>2</sub>) to make a comparative study of different Nobel oxides. The magnesium borate (MBO) whisker was made using hydrolyzation route using magnesia and boric acid after sintering and coating of various oxide is done by the sol-gel method. To confirm the microstructural properties after coating were done by SEM and EDS analysis. XRD was performed for phase identification at two different temperatures. The physical properties such as bulk density, apparent porosity and thermo-mechanical properties such as cold modulus of rupture, hot modulus of rupture, hardness and wear properties were measured for different coated samples. The comparative study of synthesized coated sample was presented at different parameters. Resultant was observed that the SiO<sub>2</sub> coated sample shows remarkable improvement in properties as compared to other coated samples.

**(PACC-P018-2022) Structural and ferroic properties of compounds based on BiFeO<sub>3</sub> by First principles study**

I. B. Catellani<sup>\*1</sup>; O. G. Oliveira<sup>2</sup>; G. Perin<sup>1</sup>; L. F. Cótica<sup>1</sup>; I. A. Santos<sup>3</sup>

1. State University of Maringá, Physics, Brazil
2. Maringá State University, Brazil
3. State University of Maringá, Physics, Brazil

During the last decade, considerable attention has been devoted to the investigation of perovskite-type crystals that have multiferroic properties due to their possibilities of applications. In this class of materials, is one of the most studied multiferroics, as it presents ferroelectric and magnetic orders at temperatures well above room temperature, makes this material a candidate promising for multifunctional devices. There are drawbacks that impair ferroelectricity,

which are the low resistivity and the high coercive field, which are problematic for application in real devices. One of the approaches to improve the ferroelectric property is the synthesis of a solid solution with other ferroelectric materials. In this work we chose to study pure, the solid solutions and (these combinations improve the ferroelectric and magnetic properties, compared pure. The goal of this present study is to use the density functional theory implemented in the OpenMx software to obtain structural and electronic properties of the compounds. From this technique, analyzes of the behavior of the structural, electrical and magnetic properties of this system were performed. Finally, analyzes of the electronic densities calculated by DFT were carried out, investigating the origin of ferroelectricity, and from the electronic densities we can confirm the performance of lone pairs distorting the structure.

**(PACC-P019-2022) Polymer- ceramic composites**

J. M. Rosso<sup>\*1</sup>; J. Burato<sup>1</sup>; D. M. Silva<sup>1</sup>; T. G. Bonadio<sup>2</sup>; V. F. Freitas<sup>2</sup>; G. S. Dias<sup>1</sup>; L. F. Cótica<sup>1</sup>; I. A. Santos<sup>1</sup>

1. Maringá State University, Physics, Brazil
2. Midwest State University, Physics, Brazil

Composites of ferroelectric ceramic inclusions in a polymer matrix have been widely investigated as promising candidates for many applications such as pressure and pyroelectric sensors. These composites combine the advantages of the ceramic phase with those of the polymer matrix, such as high piezoelectric and pyroelectric properties with good mechanical properties, such as low density and flexibility. However desirable properties must be optimized with processing techniques. In the present work was mixed the polymer powder commercial PVDF obtained from Alfa Aesar with 0.3 volume fraction of ceramic powder Ba<sub>0.2</sub>Na<sub>0.8</sub>Ti<sub>0.2</sub>Nb<sub>0.8</sub>O<sub>3</sub> (BTNN0.80) which was prepared by high energy milling followed of conventional ceramic fabrication technique. XDR analysis of BTNN0.80 ceramic shows that the sample to be single phase. Dielectric measurements show that the real dielectric constant (ε') increases with increasing temperature, with a significant increase in the range from 250 K to 300 K. For lower frequencies, there is also a significant increase at temperatures close to 360 K.

**(PACC-P020-2022) Dielectric Behaviour of Ba<sub>0.25</sub>Na<sub>0.75</sub>Ti<sub>0.25</sub>Nb<sub>0.75</sub>O<sub>3</sub> System**

J. M. Rosso<sup>\*1</sup>; D. M. Silva<sup>1</sup>; G. M. Santos<sup>1</sup>; J. Burato<sup>1</sup>; T. G. Bonadio<sup>2</sup>; V. F. Freitas<sup>2</sup>; G. S. Dias<sup>1</sup>; L. F. Cótica<sup>1</sup>; I. A. Santos<sup>1</sup>

1. Maringá State University, Physics, Brazil
2. Midwest State University, Physics, Brazil

Ceramic materials based on barium titanate (BaTiO<sub>3</sub>) they have a wide application as multilayer ceramic capacitors, mainly due to its high dielectric constant and a good stability with temperature variation. In this work, the BaTiO<sub>3</sub> was added to sodium niobate (NaNbO<sub>3</sub>), in order to improve the dielectric properties and makes it ferroelectric room temperature, this material were synthesized using the following chemical reaction: (1-x)BaCO<sub>3</sub>+(1-x)TiO<sub>2</sub>+(x/2)Nb<sub>2</sub>O<sub>5</sub>+(x/2)Na<sub>2</sub>CO<sub>3</sub>→ Ba<sub>1-x</sub>Na<sub>x</sub>Ti<sub>1-x/2</sub>Nb<sub>x/2</sub>O<sub>3</sub>+[(1-x)/2]CO<sub>2</sub> The single-phased Ba<sub>0.25</sub>Na<sub>0.75</sub>Ti<sub>0.25</sub>Nb<sub>0.75</sub>O<sub>3</sub> (BTNN70) were then processed by dry high-energy ball milling (HEBM) and heat treatments in an oxygen atmosphere. In this work, the BaTiO<sub>3</sub> was added to sodium niobate (NaNbO<sub>3</sub>), in order to improve the dielectric properties and makes it ferroelectric. X-ray diffraction (XRD), were performed in powers ceramics at room temperature, was determined using the BTNN25/75 structural lattice parameters obtained by Rietveld refinement. Then were and dielectric investigations performed on polished ceramic disks with silver electrodes on the disks' face.

**(PACC-P021-2022) Structure, morphology, and magnetism of SCTFO hexaferrite synthesized by Citrate's method**W. Salazar González<sup>\*1</sup>; J. W. Sandino del Busto<sup>1</sup>; L. C. Moreno Aldana<sup>1</sup>

1. Universidad Nacional de Colombia, Physics, Colombia

The SCTFO ferrite ( $\text{SrCo}_2\text{Ti}_2\text{Fe}_8\text{O}_{19}$ ) is of interest due to its wide variety in possible technological applications due to their uncommon effects like the theoretical presence of magnetic Skyrmions and magnetics switching [1]. This type of ferrite has shown magneto-electric effect at room temperature due to the Dzyaloshinskii-Moriya interaction. The manufacture of SCTFO is fundamental because of the desired properties are dependent on the synthesis method [2]. Among the different methods applied to prepare this ferrite, the citrate method has as advantages its relatively simplicity and almost independence in the chemical process. In this work synthesis procedure through of the Citrate method and precise annealing of specimens by a well-controlled thermal treatment is showed to obtain the hexagonal ferrite SCTFO. The samples obtained were characterized structurally by X-Ray diffraction, morphologically by scanning electron microscopy and magnetically vibrant sample magnetometry. It was observed that for the synthesis temperature is obtained the predominant M phase. Electron micrographs indicated hexagonal-like morphology and phase homogeneity. Magnetic measurements show a soft ferrite and transitions from helical to ferrimagnetic structure, these measurements were correlated with the magnetoelectric couplings. Finally, the results obtained are compared with measurements of samples manufactured by state solid method.

**(PACC-P022-2022) Origin of ferroelectricity in  $\text{Zn}_{1-x}\text{Mg}_x\text{O}$  by first-principles study**E. Martínez-Aguilar<sup>\*3</sup>; H. HMok<sup>2</sup>; J. Siqueiros<sup>1</sup>; R. López-Juárez<sup>3</sup>

1. Universidad Nacional Autonoma De Mexico, Centro De Nanociencias y Nanotecnologia, Mexico
2. Van Lang University, Simulation in Materials Science Research Group, Science and Technology Advanced Institute, Viet Nam
3. Universidad Nacional Autonoma de Mexico, Unidad Morelia del Instituto de Investigaciones en Materiales, Mexico

First-principles calculations based on the density functional theory to identify the effects on the structural, electronic, and polar properties of ZnO suffers when it is doped with  $\text{Mg}^{2+}$  ions are presented. The results show that the lattice parameters decrease with increasing  $\text{Mg}^{2+}$  concentration up to 37%. The calculated gap value of 3.056 eV for the undoped ZnO increase with the  $\text{Mg}^{2+}$  concentration. Using the modern theory of polarization, a spontaneous polarization of  $\sim 134 \mu\text{C}/\text{cm}^2$  for 37% Mg-doped ZnO along the [0001] direction was calculated. The high polarization values of the Mg-doped ZnO are due to local distortion and increased ionicity of the compound along the [0001] direction, accentuated by the structural changes and corresponding bond lengths that ZnO undergoes. These results agree with those reported experimentally and clarify the origin of the high ferroelectric polarization values measured in  $\text{Zn}_{1-x}\text{Mg}_x\text{O}$ . \*Corresponding author's email: hlinhmok@vlu.edu.vn Acknowledgments The authors thank DGTIC-UNAM for computer support through Project LANCAD-UNAM-DGTIC-348. E. Martínez-Aguilar thanks DGAPA-UNAM for Scholarship grant No. CJIC/CTIC/4636/2021. H.Linh Hmok thanks Van Lang University for support. JMS acknowledges support by DGAPA-UNAM project IN104320. R. López-Juárez thanks DGAPA-UNAM for financial support under project PAPIIT-IN113420.

**(PACC-P023-2022) Determination of the Polymorphic Transition Zone in  $\text{KNNLiTaLa}_{0.01}$  by Raman Spectroscopy**Y. De Armas<sup>2</sup>; J. Portelles<sup>3</sup>; R. López-Noda<sup>2</sup>; J. Fuentes<sup>2</sup>;H. Hmok<sup>\*5</sup>; Bedolla-Valdez<sup>4</sup>; J. Siqueiros<sup>1</sup>

1. Universidad Nacional Autonoma De Mexico, Centro De Nanociencias y Nanotecnologia, Mexico
2. Instituto de Cibernética, Matemática y Física, CITMA, Departamento de Física Aplicada, Cuba
3. Universidad de La Habana, Facultad de Física, Cuba
4. Instituto Tecnológico Superior de Uruapan, Mexico
5. Science and Technology Advanced Institute, Van Lang University, Simulation in Materials Science Research Group, Viet Nam

The ( $\text{K}_{0.44}\text{Na}_{0.52}\text{Li}_{0.04}\text{La}_{0.01}\text{Nb}_{0.9}\text{Ta}_{0.1}\text{O}_3$  ( $\text{KNNLiTaLa}_{0.01}$ ) composition was synthesized using a combination of the reactive templated grain growth method (RTGG) and the conventional ceramic method. Using X-ray diffraction (XRD) analysis at room temperature, the coexistence of Orthorhombic Amm2, Tetragonal P4mm and Tetragonal P4/mbm phases was determined. Using Raman Spectroscopy, the study of a polymorphic phase transition in the  $\text{KNNLiTaLa}_{0.01}$  compound is presented. This analysis determined that the polymorphic phase transition of the  $\text{KNNLiTaLa}_{0.01}$  compound occurs in the range of 90 °C to 105 °C. Using the Hard Mode Spectroscopy method, the value of the critical exponent of the order parameter was determined to be  $\beta = 1/2$ , indicative of a second order phase transition. \* H'Linh Hmok, corresponding author: hlinhmok@vlu.edu.vn Acknowledgment This work was partially supported by PAPIIT-DGAPA-UNAM Grant IN104320. H'Linh Hmok thanks to the support of Van Lang University

**(PACC-P024-2022) Experimental and theoretical study of ferromagnetic ordering and semiconductor response in the  $\text{La}_2\text{CoFeO}_6$  ceramic material**K. Muñoz Pulido<sup>\*1</sup>; J. Jaramillo Palacio<sup>1</sup>; C. E. Deluque Toro<sup>2</sup>; D. A. Landínez Téllez<sup>1</sup>; J. Roa-Rojas<sup>1</sup>

1. Grupo de Física de Nuevos Materiales, Universidad Nacional de Colombia, Física, Colombia
2. Universidad del Magdalena, Colombia

Structural, magnetic and electric measurements of the  $\text{La}_2\text{CoFeO}_6$  perovskite produced by the Pechini technique are reported. Ab initio calculations of the electronic and thermodynamic properties for these oxide ferrocobaltite were carried out by means of first principles calculations, using the formalism of the Functional Density Theory and the Plane Wave and Pseudopotential method through the VASP code. Exchange and correlation energy was described using the Generalized Gradient Approximation, including spin polarization and Hubbard potential correction due to the presence of Fe-3d and Co-3d orbitals. The ferromagnetic semiconductor behavior of the material was established by obtaining a band gap of 2.35 eV. Strong hybridizations between the 2p oxygen orbitals in the valence band with  $\text{Fe}^{2+}$ -3d and  $\text{Co}^{4+}$ -3d states allow us to explain the ferromagnetic nature through the superexchange mechanism between high-spin states of  $\text{Fe}^{2+}$  with low-spin states of  $\text{Co}^{4+}$  mediated by  $\text{O}^{2-}$  orbitals. The theoretical results are in agreement with the values obtained from experimental measurement.

**(PACC-P025-2022) Fabrication and Structural Characterization of Intermetallic Compounds of the  $\text{RT}_2\text{Al}_{10}$  Family -**J. C. Delgado<sup>\*1</sup>; M. Cabrera<sup>2</sup>; L. Huertas Pulido<sup>1</sup>; D. A. Landínez Téllez<sup>1</sup>;J. Roa-Rojas<sup>1</sup>

1. Grupo de Física de Nuevos Materiales, Universidad Nacional de Colombia, Física, Colombia
2. Universidade Federal de Pernambuco, Física, Brazil

In the present work, an overview is presented on the fabrication and structural characterization of single crystals of the  $\text{RT}_2\text{Al}_{10}$  family (R: rare earth, T: transition metal) using the self-flux method with an excess of Al. Specifically, the compounds ( $\text{YFe}_2\text{Al}_{10}$ ),

$\text{YbFe}_2\text{Al}_{10}$ ,  $\text{GdFe}_2\text{Al}_{10}$ ) were made. The initial reagents were 99.9% Y, 99.9% Yb, 99.9% Gd, 99.9% Fe and 99.9% Al. Initial ratios of elements were 1:2:30 for the pure ternaries Y:Fe:Al, Yb:Fe:Al and Gd:Fe:Al. The elemental mixtures were sealed in an evacuated quartz ampoule and placed in a furnace for the temperature ramping. Crystals were grown by slowly cooling the melt between  $1090^\circ\text{C}$  and  $750^\circ\text{C}$  over 100 h. At  $750^\circ\text{C}$  the ampoules were removed from the furnace, inverted, and placed in a manual centrifuge to spin off the excess flux. Powder X-ray diffraction on crushed crystals was used to determine the structure of the compounds, obtaining well-defined pure phases for each compound, and finally some images of the compounds were taken using Scanning Electron Microscope (SEM).

### (PACC-P026-2022) Refining structural and density calculation electronic system multiferroic $(\text{Bi}_{1-x}\text{Nd}_x)\text{FeO}_3$

O. G. Oliveira<sup>\*1</sup>

1. Maringá State University, Brazil

The need for new technologies in our society caused a greater interest in research on materials used in electronics applications, it made the multiferroic crystalline materials very promising and of great and technological academic interest materials due to correlation between the ferroelectric and (anti)ferromagnetic properties. Among these materials, compounds with perovskite structures, as those arising from the doping of  $\text{BiFeO}_3$ , can be mentioned. In this work ceramic powders of  $(\text{Bi}_{1-x}\text{Nd}_x)\text{FeO}_3$  compositions, for  $x = 0.025, 0.05, 0.10, 0.125, 0.15$  and  $0.20$ , were processed using high-energy ball-milling followed by sintering in a free atmosphere. Also it was used the fast sintering technique followed by quenching. Through the Rietveld refinement, associated with the Maximum Entropy Method (MEM), we found that a gradual increase of neodymium substitution induces a phase transition from rhombohedral R3c to orthorhombic Pbam phase. However, the presence of a third phase, that assists in the transition from rhombohedral to orthorhombic phase was identified. The electron density calculations allowed better analysis on the bonding character between the  $\text{Bi}^{3+}/\text{Nd}^{3+}$  and  $\text{O}^{2-}$  ions, and between the  $\text{Fe}^{3+}$  and  $\text{O}^{2-}$  ions in the  $(\text{Bi}_{1-x}\text{Nd}_x)\text{FeO}_3$  compositions. The graduated substitution with  $\text{Nd}^{3+}$  ions showed a decrease in the lattice parameters, in addition to weakening the lone pair stereochemical activity.

### (PACC-P027-2022) High resolution laser assisted load dilatometry focused on simultaneous axial and radial strain measurements for sintering characterization

H. Camacho Montes<sup>\*1</sup>; L. H. Montes<sup>2</sup>; H. M. Loya Caraveo<sup>2</sup>; A. Delgado Salido<sup>2</sup>; A. García Reyes<sup>3</sup>; I. M. Espinoza Ochoa<sup>1</sup>; R. Bordia<sup>4</sup>

1. Universidad Autonoma de Ciudad Juarez, Physics and Mathematics, Mexico
2. Universidad Autonoma de Ciudad Juarez, Eléctrica y Computación, Mexico
3. PROQUIMAR, Mexico
4. Clemson University, Materials Science and Engineering, USA

Continuum description is a useful tool for sintering characterization. Homogeneous sample with uniform distribution of temperature and green density can be easily characterized by traditional dilatometry. However, this case is rather scarce. Constrained sintering is a common case where the useful information of traditional dilatometry may not be enough. E. Aulbach et al. reported a new dilatometer design where is possible to simultaneously measure axial and radial strains. This is an important step forward because, for a cylindrical shape sample, it is possible to measure the entire strain tensor. Continuum description requires constitutive relations that relates strains and stress. In order to find this relation, E. Aulbach et al. included a pressing system in their dilatometer. The present load dilatometer design is inspired in the sintering continuum description. It is similar to the system developed by E. Aulbach et al. The main difference is the optical table that allows a change

of the laser sensors. In addition, the pressing direction is free of any other mechanisms. The optical table includes New Ports accessories (servomotors and plates) for the laser sensors positioning. Laser sensors are from Beta LaserMike, the furnace is from Carbolite and stress is applied to samples by mean of an Instron 5960.

### (PACC-P028-2022) Properties of Mullite-Ag Cermets

M. G. Téllez Arias<sup>\*1</sup>; E. Terrés<sup>2</sup>; A. Reyes-Montero<sup>3</sup>; L. Lartundo<sup>4</sup>

1. Universidad Michoacana de San Nicolas de Hidalgo, Facultad de Ingeniería Química, Mexico
2. Instituto Mexicano del Petróleo, Mexico
3. Universidad Nacional Autónoma de México, Instituto de Investigaciones en Materiales, Mexico
4. Instituto Politécnico Nacional, Centro de Nanociencias y Micro y Nanotecnologías, Mexico

In this work the mechanical and electrical properties of a mullite-Ag system with 0 to 30% of Ag are presented, the integration of the powders was carried out by high-energy dry grinding, cylindrical pellets were formed by applying uniaxial load cold at 200 MPa and subsequent pyrolysis at  $1500^\circ\text{C}$  and  $1600^\circ\text{C}$  in a nitrogen atmosphere. The cermets were characterized by X-ray diffraction, the mullite phase is maintained and a better definition of the diffraction peaks is achieved, because of recrystallization. By Scanning Electron Microscopy, changes in grain size were observed, images of the cermets with high concentrations of Ag (20 and 30%) the largest grain sizes can be seen in addition to being highly homogenized, the nanometric size of the Ag particles also was determined low voltages; with confocal microscopy it was possible to observe the dispersion of silver in the mullite matrix. X-ray photoelectron spectroscopy (XPS) determined that the silver nanoparticles are present in a combination of  $\text{Ag}^0$  and  $\text{AgO}$ . Vickers indentation technique, finding that the effect of incorporating Ag nanoparticles in Mullite is to increase the value of fracture toughness. The electrical properties of Mullite-Ag cermets were analyzed, between  $400^\circ\text{C}$  and  $700^\circ\text{C}$  and a  $0.01\text{Hz} - 10\text{MHz}$ , in cermets with only 1% Ag, the electrical conductivity increases markedly at relatively low activation energy, where conduction phenomena occur at the grains and grain boundaries. The charge carriers associated with the conduction mechanism are related to electrons.

### (PACC-P029-2022) Lithium Aluminium Silicate ceramic glass densification during sintering

I. M. Espinoza Ochoa<sup>\*1</sup>

1. Universidad Autónoma de Ciudad Juárez, Física y Matemáticas, Mexico

Densification of lithium aluminium silicate glass (LAS) during sintering is characterized by means of a laser assisted load dilatometer. This dilatometer is assisted by two high-resolution lasers scans for continuous measurements of radial and axial strains of the cylindrical ceramic sample during hot forging. A uniform load is applied in a consistent way that favours the determination of reliable viscoelastic parameters. It is observed that densification is interrupted at different temperatures for different heating rates, and, isothermal densification is stopped depending on the dwelling temperature. This behaviour can be related to the crystallization that takes place approximately at  $800^\circ\text{C}$ . Then, the crystallization kinetics is also studied by means of Differential Scanning Calorimetry (DSC) and complemented with X Ray Diffraction (XRD) and Scanning Electron Microscopy (SEM), and it is described with the help of Kolmogorov-Johnson-Mehl-Avrami rate equation. The connection between densification and crystallization is established considering that sintering takes place in a viscous matrix where rigid inclusions are growing up. Hence, a phenomenological model is stated where the Mackenzie and Shuttleworth phenomenological theory is used to describe the free sintering component where the temperature effect is considered by the Arrhenius equation.

**(PACC-P030-2022) Influence of grain size on uniaxial viscosity during sintering**

A. Vega Siverio<sup>\*1</sup>; H. Camacho Montes<sup>2</sup>; B. M. Madrazo<sup>1</sup>; I. M. Espinoza Ochoa<sup>1</sup>

1. Universidad Autónoma de Ciudad Juárez, Física y Matemáticas, Mexico
2. Universidad Autonoma de Ciudad Juarez, Physics and Mathematics, Mexico

The present work aims to investigate the dependence of uniaxial viscosity on the grain size during the sintering process in ceramics. Measurements of powder compact height and diameter were performed in a high precision load dilatometry during sintering applying different compression loads to induce different grain sizes for the sintered samples. Data cleaning is necessary in order to obtain an accurate strain rate. Uniaxial viscosity is estimated considering the relation between the applied stress and the resulting difference between the axial strain rate with load and the free axial strain rate. Characterizations were carried out on the microstructure of the samples by means of scanning electron microscopy (SEM) and X-ray diffraction (XRD) and finally a correlation was established between the uniaxial viscosity and the grain size.

**(PACC-P031-2022) Grain size and crystallographic texture effect on the piezoelectric coefficient  $d_{33}$  of BaTiO<sub>3</sub> ceramics**

B. Olmos<sup>\*1</sup>; O. Raymond<sup>4</sup>; G. M. Herrera-Perez<sup>2</sup>; H. Camacho Montes<sup>3</sup>

1. Universidad Autónoma de Ciudad Juárez, Mexico
2. CONACYT, CIMAV, Mexico
3. Universidad Autonoma de Ciudad Juarez, Physics and Mathematics, Mexico
4. Centro de Nanociencias y Nanotecnología-Universidad Nacional Autónoma de México, Mexico

The following investigation has the purpose to describe the effect of grain size and the crystallographic texture on the piezoelectric coefficient  $d_{33}$  for BaTiO<sub>3</sub>. Dense BaTiO<sub>3</sub> ceramics with different grain sizes were fabricated by stress assisted sintering in sinter-forging unit using microsize powders. Different temperatures and forces were applied to create different grain sizes and texture on the BaTiO<sub>3</sub> pellet samples. The results show density above 96.5% for all the samples. The average grain sizes range is 0.8-1.8  $\mu\text{m}$ . The DRX analysis shows some preferred orientation on the samples with higher applied force during sintering. The direct piezoelectric coefficient  $d_{33}$  shows different values at different conditions. Also, the converse piezoelectric coefficient  $d_{33}^*$  presented a similar tendency.

**(PACC-P032-2022) Mechanism of Hydration of Belite Nanoparticles made from Flame Spray Pyrolysis**

J. J. Pérez Molina<sup>\*1</sup>; D. Gil Velasquez<sup>1</sup>; O. J. Restrepo<sup>3</sup>; J. I. Tobón<sup>3</sup>; N. Betancur-Granados<sup>2</sup>

1. Universidad Nacional de Colombia, Department of Construction, Colombia
2. Corporación Universitaria Minuto de Dios-UNIMINUTO, Department of Basic Sciences, Colombia
3. Universidad Nacional de Colombia, Department of Minerals and Materials, Colombia

Belite cement is considered an environmentally friendly material due to the lower CO emissions during its production and an important material for engineering for hydraulic applications considering its high sulfate attack resistance and reduction of cracks. However, it has as a technological disadvantage its low kinetic of hydration, therefore, increase the specific surface area could improve it. In order to reveal the hydration of nanoparticles belite were evaluated the role of three different calcium resources and their temperature in relation with to the reaction stages vs traditional cement. The precursors tetraethyl orthosilicate or TEOS (Si(OC H), 98 %), calcium nitrate tetrahydrate (Ca(NO). 4H O, 98 %) and calcium propionate (Ca(O CCH CH)) have been studied through microcalorimetry, whose result showed a time decrease in latent

period and a time increase the second heat peak in comparison at the traditional cement, revealing as well that calcium propionate promotes a better formation of belite cements. The cumulative heat plots showed that the complete hydration of the samples was achieved after 48 h of reaction, indicating the formation of a highly-reactive material in comparison to belites obtained by the traditional solid-state method, which require months even years to get a complete hydration.

**(PACC-P033-2022) Study of the reactivity of Alkali-activated cements added with nanoparticles of SiO<sub>2</sub>**

I. Taborda Llano<sup>2</sup>; N. Betancur-Granados<sup>1</sup>; J. I. Tobón<sup>3</sup>; A. A. Hoyos Montilla<sup>2</sup>

1. Corporación Universitaria Minuto de Dios - UNIMINUTO, Faculty of Engineering, Colombia
2. Universidad Nacional de Colombia, School of Architecture, Colombia
3. Universidad Nacional de Colombia, Department of Materials and Minerals, Colombia

Ordinary Portland cement (OPC) presents a high demand for the manufacture of concrete, implying high CO<sub>2</sub> emissions to the atmosphere and a high consumption of natural resources. For these reasons, alternative cements are gaining more attention. Alkaline activated cements (AAC) are considered as green cements, providing excellent cementitious properties, and releasing less CO<sub>2</sub> emissions into the atmosphere. The addition of nanoparticles to cementitious materials has contributed to improved setting times, durability to environmental attacks, reduced cracking, and reduced shrinkage in concrete. Therefore, this research shows the study of the reactivity of AAC after adding nanoparticles of SiO<sub>2</sub>, in percentages in weight of 0%, 1%, 2%, 3%, 5%. The alkaline activation was done with calcium hydroxide (10%) and sodium silicate (2%), and the aluminosilicate source will be fly ash. The chemical reactions were studied using isothermal microcalorimetry using temperatures of 25°, 35° and 45° at 14 and 28 days. Finally, microstructural characteristics were obtained by means of FTIR and SEM techniques.

**(PACC-P034-2022) Study on interfacial transition zone properties of lightweight aggregates in concrete**

D. Gonzalez<sup>\*3</sup>; N. Betancur-Granados<sup>1</sup>; J. I. Tobón<sup>3</sup>; A. A. Hoyos Montilla<sup>2</sup>

1. Corporación Universitaria Minuto de Dios - UNIMINUTO, Faculty of Engineering, Colombia
2. Universidad Nacional de Colombia, School of Architecture, Colombia
3. Universidad Nacional de Colombia, Department of Materials and Minerals, Colombia

Lightweight concrete demand has increased due to interesting features as its adaptability to seismic design since the significant reduction of the inertial forces in the elements. Artificial lightweight aggregates contribute to the preservation of the environment since they recycle by-products and reduce the consumption of the natural aggregates, however, some mechanical problems have limited their use as structural elements in the construction industry. The mechanical properties of lightweight concretes are affected by factors such as the stiffness of the aggregate particles, the water to cement ratio (a/c), the cement content and density, whereby significant efforts to optimizing their dosage and improving their mechanical properties are made. This tendency has led to the study of microstructure, particularly the mechanisms responsible for the internal transition zone (ITZ) formation, related with absorption and water release. Therefore, this research focuses on analyze the morphological and physical properties such as water absorption and density of expanded clay and polymeric wastes lightweight aggregates to determine their impact on the microstructure of the ITZ.

### **(PACC-P035-2022) Hydrothermal Transformation of Kaolinite to Kalsilite Using Potassium Carbonate**

E. F. Yusslee\*<sup>1</sup>; N. Dahon<sup>1</sup>; M. Abdul Rajak<sup>1</sup>; S. E. Arshad<sup>2</sup>

1. Universiti Malaysia Sabah, Pusat Peralaksanaan Sains & Teknologi, Malaysia
2. Universiti Malaysia Sabah, Faculty of Science and Natural Resources, Malaysia

Kalsilite has a high melting temperature (1600°C) and resistance to alkali attack, making it suitable to be used as a refractory material. In this study, hydrothermal synthesis of kalsilite was facilitated by the inclusion of potassium carbonate ( $K_2CO_3$ ) as the source of potassium and kaolin clay as precursors. After a 24-hour reaction at 220°C, kaolin clay treated with 1.25M  $K_2CO_3$  showed peaks at 28.5° and 34.7° are the most significant under X-ray diffraction (XRD) corresponded to hexagonal kalsilite (space group  $P6_3$ , PDF 11-0579). In addition, Field Emission Scanning Electron Microscopy (FESEM) images also revealed nano-sized hexagonal particles proving the formation of the desired mineral. At lower  $K_2CO_3$  molarity (<1.0M), orthorhombic boehmite and monoclinic bayerite were acknowledged as the major crystalline phases, while kalsilite formed as a minor phase. The crystallinity of hexagonal kalsilite increased at higher  $K_2CO_3$  concentration (>1.0M) while the reaction temperature remained at 220°C. On the other hand, zeolite W and muscovite are the major products when the reaction temperature is below 220°C. Besides, a significant atomic percentage of potassium in the aluminosilicate material was observed in Energy Dispersive Spectroscopy (EDS) pattern of kalsilite, proving its formation.

### **(PACC-P036-2022) The use of steelmaking slag as protection for oxidation of MgO-C refractories**

M. N. Moliné<sup>1</sup>; W. A. Calvo<sup>1</sup>; S. E. Gass<sup>1</sup>; D. Gutiérrez-Campos\*<sup>3</sup>; P. G. Galliano<sup>2</sup>; A. G. Tomba Martínez<sup>1</sup>

1. INTEMA (CONICET), Argentina
2. CINI - Tenaris REDE AR, Argentina
3. Universidad Simón Bolívar, Venezuela, Bolivarian Republic of

MgO-C is one of the most important refractories for steelmaking ladles. Carbon is a key component which allows the refractory to have high resistance to thermal shock and to slag attack. However, C oxidizes in air; this risk is currently found during the pre-heating of the ladle (at the beginning and between production cycles). During the operation, the liquid steel is evacuated through ladle bottom leaving a slag layer adhered to the working lining which serves as protection against oxidation of refractories' carbon. Nevertheless, this layer could suffer degradation by ambient humidity which affects its role as an oxygen diffusion barrier. This work analyzes how the refractory composition (graphite content, type of binder) and the slag degradation affect the oxidation resistance of MgO-C materials. For testing, a slag layer was generated over one of the plane surface of the refractory cylinder (25x25 mm<sup>2</sup>) by treatment at 1400°C (graphite bed). Only this face was exposed to air (unidirectional test) at 1000°C (2 h). Variations in weight, depth of decarburized layer and graphite content were used as oxidation indicators. To evaluate the effect of slag weathering, tests were carried out after 2 and 10 weeks from the sample conditioning.

### **(PACC-P037-2022) High-temperature Young's modulus of alumina-containing kaolin-based silicate ceramics and its evolution during sintering**

E. Gregorova\*<sup>1</sup>; W. Pabst<sup>1</sup>

1. UCT Prague, Department of Glass and Ceramics, Czechia

Mullite is the main crystalline phase of kaolin-based silicate ceramics and refractories, while the addition of alumina enhances strength and stiffness and improves the refractoriness and high-temperature mechanical properties. Therefore the temperature dependence of elastic properties and their evolution during sintering is of considerable interest. This work focuses on the temperature dependence

of Young's modulus of alumina-containing kaolin-based silicate ceramics from 20 to 1500 °C. Samples were prepared from Czech kaolin (Sedlec Ia) and two grades of commercial alumina (Almatis), namely tabular alumina with a particle size up to 200 μm (T60) and submicron alumina with a median particle size of 0.7 μm (CT 3000 SG) in the mass ratio 60:40. The components were mixed by co-milling in aqueous suspension, dewatered, dried and crushed. Bar-shaped specimens were prepared by uniaxial pressing at 50 MPa and firing at 1100, 1200, 1300, 1400 and 1500 °C (heating rate 2°C/min, dwell 2 h). The temperature dependence of Young's modulus and its further evolution after exceeding the original sintering temperature was measured via high-temperature impulse excitation. The resulting differences for materials with fine-grained and coarse-grained alumina are compared and discussed with respect to phase composition and porosity.

### **(PACC-P038-2022) Temperature dependence of Young's modulus of silicon carbide refractories after up to 250 firing cycles determined via impulse excitation**

W. Pabst\*<sup>1</sup>; E. Gregorova<sup>1</sup>

1. University of Chemistry and Technology, Prague, Department of Glass and Ceramics, Czechia

The temperature dependence of elastic properties provides fundamental information on the high-temperature performance of refractories. In this work, the temperature dependence of Young's modulus is determined via impulse excitation for commercial silicon carbide (SiC) refractories in the as-supplied state and after up to 250 firing cycles. It is found that Young's modulus of as-supplied SiC decreases from 272–281 GPa at room temperature to 250–262 GPa at 1500 °C during heating but recovers during cooling. After 67–126 firing cycles in air at 1600 °C the room temperature values of Young's modulus are as low as 234–260 GPa, due to the presence of cristobalite, which is a natural product of oxidation. During heating, Young's modulus exhibits a steep increase at 230 °C to values of 250–275 GPa at around 400 °C, followed by a slight decrease during further heating. During cooling a steep decrease occurs at 200 °C, due to the re-opening of microcracks (phase transition of cristobalite). The oxidation layers formed in the bulk material (at the grain boundaries) passivate the material against further oxidation, so that even after 250 firing cycles the samples still exhibit full shape integrity and Young's modulus values of 230 GPa at room temperature and 250 GPa at 400 °C, followed by the typical slight decrease towards 240 GPa at 1500 °C.

### **(PACC-P039-2022) New understanding of liquid thermodynamics, viscosity and its lower bounds**

K. Trachenko\*<sup>1</sup>

1. Queen Mary University of London, Physics, United Kingdom

Understanding most basic thermodynamic properties of the liquid state such as energy and heat capacity turned out to be a long-standing problem: Landau&Lifshitz textbook states that no general formulas can be derived for liquid thermodynamic functions because the interactions are both strong and system-specific. Recent theoretical results open a new way to understand liquid thermodynamics on the basis of collective excitations (phonons) as is done in the solid state theory. Differently from solids, the phase space for these excitations reduces with temperature, explaining the universal decrease of liquid constant-volume specific heat. I will discuss the implication of the above theory for fundamental understanding of liquids. I will also explain how this picture extends above the critical point where the Frenkel line separates two physically distinct states on the supercritical phase diagram. I will subsequently describe how this leads to the theory of minimal quantum viscosity in terms of fundamental physical constants. This answers the long-standing question discussed by Purcell and Weisskopf of why viscosity never drops below a certain value. This also means that water and life and

well attuned to the degree of quantumness of the physical world. I will finally note that the kinematic viscosity of the quark-gluon plasma is surprisingly close to the kinematic viscosity of liquids at their minimum.

**(PACC-P040-2022) Rare-Earth-doped Chalcogenide Glasses: On the Path from Passive to Active Applications**

Y. Shpotyuk<sup>1</sup>; B. Mahlovany<sup>1</sup>; C. Boussard-Pledel<sup>2</sup>; R. Golovchak<sup>3</sup>; J. Cebulski<sup>1</sup>; O. Shpotyuk<sup>4</sup>; B. Bureau<sup>5</sup>

1. University of Rzeszow, Poland
2. University of Rennes, France
3. Austin Peay State University, Physics and Astronomy, USA
4. Jan Dlugosz University in Czestochowa, Poland
5. University of Rennes 1, Institute of Chemical Sciences, France

Chalcogenide glasses (ChG) possess exceptional transparency in the IR and favorable thermal properties allowing to use them for different photonic applications. In most cases, ChG are used as passive elements to transmit light from one point to another. By doping with rare-earth (RE) ions, these glasses significantly extend their functionality due to the appearance of numerous fluorescence emissions in the IR. This allows the ChG to be considered for active applications, where RE emissions create the second remote source of light in the IR. Indeed, RE solubility in “pure” covalently-bonded glass matrix is known to be very low, provoking clustering of RE ions and depression of the luminescence. By modifying the ChG with Ga (or In), the Ga (S, Se, Te)<sub>4</sub> tetrahedral units are formed, allowing much better solubility of RE ions. In this work the structure and properties of the canonical ChG systems (such as As<sub>2</sub>Se<sub>3</sub>, 2G2S) under the subsequent stages of their modification (Ga, In co-doping and RE-doping) are investigated. Besides the changes in optical properties, the RE-doping is shown to provoke significant changes in the structure (void structure) of ChG. It was shown that devitrification processes provoked by Ga addition could be significantly reduced by As to Sb substitution in ChG of binary As-Se system. This aspect of RE modification was also examined employing positron annihilation technique.

**(PACC-P041-2022) Electrical conductivity of vanado-tellurite glass-ceramics doped with CuO, Cu<sub>2</sub>O, FeO and Fe<sub>2</sub>O<sub>3</sub>**

M. Vacchi<sup>1</sup>; M. Affatigato<sup>2</sup>; E. I. Cedillo-González<sup>1</sup>; C. Siligardi<sup>1</sup>

1. Università degli studi di Modena e Reggio Emilia, Italy
2. Coe College, Physics Department, USA

Glasses containing transition metal oxides (TMO) are systems of interest due to optical and electrical properties that make them suitable for many uses, including solid-state devices and detectors for physical or medical applications. Among them, vanado-tellurite glasses are well-known for their semiconductor behavior. In this work, two series of glasses, i.e. (68-x) CuO - xV<sub>2</sub>O<sub>5</sub> - 32TeO<sub>2</sub> (x = 0 - 68 mol%, Te<sub>32</sub> series) and (35-x) CuO - xV<sub>2</sub>O<sub>5</sub> - 65TeO<sub>2</sub> (x = 0 - 35 mol%, Te<sub>65</sub> series), were subjected to physical, thermal and electrical characterization. After identifying the best performing formulation in terms of electrical conductivity, CuO was replaced by Cu<sub>2</sub>O, FeO, Fe<sub>2</sub>O<sub>3</sub> with the goal of further enhancing their electronic conductivity. Samples were prepared by melt-quenching and subsequent thermal treatment to promote crystallization. Electrical properties were measured on both amorphous and crystalline samples through impedance spectroscopy and high resistance electrometry. To investigate the influence of the presence and nature of crystalline phase, the samples were investigated by XRD, FEG-SEM-EDS, Raman, FTIR, and density and thermal properties (T<sub>g</sub> and ΔT) were also compared. The best conductivity results were mainly obtained for short annealing processes, where morphologically and compositionally homogeneous microstructures were developed.

**(PACC-P042-2022) SERS using sodium-titanium phosphate glasses containing Ag-NP for photocatalysis application**

D. Manzani<sup>1</sup>; T. I. Rubio<sup>1</sup>

1. University of São Paulo, São Carlos Institute of Chemistry, Brazil

Glass is a versatile material that can be applied in a great variety of uses, and its utilization in heterogeneous photocatalysis is currently a growing field of research. Adding plasmonic nanoparticles to the substrate is a method employed in the enhancement of photocatalytic activity. This work aimed to obtain silver nanoparticles (Ag-NPs) on the surface of sodium-titanium phosphate glass systems through Na<sup>+</sup>/Ag<sup>+</sup> ion exchange followed by heat treatment. Besides the detection of low concentration of organic molecules by SERS spectroscopy (10<sup>-5</sup> - 10<sup>-6</sup> M), the synthesized glass was used to evaluate photocatalysis activity towards methylene blue (MB), an organic dye that its degradation has a strong environmental remediation claim. Two different experimental approaches were carried out to have its photocatalytic activity assessed: using glass powder as a suspension with MB aqueous solution, and glass bulk placed at the inner surfaces of a cuvette. The photodegradation of MB was monitored via its absorption band in the electronic spectra every 10 min for 1 h, allowing to obtain a maximum of 57.8% of photodegradation for the suspension method and 68.3% for the bulk method. Despite photodegradation using glass is still a harsh area of investigation, the results obtained here showed that this field is a bright one, in which is possible to combine the versatility of glass materials tailoring to innovative applications in the environmental remediation of organic pollutants.

**(PACC-P043-2022) Hierarchical porous ceramics developed by using a Si-based preceramic polymer**

C. S. Certuche Arenas<sup>1</sup>; J. O. Bolaños Rivera<sup>1</sup>; Y. X. Hung Hung<sup>\*1</sup>; M. L. Sandoval<sup>1</sup>; M. H. Talou<sup>1</sup>; M. A. Camerucci<sup>1</sup>

1. INTEMA - CONICET, Argentina

Silicon-based preceramic polymers are an important type of precursors used in the processing of novel silicon-based ceramics. Different processing routes based on the consolidation of a hybrid body from the preceramic crosslinking reaction or the infiltration of a carbon-based template with the precursor, and then pyrolysis in controlled atmosphere, are proposed to develop hierarchical porous ceramics with unique chemical compositions. In this work, a partially condensed polysilsesquioxane (MP-SSO) synthesized by sol-gel method from 3-methacryloxypropyl-trimethoxysilane was used as consolidating or infiltration agent of poplar templates. The MP-SSO was characterized by ATR-FTIR, <sup>1</sup>H, <sup>13</sup>C and <sup>29</sup>Si NMR, DSC and rheological tests. Porous hybrid bodies were prepared by crosslinking (25°C, 72h; 10 vol% of TETA) of MP-SSO/sucrose/SiOC (preceramic/porogen/filler) mixtures (50/40/10 vol%) and calcining (300°C, 1h), and were characterized by porosity measuring and SEM. The templates were infiltrated at 50 bar, cured (135°C, 3h) and characterized by infiltration degree, porosity measuring, TGA, and SEM/EDS. All samples were pyrolyzed in N<sub>2</sub> (1000-1600°C, 2-4h) and characterized by porosity measuring, XRD, Leco, <sup>29</sup>Si NMR, Raman and SEM/EDS. The materials shown high hierarchical porosity, SiC nanowires, Si<sub>3</sub>N<sub>4</sub> crystals and SiOC amorphous phase, whose amounts and features depended on the processing conditions.

**(PACC-P044-2022) Porous ceramic structures obtained by using novel polymer-ceramic systems via additive manufacturing technologies**

Y. X. Hung Hung<sup>\*1</sup>; D. Gutiérrez-Campos<sup>2</sup>; M. L. Sandoval<sup>1</sup>; M. A. Camerucci<sup>1</sup>; M. H. Talou<sup>1</sup>

1. INTEMA - CONICET, Argentina
2. Universidad Simón Bolívar, Ciencias de los Materiales, Venezuela, Bolivarian Republic of

Additive manufacturing refers to different near-net shape fabrication techniques in which a part is generated from 3D model data



by adding material. These technologies allow the direct production of components with complex shapes, which are difficult to fabricate using conventional forming methods. Among them, fused deposition modeling (FDM) and selective laser sintering (SLS) are highlighted in the ceramic processing field. In this context, the design and preparation of appropriate feed systems constitutes still a challenge to solve. In this work, porous ceramic structures developed from novel polymer-ceramic systems via FDM and SLS were obtained. Alumina and polyamide (PA612) powders were used as ceramic and polymeric materials. PA612-alumina granules were prepared by thermally induced phase separation (TIPS) to be used as a printer feed material alternative to the composite filament for FDM, while the PA612-alumina-micrographite granules prepared also by TIPS and then milled and spray dried were used as a new feed system for SLS. Both types of granules were characterized by granulometric distribution, density and SEM/EDS. Printed, burned (800-1200 °C) and sintered (1580 °C) porous ceramic structures were characterized by density and porosity measurements, and SEM. The parts showed good intra and interlayer adhesion, high skeletal densification and macroporous structure control.

### **(PACC-P045-2022) The effective role of CaO/SiO<sub>2</sub> ratio on the binary system based on CaO-SiO<sub>2</sub>**

M. H. Kaou<sup>\*1</sup>; H. R. Ben Zine<sup>2</sup>; C. Balazsi<sup>2</sup>; K. Balazsi<sup>2</sup>

1. Óbuda University, Doctoral School on Materials Sciences and Technologies, Hungary
2. Institute of Technical Physics and Materials Science, Centre for Energy Research, ELKH, Hungary

The biological characteristics of calcium silicate based system have highlighted them as promising materials for bio-applications such in bone repairing, tissue engineering, drug carrier, and dental restoration. These applications are accompanied by the phenomenon of formation of an apatite layer on the surface upon implantation when it is connected to biological fluids. This last helps in inducing the bonding to the surrounding tissues to the hard tissues and soft tissues with certain compositions. On the other hand, the structure of calcium silicates is determining the biological behavior that can be manipulated by different factors such as: sintering temperature, porosity, precursors, composition, and fabrication method. Therefore, our work aimed to investigate the effective role of CaO/SiO<sub>2</sub> ratio on the composition and recycle the natural waste represented in chicken eggshells as calcium oxide (CaO) source. The current study focused on preparing calcium silicates by environmental method. For this reason, the eggshells have been subjected to heat treatment in the air at 900 °C for 12 hours, to extract CaO. Whereas the silica (SiO<sub>2</sub>) has been prepared as following starting from silica gel by intensive ball milling for 3 hours in dry conditions. Different ratios have been produced, pressed in dry conditions at room temperature, and heated at 800 °C for 1 hour. The elemental composition, structural and morphological properties have been investigated by extensive analytical tools.

### **(PACC-P046-2022) Glass for Environmental Sustainability – An Overview**

M. Mahapatra<sup>\*1</sup>; S. Gupta<sup>2</sup>

1. University of Alabama at Birmingham, Materials Science and Engineering, USA
2. University of North Dakota, Mechanical Engineering, USA

Multicomponent glasses are reliable sources of various ions, and macro and micronutrients for plant growth. Flexibility in chemistry modification is the major advantage to introduce desired ions and inorganic nutrients into a glass system for tuning physicochemical properties. Controlled leaching of selective ions from glass can be exploited for immobilization of toxic elements in water and soil and smart fertilizer use for environmental sustainability. This study highlights the prospects of inorganic glasses for water and soil treatment as well as corrosion prevention in water supply infrastructure.

We shall provide an overview on the R&D progress in this area based on literature review. We shall focus on the role of different glass network formers and modifiers on controlled ion release mechanisms.

**Tuesday, July 26, 2022**

## **PACC2: Advanced Ceramics and Composites**

### **Advanced Ceramics; Novel Synthesis; Structural Ceramics and Composites**

Room: Vitri (Level M)

Session Chair: Mangalaraja Ramalinga Viswanathan, Universidad Adolfo Ibáñez

**8:30 AM**

#### **(PACC-S2-006-2022) Bidisperse magneto-rheological fluids consisting of functional SPIONs added to commercial MRF (Invited)**

M. Nejatpour<sup>\*1</sup>

1. Sabanci University, Material Science Engineering, Turkey

Magnetorheological fluids (MRFs) are smart materials with a reversible and fast transition from a liquid to a semi-solid state when an external magnetic field is applied (magnetorheological effect). The sedimentation of micron-sized magnetic particles in commercial MRFs is a crucial problem limiting the long-term use in industrial applications. Here, we develop a new MRF based on commercial 140-CG LORD<sup>®</sup> with the addition of surface functional superparamagnetic iron oxide nanoparticles (SPIONs). These new bidisperse MRFs are comprised of either poly(acrylic acid) (PAA) coated SPIONs or lauric acid (LA) coated SPIONs and micron-sized fatty acid-coated magnetic particles of the commercial MRF. SPIONs have specific coatings to interact with the fatty acid coating of the micron-sized Fe-particles. Sedimentation behaviour and the magnetorheological properties of these bidisperse MRFs with 6–12 wt% SPION were examined. Bidisperse MRFs improved the stability and redispersibility of MRFs. Bidisperse MRFs with 12 wt% SPION-PAA showed similar or better magnetorheological behaviour than the commercial MRF despite lower content of the micron size Fe-particles.

**9:00 AM**

#### **(PACC-S2-007-2022) Tb<sub>2</sub>CoFeO<sub>6</sub> ferromagnetic semiconductor: An experimental and theoretical correlation of physical properties**

X. A. Velásquez<sup>\*1</sup>; V. Estrada Contreras<sup>1</sup>; C. E. Deluque Toro<sup>2</sup>; D. A. Landínez Téllez<sup>1</sup>; J. Roa-Rojas<sup>3</sup>

1. Grupo de Física de Nuevos Materiales, Universidad Nacional de Colombia, Física, Colombia
2. Universidad del Magdalena, Colombia
3. Universidad Nacional de Colombia, Physics, Colombia

Complex perovskite-type compounds constitute one of the most studied families of materials due to the wide range of applications based on the compositional tunability of their physical properties. In the present work we report the study of the structural, magnetic, semiconducting, electronic and thermophysical properties of complex perovskites with stoichiometric formula Tb<sub>2</sub>CoFeO<sub>6</sub>. An exhaustive theoretical-experimental study of this double perovskite type compound is carried out by correlating the responses measured by different experimental techniques with ab-initio calculations in the framework of the Density Functional Theory and thermodynamic properties by means of the Debye quasi-harmonic

model. The results obtained reveal the applicability of this type of complex perovskites in spintronics technology.

**9:20 AM**

**(PACC-S2-008-2022) Progress and challenges towards additive manufacturing of ceramic**

Y. Yang\*<sup>1</sup>

1. Shanghai Institute of Ceramics, Chinese Academy of Sciences, China

Ceramic and related materials are widely used in various industry, military and engineering fields. The emergence of additive manufacturing (AM) technologies provides a new approach for the fabrication of structural and functional ceramic products. This submission systematically reviews the additive manufacturing technologies of ceramic developed in recent years, including Indirect Additive Manufacturing (Indirect AM) and Direct Additive Manufacturing (Direct AM) technologies. This submission also summarizes the key scientific and technological challenges for the additive manufacturing of ceramic, and also forecasts its possible future opportunities.

**9:40 AM**

**(PACC-S2-009-2022) Garnet-based All-Solid-State Li Batteries by advanced sintering**

M. Ihrig\*<sup>1</sup>; A. M. Laptev<sup>1</sup>; T. Mishra<sup>2</sup>; M. Finsterbusch<sup>3</sup>; O. Guillon<sup>4</sup>

1. Forschungszentrum Juelich, IEK-1, Germany
2. Institute of Energy and Climate Research IEK-1: Materials Synthesis and Processing, Forschungszentrum Jülich GmbH, Germany
3. Forschungszentrum Juelich, IEK-1, Germany
4. Forschungszentrum Juelich, IEK-1, Germany

Garnet-based  $\text{Li}_7\text{La}_3\text{Zr}_2\text{O}_{12}$  (LLZ) all-solid-state Li batteries (ASBs) are considered the next generation of Li batteries. Fabrication of such ASBs requires co-sintering of the cathode active material (CAM) and electrolyte. However, the conventional co-sintering of CAM and LLZ leads to non-conductive side phases as a result of long exposure to high temperatures. Advanced sintering shortens the dwell time and reduces the sintering temperature are required to maintain phase purity. Ultrafast high-temperature sintering (UHS) can sinter bulk sinter-additive-free LLZ pellets within seconds, kinetically inhibiting side reactions. Although the sintering process is short, a mechanically stable, phase pure, and sufficiently dense LLZ with good ionic conductivity is obtained. The introduced UHS process is predestined for co-sintering of LLZ and CAMs, as it could help to overcome thermodynamic limitations and avoid the formation of a diffusion-based secondary phase, which enables CAM/LLZ combinations which were unsuitable so far. Another technique is Field Assisted Sintering Technique/Spark Plasma Sintering. The application of high mechanical pressure allows to lower the sintering temperature and reduce the dwell time to minutes for the fabrication of functional  $\text{LiCoCO}_2$  (LCO)/LLZ solid-state battery components e.g. dense and thick LCO/LLZ composite cathodes providing a good utilization of LCO and leading to a high areal capacity.

**10:20 AM**

**(PACC-S2-010-2022) High Reliable High-K Dielectric Oxide-Based Nanolaminates for Next Generation Logic Analog and Memory Semiconductor Devices**

E. De Obaldía\*<sup>1</sup>; Y. Chen<sup>2</sup>; O. Auciello<sup>3</sup>

1. Universidad Tecnológica de Panamá, Facultad de Ciencias y Tecnología, Panamá
2. MicroSol Technologies Inc, USA
3. University of Texas at Dallas, Material Science Engineering, USA

A novel material structured in thin film form, Sub-Nanometer Periodic Stack Dielectrics (SN-PSD) has been developed for applications to a new generation of logic analog and memory semiconductor micro/nano-devices. Compared with conventional single

layer dielectric films, SN-PSD exhibits substantial improvement in dielectric breakdown voltage ( $\sim 2.4\text{V}$ , or 35% improvement), and reduced leakage current by about one order of magnitude. The SN-PSD would also be suitable for use as a gate dielectric in silicon carbide (SiC) CMOS FETs for its low leakage current and high breakdown voltage. Existing single-layer-dielectric capacitors often have a large footprint and have issues with high leakage current and early dielectric breakdown, making their use in developing devices problematic. Compared to single layer  $\text{HfO}_2$  capacitors, the breakdown mechanism of the newly developed  $\text{HfO}_2/\text{TiO}_2$  SN-PSD capacitors have been changed from hard breakdown to soft breakdown. The capacitance voltage (C-V) characteristics have been analyzed. The charge and discharge cycle has been studied for 10,000 cycles without degradation. The frequency response of capacitor has been characterized for frequencies of 10Hz, 100KHz, and 1MHz. Underlying mechanisms for the SN-PSD functionalities will be discussed.

**10:40 AM**

**(PACC-S2-011-2022) Spark plasma sintered triplet composites of SiC,  $\text{TiB}_2$  and ZrN**

S. Chodisetti\*<sup>1</sup>; V. B<sup>1</sup>

1. Indian Institute of Technology Roorkee, Department of Metallurgical and Materials ENgineering, India

Highly dense triplet composites of SiC with  $\text{TiB}_2$  and ZrN were processed at a relatively lower sintering temperature ( $1800\text{ }^\circ\text{C}$ ) and shorter holding time (5 min) under 30 MPa pressure in a nitrogen atmosphere. The influence of 10 to 30 vol % ( $\text{TiB}_2 + \text{ZrN}$ ) reinforcement on density, mechanical properties, and electrical properties of the composites was investigated. The microstructures and phase analysis of sintered composites confirm suppression of grain growth and  $\beta \rightarrow \alpha$  phase transformation in the SiC matrix. Fracture toughness varied from 4.1 to 4.6  $\text{MPa}\cdot\text{m}^{0.5}$ , and hardness varied from 19.2 to 20.3 GPa with a change in reinforcement amount. The electrical conductivity of the triplet composites continuously increased with reinforcement amount. The sintered triplet composites were successfully cut using wire-EDM to demonstrate possible alternatives for conventional machining of non-oxide ceramics.

## **PACC1: Ceramics for Energy and Environment**

### **Fuel, Oxide Cells and Similar Topics**

Room: Revolution (Level B)

Session Chair: Henry Colorado L., Universidad de Antioquia

**10:20 AM**

**(PACC-S1-007-2022) Glasses and ceramics as joining and coating materials for energy conversion: Issues and perspectives (Invited)**

F. Smeacetto\*<sup>1</sup>; M. Salvo<sup>2</sup>; M. Ferraris<sup>3</sup>

1. Politecnico di Torino, Applied Science and Technology, Italy
2. Politecnico di Torino, Italy
3. Politecnico di Torino, Department of Applied Science and Technology, Italy

Enhanced efficiency and durable electrochemical energy conversion systems (i. e. solid oxide cells, SOC) can be achieved only by a reliable joining and integration technology. The development of seals for SOCs is still a significant challenge as they must meet very restrictive requirements, withstand the severe environment of the solid oxide cells and be thermo-mechanically compatible with ceramic and metallic substrates. Glasses and glass-ceramics are likely to be the materials of choice, because of superior gas tightness in comparison with other types of sealants and higher stability in extreme working conditions, depending on the stack operating temperature (T range  $750\text{-}850^\circ\text{C}$ ). Another key aspect concerning

durability of solid oxide cells is to produce well performing protective ceramic coatings for metallic interconnects, with particular focus on the deposition method and the sintering treatment. This presentation will give a review of current solutions and challenges related to design processing and sintering behavior of different glass-ceramics and ceramics. It will show how these materials play a fundamental role in the SOC integration technology, pointing out some unanswered questions about their stability and perspectives for further research.

**10:50 AM**

**(PACC-S1-008-2022) Advanced Ceramics for Energy Systems and Environmental Technology (Invited)**

A. Michaelis\*<sup>1</sup>

1. Fraunhofer IKTS, Germany

Advanced ceramic materials and manufacturing technologies offer enormous potential for disruptive innovations in the fields of energy conversion and storage. We present new results for the development of Fuel Cell, Electrolysis Systems, Li-Ion and high temperature NaNiCl batteries for mobile and stationary applications. For the illustration of the potential of advanced ceramic materials in environmental technology, ceramic membrane systems are discussed. Ceramic membranes can be used for micro-, ultra- or nano- filtration of liquids, e.g. for the treatment of industrial waste water. Further innovations require an improved control and reduction of pore size. This allows for new applications in gas separation and pervaporation. For this, pores sizes below 1 nm have to be generated using specific structural features of selected materials. Several new methods for preparation of such nano-porous membranes are presented.

**11:20 AM**

**(PACC-S1-009-2022) Optimized Strategies for the Recovery of Critical Raw Materials from end-of-life Solid Oxide Cells**

S. Fiorilli\*<sup>1</sup>; S. Saffirio<sup>1</sup>; S. Fiore<sup>6</sup>; M. Santarelli<sup>2</sup>; I. Schiavi<sup>3</sup>; S. Pylypko<sup>4</sup>; F. Smeacetto<sup>5</sup>

1. Politecnico di Torino, Applied Science and Technology, Italy
2. Politecnico di Torino, Energy, Italy
3. Environment Park S.p.A., Italy
4. Elcogen AS, Estonia
5. Politecnico di Torino, Applied Science and Technology, Italy
6. Politecnico di Torino, Environment, Italy

As part of FCH (fuel-cell and hydrogen) technologies, solid oxide cells (SOCs) provide a mature alternative solution to conventional power-generation sources to achieve the EU carbon-neutrality goal set for 2050. However, the full deployment of SOC is still hindered by the lack of efficient, scalable and cost-effective end-of-life (EoL) strategies enabling the management and valorization of waste products derived from stacks operation and avoiding their landfill disposal. The BEST4Hy project, funded by the EU's Horizon 2020, aims at the development and validation of efficient and scalable recovery pathways for critical raw and hazardous materials including rare earth elements, cobalt and nickel from EoL SOC in view of recycling for cells re-manufacturing. The present study aims at the development of a process specifically adapted for SOC dismantled from stacks for the efficient recovery of yttria-stabilized zirconia and Ni, contained in both fuel electrode and electrolyte, and La and Co (as critical raw material) both present in the perovskite structure of the oxygen electrode. This project has received funding from the Fuel Cells and Hydrogen 2 Joint Undertaking under grant agreement No 101007216. This Joint Undertaking receives support from the European Union's Horizon 2020 research and innovation programme, Hydrogen Europe and Hydrogen Europe research.

## **PACC3: Densification and Microstructural Evolution in Ceramics During Sintering**

### **Sintering II**

Room: Millennium (Level B)

Session Chair: Hector Camacho Montes, Universidad Autonoma de Ciudad Juarez

**8:30 AM**

**(PACC-S3-007-2022) Supercompatibility in Ceramic Micropillars of LaNbO<sub>4</sub> (Invited)**

O. A. Graeve\*<sup>1</sup>; H. Hosseini-Toudeshki<sup>1</sup>

1. University of California, San Diego, Mechanical and Aerospace Engineering, USA

Superelastic materials represent a distinct family of compounds with the ability to manifest reversible deformation in response to an applied stress. Generally, superelastic materials are metallic in nature, and only very few ceramics have been shown to fully or partially display this response. Here, we describe exceptional superelasticity and enhanced reversibility on micropillars of LaNbO<sub>4</sub> ceramic in response to compressive stresses up to 1100 MPa without fracture. The micropillars were prepared by focused ion beam machining from specimens consolidated by spark plasma sintering. The material response to stress is consistent with the theory of supercompatibility (cofactor theory) that has been reported to address the enhanced reversibility and low-hysteresis behavior (i.e., improved superelasticity) of certain shape memory metallic alloys. This makes LaNbO<sub>4</sub> a unique addition to the germane family of smart materials for applications as long-lived actuators impacting the automotive, energy and aerospace sectors, among many other technologically significant fields, especially in extreme conditions (i.e., higher temperatures or pressures) under which ceramics excel compared to metals.

**9:00 AM**

**(PACC-S3-008-2022) Structural and microstructural evolution of BCZT perovskite doped with vanadium**

G. M. Herrera-Perez\*<sup>1</sup>; R. Borja-Urby<sup>2</sup>; C. Ornelas-Gutierrez<sup>3</sup>; A. Reyes-Rojas<sup>4</sup>; F. Paraguay-Delgado<sup>5</sup>; L. Fuentes-Cobas<sup>6</sup>

1. CONACYT, Mexico
2. CNMN-IPN, Mexico
3. Nanotech-CIMAV, Mexico
4. CIMAV, Mexico
5. CIMAV, Mexico
6. CIMAV, Mexico

In this work, we present the structural, microstructural evolution, and multiplet structure of vanadium-doped Ba<sub>0.9</sub>Ca<sub>0.1</sub>Ti<sub>0.9-x</sub>Zr<sub>0.1</sub>V<sub>x</sub>O<sub>3</sub> ceramics. All the ceramics were prepared by the modified Pechini method. The Rietveld refinement of x-ray diffraction patterns using the Fullprof suite software, suggests a perovskite structure with a single tetragonal phase, where Ca<sup>2+</sup> ions occupied the Ba<sup>2+</sup> sites and Zr<sup>4+</sup> and V ions occupied the Ti sites. An increase in lattice volume has been observed in the substitutions of Ti ions for vanadium ions. The morphology of grains, monitored by scanning electron micrographs, exhibits irregular faceted polyhedral shapes with inter-granular and intra-grain porosity. The vanadium L<sub>2,3</sub>-edge core-electron energy loss spectrum analyzed by the multiplet calculation using CTM4XAS software proposes an important presence of a V<sup>3+</sup> oxidation state. Our spectroscopy analysis agrees well with the expected V<sup>3+</sup> substitution in Ti sites that increases the lattice volume. Thermal analysis and Raman spectroscopy complement the characterization of these ceramics. G. H-P thanks to CONACYT-SEP Basic Research Project No. 253605, catedras-CONACYT program No. 580, CONACYT sabbatical award at CNMN-IPN, and CIMAV for the sample preparation and technical assistance.

9:20 AM

**(PACC-S3-009-2022) Transparent magnesium aluminate spinel obtained by spark plasma sintering of sol-gel powders**H. Balmori<sup>\*1</sup>; L. Zarazua<sup>1</sup>; L. Tellez-Jurado<sup>1</sup>

1. National Polytechnic Institute, Metallurgical Eng., Mexico

The aim of this work is to explore the effect of the characteristics of sol-gel powders on the production of transparent magnesium aluminate spinel by spark plasma sintering. Three types of sol-gel nanosize powders were synthesized: Powder 1: amorphous; powder 2: incipient transformation to spinel, and powder 3: fully transformed spinel. The powders were densified by SPS following specific procedures for each one at temperatures of 1250 to 1350°C. Powders 1 and 2 transformed to spinel after SPS. Opaque discs were obtained with powder 1 because it released gases upon heating that generated defects that could not be eliminated by SPS. The densification of powders 2 and 3 was followed with measurements of the grain size and relative density as a function of the SPS temperature. The grain size (GS) of the samples obtained with the powders 2 and 3 were < 500 nm, except for the specimen obtained with powder 3 fired at 1300°C, which had a GS = 1098 nm. The powder 2 had better sinterability than powder 3 because it achieved higher density and smaller grain size upon sintering at similar conditions. Maximum in-line transmittance of 71 %, 99.98 % relative density and GS = 604 nm were obtained with the powder 2 sintered at 1325°C. It is shown that transparent magnesium aluminate spinel is obtained with a nanosize untransformed spinel sol-gel powder and spark reaction sintering.

9:40 AM

**(PACC-S3-010-2022) Densification behavior of Yb<sub>2</sub>O<sub>3</sub> with an addition of TiO<sub>2</sub>**S. Mait<sup>\*1</sup>; Q. Li<sup>1</sup>; F. Peng<sup>1</sup>; R. Bordia<sup>1</sup>

1. Clemson University, Materials Science and Engineering, USA

The densification behavior of ytterbia (Yb<sub>2</sub>O<sub>3</sub>) in presence of titania doping at different temperatures was investigated and compared with pure ytterbia. The cross-sectioned surfaces of doped and pure ytterbia were examined with a scanning electron microscope (SEM). It was found that titania doping has significant influence on densification of ytterbia up to a certain doping level. The result of titania doping on crystal structure confirms that titania is substituted into ytterbia up to the solubility limit, which is in agreement with the densification results. It is postulated that titania-doped ytterbia densifies faster because of cation vacancy formation and lattice distortion. The activation energy for densification has been determined by constant heating rate experiments. The results indicate that the activation energy is independent of the density in the intermediate stage of sintering (60 to 85%). Titanium doped ytterbia have a higher activation energy for densification than pure ytterbia.

10:20 AM

**(PACC-S3-011-2022) Advanced processing of oxide ceramics for energy applications by cold sintering (Invited)**M. Bram<sup>\*3</sup>; K. Nur<sup>1</sup>; M. Kindelmann<sup>1</sup>; O. Guillon<sup>2</sup>

1. Forschungszentrum Juelich, Institute IEK-1, Germany
2. Forschungszentrum Juelich, IEK-1, Germany
3. Forschungszentrum Juelich, Institute IEK-1, Germany

A promising new way of processing ceramics is cold sintering, which relies on the densification of ceramic powders at significantly reduced sintering temperatures. Cold sintering is based on the application of high pressure in combination with liquid sintering aids like pure water, dissolved precursors or pH modifiers. Using ZnO as model material, role of starting powder characteristics like agglomeration propensity on densification was investigated. For better understanding the microstructure evolution during cold sintering, related TEM investigations revealed formation of stacking faults and residual amorphous phases on grain boundaries as important influencing factors on densification and resulting mechanical properties.

Hardness, elastic modulus and compressive strength were measured by nano-indentation and micro-pillar tests. It has been found that mechanical properties of cold sintered ZnO were quite comparable to conventionally sintered ZnO. Based on the findings of this fundamental study, cold sintering has been successfully integrated in the processing chain of advanced ceramic materials for energy applications. Cold sintering of lithium manganese oxide powders enabled manufacturing of high rate/capability lithium-ion battery cathodes. Cold sintering of barium cerate zirconate powders was found to improve manufacturing of proton conducting membranes for hydrogen applications.

10:50 AM

**(PACC-S3-012-2022) Fast Firing of Porcelain Stoneware Tiles in 20 Minutes Cold-to-Cold**C. Conceição<sup>1</sup>; D. E. Garcia<sup>1</sup>; A. De Noni Junior<sup>1</sup>; D. Hotza<sup>\*1</sup>

1. Federal University of Santa Catarina, Brazil

Dense and crack-free porcelain stoneware showing water absorption ≤ 0.1% and fracture strength ≥ 50 MPa has been fabricated by fast firing in about ¼ of the time required by a conventional schedule. Powder compacts formed by uniaxial pressing were introduced in a preheated furnace at temperatures between 1190 and 1240 °C, hold during 5 to 15 min, removed from the furnace and allowed to cool in air. The short residence time in low temperature regions prior to melt formation enhanced densification with respect to pore growth. Moreover, reduced soaking time at high firing temperatures affected the physical and chemical properties of liquid phase formed and the amount, morphology and size of the porosity.

11:10 AM

**(PACC-S3-013-2022) Microstructure and mechanical properties of B<sub>4</sub>C–TiB<sub>2</sub> ceramic composites prepared via a two-step method**Q. He<sup>\*1</sup>; W. Guo<sup>1</sup>; W. Wang<sup>1</sup>

1. Wuhan University of Technology, China

B<sub>4</sub>C–TiB<sub>2</sub> ceramic composites were fabricated by a two-step method. First, B<sub>4</sub>C–TiB<sub>2</sub> composite powders were synthesized from TiC–B powder mixtures at 1400 degrees, then mixed with commercial B<sub>4</sub>C powders by ball milling and the B<sub>4</sub>C–TiB<sub>2</sub> ceramic composites were prepared by hot pressing at 1950 degrees. This two-step method not only effectively refined TiB<sub>2</sub> grains, but also allowed the composition of the composites to be freely designed. The microstructure and mechanical properties of the composites were investigated. The results showed that the B<sub>4</sub>C–TiB<sub>2</sub> ceramic composite with a 10 wt% TiB<sub>2</sub> content obtained the ideal comprehensive performance, with a volume density, Vickers hardness, bending strength, and fracture toughness of 2.61 g/cm<sup>3</sup>, 35.3 GPa, 708 MPa, and 5.82 MPa•m<sup>1/2</sup>, respectively. The advantages of the in-situ reaction process were fully exerted by the two-step method, which made a remarkable contribution to the excellent properties of B<sub>4</sub>C–TiB<sub>2</sub> ceramic composites.

11:30 AM

**(PACC-S3-014-2022) Temperature-dependent impulse excitation as a tool for monitoring phase transitions and microstructural changes in ceramics**W. Pabst<sup>\*1</sup>; E. Gregorova<sup>1</sup>; P. Simonova<sup>1</sup>

1. University of Chemistry and Technology, Prague, Department of Glass and Ceramics, Czechia

The impulse excitation technique / IET is a well-established method for measuring elastic constants and damping of ceramics. While IET measurements at room temperature can provide useful information which may be confronted theoretical predictions (e.g. elastic moduli predicted for a given phase composition and porosity via rigorous micromechanical bounds or model relations such as effective medium approximations), temperature-dependent IET measurements can provide much more information. This contribution gives an overview of temperature-dependent IET measurements, with a

focus on recent results concerning silica-based materials, including sandstone, mullite-based ceramics and oxide ceramics, mainly the intriguing case of tin oxide, where sintering occurs without shrinkage and thus changes in elastic properties are exclusively due to pore surface curvature changes. It is shown that the elastic anomaly of sandstone (due to the transition from low-temperature to high-temperature quartz), as determined by the IET, may throw new light on the question of auxetic behavior. Further it is shown that some IET results indicate a diffuse phase transition in mullite-based ceramics. And last but not least, it is shown that the elastic moduli of tin oxide ceramics increase when the pore surface curvature decreases, although the porosity remains the same.

### **PACC8: Novel, Green, and Strategic Processing and Manufacturing Technologies**

#### **Novel, Green, and Strategic Processing II**

Room: Bellagio (Level B)

Session Chair: Vania Salvini, UFSCar, Brazil

**8:30 AM**

#### **(PACC-S8-001-2022) Efficient Water Splitting on Hematite Thin Films – A Pathway to Solar Hydrogen (Invited)**

S. Mathur\*<sup>1</sup>

1. University of Cologne, Institute of Inorganic Chemistry, Germany

Metal oxide nanostructures with hetero-contacts and phase boundaries offer unique platform for designing materials architectures for energy harvesting applications. Photoelectrochemical (PEC) water splitting has emerged as a competitive technology being capable of converting solar energy directly into chemical energy using stable and efficient photocatalysts for solar hydrogen production. Besides the size and surface effects, the modulation of electronic behaviour due to junction properties leads to modified surface states that promote selective decomposition of analytes and adsorbates. The growing possibilities of engineering nanostructures in various compositions (pure, doped, composites, heterostructures) and forms has intensified the research on the integration of different functional material units in a single architecture to obtain new photocatalytic materials. We report here on the influence of external magnetic fields applied parallel or perpendicular to the substrate during plasma enhanced chemical vapor deposition (PECVD) of hematite ( $\alpha$ -Fe<sub>2</sub>O<sub>3</sub>) nanostructures. Investigations on the water splitting properties of the hematite films in a photoelectrochemical reactor revealed superior photocurrent values of hematite photoanodes deposited in external magnetic field.

**9:00 AM**

#### **(PACC-S8-008-2022) Silicon-Based Anode Materials for Advanced Lithium and Sodium Ion Batteries (Invited)**

R. Riedel\*<sup>1</sup>; M. Graczyk-Zajac<sup>2</sup>

1. TU Darmstadt, Materials Science, Germany
2. EnBW, Germany

The increase in energy density and power density requirements for lithium and sodium ion batteries leads to continuous research for new electrode materials. Various insertion materials have been proposed as negative electrodes for rechargeable batteries. In Li-ion batteries, the highest theoretical capacity can be obtained when using metallic lithium (3862 mAh/g)

or elemental silicon forming lithium rich alloys (3578 mAh/g), however these materials are not commercialized due to safety reasons and rapid capacity fading, respectively. At present, mostly graphitic materials are used due to low price and high reversibility despite relatively low capacity (372 mAh/g), instability during long time cycling and inadequacy high power applications. Therefore, new materials, which are economically interesting but demonstrate higher capacity, longer life time and better high rate capability are urgently required to meet the technological demands of our future electromobility and energy storage applications. In this context, novel anode materials based on ceramic nanocomposites comprised of ternary SiCN and SiOC systems are discussed and evaluated in terms of their electrochemical performance with respect to application in Li- and Na-ion batteries.

**9:30 AM**

#### **(PACC-S8-009-2022) Colloidal methods for fabrication of supercapacitor electrodes with high active mass (Invited)**

I. Zhitomirsky\*<sup>1</sup>

1. McMaster University, Canada

New colloidal methods have been developed for the fabrication of composites for energy storage in supercapacitors with high active mass loadings. The methods allowed for enhanced performance and facilitated the fabrication of electrodes and devices with high areal capacitance. Biosurfactants were used as capping agents for synthesis of Mn<sub>3</sub>O<sub>4</sub> nanoparticles for cathodes and Fe<sub>3</sub>O<sub>4</sub> nanoparticles for anodes. The shape and size of the nanoparticles were influenced by the capping agents. New co-dispersants were developed for co-dispersion of oxide nanoparticles, MXenes and carbon nanotubes for the fabrication of composite electrodes. The analysis of electrochemical testing results provided an insight into the influence of the chemical structure of the dispersants on their adsorption on different materials and co-dispersion. New redox-active dispersants were developed, which facilitated charge transfer and allowed for high capacitance. Advanced dispersants were developed, for the formation of coated nanoparticles. Heterocoagulation techniques were developed for the fabrication of advanced nanocomposites, which were based on two different types of surfactants and different heterocoagulation mechanisms, such as electrostatic heterocoagulation or Schiff base reactions. The obtained electrodes and devices showed promising performance for energy storage in supercapacitors.

**10:20 AM**

#### **(PACC-S8-010-2022) Aqueous Processing of Garnet-Type Li-Ion Conductors Enabled by Reversible Li<sup>+</sup>/H<sup>+</sup> Exchange**

R. Ye\*<sup>1</sup>; M. Finsterbusch<sup>2</sup>; E. Figgemeier<sup>3</sup>

1. Forschungszentrum Jülich Institut für Energie- und Klimaforschung, Materials Synthesis and Processing (IEK-1), Germany
2. Forschungszentrum Jülich, IEK-1, Germany
3. Institute for Power Electronics and Electrical Drives (ISEA), RWTH Aachen University, Germany

The garnet-type Li-ion conductor is regarded as one promising oxide-ceramic solid electrolyte material. However, a spontaneous Li<sup>+</sup>/H<sup>+</sup> exchange reaction<sup>1</sup> takes place when garnets are processed in protic solvents or even in ambient air. The protonated garnets impair the Li-conducting performance, and the degraded surface hinders the Li-ion transport with the Li metal anode. Recent findings about the underlying chemical mechanisms lead to the development of mitigation strategies. The Li<sup>+</sup>/H<sup>+</sup> exchange can be reversed at elevated temperature in the presence of excess Li sources, for which LiOH and Li<sub>2</sub>CO<sub>3</sub> are commonly used. Herein, we demonstrated a water-based tape casting route to fabricate free-standing garnet separators with thicknesses below 150  $\mu$ m.<sup>2</sup> In this sustainable processing route, the water-soluble biopolymer methylcellulose is used as binder, and the eco-friendly polyethylene glycol and glycerol as plasticizers. After sintering at 1175 °C, excess Li species reentered the garnet structure and underwent reversed Li<sup>+</sup>/H<sup>+</sup> exchange,

resulting in the formation of stoichiometric cubic garnet phase with the ionic conductivity of  $0.15 \text{ mS cm}^{-1}$  at room temperature. Our developed aqueous tape-casting process paves a green way to fabricate garnet separators, which is suitable to be employed in solid-state lithium batteries.

#### 10:40 AM

##### (PACC-S8-011-2022) Novel single crystalline materials, growth and characteristics (Invited)

K. Shimamura<sup>\*1</sup>; E. G. Villora<sup>2</sup>; D. Yuan<sup>2</sup>; L. Vaschalde<sup>2</sup>

1. National Institute for Materials Science, Japan
2. National Institute for Materials Science (NIMS), Japan

Optoelectronic technology progress in a wide range of applications, and still demands the further development. Here, novel single crystalline materials with advantageous characteristics will be introduced. Ce:YAG single-crystal phosphors (SCPs) which could be promising for high-brightness (HB) lighting, have been proposed. SCPs exhibit an outstanding internal quantum efficiency (QE); over 95%, until 300°C. Binder-free SCP powder plate is also demonstrated, and it has shown the same performance. Authors would like to thank to Tamura Corp. for the collaboration. Ce:Li<sub>6</sub>Y(BO<sub>3</sub>)<sub>3</sub> (LYBO) is a promising thermal neutron scintillator. 1 inch crack-free bulk single crystals of Ce:LYBO were grown by optimizing the growth conditions. The grown crystals show significant rise in quantum efficiency (QE), which was enhanced from zero to > 40%. Consequently, the scintillation performance of LYBO was improved, showing great potential for thermal neutron scintillation applications. PZT ceramics that exhibit large piezoelectric coefficients show very low Curie Temperatures T<sub>c</sub>, and vice-versa. Furthermore, PZT contains toxic Pb, which is recommended to be replaced by RoHS and WEEE regulations. Present work focuses on the alternative family of the Potassium-Sodium-Niobates (KNN). Optimized conditions led to highly reproducible results with record values for undoped KNN.

#### 11:10 AM

##### (PACC-S8-012-2022) Green synthesis of metal-carbon nanocomposites for energy- and bio-related applications (Invited)

W. Lin<sup>1</sup>; S. Ozeki<sup>1</sup>; T. Akiyama<sup>2</sup>; S. Sharma<sup>1</sup>; S. Elnobi<sup>1</sup>; Y. Yaakob<sup>3</sup>; M. Yusop<sup>4</sup>; Y. Yang<sup>5</sup>; M. Tanemura<sup>\*1</sup>

1. Nagoya Institute of Technology, Department of Physical Science and Engineering, Japan
2. F.C.C. Co., Ltd, Japan
3. Universiti Putra Malaysia, Department of Physics, Faculty of Science, Malaysia
4. Universiti Teknologi Malaysia, Department of Materials, Faculty of Mechanical Engineering, Malaysia
5. Shanghai Institute of Ceramics, Chinese Academy of Sciences, China

Carbon-based nanomaterials, such as graphene, is one of the key materials in nanotechnology and energy-related devices. For their applications especially for the green manufacturing, the synthesis temperature should be reduced as low as possible, ideally to room temperature (RT). Ion irradiation onto the solid surface sometimes entails the formation of various types of surface nanostructures even at RT, and their composition is readily controllable by a simultaneous supply of other elements during ion irradiation. So, the ion irradiation is promising for the green synthesis of nanomaterials, being dealt with in this talk. For the carbon-based nanomaterials, graphitization is also the important factor. The selection of the metal included in the carbon-based nanomaterials leads even to the spontaneous local graphitization at RT. Surprisingly, the metallic state is still preserved even after the air exposure for the Li-carbon nanocomposites prepared by the ion irradiation method, which will be usable for the future battery application. In this talk, the highly sensitive detection of COVID-19 virus using ion-induced nanostructures will be also demonstrated.

#### 11:40 AM

##### (PACC-S8-013-2022) Fabrication of Nanomaterial processing for SDGs (Invited)

Y. Hayashi<sup>\*1</sup>

1. Tohoku University, School of Engineering, Japan

Nanomaterial is useful of energy saving and environmental purification for SDGs. However the practical use of the nanomaterial did not advance very much, because of nanomaterial price. In general, nanomaterial synthesis is low yield and high environment impact, high cost in traditional processing. The innovative processing with new concept is necessary for the promotion in practical use of the nanomaterial. We developed the nanomaterial processing of the new concept to solve a conventional problem. It is our process using liquid-solid reaction which raw materials do not dissolve in a solvent. Liquid-solid reaction enable high concentrated synthesis. Our process uses oxide and metal to solid raw materials. Therefore harmful counter anion such as the nitric acid does not exist. Ultrasound and Microwave is used as reaction energy. Everyone can use it as ultrasonic cleaner and microwave oven in laboratory. By these combinations, our process can realize SDGs in the processing of the nanomaterial. In presentation, various nanomaterials (metal, ceramics, nanocomposite) are introduced by application of this concepts for SDGs.

### PACC11: Materials Approach to Art, Architecture, and Archaeology in the Americas

#### Petrography & Technology

Room: Venetian (Level B)

Session Chair: Christina Bisulca, Detroit Institute of Arts

#### 8:30 AM

##### (PACC-S11-001-2022) Anna O. Shephard (1903–1973): Materials Science Methods in Archaeological Ceramic Analysis

M. D. Jackson<sup>\*1</sup>; C. Bisulca<sup>2</sup>

1. University of Utah, Geology and Geophysics, USA
2. Detroit Institute of Arts, USA

Anna O. Shepard developed interdisciplinary methods of ceramic analysis to describe the physical and material properties of pottery and compositions, sources and properties of its raw constituents. She created a materials science foundation for ceramic cultural heritage, yet reflections on her contributions focus mainly on anthropological pottery making techniques and recognition of these techniques in archaeological potsherds. Shepard emphasized mineralogical analyses with X-ray diffraction and petrographic microscopy since “minerals and rocks are the potter’s principal materials.” They are also the materials of pigments, glazes, stone artifacts, and ancient concretes. Shepard used microchemical, spectroscopic and thermal analyses to describe archaeological ceramics and crystallographic properties of clays and tempers; she reverse engineered these materials to gain insights into production methods. She foreshadowed in situ spectroscopic, X-ray microdiffraction and microfluorescence, and neutron activation applications in ceramic technology studies. The Art, Archaeology and Conservation Science award of the American Ceramic Society brings recognition to her contributions to chemical, physical and crystallographic properties of art and archaeological materials, geological and natural resources used in their fabrication, and cultural archaeological and artistic interpretation of these data.

8:50 AM - **WITHDRAWN**

**(PACC-S11-002-2022) Conventional Microscopy and Thin Section Petrography in the Reduction of Ceramic Typological Variability at the Olmec Site of Los Soldados, Mexico (Invited)**

E. H. Huerta\*<sup>1</sup>

1. UC Davis/CSU Fullerton, Anthropology, USA

The degradation of archaeological ceramic materials in tropical environments presents a challenge to archaeologists attempting to reconstruct typologies, chronologies, and the organization of craft production. This challenge becomes more relevant in archaeological sites excavated for the first time lacking an established comparative collection. While regional comparative collections offer a possible solution to the problem, it is important to understand the organization of pottery production for newly excavated sites in order to maximize the use of regional comparative collections. This paper presents the results of conventional microscopy and thin-section petrographic analysis identifying paste properties and temper distribution in the pottery assemblage from the Olmec Middle Formative (1000 - 400 BC) site of Los Soldados, Mexico. This study attempts to illustrate the usefulness of conventional microscopy coupled with petrographic analysis in order to reduce typological variation, reduce uncertainty regarding highly fragmented or eroded pottery fragments, maximize the use of available regional comparative collections, and minimize the inherent damage of the technique to cultural materials.

9:20 AM

**(PACC-S11-003-2022) Early Formative ceramic production in western Mesoamerica: First results of the technological study of Capacha pottery (Invited)**

C. Salgado-Ceballos\*<sup>1</sup>

1. Universidad de Guadalajara, Departamento de Estudios Mesoamericanos y Mexicanos, Mexico

Capacha (1200-900 BCE) is one of the two oldest ceramic complexes known from western Mesoamerica, and the one that all later pottery complexes in the core Colima-Jalisco-Nayarit area seem to stem. Capacha's ceramic repertoire is relatively well known, and while a lot has been written on its resemblances to pottery found elsewhere in the Americas, there is little known regarding the technology and the organization of its production. Using a multi-analytical approach (thin-section petrography, X-ray fluorescence, paleodermatoglyphics), this study assess the technological patterns observed in the raw material selection and processing steps of the production of Capacha pottery in the Colima Valley, the material constraints, such as resource availability, and the sexual divisions of labor behind its production. This study represents the largest and first proper archaeometry-based study of Capacha pottery production, and provides an introduction to our understanding of the organization of Capacha society more broadly.

9:50 AM

**(PACC-S11-004-2022) Early ceramic technology from La Isleta del Pozon and Puerto Hormiga (Colombia)**

D. R. Carvajal Contreras\*<sup>1</sup>

1. Universidad Externado, Archaeology, Colombia

Many archaeological sites on the Caribbean coast of Colombia are characterized by the presence of pottery with diverse decorative features and tempers. These sites with early pottery are located near the coast or inland and are associated with other behavioral traits such as plant production, high mobility and exploitation of animals from estuarine environments. The purpose of this paper is the analysis of two early pottery sites from two shell-mound near Cartagena associated with the Formative period. Using X-ray and visual analysis, this study identifies the pottery manufacturing techniques. The data contribute to the scarcity of regional studies on early

pottery and the variability of its production. Additionally, in order to critically evaluate pottery manufacturing and previous behavioral traits such as mobility, I include environmental and subsistence reconstruction.

### Organics

Room: Venetian (Level B)

Session Chair: Fumie Iizuka, University of California Merced

10:30 AM

**(PACC-S11-005-2022) The Common Thread: Authenticating a Nazca tunic using combined dye analysis by LCMS and radiocarbon dating on a single fiber**

G. D. Smith\*<sup>1</sup>; V. J. Chen<sup>1</sup>; A. Holden<sup>1</sup>; L. Hendriks<sup>2</sup>; N. Haghypour<sup>3</sup>

1. Indianapolis Museum of Art at Newfields, Conservation Science Lab, USA
2. Haute Ecole d'Ingénierie et d'Architecture, Switzerland
3. ETH-Zurich, Laboratory of Ion Beam Physics, Switzerland

Accessioning historic textiles into museum collections requires objective information regarding the object's appropriateness and authenticity. In the case of dyed fibers, evidence of period appropriate dyes builds confidence and reduces the chances of the object being a simple fake produced using modern materials. Increasingly, objective age estimates in the form of <sup>14</sup>C dating are needed to further prove that the naturally occurring materials match the purported date of the textile. These techniques are destructive, requiring a small sample of the object, and are typically conducted separately on individual samples. In 2020, the Indianapolis Museum of Art considered the purchase of a Nazca dyed camelid wool tunic dated to the period 100 BCE – 600 CE. Because of the supple feel and excellent condition of the artifact, concerns were raised internally over its purported age. This report demonstrates for the first time the successful analysis of dyes by liquid chromatography-diode array detection-mass spectrometry and subsequent <sup>14</sup>C dating of the same extracted fibers. The analysis confirmed that the wool fibers were most likely dyed with the common Peruvian dyestuffs *Relbunium ssp* and natural indigo, while the same fibers were dated between 550 and 650 CE. Based on these confirmatory findings, the Nazca tunic was accessioned into the collection.

10:50 AM

**(PACC-S11-006-2022) Physical Characterization of Prehispanic Ceramic Technologies in the Upper Basin of the Ariari River (Colombia)**

R. R. Galindo\*<sup>1</sup>; L. Laura<sup>3</sup>; M. Lopez<sup>2</sup>; D. Contreras<sup>4</sup>; V. Benavides<sup>5</sup>; J. Jaramillo<sup>3</sup>; S. Fajardo<sup>6</sup>

1. Universidad del Magdalena, Antropología, Colombia
2. Universidad de los Andes, Colombia
3. Independiente, Colombia
4. Servicio Geológico Colombiano, Colombia
5. Gmas Lab, Colombia
6. TU-Delft, Faculty of Mechanical, Maritime and Materials Engineering (3mE), Netherlands

Archaeological remains and historical accounts of the Colombian Eastern Plains suggest that ceramic production processes were embedded within an intricate and complex network of local and regional interactions. Archaeological research along the Ariari River about the Guayupe culture dates back to 1970s and have identified abundant ceramic shapes and elaborated decorative motifs. Recently, Cultural Heritage Management projects recorded more variability in terms of shapes and preservation conditions of the ceramics of the region. Nevertheless, it is still unclear how these ceramics were produced and what material properties they had in prehispanic times. This research focused on understanding the production process of ceramics between 1000 and 1330 CE. Conventional thin section petrography, SEM-EDX, FT-IR and DRx techniques allowed

to document physical aspects. These techniques were conducted on eight samples representing a collection of 3000 ceramic sherds. Constant use of organic material as temper was observed in seven of the eight samples. Moreover, among other materials, presence of sedimentary rock and cauxí (*Tubella reticulata* and *Parnula Betesil*) was also observed. DRx analysis on oriented clays presented a challenge in methodological terms due to the presence of large proportion of organic matter (amorphous phases) and non-crystalline material.

**11:10 AM**

**(PACC-S11-007-2022) Phenolic Plant Exudates in the Archaeology of the American Southwest**

C. Bisulca\*<sup>1</sup>; J. B. Lambert<sup>2</sup>; J. A. Santiago-Blay<sup>3</sup>

1. Detroit Institute of Arts, USA
2. Trinity University, Department of Chemistry, USA
3. National Museum of Natural History, Department of Paleobiology, USA

Various plant exudates were utilized as adhesives, coatings, paints, dyes, as well as for medicinal purposes throughout the American Southwest. Anthropological sources document the use of these materials from pines, mesquite, creosote, brittlebush, as well as various polysaccharides derived from seeds, roots and cacti. As part of a long-term study, a comprehensive survey of collections was undertaken spanning the archaeological through to the historic periods. Over 300 samples of resinous materials from artifacts in four different institutions have been characterized with Fourier transform infrared spectroscopy (FTIR). During this survey, a previously unknown phenolic exudate was identified in several artifacts. With further analysis and through collaboration with a larger study on plant exudates using nuclear magnetic resonance (NMR), it was found that pines in addition to the well-known terpenoid exudates also produce a phenolic exudate. This phenolic exudate, likely from Pinyon pine, has been found in Ancestral Puebloan, Mogollon, and Zuni artifacts. Based on use patterns noted in this study, it does not appear that cultures distinguished between the two types of pine exudate. This study will also highlight the importance of correct identification of plant source of exudates to understand their use, processing and trade.

**11:30 AM**

**(PACC-S11-008-2022) 19<sup>th</sup> Century Rubber Manufacture in the United States: Analysis of Objects from the USS Monitor Wreck**

M. K. McGath\*<sup>1</sup>; L. King<sup>1</sup>; L. Haines<sup>1</sup>; H. Fleming<sup>2</sup>

1. The Mariners' Museum and Park, Batten Conservation Complex, USA
2. Henry M. Jackson Foundation supporting supporting Defense POW/MIA Accounting Agency, USA

This paper discusses the manufacture of rubber during the United States of America's Civil War and the conservation of such objects by investigating the composition of objects recovered from the USS Monitor, a marine shipwreck, and treated by conservators at The Mariners' Museum and Park. The composition of rubber artifacts was evaluated using attenuated total reflectance-Fourier transform infrared spectroscopy. The test results reveal the compositions for rubber gaskets from USS Monitor, providing us with a better understanding of rubber manufacture in the 19<sup>th</sup> century as well as how treatment impacts the objects. The majority of tested rubber objects are made with rubber comprised of 1,4-cis-polyisoprene, which is most commonly found from the *Hevea brasiliensis* tree native to South and Central America. Additional tests were conducted to monitor the change in chemistry of three rubber gaskets as they dried to evaluate the effects of drying on the oxidation of the isoprene units. From these experiments it was determined that the most change in the rubber occurs within the first 24 hours. This paper delves into the infrared spectroscopic analyses with the goal of highlighting what this means for the collection and its conservation.

**11:50 AM**

**(PACC-S11-009-2022) Vis-NIR Reflectance Spectroscopy of Plastics in Contemporary Art**

C. L. Bailin\*<sup>1</sup>; E. Homberger<sup>1</sup>; C. Bisulca<sup>1</sup>

1. Detroit Institute of Arts, USA

Rapid, non-invasive plastic identification using NIR reflectance spectroscopy has received limited attention in museum contexts despite its widespread use in industry and its potential to provide insight into the preservation needs of modern and contemporary art collections. Recognizing this, the Detroit Institute of Arts Conservation Department began investigating the technology's efficacy in identifying polymers and gauging the degree of deterioration present in its own collection. A selection of contemporary objects was examined, including the discolored and embrittled original Quasar CRT televisions and display structure from Nam June Paik's Video Flag x (1984); components of Sarah Sze's Sexton (from Triple Point of Water) (2004-5); and Claes Oldenburg's Alphabet/Good Humor (1975) and Profile Airflow (1969). Using a vis-NIR spectrometer (350-2500 nm) with a fiber optic probe, a searchable plastics database was created using reference materials with known compositions, sampled before and after accelerated aging. This technique proved effective in separating common plastics using derivative spectroscopy, and in some cases could also detect additives such as flame retardants and plasticizers. Since recorded spectra includes the visible range, it was often possible to simultaneously determine the colorants used.

**Ferroelectrics Meeting of Americas**

**Dielectrics/Composites/Growth I**

Room: Mirage (Level B)

Session Chair: Jei-Chao, University of Texas, Dallas

**8:30 AM**

**(FMAs-009-2022) Potentials of Biodegradable composite for Energy Storage Devices : Flexible Dielectric Film derived by PLA/PBAT Blends and Porous Clay Heterostructures (Invited)**

H. Manusiya\*<sup>1</sup>

1. Chulalongkorn University, Petroleum and Petrochemical College, Thailand

Polymer materials have distinguished themselves from other materials and have become the dominant dielectrics in film capacitors due to their cost-effectiveness, flexibility, and tailorable functional properties. This work is dedicated to developing a dielectric film from a nanocomposite between biodegradable polymers and modified porous clay with a high dielectric constant but low dielectric loss. Polylactic acid (PLA) is a promising alternative biodegradable polymer to use in a variety of commodity and engineering applications. However, PLA is relatively brittle, with less than 5% elongation at break, which limits its use in some applications. Poly(butylene adipate-co-terephthalate) (PBAT) was used to enhance the flexibility of PLA via polymer blending. To enhance the dielectric constant, the porous clay heterostructure from mixed surfactant systems (BC-PCH) was used as filler to enhance the total polarization. Furthermore, BC-PCH was modified with transition metal cation doping to increase dipole density and dipole moment in the system. The highest dielectric constant was found at Mn/B1C2-PCH because manganese atoms had the greatest ionic radius. These efforts revealed a roughly four-times increase in biodegradable nanocomposite film dielectric constant (at 1 kHz).



9:00 AM

**(FMAs-010-2022) Perspective on Dielectric Properties of Calcium Copper Titanate Ceramics (Invited)**

R. N. Singh\*<sup>1</sup>

1. Oklahoma State University, School of Materials Science and Engineering, USA

Calcium Copper Titanium Oxide (CCTO) Ceramics of composition  $\text{CaCu}_3\text{Ti}_4\text{O}_{12}$  has emerged as a lead-free ceramic supercapacitor with a large dielectric constant of  $10^4 - 10^5$  at room temperature. The CCTO microstructure is electrically heterogeneous composed of semiconducting grains and insulating grain boundaries. Origin of the large dielectric constant has therefore been widely attributed to barrier layer capacitance originated at grain boundaries. Our research is focused on understanding the stability and reproducibility of the measured electrical and dielectric properties when they are used as capacitor dielectrics because of the inconsistent results obtained when tested in ambient conditions. The origin of this inconsistency is investigated through the roles of testing atmosphere, sample thickness and doping with alumina on the stability and reproducibility of dielectric properties of CCTO. Solid state reaction method is used to fabricate phase pure and dense samples. AC impedance spectroscopy is used to study the roles of testing atmospheres, temperatures, microstructures, grain boundaries, sample thickness, alumina doping and frequency on the dielectric properties. It is shown that this approach of characterizing fundamental electrical properties of CCTO can be used to eliminate hysteresis to produce stable and reproducible dielectric properties. These perspectives will be presented and discussed.

9:20 AM - **WITHDRAWN**

**(FMAs-011-2022) Nanoscale Dipole Engineering of BaTiO<sub>3</sub> Using La<sup>3+</sup>-Ta<sup>5+</sup> Dipoles**

C. J. Mayo\*<sup>1</sup>; V. Pellegrino<sup>2</sup>; K. Ning<sup>3</sup>; S. Tidrow<sup>4</sup>

1. Alfred University, Materials Science and Biomaterials Engineering, USA
2. Alfred University, USA
3. Alfred University, New York State College of Ceramics, School of Engineering, USA
4. Alfred University, USA

Christopher Mayo, Victoria Pellegrino, Kaijie Ning, Steven C. Tidrow Electric-field (E) dipole engineering at the nanoscale (E-DENS) is a methodology used to investigate interactions between E and atoms within  $\text{ABX}_3$  perovskites and to modify or engineer material properties. Previously,  $\text{Y}^{5+} - \text{Ta}^{3+}$ , and  $\text{Ga}^{3+} - \text{Ta}^{3+}$  dipole pairs have been substituted for pairs of  $\text{Ti}^{4+}$  to form  $\text{Ba}\{[\text{Y}^{3+}_x, \text{Ta}^{5+}_x] \text{Ti}_{(1-2x)}\}\text{O}_3$  and  $\text{Ba}\{[\text{Ga}^{3+}_x, \text{Ta}^{5+}_x] \text{Ti}_{(1-2x)}\}\text{O}_3$ , respectively. These materials transition from ferroelectric to diffuse phase to a relaxor-like material within a solid solution range of  $0.0000 \leq x \leq 0.0500$ . Due to the higher polarizability of  $\text{Y}^{3+}$  relative to  $\text{Ga}^{3+}$ ,  $3.84 \text{ \AA}^3$  to  $1.50 \text{ \AA}^3$ , and larger radii,  $1.040 \text{ \AA}$  to  $0.76 \text{ \AA}$ ,  $T_m$  and  $T_c$  increased while diffuseness decreased slightly due to a decrease in dipole field strength of  $\text{Ba}\{[\text{Y}^{3+}_x, \text{Ta}^{5+}_x] \text{Ti}_{(1-2x)}\}\text{O}_3$  compared to  $\text{Ba}\{[\text{Ga}^{3+}_x, \text{Ta}^{5+}_x] \text{Ti}_{(1-2x)}\}\text{O}_3$ . Using these results and the Clausius - Mossotti relation, it is anticipated use of  $\text{La}^{3+}$ , which possessing an even larger radii and polarizability,  $1.172 \text{ \AA}^3$  and  $6.03 \text{ \AA}^3$ , respectively, than either  $\text{Y}^{3+}$  or  $\text{Ga}^{3+}$ , with  $\text{Ta}^{5+}$  as the dipole pair in  $\text{Ba}\{[\text{La}_x, \text{Ta}_x] \text{Ti}_{(1-2x)}\}\text{O}_3$  will further increase  $T_m$  and  $T_c$  and will cause a slight decrease in diffuseness due to decrease in dipole strength. Design, fabrication, and characterization of  $\text{Ba}\{[\text{La}_x, \text{Ta}_x] \text{Ti}_{(1-2x)}\}\text{O}_3$  are reported and characteristics of the material are compared with anticipated properties.

9:40 AM

**(FMAs-012-2022) Structural, Dielectric and Ferroelectric Behaviour of BaTiO<sub>3</sub>-PbZrO<sub>3</sub>-SmFeO<sub>3</sub> Solid Solution**

P. Kumar\*<sup>1</sup>; K.<sup>1</sup>

1. DIT University, Department of Physics, School of Physical Sciences, India

In the present report, the ternary solid solution of ferroelectric  $\text{BaTiO}_3$ , antiferroelectric  $\text{PbZrO}_3$  and semiconducting  $\text{SmFeO}_3$  is selected for structural, dielectric and ferroelectric investigations. The materials with compositional formula  $(\text{Ba}_{1-x-y}\text{Pb}_x\text{Sm}_y)(\text{Ti}_{1-x-y}\text{Zr}_x\text{Fe}_y)\text{O}_3$  with (x,y) equals to (0.035, 0.003), (0.0525, 0.0045) and (0.07, 0.006) are prepared by conventional solid-state reaction route and sintered at  $1325^\circ\text{C}$  for 4 hours in lead-rich environment. Sintered samples were subjected to X-ray diffraction (XRD) and SEM analyses to investigate their structural properties. The relative density is found to be greater than 94% for all the samples. Dielectric constant ' $\epsilon'$ ' is measured as a function of temperature (30 to  $175^\circ\text{C}$ ) at different frequencies (1, 5, 10, 50, 100, 500 and 1000 kHz) for all the samples. In order to confirm the ferroelectricity in the prepared samples, PE-loops are recorded at 50Hz at  $30^\circ\text{C}$  for all the samples.

10:20 AM

**(FMAs-013-2022) Morphological evolution and transition at nanoscale in multifunctional ceramic materials (Invited)**

N. B. Singh\*<sup>1</sup>; C. H. Su<sup>2</sup>; F. Choa<sup>1</sup>; B. R. Arnold<sup>1</sup>; B. Cullum<sup>1</sup>; K. Mandal<sup>3</sup>

1. University of Maryland Baltimore County, Chemistry and Biochemistry, USA
2. NASA Marshall Space Flight Center, EM, USA
3. Indian Institute of Technology (BHU), Chemistry, India

Since past few years we have been studying synthesis and characterization of bulk and nanoengineered multifunctional industrially important dielectric and ferroelectric materials for variety of optical and electronic devices, energy storage, ferroelectric and magnetic devices and systems. Measured properties such as bandgap, resistivity and dielectric constant value are highly process dependent and show variation with particle size of source material, temperature and cooling conditions during processing. This may be the reason for different values reported by different investigators in perovskite materials such as calcium copper titanate. To understand the problems related to uncertainty and variation of electrical properties, we have prepared nanoparticles based ternary compounds and studied electronic, optical and thermal characteristics including phase transition. We observed that similar to the solid-liquid breakdown, nano- and microparticles show huge transition into nanowires and fibers. This transition enables possibility of designing conformal materials for variety of applications without significant decrease in their performance.

10:50 AM

**(FMAs-014-2022) Preparation and characterizations of Bi<sub>0.617</sub>Y<sub>0.05</sub>Cu<sub>3</sub>Ti<sub>4</sub>O<sub>12</sub> ceramic**

K. Mandal<sup>1</sup>, D. Prajapati\*<sup>1</sup>

1. Indian Institute of Technology (BHU), Chemistry, India

$\text{Bi}_{0.617}\text{Y}_{0.05}\text{Cu}_3\text{Ti}_4\text{O}_{12}$  (BYCTO) was successfully synthesized through an economically semi-wet route using metals nitrates, acetate, and  $\text{TiO}_2$  precursor and sintered at 1173 K for 8 h. The single phase of ceramic was authorized by XRD analysis. The crystallite size of BYCTO ceramic was calculated to be 62.3 nm through XRD measurement. The particle size obtained by TEM analysis was to be in the range of  $55 \pm 7$  nm. The average grain size observed through the SEM technique was 0.783  $\mu\text{m}$ . The dielectric constant ( $\epsilon_r$ ) of BYCTO was measured to be 1481 at 307 K and 100 Hz. The tangent loss (tan d) was observed to be in the range of 0.13–0.29 at all selected temperatures (307–487 K) and 10 kHz which is lower than that of  $\text{Bi}_{2/3}\text{Cu}_3\text{Ti}_4\text{O}_{12}$ .

**11:10 AM - WITHDRAWN****(FMAs-015-2022) Effect of DC Poling on Dielectric Properties of Lead-Free Ferroelectric Ceramics**N. Gugar<sup>\*1</sup>; P. Kumar<sup>2</sup>; C. Prakash<sup>3</sup>

1. DIT University, India
2. DIT University, Physics, India
3. Maharaja Agrasen Institute of Technology, Applied Sciences, India

This study explores the effect of electrical poling, Lead-free polycrystalline ferroelectric ceramics with compositional formula  $(\text{Ba}_{0.70-x}\text{Sm}_x\text{Ca}_{0.30})\text{TiO}_3$  with  $x = 0, 0.005, 0.010, 0.015, 0.020$  and  $0.030$ . The samples were prepared by solid-state reaction route and sintered at  $1325^\circ\text{C}$  for 4 hours. The phase was confirmed by X-ray diffraction 'XRD' technique. The prepared ceramic samples were heated upto  $80^\circ\text{C}$  in an oil bath and electrically poled using a DC field. Dielectric constant and tangent loss was measured before and after poling over a frequency range from 100Hz to 100kHz. The dielectric properties were compared and analyzed. A decrease in the value of dielectric constant was observed after poling, which shows reduction in the anisotropy by electric poling.

**11:30 AM****(FMAs-016-2022) Obtaining the rod-shaped barium titanate single crystal from glycolate**O. Kovalenko<sup>\*1</sup>; S. Škapin<sup>2</sup>; M. Maček Krzmann<sup>2</sup>; D. Vengust<sup>2</sup>; M. Spreitzer<sup>2</sup>; Z. Kutnjak<sup>2</sup>; A. Ragulya<sup>1</sup>

1. LLC NanoTechCenter, Ukraine, Ukraine
2. Jozef Stefan Institute, Slovenia

In this paper, we have studied the effect of supersaturation on the development of structure and morphology from lamellar glycolate intermediate phase to single-crystalline barium titanate nanorods. It was shown that a single-phase rod-shaped  $\text{BaTiO}_3$  nanoparticle with a tetragonality of 1.013, aspect ratio of 6–9, and width less than 100 nm is formed when the supersaturation was set at a range of 19–29. Below this range, we observed the formation of the plate-shaped glycolate-based intermediates with a size of 0.7–1  $\mu\text{m}$ , while above the supersaturation value of 29, the formation of nanoparticles with irregular shapes, a diameter of 50 nm, and cubic structure have occurred. The prevailing crystallization path in-situ is altered into a dissolution-precipitation path above the supersaturation value of 19. It was shown that the structure and morphology of the obtained  $\text{BaTiO}_3$  nanoparticles can be well-tuned by a simple regulation of supersaturation.

**11:50 AM****(FMAs-017-2022) Dielectric and electrical properties of Zn doped and undoped  $\text{Bi}_{2/3}\text{Cu}_3\text{Ti}_4\text{O}_{12}$  ceramic (Invited)**K. Mandal<sup>1</sup>, V. Shankar Rai<sup>1</sup>, N.B. Singh<sup>\*2</sup>

1. Indian Institute of Technology (BHU), Chemistry, India
2. University of Maryland Baltimore County, USA

Zn-doped and un-doped BCTO ceramics ( $\text{Bi}_{2/3}\text{Cu}_{3-x}\text{Zn}_x\text{Ti}_4\text{O}_{12}$ ,  $x=0, 0.05, 0.1, \text{ and } 0.2$ ) were prepared by chemical route sintered at 1123 K for 8 h. The Phase formation of ceramics were confirmed by X-ray Diffraction. Their microstructural properties were examined through SEM, EDX, and TEM. The dielectric constant of Zn doped BCTO ceramics were obtained higher than undoped BCTO ceramics at 100 Hz and room temperature (310 K). The tangent loss (tan) value for Zn doped BCTO ceramics were found to be lower than undoped BCTO ceramics at 10 kHz and 310 K. The conductivity dependence of  $\text{Bi}_{2/3}\text{Cu}_{3-x}\text{Zn}_x\text{Ti}_4\text{O}_{12}$  ceramics (where  $x=0, 0.05, 0.1, \text{ and } 0.2$ ), with the inverse of temperature follows the Arrhenius equation, with a major temperature range of 300–500 K.

**Ferroic Domains and Modeling**

Room: Star Bay 3 (Level B)

Session Chair: Ruyan Guo, University of Texas, San Antonio

**8:30 AM****(FMAs-018-2022) Topological Defects in Ferroelectrics and Functional Materials (Invited)**A. Saxena<sup>\*1</sup>

1. Los Alamos National Lab, USA

Materials properties crucially depend on defects, and even more so if the defects are topological in nature, i.e. they cannot be removed by a simple deformation of the material. Some examples of such defects are the celebrated domain walls, vortices as well as dislocations. More exotic ones include disclinations, skyrmions (non-collinear spin textures), vortex rings, merons (or half skyrmions), hopfions, torons and monopoles. Many of these topological defects have now been observed in ferroelectrics, chiral magnets, multiferroics, nematic liquid crystals and a variety of other functional materials. They can be studied within a mesoscopic model based on the order parameter (polarization, strain, magnetization, director field, etc.) and relevant crystal symmetries. Such a model is then capable of explaining experimental observations and describing the change in materials properties as a function of defect distribution, density and interaction among the defects.

**9:00 AM****(FMAs-019-2022) Switchable negative capacitance in ultrathin ferroelectric/dielectric bilayer capacitors (Invited)**J. Wu<sup>\*1</sup>

1. University of Kansas, USA

Ultrathin ferroelectric (FE) and dielectric (DE) insulator bilayer stacks provide a promising gate for low-power microelectronic devices. To fully realize the FE polarization switching, the DE layer must be ultrathin in the FE/DE bilayer stack. In this talk, I will present the first successful fabrication and characterization of  $\text{FeOx}/\text{Al}_2\text{O}_3$  FE/DE bilayer capacitors using in vacuo atomic layer deposition (ALD) with a total FE/DE stack thickness  $\sim 3\text{--}4$  nm. Without the FE layer, high-quality conventional DE capacitors of 2.2 nm thick ALD- $\text{Al}_2\text{O}_3$  were obtained with dielectric constant ( $\epsilon_r$ )  $\sim 8.0$  that is close to  $\epsilon_r \sim 9.2$  for the  $\text{Al}_2\text{O}_3$  bulk single crystal with an effective oxide thickness (EOT) of 1.0 nm. By introducing a thin ferroelectric  $\text{FeOx}$  interfacial layer of a thickness of 1–2 nm, the ultrathin FE/DE bilayer capacitor exhibits a static negative capacitance, which may be explained by the interfacial charge (or dipole) induced at the FE/DE interface. In addition, the negative capacitance can dynamically switched on/off under the application of an external force on the ultrathin FE/DE capacitors through manipulation of the electric dipoles. This result not only provides a viable approach for generating ultrathin FE/DE bilayer capacitors but also offers a promising solution to low-power consumption microelectronics.

**9:20 AM****(FMAs-020-2022) Creating Giant Permittivity in  $\text{BaTiO}_3$  Ceramics Using Defect**Z. Cheng<sup>\*1</sup>

1. Auburn University, Materials Engineering, USA

Dielectrics with a high permittivity and a weak temperature dependence are highly desirable for various development. Normally, nonpolar dielectrics exhibit a low permittivity with a weak temperature dependence and the polar dielectrics, especially ferroelectrics, exhibit a high dielectric constant with a strong temperature dependence. Therefore, composites consisting of polar and nonpolar dielectrics have been studied to create dielectrics. The permittivity of a composite is usually somewhere between the two constituents.  $\text{BaTiO}_3\text{-SiO}_2$  ceramics have been studied to weaken the temperature

dependence of the permittivity. The permittivity of BaTiO<sub>3</sub>-SiO<sub>2</sub> decreases with increasing TiO<sub>2</sub>, when TiO<sub>2</sub> is about 20%, the permittivity of BaTiO<sub>3</sub>-SiO<sub>2</sub> is only about 20. In this study, to increase the permittivity, defects were induced to the ceramic composites. A giant permittivity ( $\sim 10^6$ ) with a low loss at 100 Hz was achieved in BaTiO<sub>3</sub>-SiO<sub>2</sub> ceramic composites in which the phase transitions of BaTiO<sub>3</sub> at 0 °C and 120 °C were barely observed. The temperature dependence of the permittivity is significantly smaller than that of BaTiO<sub>3</sub>. Additionally, the higher permittivity of the ceramics can be tuned over more than 100% with the electric field. The ceramics are a great candidate for the development of high performance ultracapacitors.

### 9:40 AM - **WITHDRAWN**

#### (FMAs-021-2022) Frequency & temperature-dependent dielectric and ferroelectric properties of Mg-substituted BST ceramics

C. Prakash<sup>\*1</sup>

1. Maharaja Agrasen Institute of Technology, Applied Sciences, India

Barium titanate based ferroelectric materials, due to their excellent properties, find applications in a variety of components including capacitors, sensors, actuators etc. They are potential candidates to replace lead base materials which are toxic in nature. Here, we present synthesis and dielectric & ferroelectric properties of Mg substituted Barium-Strontium Titanate (BST) compositions. Samples with representative formula Ba<sub>0.95-x</sub>Sr<sub>0.05</sub>Mg<sub>x</sub>TiO<sub>3</sub> (BMST) with x = 0, 0.005, 0.01 and 0.015 were prepared by the conventional solid state reaction process. The circular pellets of calcined powders were sintered at 1325°C for 4 hours in a closed alumina crucibles. Single phase formation with perovskite structure was confirmed by XRD analysis. Dielectric properties were studied as a function of frequency in the range of 100 Hz to 100 kHz at room temperature and as a function of temperature in the range of 20 °C to 150 °C at different selected frequencies. Ferroelectric PE loops were recorded using an automated loop tracer. All the samples show well defined ferroelectric behaviour. The composition with Mg = 0.015 gives highest value of dielectric constant and lowest value of loss tangent. The detailed study will be present in the meeting.

### 10:20 AM

#### (FMAs-022-2022) On the DC nonlinear dielectric permittivity and its correlation with the macroscopic polarization state in ferroelectrics (Invited)

J. A. Eiras<sup>\*1</sup>; A. M. Gonçalves<sup>1</sup>; E. B. Araujo<sup>2</sup>; R. Placeres-Jiménez<sup>1</sup>

1. Federal University of Sao Carlos, Physics, Brazil

2. São State University, Physics, Brazil

Ferroelectrics are dielectrics in which many practical applications are based on their nonlinear behavior. For any application, as memories or tunable microwave devices, the polarization reorientation and the dielectric permittivity changes under external electric fields must be explored. Different mechanisms (domain wall pinning, domain structure, grain size,...) impact as well the polarization reorientation as the tunability. Recently we proposed two different empirical models to correlate the dependence of the dielectric permittivity, under an DC electric field  $\epsilon'(E)$ , with the hysteresis loop  $P(E)$ . One of the strengths of these models is to reproduce the ferroelectric  $P(E)$  loops using parameters from fits. The first model uses the hyperbolic tangent function to represent the polarization curve. The second one considers that the  $\epsilon'(E)$  dependence on the electric field is proportional to the reciprocal of a quadratic function of the electric field  $(E)$ . Using parameters of both models, we aim to correlate the ferroelectric domain structure with the polarization reorientation process. Experimental results obtained in Pb(Zr<sub>0.20</sub>Ti<sub>0.80</sub>)O<sub>3</sub> and (Pb<sub>1-x</sub>La<sub>x</sub>)(Zr<sub>0.52</sub>Ti<sub>0.48</sub>)O<sub>3</sub> (0 ≤ x ≤ 0.15) polycrystalline thin films will be discussed.

### 10:50 AM

#### (FMAs-023-2022) Halide Perovskites: NSMM versus Goldschmidt's Tolerance Factor Formalism (Invited)

S. Tidrow<sup>\*1</sup>

1. Alfred University, USA

Properties of a material depend upon the atoms utilized and their positions in space with respect to time. Here, we discuss the extendable new simple material model (NSMM), a spreadsheet calculation, as applied to halide perovskites which are of recent interest for sustainable, renewable energy engineering of photovoltaic cells. Using physical constraints, NSMM has previously been shown to outperform Goldschmidt's tolerance factor formalism (GTFF), a correlation relation, for modeling a wide range of "simple" and "simply mixed" perovskite oxide materials. NSMM utilizes physical constraints, lattice, volume, packing density, and temperature dependent radii and polarizability, to determine whether or not a material will form and if it forms to model the lattice structure, lattice constant and volume, relative permittivity, and some temperature dependent phase transitions. Here, for halide perovskites, NSMM is shown to significantly outperform the coin-toss, which outperforms Goldschmidt's tolerance formalism, for identifying which materials will form and which materials will not form the perovskite structure using standard processing conditions. Of the 864 materials investigated, roughly 260 or 30% are reported to form the simple perovskite structure and roughly 600 or 70% are not reported of which NSMM accurately identifies 214 or 82% of those that are reported and 392 or 65% of those not reported.

### 11:20 AM

#### (FMAs-024-2022) Sensitivity analysis on the application of direct piezo-electric effect to predict the influence of variations in the material properties

C. Acosta<sup>\*1</sup>; J. de los Santos Guerra<sup>2</sup>; A. S. Bhalla<sup>1</sup>; R. Guo<sup>1</sup>

1. University of Texas, San Antonio, USA

2. Federal University of Uberlandia, Institute of Physics, Brazil

Piezoelectric materials have anisotropic coupling between the electric and elastic fields at different lengths scales. Different attributes such as symmetry and orientation result in independent configurations of elastic, dielectric, and piezo-electric material properties. Also, the synthesis processes of ceramics can add variability to such properties due to the arrangement of grains in the polycrystalline samples. These variations affect the response and performance of the domain due to internal microstructural defects. The goal of this research is to predict the response of the mechanical and electric fields given microstructural defects that render variations in the material properties. Such variations are studied under a numerical sensitivity analysis approach derived from the Complex Taylor Series Method incorporated into the traditional Galerkin finite element approximation. Results show that when a longitudinal load is applied to a PZT-5H material, the electric field is most affected by variations in  $\epsilon_{33}$  followed by defects in  $\epsilon_{33}$ , whereas the mechanical displacements show larger sensitivity from variations in the elastic constant  $C_{31}$  and  $C_{33}$ .

### 11:40 AM

#### (FMAs-025-2022) Nanoscale Dipole Engineering of Barium Titanate Using Yttrium (III) - Tantalum (V) Dipoles

V. Pellegrino<sup>\*1</sup>; K. Ning<sup>1</sup>; S. Tidrow<sup>1</sup>

1. Alfred University, New York State College of Ceramics, School of Engineering, USA

Electric-field dipole engineering at the nanoscale (E-DENS) allows for a thorough investigation on the effects of substitutions on relaxor/relaxor-like ferroelectrics, which play significant roles in numerous electronic devices. The search for relaxor/relaxor-like ferroelectrics has primarily focused on perovskite materials with morphotrophic phase boundary (MPB). Nanoscale dipole engineering

is a novel alternative approach for the development of relaxor/relaxor-like ferroelectrics. In this work, nanoscale dipole-pair engineered [Y, Ta]: BaTiO<sub>3</sub> (BaTi<sub>1-2x</sub>[Y, Ta]<sub>x</sub>O<sub>3</sub>, x = 0.0000 to 0.0500) ceramics has been manufactured based on two-step, solid-reaction sintering, with the [Y, Ta] dipoles being substituted into the Ti location in the structure. The dielectric relaxor behavior has been investigated from aspects of temperature, frequency, dipole concentration, crystal structure, microstructure, and optical bandgap. The results indicate that [Y, Ta] acts as an effective dipole in BaTiO<sub>3</sub> to produce relaxor-like ferroelectric material that possesses enhanced properties in the aforementioned fields.

12:00 PM

**(FMA-026-2022) Domain engineering of ferroelectric single crystal architecture in glass for integrated optics applications**

K. J. Veenhuizen<sup>1</sup>; S. McAnany<sup>2</sup>; R. Vasudevan<sup>6</sup>; D. Nolan<sup>3</sup>; B. Aitken<sup>3</sup>; S. Jesse<sup>6</sup>; V. Dierolf<sup>4</sup>; H. Jain<sup>4,5</sup>

1. Lebanon Valley College, Physics, USA
2. II-VI M Cubed, USA
3. Corning Incorporated, USA
4. Lehigh University, Physics, USA
5. Lehigh University, International Materials Institute for New Functionality in Glass, USA
6. Oak Ridge National Lab, USA

A new class of metamaterials known as ferroelectric single crystal architectures in glass can be fabricated via spatially-selective laser irradiation of the glass. Depending on the glass composition, waveguides of single crystals lacking inversion symmetry have been laser-written. These crystals possess ferroelectric, nonlinear optical, and electro-optic properties, enabling a host of integrated optics applications that would be impossible using amorphous waveguides. This presentation will focus on the formation of LiNbO<sub>3</sub> and LaGeO<sub>3</sub> in lithium niobosilicate and lanthanum borogermanate glasses, respectively. The ferroelectric domain structure of these crystals is characterized using piezoresponse force microscopy (PFM). As the LiNbO<sub>3</sub> crystals exhibit a non-uniform domain structure at the micro- and nano-scale, engineering the domain structure is crucial for potential device applications. PFM is used to apply a DC bias to reverse and uniformly orient the ferroelectric domains. The effect of spatial and dielectric confinement on the piezoelectric properties of the crystals in glass is unclear at the outset. PFM is used to map the spatial variation of the piezoresponse within the LiNbO<sub>3</sub> crystals. This measurement is compared to the simulated response using crystal lattice orientation information and piezoelectric coefficients of bulk single crystal.

**PACC1: Ceramics for Energy and Environment**

**Batteries and Various Topics**

Room: Revolution (Level B)

Session Chair: Henry Colorado L., Universidad de Antioquia

1:30 PM

**(PACC-S1-011-2022) A first-principles study of the origin of structural changes in Li<sub>x</sub>Ni<sub>1/3</sub>Co<sub>1/3</sub>Mn<sub>1/3</sub>O<sub>2</sub> and Li<sub>x</sub>Ni<sub>0.8</sub>Co<sub>0.1</sub>Mn<sub>0.1</sub>O<sub>2</sub> cathode materials with lithiation/delithiation (Invited)**

L. Kuo<sup>1</sup>; O. Guillon<sup>2</sup>; P. Kaghazchi<sup>3</sup>

1. Ming Chi University of Technology, Chemical Engineering, Taiwan
2. Forschungszentrum Juelich, IEK-1, Germany
3. Forschungszentrum Juelich, Germany

In this work, an extensive set of electrostatic and density functional theory (DFT) calculations were combined to determine the crystal, atomic and electronic structures of Li<sub>x</sub>Ni<sub>1/3</sub>Co<sub>1/3</sub>Mn<sub>1/3</sub>O<sub>2</sub> (NCM111)

and Ni-rich Li<sub>x</sub>Ni<sub>0.8</sub>Co<sub>0.1</sub>Mn<sub>0.1</sub>O<sub>2</sub> (NCM811) cathode materials. A detailed analysis of the number of unpaired spins (NUS), spin density difference (SDD), density of state (DOS) and Bader charges (BCs) was applied to explain the reason behind the non-monotonic variation of lattice parameters and structural phase transitions. The O-stacking induced phase transition at x = 0.00, which has not been well understood, is shown to be driven by electrostatic forces. To our knowledge, for the first time, we explained the hexagonal to monoclinic (H-M) phase transition at x = 0.50 for Ni-rich NCM811. It is found that the H-M phase transition is driven by the Jahn-Teller (J-T) distortion. Our results indicate that the presence/absence of Li-O attractions, charges on transition metals (TMs) and O anions, J-T distortion and electrostatic interactions are key factors to control the lattice parameters change.

2:00 PM

**(PACC-S1-012-2022) Ferroelectric Implanted Cathodes for Lithium Sulfur Batteries for High-Capacity Performance**

C. C. Zuluaga-Gomez<sup>1</sup>; C. Plaza<sup>2</sup>; G. Morell<sup>1</sup>; Y. Lin<sup>3</sup>; M. Correa<sup>4</sup>; R. Katiyar<sup>1</sup>

1. Universidad de Puerto Rico Recinto de Rio Piedras, Puerto Rico
2. Massachusetts Institute of Technology, USA
3. National Institute of Aerospace, USA
4. Universidad del Atlántico, Colombia

Lithium-Sulfur (Li-S) batteries have been vigorously revisited in recent years due to need of advanced energy storage technologies for transportation and large-scale energy storage applications. Sulfur is a promising cathode material for lithium sulfur batteries due to its high theoretical capacity (1675 mAh/g). Although Li-S batteries are in great demand, their real applications are still plagued by rapid capacity fading mainly stemming from the polysulfide shuttle. Coupling of highly polarized ferroelectric Bismuth Ferrite BiFeO<sub>3</sub> (BFO) layer is an approach that can be used to enhance the higher rate characteristics and trapping of shuttle mechanism because ferroelectrics provide higher polarization which help to build up an internal electric field and induce macroscopic charges separation on the surface of the cathode. To improve the electrochemical performance of the cathode in Lithium-Sulfur batteries, holey graphene and carbon-based materials are employed. This allows for a dry compression manufacturing process to facilitate the bonding between the Sulfur and the ferroelectric nanoparticles layer to generate a more stable cathode. We can speculate that polysulfides are heteropolar in which spontaneous polarization of ferroelectrics BFO may reduce the shuttle effect and can trap its formation thus yielding high-rate performance of Li-S batteries. XRD and Raman spectroscopy reveal that the synthesized BFO exhibits rhombohedral perovskite structure. The result is less polysulfide shuttling to achieve the high-capacity storage required for the Li-S batteries to become the power source of today. The current research has the desired preliminary results of cathode composition S<sub>47.5</sub>(BiFeO<sub>3</sub>)<sub>3</sub>hG<sub>47.5</sub> in discharge specific capacity as a function of the cycle number: a reversible capacity of ~1,388 mAh/g<sub>s</sub> was achieved with high coulombic efficiencies (> 87%) and active sulfur mass loading of 6.908 mgs/cm<sup>2</sup>.

2:20 PM

**(PACC-S1-013-2022) Supplementing Rate Capability and Cycling Efficiency of Li-ion Battery Anodes using MoSe<sub>2</sub>/SiOC self-supporting Structure - *WITHDRAWN***

S. Dey<sup>1</sup>; G. Singh<sup>2</sup>

1. Kansas State University, Mechanical Engineering, USA
2. Kansas State University, Mechanical and Nuclear Engineering Dept., USA

Keeping in mind the various hurdles of components used in traditional secondary electrochemical energy storage devices, the center of focus nowadays is on producing electrodes that are portable, lightweight, wearable, and mechanically flexible; which offer more active sites and shorter diffusion paths for Li<sup>+</sup> ions. While various

transition metal dichalcogenides (TMDs) have been widely studied for practical applications in Li-ion batteries, MoSe<sub>2</sub> has been less investigated. By incorporating carbonaceous materials, the conductivity, and active sites of electrodes fabricated with such materials can be increased. Interestingly, polymeric precursor-derived silicon oxycarbide (SiOC) being termed as an “all-rounder” material for various applications, has also been applied in LiBs and was reported to bring better cycling stability and rate capability by providing free carbons in the ceramic form. In this study, for the first time we report the fabrication of a freestanding electrode material with a small amount of two dimensional MoSe<sub>2</sub> along with SiOC fiber mats. After characterizing the structure of the fiber mat with microscopic techniques (such as SEM, TEM, and XPS) and spectroscopic techniques (such as Raman spectroscopy and FTIR) a lithium-ion half-cell was assembled using the material which showed improved cycling stability and rate capability.

**2:40 PM**

### **(PACC-S1-014-2022) Mitigation of Environmental Noise Through the Use of Composite Materials Containing Nanoparticles of Rice Husk**

J. Rendon\*<sup>1</sup>; C. H. Giraldo<sup>3</sup>; H. A. Colorado L.<sup>2</sup>

1. Universidad de Antioquia, CCOMposites Laboratory, Colombia
2. Universidad de Antioquia, Colombia
3. Missouri University of Science and Technology, USA

Currently the facades of the buildings are increasing the levels of urban noise. This is because they have highly reflective surfaces which increases reverberation levels and therefore the energy produced by noise. The following work studies the behavior of materials commonly used in facades in combination with rice husk nanoparticles (RHNP). For this, different mixtures of mortar, concrete, putty, and resin with RHNP are implemented. The results show an upward trend in sound absorption as RHNP increases.

**3:20 PM**

### **(PACC-S1-015-2022) Sustainable synthesis of advanced functional ceramics for energy applications (Invited)**

J. C. Nino\*<sup>1</sup>

1. University of Florida, Materials Science and Engineering, USA

Synthesis of nanopowders of advanced functional ceramics is of fundamental interest to industry and there are numerous methods currently employed including sol-gel, solvothermal, combustion reaction, microwave, sonochemical, co-precipitation, electrospraying, solution evaporation, molten salt, etc. These methods vary substantially in their simplicity, capital and operating expense, and their overall environmental hazard and safety. Therefore, there is significant interest in developing new, environmentally benign and more efficient methods for obtaining high purity nanopowders of advanced ceramics. Here we describe our use of a solvent deficient method for the synthesis of high surface area metal oxide nanomaterials that does not employ traditional organic solvents during the mixing the reagents, and does not require a complex apparatus or setup. Based on the solid mixture of nitrate precursors and ammonium bicarbonate, the synthesis process involves low energy and time consumption. We show the solvent deficient synthesis of nanoparticles of CeO<sub>2</sub>, Gd-doped CeO<sub>2</sub>, and BiFeO<sub>3</sub>. The synthesis reactions and kinetics investigated by simultaneous thermogravimetric analysis-differential scanning calorimetry, and x-ray diffraction will be discussed. Moreover, the powder morphology, sintering behavior, resulting microstructure, and the electrical and magnetic properties of the compounds will be presented.

**3:50 PM**

### **(PACC-S1-016-2022) Development of Ultra-High Temperature Ceramic Additively Manufactured Compact Heat Exchangers (Invited)**

N. Timme<sup>1</sup>; V. Anthony<sup>4</sup>; M. Lakusta<sup>1</sup>; G. Basler<sup>1</sup>; S. Grier<sup>1</sup>; T. Plateau<sup>4</sup>; E. Olugbade<sup>4</sup>; P. Rao<sup>1</sup>; S. Jape<sup>6</sup>; P. Davenport<sup>6</sup>; Z. Ma<sup>4</sup>; T. Held<sup>3</sup>; G. Hilmas<sup>1</sup>; W. Fahrenholtz<sup>2</sup>; J. Watts<sup>3</sup>; M. Leu<sup>4</sup>; J. Park<sup>4</sup>; D. Lipke\*<sup>1</sup>

1. Missouri University of Science & Technology, Materials Science & Engineering, USA
2. Missouri University of Science & Technology, Dept. of Materials Science and Engineering, USA
3. Missouri University of Science & Technology, Materials Science and Engineering, USA
4. Missouri University of Science & Technology, Mechanical & Aerospace Engineering, USA
5. Echogen Power Systems, USA
6. National Renewable Energy Laboratory, USA

Heat exchangers that can operate with dense hot fluids, such as supercritical carbon dioxide at temperatures above 1100°C, are thermal exchange components critical to ultra-compact and efficient electrical power generation. The combination of emergent materials, manufacturing methods, and modeling techniques may be poised to bring about disruptive innovation resulting in step reductions in fuel consumption, technological footprint, and capital expenditures. This presentation will describe activities at Missouri University of Science and Technology and project partners to leverage recent advances in ceramic additive manufacturing and materials for extreme environments to fabricate microchannel-style heat exchangers for use in power cycles with intense heat sources. Key challenges relating to materials selection and heat exchanger design will be highlighted, and perspectives as how to overcome historical roadblocks will be shared.

**4:20 PM**

### **(PACC-S1-017-2022) Electrocatalytically Active Staggered Gap-Based g-C<sub>3</sub>N<sub>4</sub>/WS<sub>2</sub> for Robust Water Splitting**

A. Arunachalam\*<sup>1</sup>; M. Viswanathan<sup>1</sup>

1. Universidad de Concepcion, Materials Engineering, Chile

The electrocatalytic decomposition of water is an effective method for addressing the energy and environmental crises. For large-scale water splitting, the development of low-cost, high-efficiency, and stable bifunctional electrocatalysts for the hydrogen evolution reaction (HER) and oxygen evolution reaction (OER) is critical. The non-precious metal catalysts have advanced rapidly due to their low cost and abundant resources, and are now widely used for the electrolysis of water. Among the various non-metal catalysts, the two-dimensional (2D) tungsten disulphide (WS<sub>2</sub>) is known to be one of the potential candidates in electrolyzing water into oxygen and hydrogen fuels owing to its physicochemical characteristics. Here, we design the synergistic electrocatalytic composites composed of graphitic carbon nitride (g-C<sub>3</sub>N<sub>4</sub>) and WS<sub>2</sub>, which not only combines the intrinsic properties of individuals but also has significantly higher HER and OER activities. Furthermore, it enables an alkaline electrolyser with a current density of 15.9 mA cm<sup>-2</sup> at 1.23V RHE. The outstanding performance is primarily due to the unique configuration and multicomponent synergies between g-C<sub>3</sub>N<sub>4</sub> and WS<sub>2</sub>.

## **PACC3: Densification and Microstructural Evolution in Ceramics During Sintering**

### **Sintering III**

Room: Millennium (Level B)

Session Chair: Rajendra Bordia, Clemson University

**1:30 PM**

#### **(PACC-S3-015-2022) Sintering-Assisted Additive Manufacturing of Powder Components: Effect of Gravity (Invited)**

E. Olevsky<sup>\*1</sup>; E. Torresani<sup>1</sup>; R. Bordia<sup>2</sup>; R. M. German<sup>1</sup>

1. San Diego State University, College of Engineering, USA
2. Clemson University, Materials Science and Engineering, USA

Additive manufacturing is increasingly used to make porous preforms followed by sintering to fabricate the final component. The effects of gravity on micro- and macro-structure of sintered component are still poorly understood. Present technologies of additive manufacturing (such as binder-jetting, stereolithography, robocasting, etc.) of complex-shape powder-components necessitate fine-tuning of sintering as applied to porous 3D-printing products. The densification of complex shapes requires control of the gravity-related phenomena to ensure a nearly full and distortion-free densification. The present study addresses these issues through the involvement of comprehensive finite element simulations, the determination of the additively manufactured powder specimens' sintering behavior, and the experimental validation of the developed models describing sintering of 3D-printed objects. The presentation describes the application of a numerical approach based on continuum mechanics-based modeling of the gravity-induced distortions during sintering of 3D-printed powder components. The validation of the model is conducted through the comparison with the experimental results obtained for the sintering of the beam-shape components printed using ceramic stereolithography technology. A semi-analytical criterion, which can be used for sintered 3D-printed parts' design recommendations, is derived.

**2:00 PM**

#### **(PACC-S3-016-2022) Densification and shape deformation cases descriptions for sintering based on solid mechanics**

H. Camacho Montes<sup>\*1</sup>; A. Gracia Reyes<sup>2</sup>; I. M. Espinoza Ochoa<sup>3</sup>; Y. Espinosa Almeyda<sup>1</sup>; A. Vega Siverio<sup>4</sup>; B. Olmos<sup>5</sup>; R. Bordia<sup>6</sup>

1. Universidad Autonoma de Ciudad Juarez, Physics and Mathematics, Mexico
2. PROQUIMAR, Mexico
3. Universidad Autónoma de Ciudad Juárez, Física y Matemáticas, Mexico
4. Universidad Autónoma de Ciudad Juárez, Física y Matemáticas, Mexico
5. Universidad Autónoma de Ciudad Juárez, Mexico
6. Clemson University, Materials Science and Engineering, USA

Continuum Mechanics offers a useful tool to describe macroscopic aspects of powder compact sintering. Densification and shape deformations are two examples where solid mechanics can provide an accurate description. A resume of the viscous elastic analogy and the stress equilibrium problem statement are presented. Constitutive parameters such as uniaxial viscosity, viscous Poisson ratio and free sintering rate can be obtained from measurements performed in a sinter forging unit or considering constitutive laws reported in the literature. Cases such as clay ceramics tiles and electronic packaging are studied with special attention on shape deformation, although densification is also important because nonuniform density maps potentially affect mechanical strength. Stress assisted sintering cases are also reported as an example to control densification.

**2:20 PM**

#### **(PACC-S3-017-2022) Viscous Composite Sintering of Triaxial Ceramics**

D. Hotza<sup>\*1</sup>

1. Federal University of Santa Catarina, Brazil

A liquid phase is fundamental to the densification of traditional ceramics, especially porcelain-like products such as tableware, sanitaryware, and stoneware tiles. Liquid Phase Sintering (LPS) with <20 vol.% liquid improves diffusion and material transport and increases the pore removal rate. Viscous Composite Sintering (VCS) or vitrification occurs when larger amounts of liquid are present. In VCS, a viscous liquid forms at a relatively low temperature. The resulting vitrified bodies are known as triaxial ceramics and contain clay (plasticizer), feldspar (flux), and quartz (filler). When heated, clay decomposes into an amorphous phase, which reacts with the low-melting, alkaline-rich flux to form a large amount of liquid (~60 vol.%). After cooling to room temperature, the microstructure of vitrified porcelain is complex and contains quartz, mullite, and glass. This microstructure and processing route leaves a product with low porosity and a smooth surface for traditional ceramic applications. However, the mechanism and microstructure evolution remain partially unexplained, given the high heating and cooling rates found in industrial sintering processes. This environment, far from thermodynamic equilibrium, hampers prediction and control by modeling and simulation tools. This work will provide an overview of efforts to shed light on the VCS of triaxial ceramics, particularly those subjected to fast firing in industrial kilns.

**2:40 PM**

#### **(PACC-S3-018-2022) Modeling of Rapid Sintering by the Discrete Element Method**

M. H. Teixeira<sup>\*1</sup>; J. R. Neto<sup>1</sup>; D. Hotza<sup>2</sup>; R. Janssen<sup>3</sup>

1. Federal University of Santa Catarina (UFSC), Graduate Program in Materials Science and Engineering, Brazil
2. Federal University of Santa Catarina (UFSC), Department of Chemical and Food Engineering, Brazil
3. TU Hamburg-Harburg, Inst. of Advanced Ceramics, Germany

The macroscopic behavior of powder compacts during sintering has its source at the microscopic level. Despite the significant progress in analytical techniques, micro-scale features of ceramic systems under fast-firing have been challenging to fully understand via experimentation only. Here we have incorporated concepts of heat transfer, transient temperature regime, and sintering/contact forces to build a numerical model for exploring and forecasting microscale details of the densification and defects propagation of ceramic parts consolidated by non-isothermal sintering. The model has been implemented within the framework of the Discrete Element Method (DEM) using the software Musen. The paper scope includes the model application to a ceramic system based on micrometric-sized alumina (Al<sub>2</sub>O<sub>3</sub>). Relationships between defects, microstructure, and sintering parameters were also explored. Micro-kinetics investigation on the simulation sample disclosed that densification did not occur homogeneously over the sample's length and the gradients of density tended to be accentuated at higher sintering temperatures. The thermal gradients were foreseen by the numerical model showing a correlation coefficient of 0.99 and r<sup>2</sup> equal to 0.98 in the range analyzed. Besides, our model corroborates with the digitalization trend of Industry 4.0.

3:20 PM

## (PACC-S3-019-2022) Machine-learning-based Microstructure-property Prediction Enabled by High-throughput Ceramic Sample-array Preparation Using Integrated Additive/Subtractive Manufacturing (Invited)

F. Peng<sup>\*2</sup>; X. Geng<sup>2</sup>; J. Tang<sup>3</sup>; Y. Shi<sup>1</sup>; D. Li<sup>4</sup>; R. Bordia<sup>2</sup>; J. Tong<sup>2</sup>; H. Xiao<sup>3</sup>

1. Rensselaer Polytechnic Institute, USA
2. Clemson University, Materials Science and Engineering, USA
3. Clemson University, Electrical and Computer Engineering, USA
4. Advanced Manufacturing LLC, USA

We demonstrate a high throughput sample fabrication method and a novel machine-learning algorithm that can predict the microstructure of laser-sintered alumina. The alumina sample array was prepared using the laser-based integrated additive/subtractive manufacturing (IASM) method. We can simultaneously fabricate a sample array that contains hundreds of individual sample units. These sample units have their own microstructure, depending on the laser power distribution and the sample locations. Micro-indentation was carried out to measure the hardness of all the sample units. The microstructure of selected sample units was characterized using SEM. Thus, we efficiently established a database of microstructure and hardness of laser-sintered alumina. We developed a novel machine-learning algorithm, regression-based conditional generative adversarial networks (GANs) with Wasserstein loss function and gradient penalty (RCWGAN-GP). We found that RCWGAN-GP can not only accurately regenerate the microstructure of alumina with measured hardness, but also accurately predict the microstructure of alumina of arbitrary hardness.

## PACC8: Novel, Green, and Strategic Processing and Manufacturing Technologies

### Novel, Green, and Strategic Processing III

Room: Bellagio (Level B)

Session Chair: Gloria Wie-Addo, Sheffield Hallam University

1:30 PM

## (PACC-S8-014-2022) Overview of pressureless electric field-assisted sintering solid electrolytes (Invited)

R. Muccillo<sup>\*1</sup>

1. IPEN, Brazil

Sintering, one of the final experimental steps towards preparing ceramic materials for inclusion in devices, usually requires between 1/2 and 3/4 of the absolute melting point, and long times. Alternatives for decreasing the temperature and time for energy saving were proposed consistently in the last decades, the application of electric fields being one of those. In the last ten years a great effort was put on sintering ceramic compacts supplying additional heat (Joule) by applying an electric field at temperatures and times shorter than those used in conventional sintering. The following compositions of solid electrolytes were pressureless sintered under DC or AC electric fields at temperatures below the reported temperatures for conventional sintering: zirconia: (3 and 8) mol% yttria, ceria: 20 mol% samaria, BITVOX, and barium cerate doped with either gadolinium, yttrium or samarium. The main results on (enhanced) electrical properties, microstructural features (grain growth inhibition) as well as proposed mechanisms (defect creation, particle surface melting, dielectric breakdown, space charge deployment) concerning the pressureless electric field-assisted densification of these solid electrolytes will be presented.

2:00 PM

## (PACC-S8-015-2022) Fabrication of transparent ceramics by colloidal processing and Spark Plasma Sintering (Invited)

T. S. Suzuki<sup>\*1</sup>; K. Morita<sup>2</sup>; J. Li<sup>2</sup>; B. Kim<sup>2</sup>

1. National Institute for Materials Science, Ceramics Processing Group, Japan
2. National Institute for Materials Science (NIMS), Japan

Densification is necessary for fabrication of transparent ceramics to require extremely low porosities. The packing structure is important to reduce porosities during sintering and can be controlled by the colloidal processing. In general, high transparent g-AlON can be fabricated by two-step method consisting of powder synthesis and densification. In this presentation, one-step method was attempted for fabricating the transparency g-AlON by colloidal processing and reactive SPS. Colloidal processing was used for fabrication of green compact with mixture powder of Al<sub>2</sub>O<sub>3</sub> and AlN. Subsequently, SPS was used as one-step method for both reaction of Al<sub>2</sub>O<sub>3</sub> with AlN and densification. Reaction between Al<sub>2</sub>O<sub>3</sub> and AlN powder was completed at 1650C during SPS, but higher temperature was needed to fabricate the transparent AlN. The total transmittance of the sample with even thickness of 2 mm was 60%. The high transparency g-AlON was successfully fabricated by one-step method using colloidal processing and reactive SPS. In the case of monolithic Al<sub>2</sub>O<sub>3</sub> and AlN, the crystallographic orientation is effective for improvement of transmittance because of anisotropic crystal structure. Orientation can be controlled by a magnetic field and alignment of the c-axis was useful for increasing their transmittance due to reduction of the birefringence at the grain boundary.

2:30 PM

## (PACC-S8-016-2022) Ultra-Fast Laser Fabrication of Alumina Micro-Sample Array and High-Throughput Characterization of Microstructure and Hardness

X. Geng<sup>\*1</sup>; J. Tang<sup>3</sup>; B. Sheridan<sup>1</sup>; S. Sarkar<sup>1</sup>; J. Tong<sup>1</sup>; H. Xiao<sup>3</sup>; D. Li<sup>4</sup>; R. Bordia<sup>2</sup>; F. Peng<sup>1</sup>

1. Clemson University, Materials Science and Engineering, USA
2. Clemson University, Materials Science and Engineering, USA
3. Clemson University, Electrical and Computer Engineering, USA
4. Advanced Manufacturing LLC, USA

The high-throughput approach for fast sampling of the microstructure and the correlated properties is still a blank in current study. In this paper, we demonstrate the ultra-fast fabrication of an alumina sample array and the high-throughput hardness characterization of these sample units. The alumina sample array was fabricated using picosecond (PS) laser micromachining and CO<sub>2</sub> laser sintering within a few minutes. Hardness of laser sintered samples were characterized by micro-indentation and their microstructures were captured using scanning electron microscopy (SEM). In our ultra-fast fabricated high-throughput samples, the relative density (RD) and corresponding micro-hardness was found to continuously vary over a wide range from 89% RD with 600 kgf/mm<sup>2</sup> hardness to 99% RD with 1609 kgf/mm<sup>2</sup> hardness, which matched well with the literature reports on conventional low-throughput furnace sintering experiments. It indicates that the database of the microstructure and hardness of laser-sintered alumina can be efficiently established through this high-throughput laser sintering approach.

3:10 PM

## (PACC-S8-017-2022) Effect of the pressureless post-sintering on the hot isostatic pressed Al<sub>2</sub>O<sub>3</sub> prepared from the oxidized AlN powder (Invited)

C. Balazsi<sup>\*1</sup>; K. Balazsi<sup>2</sup>

1. ELKH Centre for Energy Research, Hungary
2. Centre for Energy Research ELKH, Thin Film Physics, Hungary

The effect of the pressureless post-sintering in hydrogen on the structural and mechanical properties of the hot isostatic pressed Al<sub>2</sub>O<sub>3</sub> prepared by oxidized AlN powder has been studied. The

micrometer size AlN powder has been oxidized in air at 900° C and sintered by hot isostatic pressing (HIP) at 1700°C, 20 MPa nitrogen atmosphere for 5h. Pressureless sintering (PS) has been applied for all HIP sintered samples in H<sub>2</sub> gas at 1800° C for 10 hours. It has been shown that the oxidation caused a core-shell AlN/Al<sub>2</sub>O<sub>3</sub> structure and the amount of Al<sub>2</sub>O<sub>3</sub> increased with increasing of the oxidation time of the AlN powder. For the first time, the green samples obtained from oxidized AlN powder have been successfully sintered first by HIP followed by post-sintering by PS under hydrogen without adding any sintering additives. All post-sintered samples exhibited the main  $\alpha$ -Al<sub>2</sub>O<sub>3</sub> phase. Sintering in H<sub>2</sub> caused the full transformation of AlN to  $\alpha$ -Al<sub>2</sub>O<sub>3</sub> phase and their better densification. Therefore, the hardness values of post-sintered samples have been increased to 17-18 GPa having apparent densities between 3.11 and 3.39 g/cm<sup>3</sup>.

**3:40 PM**

**(PACC-S8-018-2022) Microstructure and properties of B-rich boron carbide fabricated by hot-pressing sintering (Invited)**

W. Wang<sup>\*1</sup>; T. Tian<sup>1</sup>; A. Wang<sup>1</sup>; W. Ji<sup>1</sup>; H. Wang<sup>1</sup>; Z. Fu<sup>1</sup>

1. Wuhan University of Technology, State Key Lab of Advanced Technology for Materials Synthesis and Processing, China

Boron carbide has a wide solubility range owing to the substitution of B and C atoms in the crystal. In this study, boron carbides with different stoichiometric ratios were prepared using a hot-pressing sintering method, and the influences of the B/C atomic ratio on the microstructures and properties were explored in detail. X-ray diffraction analysis showed that excessive B atoms caused lattice expansion. Raman spectroscopy analysis showed disordered substitution of B atoms in the chains and icosahedra. Analysis of the densification process and microstructure evolution revealed that the addition of B promoted densification, and more stacking faults and twins occurred in B-rich boron carbide, and result in the densification mechanism gradually changes from atomic diffusion mechanism driven by thermal energy to plastic deformation mechanism dominated by the proliferation of dislocation and substructures. The introduction of chemical composition changes by dissolving excessive B into boron carbide further affected the microstructure and consequently the mechanical response. The Vickers hardness, modulus, and sound velocity all decreased with the increase in B content. Moreover, the fracture toughness improved with increased B content. The flexural strength of the samples was optimized at the B/C stoichiometric ratio of 6.1.

**4:10 PM**

**(PACC-S8-019-2022) Aluminum-to-Ceramics Joining Method by Polysiloxane**

K. Kita<sup>1</sup>; T. Ohji<sup>\*1</sup>; N. Kondo<sup>1</sup>; M. Fukushima<sup>2</sup>; M. Hotta<sup>1</sup>

1. National Institute of Advanced Industrial Science and Technology (AIST), Japan
2. National Institute of Advanced Industrial Science and Technology (AIST), Japan

Multi-material structure using “the right materials in the right parts” is a promising design approach for improving performance and functionality of the products and systems. For utilizing this approach, a reliable technique of joining dissimilar materials is critically essential. Particularly, a joining method between aluminum and ceramics has a great demand from industry, because a multi-material composed of these materials has a combination of good conductor and insulator. This joining is, however, considered extremely challenging because of their stable surfaces. Utilization of polysiloxane is an innovative method of aluminum/ceramics joining process. Its thermal decomposition and reaction to aluminum enable easy and robust joining without any additional preparations such as a deoxidation of an oxidized layer on aluminum, surface modification of a ceramic substrate by metal coating, etc. The thickness of the joining layer is approximately 100 nm with the minimum of

less than 10 nm, and therefore, relatively good thermal conductivity and bending strength can be expected. This paper will first address a general outline of this joining method and then address a multi-material containing aluminum and silicon nitride substrate joined by this technique, which has a great thermal conductivity.

**PACC10: Ceramics for Sustainable Agriculture**

**Water Management and Waste Recycling**

Room: Vitri (Level M)

Session Chairs: Allen Apblett, Oklahoma State University; Dileep Singh, Argonne National Lab

**1:30 PM**

**(PACC-S10-001-2022) Synthesis and Corrosion Study of Polymer-Derived Ceramic Coatings on 304 Stainless Steel (Invited)**

K. Lu<sup>\*1</sup>; H. Choi<sup>1</sup>; W. Wang<sup>1</sup>; R. Cai<sup>1</sup>

1. Virginia Tech, USA

Corrosion of nuclear spent fuel storage canister is a serious concern due to deposition of corrosive marine salts by inducing chloride-induced pitting corrosion. Ceramic-based coatings such as silicon-based oxide are promising materials to protect canisters due to their low cost as well as excellent wear and corrosion resistance. In this work, SiON ceramic coatings were synthesized on 304 stainless steel substrate by crosslinking polysilazane (PHPS) precursor at room temperature and by pyrolysis at 600°C. Potentiodynamic test indicated that the corrosion resistance of the substrate in a 0.6 M NaCl aqueous solution is significantly improved after coating application. Better tribocorrosion resistance was observed in the coating synthesized at 600 °C. In addition, a SiOCN coating has been developed based on polysilazane (PHPS) and polysiloxane (PSO) preceramic polymers. The multilayer coating system consists of a SiON bond coat to secure adhesion, a SiONC as the main coat, and a passivated SiON/SiO<sub>2</sub> top layer. This work sheds light on the design strategy of corrosion-protective coatings for nuclear waste storage canisters used in harsh environments.

**2:00 PM - WITHDRAWN**

**(PACC-S10-002-2022) Aggressive Simulated Atmospheric Corrosion of Copper-Lignin Composites**

A. Nieto<sup>\*1</sup>; M. Dey<sup>2</sup>; S. Gupta<sup>2</sup>

1. Naval Postgraduate School, Dept. of Mechanical and Aerospace Engineering, USA
2. University of North Dakota, Mechanical Engineering, USA

There is significant interest in the materials science community in developing high performance materials from sustainable materials. To this end the harnessing of biorenewable natural or agricultural products for use in high performance metal or ceramic materials would be a milestone achievement. A promising type of biomass, lignin, has previously been explored for use in polymer matrix composites. Lignin is a complex natural polymer that is a primary constituent of structural tissues in plants such as the cell walls of wood. Here we report on the microstructure, mechanical properties, and corrosion behavior of lignin-copper hybrid composites, with the lignin content comprising 50 vol.% of the samples. Samples are evaluated in aggressive simulated atmospheric conditions using a salt fog chamber for over 3000 hours. Copper based materials have excellent corrosion resistance and the retention of improvement in corrosion resistance using bio renewable materials such as lignin would represent a new and sustainable materials approach to high performance composites. Corroded specimens are examined via scanning electron microscopy, energy dispersive spectroscopy, and x-ray diffraction analysis.



2:20 PM

**(PACC-S10-003-2022) Low-temperature Polymer-assisted Additive Manufacturing of Microchanneled Magnetocaloric Structures (Invited)**

V. Sharma<sup>2</sup>; L. Balderson<sup>1</sup>; H. Zhao<sup>1</sup>; R. Barua<sup>\*1</sup>

1. Virginia Commonwealth University, Department of Mechanical & Nuclear Engineering, USA
2. Virginia Commonwealth University, Department of Mechanical Engineering, USA

Magnetic refrigeration is an energy-efficient, sustainable, environmentally-friendly alternative to the conventional vapor-compression cooling technology. There are several magnetic refrigerator device designs in existence today that are predicted to be highly energy-efficient, on the condition that suitable working materials can be developed. This challenge in manufacturing magnetocaloric devices is unresolved, mainly due to issues related to shaping the mostly brittle magnetocaloric alloys into thin-walled channeled regenerator structures to facilitate efficient heat transfer between the solid refrigerant and the heat exchange fluid in an active magnetic regenerator (AMR) cooling device. To address this challenge, we have developed an extrusion-based additive manufacturing (AM) method to 3D print porous magnetocaloric structures with potentially controlled chemical gradients and magnetic anisotropy. Research efforts involving  $\text{La}_{0.6}\text{Ca}_{0.4}\text{MnO}_3$  nanoparticles and  $\text{AlFe}_2\text{B}_2$  powders will be presented to demonstrate the feasibility of printing spatially designed lattice structures with minimum microchannel dimensions of 150  $\mu\text{m}$ . Overall, this study provides guidelines for realizing low-cost magnetic regenerators, thus potentially eliminating one of the main barriers to the commercialization of magnetic cooling technology.

2:50 PM

**(PACC-S10-004-2022) Use of  $\alpha$ -alumina membranes with immobilized lipase for oil fouling degradation**

J. Mulinari<sup>\*1</sup>; A. Ambrosi<sup>1</sup>; M. Di Luccio<sup>1</sup>; Q. Li<sup>2</sup>; J. Oliveira<sup>1</sup>; D. Hotza<sup>1</sup>

1. Federal University of Santa Catarina, Department of Chemical Engineering and Food Engineering, Brazil
2. Rice University, Civil and Environmental Engineering Department, USA

Ceramic membranes are known for their advantages over polymeric membranes in terms of chemical, mechanical and thermal resistance. In this study, a nature-inspired coating (polydopamine) was used to immobilize the enzyme lipase on the surface of an  $\alpha$ -alumina tubular membrane. The goal was to create an active layer capable of degrading oil fouling during the oil-water separation process and membrane cleaning. The active membrane had a lower water permeance reduction after oil emulsion filtration (35%), a greater permeance increase after cleaning (25%), and a higher overall permeance recovery (90%) than the pristine membrane (that showed 62% of permeance reduction, just 10% of permeance increase after cleaning and 48% of overall permeance recovery). The use of ceramic material to provide a substrate to an active coating allows the reuse of the membrane after the enzymes lose their activity. A new coating can be applied after simple calcination or chemical cleaning. These processes do not affect the membrane physical and chemical properties, so the same modification method can be carried out to immobilize the enzyme and similar results can be expected in terms of fouling degradation.

3:30 PM

**(PACC-S10-005-2022) Biomass and wood derived materials for structural and energy applications (Invited)**

J. Ramirez-Rico<sup>\*1</sup>

1. Universidad de Sevilla, Spain

Materials development is driven by microstructural complexity, sometimes inspired by biological systems like bones, shells, and wood. In one approach, one selects the main microstructural features responsible for improved properties and designs processes to obtain materials with such microstructures. In a different approach, it is possible to use natural materials directly as microstructural templates. Among natural materials, wood is an interesting template due to its hierarchical structure and highly interconnected porosity optimized for fluid transport and mechanical strength. By thermal decomposition of wood or other vegetable templates, a porous carbon scaffold can be obtained that retains the structure of the precursor. This carbon scaffold can be infiltrated with silicon to obtain highly porous SiC ceramics with high mechanical strength, or can be functionalized to be used as an electrode in energy storage applications. Interestingly, the microstructure and porosity of the resulting material can be controlled simply by choosing from a wide range of commercially available, sustainable wood materials. In this presentation we will review the fabrication and properties of biomass templated structural and functional materials with a wide range of applications from hot-gas filtering to long-bone prosthesis, from catalyst supports to supercapacitor and battery electrodes.

4:00 PM

**(PACC-S10-006-2022) Design of Novel Membranes by Using Biomass for Different Types of Applications**

J. Zhang<sup>\*1</sup>; N. Ziamahmoodi<sup>1</sup>; S. McPherson<sup>1</sup>; G. Mackenzie<sup>1</sup>; S. Gupta<sup>1</sup>

1. University of North Dakota, Mechanical Engineering, USA

Biomass is an important source of raw materials for designing novel materials. In this paper, we will report latest development in the design of biomass based membranes from different types of biomass. We will report the microstructure, mechanical strength, and pore structure development of these solids during pyrolysis. In addition, we will also present functional application of these materials. It is expected that these materials can be commercialized and can be used in demanding applications.

4:20 PM

**(PACC-S10-007-2022) A Brief Report on Sustainable Manufacturing of Ceramics - ~~WITHDRAWN~~**

M. Dey<sup>\*1</sup>; J. Sabah<sup>1</sup>; E. Sofowora<sup>2</sup>; S. Gupta<sup>1</sup>

1. University of North Dakota, Mechanical Engineering, USA
2. University of North Dakota, Chemical Engineering, USA

Ceramics manufacturing is an energy intensive process. There is an urgent need to design ceramics by using sustainable practices. In this paper, we will report different approaches for greening of ceramics manufacturing. We will compare these novel manufacturing with literature. The characterization (microstructure and mechanical behavior) of these ceramics synthesized via sustainable methods will be presented.

## **PACC11: Materials Approach to Art, Architecture, and Archaeology in the Americas**

### **Sourcing**

Room: Venetian (Level B)

Session Chair: Molly McGath, The Mariners' Museum and Park

#### **1:30 PM**

### **(PACC-S11-010-2022) Advanced Microanalytical Approaches to the Study of Mesoamerican Obsidian and Jade**

E. P. Vicenzi<sup>\*1</sup>; T. Lam<sup>1</sup>; M. Noyes<sup>2</sup>; H. Lowers<sup>3</sup>

1. Smithsonian Institution, Museum Conservation Institute, USA
2. Rochester Institute of Technology, Image Permanence Institute, USA
3. U.S. Geological Survey, Microbeam Laboratory, USA

A suite of microscale methods was employed to examine obsidian mirrors from Central Mexico and jade beads from Chichén Itzá, Yucatan, Mexico to expand the ability to determine provenance (obsidian) and evaluate relationships between artifacts (jade). Co-located electron and micro-XRF beams were used to analyze obsidian, while correlated cathodoluminescence (CL) spectrometry and trace element analysis by wavelength dispersive X-ray spectrometry in the electron microprobe (WDS-EPMA) was utilized for the jade portion of the study. Multivariate statistical analysis of the obsidian mirrors and reference obsidian data connect the objects to two localities in the Los Azufres magmatic complex, while trace chromium has been quantitatively linked to luminescence in the near infrared within zoned jadeite crystals. The combined electron beam and micro-XRF approach provides a non-destructive technique that adds low atomic number elements to traditional higher atomic number elemental output for obsidian provenance studies, and newly established geochemical/textural fingerprints using CL and WDS-EPMA show promise for comparison among jade artifacts.

#### **1:50 PM**

### **(PACC-S11-011-2022) Pots across the Atlantic and beyond: Assessing provenance of Spanish colonial 16th-17th centuries tin-lead glazed ceramics by Non-destructive Portable X-Ray Fluorescence in the Americas**

J. G. Iñáñez<sup>\*1</sup>

1. University of the Basque Country, Geography, Prehistory and Archaeology, Spain

Non-destructive analytical techniques have emerged during the past years as an invaluable tool for archaeologists and museum professionals and are widely applied to numerous and heterogeneous kind of artifacts in museum collections. In this regard, portable x-ray fluorescence (pXRF) instruments have emerged as a virtuous tool for non-destructive elemental analyses and, although the spread of such technologies is an important step forward for the Archaeological Community, several problems may be pointed out. Thus, 16<sup>th</sup> and 17<sup>th</sup> centuries ceramics among tin-lead glazed well-established chemical reference groups of Spanish and Spanish American Colonial contexts, which were previously characterized by bulk analyses techniques (e.g. NAA, ICP-MS), will be assessed by pXRF. The strengths and limitations of pXRF for provenance studies on glazed pottery, the occurrence of complex clay matrix arrays and heavy metal coatings (e.g. lead glazes), are assessed. In light of the results, it can be concluded that nowadays pXRF instruments can become invaluable tools for screening among large set of ceramics for provenance studies, saving important efforts and resources when designing a project that includes destructive analyses.

#### **2:10 PM**

### **(PACC-S11-012-2022) Sourcing the Pottery of Machu Picchu**

L. C. Salazar<sup>\*1</sup>

1. Yale, Anthropology, USA

Machu Picchu is one of the most famous archaeological sites in the New World. Despite this, much remains to be learned about basic aspects of this site's organization and history. For example, abundant pottery has been recovered in the excavations of this Inca royal estate from domestic contexts, public settings and burials. However, there is no evidence that pottery was ever produced at the country palace itself and it is unknown how the site was provisioned with ceramics. Was the pottery produced by a single centralized workshop in the Machu Picchu area or did it acquire its pottery from multiple production centers in the Urubamba drainage and the Cuzco Valley? Neutron activation analysis of pottery recovered by Hiram Bingham in 1912 has shed light on the answer to this question and allows archaeologists to better understand how Machu Picchu was integrated into the local, regional and pan-regional Inca economy.

#### **2:30 PM**

### **(PACC-S11-013-2022) Sourcing Pottery with LA-ICP-MS and P-XRF: Monagrillo, the Earliest Ceramics of Panama**

F. Iizuka<sup>\*1</sup>

1. University of California Merced, Social Sciences, Humanities and Arts, USA

Monagrillo pottery, the earliest of Panama and Central America, ca. 5500-3300 cal BP, is found in the northeastern Azuero Peninsula and the Pacific plains, foothills, and cordillera and the Caribbean slopes of the isthmus proper of central Panama. Pottery was adopted by egalitarian farmers who had broad-spectrum diet. It was unclear earlier whether these people farmed somewhat inland during the wet season and engaged in fishing and shell-fish collecting on the coast during part of the dry season, or were sedentary people engaging in exchange of local products. I conducted a petrographic provenance study and suggested that it was produced in the Azuero coast and the Pacific slopes towards the alluvial zones. In this study, I re-evaluate the results of Monagrillo geochemical sourcing with LA-ICP-MS and pXRF. I compare the evaluated sources with petrography. The result of sourcing aligns with that based on petrography. Monagrillo vessel producers made pots in areas close to the Azuero coast and the Pacific slopes towards lowlands. Farmers of the sedentary communities met in the mid-point, in the Pacific plains and engaged in exchange of local resources using pottery as containers. Although pottery production zones did not change through time, exchange may have started later than the first use of pottery.

### **Technology**

Room: Venetian (Level B)

Session Chair: Darryl Butt, University of Utah

#### **3:10 PM**

### **(PACC-S11-014-2022) X-ray MicroCT Analysis: Using Nondestructive Imaging Technology Particularly for Studying Archaeological Ceramics of the Americas and Their Residues**

J. Henkin<sup>\*1</sup>

1. Field Museum of Natural History, USA

Residue analysis of archaeological ceramics is a complicated endeavor that usually ends up requiring (micro)destructive (sub) sampling of some sort. Surface sampling mass spectrometry and vibrational spectroscopy techniques are now more than ever enabling work with archaeological materials. Usually, analytical chemistry data for residue analysis is more deficient in microspatial data about the ceramics and their contents however. Without having

this orthogonal data such as can be provided by contemporary X-ray (micro)computed tomography analysis, archaeological interpretations of analytical chemistry data may be limited and equivocal, and there may be too little justification to (sub)sample archaeological ceramics from the perspectives of archaeologists, curators, and collection managers. Thus, two X-ray microCT instruments, a Rigaku GX 130 and a Rigaku nano3DX, were used to interrogate the microstructure of archaeological ceramics from sites in the Americas. Preliminary results for the analysis of (ethno)archaeological Wari discovered at Cerro Baúl and/or Cerro Mejía, Peru and related Peruvian materials; for exploratory residue analysis research into ceramics from Kala Uyuni, Bolivia; and for ceramics from Western Mexico promising as leads for ancient cacao beverage consumption are three applications that may be assessed herein.

### 3:30 PM - **WITHDRAWN**

#### **(PACC-S11-015-2022) The pottery collections from Puerto Nuevo on the southern coast of Perú: Insights into long-distance exchange networks of prestige pottery during the Middle and Late Formative of the Central Andes**

I. Aguirre\*<sup>1</sup>; J. Dulanto<sup>1</sup>

1. Pontificia Universidad Católica del Perú, Humanidades, Peru

In this article, we present our progress in the study of the technological, morphological, and decorative characteristics of a collection of prestige pottery vessels from the archaeological site of Puerto Nuevo, a first millennium BC fishing village on the southern coast of Perú. Our study is a contribution to our understanding of the complex interregional social interactions involved in the long-distance exchange of prestige and exotic ceramic style during the Middle and Late Formative periods in the Andes. Contrary to the current understanding of ceramic manufacture and exchange during these earlier periods, we find evidence for a continuous exchange of a few special prestige pieces, widespread local imitation of these pieces by local pottery, and the rapid emergence of new local hybrid styles on the South Coast.

### 3:50 PM

#### **(PACC-S11-016-2022) A Concurrent Analytical Study of Two Maya Incensario Supports**

E. M. Mars\*<sup>1</sup>

1. Cleveland Museum of Art, Art Conservation, USA

The Cleveland Museum of Art has two standing-figure incensario supports attributed to the Palenque region of Chiapas, Mexico. Like many pre-Columbian artworks acquired by collecting institutions outside of source countries, their provenience is unknown. Understanding of such artworks is based on form and iconography alone, which is challenging when artworks are fragmented or have undergone multiple restorations, like the Cleveland incensario supports. Additionally, regional variation is common, potentially muddying understanding of iconography when works have been removed from their original context. The rarity of standing-figure incensario supports from Palenque and the occurrence of forgeries prompt further investigation through technical analysis. This presentation will share the results of a variety of analyses including multimodal imaging, X-ray fluorescence, Fourier-transform infrared spectroscopy, Raman spectroscopy, scanning electron microscopy and energy dispersive X-ray spectroscopy, and polarized light microscopy to identify pigments and restoration materials. Thermoluminescence testing with Oxford Authentication LTD and neutron activation analysis with Iowa State University were also employed to assist with dating and identifying production locales. These analyses not only add to the growing scientific knowledge of Maya artworks but also inform decisions about conservation treatment and exhibition.

### 4:10 PM

#### **(PACC-S11-017-2022) High-resolution Micro-CT with 3D Image Analysis for Porosity Characterization of Bricks and Ceramics**

C. L. Reedy\*<sup>1</sup>

1. University of Delaware, Center for Historic Architecture and Design, USA

The study of pores in historic American bricks is important for characterizing and comparing materials, evaluating deterioration, studying the effectiveness of protective measures, and analyzing potential effects of cleaning treatments. For archaeological ceramics, analysis of pore systems can indicate intended functions and inform studies of raw materials, fabrication, and firing methods. High-resolution micro-CT coupled with 3D image analysis is a promising new approach for studying pore systems in bricks and ceramics. This paper presents a set of protocols for creating optimal images of pores in micro-CT scans of bricks and ceramic sherds, and for conducting 3D image analysis to extract both qualitative and quantitative data from those scans. Machine learning and deep learning with convoluted neural networks are important tools for better distinguishing pores from the surrounding matrix in the segmentation process, especially at the very limits of spatial resolution. Statistical analyses reveal which of the many parameters that can be measured are potentially most significant for characterizing the pore systems of bricks and ceramic sherds. These significant pore variables come from a multi-staged image analysis approach and include total volume porosity, porosity accessible to the surface, pore size and shape properties, and variables related to connections between pores.

### 4:30 PM

#### **(PACC-S11-018-2022) The technology of stirrup spout bottles from the North coast of Peru. Analysis by CT scan**

V. Wauters\*<sup>1</sup>

1. Royal Museums of Art and History of Brussels, Free University of Brussels(ULB), Belgium

The stirrup spout bottle is an emblematic ceramic form of pre-Columbian cultures, mainly those of South America. It was produced among about fifty pre-Hispanic cultures during almost 4000 years of history. It is therefore an essential element of the material culture of these civilizations. Several dozen stirrup spout vessels from the collections of the Royal Museums of Art and History of Brussels (Belgium) were analyzed using medical imaging (CT scan). They come from the Cupisnique (1200-200 ACN), Mochica (100-900 PCN) and Chimú (900-1450 PCN) cultures of the North coast of Peru. The stirrup spout bottle is an almost closed ceramic form, whose only opening is that of the spout, which is generally very narrow. Consequently, the most appropriate analysis methods are those of medical imaging. The CT scan allows to see the inner surface of the vessels and to understand how they were made. The results of these analyses allowed to identify the manufacturing processes within these three cultures and to compare them with each other.

## Ferroelectrics Meeting of Americas

### Dielectrics/Composites/Growth II

Room: Mirage (Level B)

1:30 PM

#### (FMAs-027-2022) Strontium titanate based n-type oxide thermoelectrics for low-cost electricity generation from waste heat (Invited)

T. Maiti\*<sup>1</sup>

1. IIT Kanpur, Dept. of Materials Science & Engineering, India

Thermoelectric materials are considered as cleanest source of energy generation by converting waste heat into electricity. Oxides are attractive because of their environmentally benign nature, low fabrication cost and better stability at high temperature compared to other thermoelectric materials. Recently we have investigated wide range of rare-earth-free SrTiO<sub>3</sub> based perovskites and double perovskites to evaluate their potential for high temperature thermoelectric applications. We have used various strategies such as reducing octahedral tilting, manipulating B-site cation ordering in perovskites in order to facilitate the charge transport phenomena in these oxides, which are inherently insulator in nature. It has been observed that these oxides invariably exhibit semiconductor ( $d\sigma/dT > 0$ ) to metal ( $d\sigma/dT < 0$ ) transitions. Furthermore, we achieved very high figure of merit or  $ZT > 1$  by forming nanocomposite of donor doped rare-earth free SrTiO<sub>3</sub> with graphene oxide and graphite. We have successfully demonstrated that manipulating the semiconductor to metal transition can be a robust way of enhancing ZT values of oxide thermoelectrics, which potentially opens up a new avenue of designing oxide thermoelectrics for clean energy generation from waste heat produced at high temperatures.

2:00 PM

#### (FMAs-028-2022) Some Approaches for Single Phase Room Temperature Multiferroic Materials with Strong ME Coupling (Invited)

X. Chen\*<sup>1</sup>

1. Zhengzhou University, School of Materials Science and Engineering, China

Exploring single phase multiferroic material has been a long-time-sought quest due to the promise of novel spintronic devices, and it has been a big challenge to realize the room temperature strong magnetoelectric coupling with large polarization. In the present work, some primary approaches for single phase room temperature multiferroic materials has been investigated. At first, the electric field-controlled magnetism is realized through symmetry modulation and the subsequent field-induced transition of Pn21/R3c in Bi<sub>1-x</sub>R<sub>x</sub>FeO<sub>3</sub> ceramics. Secondly, the room temperature multiferroic new system of h-Lu<sub>1-x</sub>In<sub>x</sub>FeO<sub>3</sub> has been developed, where the strong intrinsic magnetoelectric coupling could be expected through the lattice distortion which is the origin of the ferroelectricity and deeply linked with the magnetism due to Fe-O-Fe super exchange. Finally, the hybrid improper ferroelectric La<sub>0.5</sub>Y<sub>0.5</sub>FeO<sub>3</sub> ceramic with A-site ordering and strong magnetoelectric coupling has been proposed and developed.

2:30 PM

#### (FMAs-029-2022) Ferroelectric ordering and electrical energy storage in lead-free ferroelectric Ba<sub>1-x</sub>Sr<sub>x</sub>TiO<sub>3</sub> capacitors

I. W. Castillo<sup>1</sup>; K. K. Mishra<sup>1</sup>; R. Katiyar\*<sup>1</sup>

1. University of Puerto Rico, USA

Structure, phonon, and electrical energy density storage in Sr<sup>2+</sup>-substituted lead-free ferroelectric Ba<sub>1-x</sub>Sr<sub>x</sub>TiO<sub>3</sub> (BST<sub>x</sub>) (x = 0.1, 0.3, and 0.7) samples were studied utilizing X-ray diffraction, Raman spectroscopy, and ferroelectric polarization measurements. The

system is tetragonal for x = 0.1 with large c/a ratio (anisotropy) at room temperature that decreases with increasing x and it transforms into cubic phase with x = 0.7. For x ≤ 0.3, the tetragonal phase shows gradual change in the c/a ratio upon rising temperature and it stabilizes in the cubic phase at higher temperatures. The temperature dependent phonon spectroscopic results indicate reduction in tetragonal to cubic phase transition temperature upon increasing x. The overdamping of the E-soft phonon mode at ~90 cm<sup>-1</sup> and a dramatic decrease in the intensity of A-mode at ~160 cm<sup>-1</sup> were observed at the tetragonal ferroelectric to cubic paraelectric phase transition (T<sub>c</sub>). Using UV-Vis optical absorption spectra, the optical band gaps of these compounds were calculated as 1.73, 1.7, and 1.68 eV for x = 0.1, 0.3, and 0.7 respectively. The energy storage densities of the polled BST<sub>x</sub> capacitors (metal-insulator-metal) were estimated using the polarization hysteresis loops. For x = 0.7, a large energy storage density (U<sub>re</sub>) of 20 Joule/cm<sup>3</sup> with efficiency of 57 % was estimated at an applied electrical field of 88 kV/cm.

2:50 PM

#### (FMAs-030-2022) Properties of In and Ta Dipole Substituted and Doped BaTiO<sub>3</sub>

N. Betancur-Granados\*<sup>1</sup>; E. K. Merkey<sup>2</sup>; I. Chedzoy<sup>2</sup>; K. Ning<sup>2</sup>; J. I. Tobón<sup>3</sup>; O. J. Restrepo<sup>3</sup>; H. Shulman<sup>2</sup>; S. M. Pilgrim<sup>2</sup>; W. A. Schulze<sup>2</sup>; S. Tidrow<sup>2</sup>

1. Corporación Universitaria Minuto de Dios - UNIMINUTO, Faculty of engineering, Colombia
2. Alfred University, USA
3. Universidad Nacional de Colombia, Department of Materials, Colombia

Dopants play a significant role in electronic material design. In semiconductors, donor and acceptor doping enhance electron and hole conduction, respectively, while simultaneously donor and acceptor doping counteract one another. The role of dopants within dielectrics are not as well studied nor are the effects as well understood. In this investigation, both the effects of dopant and dipole dopant substitution of In and Ta within BaTiO<sub>3</sub> are systematically investigated and frequency and temperature dependent dielectric properties are reported. Experimental data indicate that doping of In and Ta within BaTiO<sub>3</sub> follows semiconductor theory; yet, dipole dopant substitution significantly reduces conductivity and results in the evolution of BaTiO<sub>3</sub> from strict ferroelectric to diffuse phase transition to a relaxor-like ferroelectric within the formed solid solution Ba(In,Ta)<sub>y</sub>Ti<sub>1-2y</sub>O<sub>3</sub>, 0 ≤ y ≤ 0.05. This work of dopant versus dipole dopant substitution within BaTiO<sub>3</sub>, provides generalized guidance for developing advanced (novel) materials.

3:30 PM

#### (FMAs-031-2022) High Impacts Inventions on Piezoelectric Ceramic Devices in the Last Four Decades (Invited)

T. Xu\*<sup>1</sup>; B. Zhao<sup>1</sup>

1. Old Dominion University, Mechanical and Aerospace Engineering, USA

In this talk, the high impact inventions on piezoelectric ceramic devices will be introduced and reviewed from several dozens of innovative piezoelectric devices in the last 4 decades. The highlighted inventions will include metal-electroactive ceramic composite actuators (Cymbal) [1-2], thin layer composite uni-morph ferroelectric driver and sensor (Thunder) [3], piezoelectric macro fiber composites (MFC) [4], polymer ceramic hybrid actuators [5], hybrid piezoelectric energy harvesting systems/transducers [6,7], hybrid piezoelectric synthetic actuators [8-10], multistage force/displacement amplification piezoelectric harvester/transducers [11], and high-power-density piezoelectric energy harvesting system [12]. In this review, the background and motivations of those inventions will be briefly introduced, and the work principles of the highlighted inventions will be explained, and the impact on increase orders of magnitude energy densities of those piezoelectric transduction devices will be summarized. The advantages performance and potential applications of those invented devices will be briefly discussed.

## 4:00 PM

### (FMAs-032-2022) Structural, Dielectric and Ferroelectric Properties of Rare Earth Doped Lead Zirconate Titanate

M. Bhattarai<sup>1</sup>; K. K. Mishra<sup>1</sup>; R. Katiyar<sup>\*1</sup>

1. University of Puerto Rico, Rio Piedras Campus, Physics, USA

The electro-ceramics with the stoichiometric formula  $(\text{PbZr}_{0.53}\text{Ti}_{0.47})_{0.90}(\text{La}_x\text{Sc}_{1-x})_{0.10}\text{O}_3$  (Viz; PLZTS10x) for  $x = 0.2, 0.4, 0.6$  &  $0.8$  were synthesized by a solid-state reaction method. Rietveld analyses of the X-ray diffraction data indicate tetragonal phase with decreasing tetragonal anisotropy. Temperature-dependent phonon spectra demonstrated tetragonal-to-cubic structural phase transition in the temperature of 80-580 K. Dielectric spectroscopic studies carried out on Ag/PLZTS10x/Ag capacitors covering the frequency range from  $10^2$ - $10^6$  Hz in the temperature range 100-600 K, exhibited high dielectric constants and low losses. Modified Curie-Weiss law analyses on the dielectric data for  $x = 0.8$  indicates diffuse phase transition with diffusivity parameter  $\gamma \sim 1.94$ . High breakdown field and spontaneous polarization were obtained from electrical hysteresis loop measurement. The remanent polarization ( $P_r$ ) was increasing upon the increasing value of  $x$  and observed high  $P_r \sim 35 \mu\text{C}/\text{cm}^2$  for  $x = 0.6$ . However, further increasing  $x$  resulted in a slimmer hysteresis loop supporting the dielectric diffusivity. A significant amount of recoverable energy density  $\sim 1162 \text{ mJ}/\text{cm}^3$  with an efficiency  $\sim 79\%$  was estimated. These results may provide insights into the PLZTS10x ferroelectric capacitor for its potential memory and power device applications.

## 4:20 PM

### (FMAs-033-2022) Synthesis and Mechanical Properties of $\text{Li}_2\text{CO}_3$ and $\text{Bi}_2\text{O}_3$ added $\text{BaTi}_{1-x}\text{Zr}_x\text{O}_3$ ( $x = 0.05$ and $0.10$ ) Ceramics

K. I.; N. Somani<sup>\*1</sup>; N. Gugar<sup>1</sup>; P. Kumar<sup>1</sup>; C. Prakash<sup>2</sup>

1. DIT University, India

2. Maharaja Agrasen Institute of Technology, Applied Sciences, India

Barium titanate based ceramics are widely used electroceramic due to their non hazardous effects and smart properties. Therefore, by increasing its mechanical strength we can increase its field of application. The purpose of this study is to check the influence of sintering aid on the mechanical properties of Barium Zirconate Titanate ' $\text{BaTi}_{1-x}\text{Zr}_x\text{O}_3$ ' with  $x = 0.05$  (BZT5) and  $0.10$  (BZT10). Here we check the effect of  $\text{Li}_2\text{CO}_3$  and  $\text{Bi}_2\text{O}_3$  addition on the mechanical properties of BZT5 and BZT10 ceramics. The samples were prepared by conventional solid state reaction method. In this method, the samples were ball milled for 12 hours, followed by calcination  $1000^\circ\text{C}$  for 4 hours and finally sintered at  $1300^\circ\text{C}$  for 4 hours. Hardness tests were done for testing the micro hardness of material. The result will be discussed according to test outputs and correlated with other properties.

## 4:40 PM

### (FMAs-034-2022) Room Temperature Dielectric and Ferroelectric Properties of Barium Titanate Ceramics Substituted Simultaneously by $\text{La}^{3+}$ at A-site and $\text{Fe}^{3+}$ at B-site

A. Mehta<sup>\*1</sup>; P. Kumar<sup>2</sup>; C. Prakash<sup>3</sup>

1. DIT University, Physics, India

2. DIT University, Physics, India

3. Maharaja Agrasen Institute of Technology, Applied Sciences, India

The material series with compositional formula  $\text{Ba}_{1-x}\text{La}_x\text{Ti}_{1-x}\text{Fe}_x\text{O}_3$ , (with  $x = 0.00, 0.005, 0.01, 0.015, 0.02$ ) was chosen and investigated. The samples were prepared by solid state reaction route and compacted in the form of circular discs which were sintered at  $1325^\circ\text{C}$  for 4 hours. Dielectric constant and tangent loss was measured as a function of frequency from 100Hz to 100kHz for all the samples. Higher values of dielectric constant were achieved in all  $\text{La}^{3+}$  and  $\text{Fe}^{3+}$  substituted samples. The variation of AC conductivity for all the samples was studied as a function of frequency and substituent content. PE hysteresis loops were recorded for all the

samples at room temperature. The variation of remanent polarization and coercive field was studied as a function of substituent content. Keywords: Solid State Reaction; dielectric constant; tangent loss; ferroelectric properties.

## Ferroics and Multiferroics I

Room: Star Bay 3 (Level B)

Session Chair: Danilo Suvorov, Jozef Stefan Institute

## 1:30 PM

### (FMAs-035-2022) Rough buffer layers as a tool for stabilizing the perovskite phase in PMN-PT thin films (Invited)

D. Suvorov<sup>\*1</sup>; M. Spreitzer<sup>2</sup>

1. Jozef Stefan Institute, Advanced Materials, Slovenia

2. Jozef Stefan Institute, Advanced Materials, Slovenia

$\text{Pb}(\text{Mg}_{1/3}\text{Nb}_{2/3})\text{O}_3$ - $\text{PbTiO}_3$  (PMN-PT) thin films exhibit numerous attractive properties that can be exploited in different applications in the field of electronics. They are usually grown on electrode layers to construct parallel plate capacitors for studying their electrical properties. While the advantages of oxide electrodes over metallic ones have been shown in several studies, the roles of specific oxide electrodes on the phase formation and functional properties of the overgrown films are often disregarded. We found that the use of a  $\text{LaNiO}_3$  bottom electrode on  $\text{SrTiO}_3$  (STO) enhances the stability of the perovskite phase in PMN-PT films. In order to find the origin of the stabilization, we prepared PMN-PT on other buffer layers, such as  $\text{SrO}$ ,  $\text{SrRuO}_3$  and  $\text{PbZr}_{0.52}\text{Ti}_{0.48}$ . We found that the main reason for the improved stability was the increased interface roughness, as compared to the bare STO substrates. A rougher surface enabled stronger binding of Pb-based species. Thus, for the purpose of preparing PMN-PT directly on STO to be used with interdigitated electrodes, we modified the surface of the substrates by growing a rough homoepitaxial layer. This way, we substantially improved the phase purity of PMN-PT on STO, which represents an important step in the fabrication of energy harvesting devices that operate in the longitudinal mode.

## 2:00 PM

### (FMAs-036-2022) Rapid discovery of superior energy storage performance in lead-free ferroelectric films with slush polar states via machine learning (Invited)

A. Chen<sup>\*1</sup>

1. Los Alamos National Lab, USA

The energy storage performance in a given ferroelectric system strongly depends on the domain structure and break-down field. Relaxor ferroelectrics with slush polar states exhibiting high density of domain walls and nanoscale domains could be an ideal candidate to achieve outstanding energy storage efficiency. In addition, doping is a common approach to suppress leakage current and improve the break-down field, which is critical to achieve excellent energy storage density. Integration of both aspects in one material is extremely challenging as it involves time-consuming optimization of multiple cations. In this work, using  $\text{BaTiO}_3$  as a model system, we demonstrated a machine learning (ML) enabled fast discovery of new relaxor ferroelectric thin films with five cations for superior energy storage performance. The formation of slush polar states at nanoscale was understood by phase field simulation and confirmed by aberration-corrected scanning transmission electron microscopy. The formation of nanoscale domains and break-down field enhancement via multiple cation doping are contributed to the excellent energy storage efficiency and density. Such a design principle can be applied to other ferroelectric systems for enhanced energy storage applications.

**2:30 PM****(FMAs-037-2022) Development of Ferroic and Multiferroic Nanomaterials for Hybrid 3D Deposition of Dynamically Tunable Electromagnetic Devices**B. D. Young<sup>\*1</sup>; R. Guo<sup>2</sup>; A. S. Bhalla<sup>2</sup>

1. Sandia National Laboratories, Microsystems Packaging and Polymer Processing, USA
2. University of Texas, San Antonio, USA

3D deposition of devices is a rapidly growing area of research given its bottom-up fabrication approach and the control this gives over the structure of the device. Implementation of ferroics and multiferroics has become increasingly attractive in this field as well, due to their potential to enable control of a device's electrical properties via an applied magnetic field and vice-versa. To this end, CoFe<sub>2</sub>O<sub>4</sub> and CoFe<sub>2</sub>O<sub>4</sub>-BaTiO<sub>3</sub> inks have been developed for implementation in 3D deposited dynamically tunable inductors and terahertz resonators. The CoFe<sub>2</sub>O<sub>4</sub>-BaTiO<sub>3</sub> nanocomposites were synthesized and then characterized via XRD/TEM/AFM studies. Both sets of inks had their jetting characteristics quantified and the printing process optimized. Before fabrication, finite element models were constructed in COMSOL Multiphysics to predict the device behavior and tunability characteristics. CoFe<sub>2</sub>O<sub>4</sub>-based tunable inductors and split ring resonators (SRRs) were then deposited using the Ceradrop F-Serie Hybrid 3D Deposition Platform (H3D); the tunable inductors then had their inductive performance and tunability measured and analyzed.

**2:50 PM****(FMAs-038-2022) Phase transitions and magnetoelectric coupling of epitaxial asymmetric multilayer heterostructures and superlattices (Invited)**D. K. Pradhan<sup>\*1</sup>

1. University of Tennessee, Department of Materials Science and Engineering, USA

Magnetoelectric (ME) materials operated at room temperature (RT) remains of keen interest due to their potential applications in ideal ultralow power and high-density memory, spintronics, magnetic field sensors, and other multifunctional devices. ME heterostructures can exhibit higher magnetic and ferroelectric ordering temperatures along with large ME coupling compared to single-phase multiferroic materials. (i) We synthesized Pb(Fe<sub>0.5</sub>Nb<sub>0.5</sub>)O<sub>3</sub>/Ni<sub>0.65</sub>Zn<sub>0.35</sub>Fe<sub>2</sub>O<sub>4</sub> multilayer heterostructures having dimensions of 40/10/40/10/40 nm. High quality epitaxial growth of these heterostructures was confirmed via XRD and SAED patterns. These nanostructures show well saturated polarization (~ 52 μC/cm<sup>2</sup>) and magnetization (~ 62 emu/cm<sup>3</sup>) at RT. The magnetic and ferroelectric transitions occur well above RT. These heterostructures exhibit relaxor behavior and undergo 2nd order FE phase transition. ME measurements show significant coupling between the magnetic and electrical order parameters at RT. (ii) We synthesized multiferroic superlattices of Pb(Zr<sub>0.53</sub>Ti<sub>0.47</sub>)<sub>0.60</sub>(Fe<sub>0.5</sub>Ta<sub>0.5</sub>)<sub>0.40</sub>O<sub>3</sub> (PZTFT) and La<sub>0.7</sub>Sr<sub>0.3</sub>MnO<sub>3</sub> (LSMO) layers on LSMO buffered LSAT substrates. These superlattices exhibit very high ME coupling (~ 480 mV/cm.Oe). The physical properties, nature of ME coupling and origin of ME coupling will be discussed in details in the meeting.

**3:30 PM****(FMAs-039-2022) Structural changes and local electric/magnetic properties of strained BiFeO<sub>3</sub> nanoparticles (Invited)**E. A. Volnistem<sup>\*1</sup>; I. A. Santos<sup>\*1</sup>

1. State University of Maringa, Physics, Brazil

Crystal imperfections such as dislocations can cause several changes in structural parameters and consequently affect the (ferro)electric and magnetic properties of multiferroics. In this sense, it is essential to understand how these imperfections affect the structure of such materials in order to correlate it to some improved or novel

physical properties. In this study, the structural changes induced by a strain-controlled BiFeO<sub>3</sub> synthesis (cryo-milling) were investigated by means of X-Ray diffraction, Rietveld Refinement and Infrared spectroscopy (FT-IR) for nanoparticles with micro-strain ranging from 0% to 1.2%. Rietveld refinement confirmed the increase of micro-strain level according to the synthesis parameters and revealed R3c space group along with some significant changes in the Fe-O-Fe bond angle (from 169.6° to 160.8°). FT-IR analysis showed a decrease in the Fe-O bond length from 1.964 Å to 1.952 Å and two additional peaks in the region of 670–490 cm<sup>-1</sup> that also suggest the increase of the internal micro-strain. Such changes were correlated with the increase of magnetization (from 0.1 to 0.6 emu/g) and the origin of local weak-ferromagnetism in small BiFeO<sub>3</sub> nanoparticles (< 50 nm). In addition, local electric and magnetic properties investigated by scanning probe techniques (KFM and MFM) showed some strain-correlated changes in the local surface potential and magnetization.

**4:00 PM - WITHDRAWN****(FMAs-040-2022) Magnetodielectric and Magnetoelectric Coupling in PZT/CFO Nanostructured Composites Fabricated by RF-Sputtering**F. L. Zabotto<sup>\*1</sup>; R. P. Bonini<sup>1</sup>; A. J. Gualdi<sup>1</sup>; J. A. Eiras<sup>1</sup>

1. Federal University of Sao Carlos, Physics Department, Brazil

The magnetoelectric coupling in nanostructured systems has attracted interests mainly due to possibility of integration between ferroelectricity and ferromagnetism through the handling of electric and magnetic order by cross coupling between electric and magnetic fields. In this work, the fabrication process was investigated by the RF-Sputtering technique and the characterization of heterostructured multiferroic composite materials of Pb(Zr<sub>0.2</sub>Ti<sub>0.8</sub>)O<sub>3</sub>/CoFe<sub>2</sub>O<sub>4</sub> were performed. The interface between phases has a significant role for the existence of coupling between the different phases, where variations of the ferroelectric and dielectric properties in the heterostructured system were correlated to strain and/or stress at the interface between the phases. It was also possible to determine the existence of magnetoelectric coupling, since an improvement of the ferroelectric properties was observed under the presence of a magnetic field of ~5 kOe. Finally, it was reported that the magnetodielectric coupling is enhanced in the dielectric dispersion region due to competition between the compressive stress in the PZT phase generated by CFO phase and the changes of electric polarization due to the ME coupling.

**4:20 PM****(FMAs-041-2022) Thallium based chalcogenide rad hard multifunctional crystals**N. B. Singh<sup>\*1</sup>; C. H. Su<sup>2</sup>; F. Choa<sup>4</sup>; B. R. Arnold<sup>3</sup>; B. Cullum<sup>3</sup>; L. R. Kelly<sup>3</sup>

1. University of Maryland Baltimore County, Chemistry and Biochemistry and Computer Science and Electrical Engineering, USA
2. NASA Marshall Space Flight Center, USA
3. University of Maryland Baltimore County, Chemistry and Biochemistry, USA
4. University of Maryland Baltimore County, Computer Science and Electrical Engineering, USA

There is a continuous need for the bulk single crystals and glasses transmitting in near infrared to mid-infrared (MWIR) and long wave infrared (LWIR) regions for variety of applications. In addition, the low absorption and good quality materials are required for achieving high power for variety of applications. We have been working with binary and multinary compounds including both classes of chalcopyrites and chalcogenides. We observed that thallium based materials such as Tl<sub>3</sub>AsSe<sub>3</sub>, Tl<sub>3</sub>PSe<sub>4</sub>, AgTlSe<sub>2</sub>, TlGaSe<sub>2</sub>, TlGaGe<sub>n</sub>Se<sub>2(n+1)</sub> and Tl<sub>0.5</sub>Ag<sub>0.5</sub>GaGe<sub>n</sub>Se<sub>2(n+1)</sub> have extremely low absorption and transmit from 0.60 to 16mm wavelength region. Most of these materials have shown congruency and were grown by Bridgman methods. This enabled preparation of glasses by

quenching methods in quartz ampoules. Details of preparation, characteristics and performance of these materials will be presented for MWIR and LWIR applications.

4:40 PM

### (FMAs-042-2022) Magneto-Electric Effects in Coaxial Nanofibers of Hexagonal Ferrites and Ferroelectrics (Invited)

G. Srinivasan<sup>\*1</sup>; Y. Liu<sup>1</sup>

1. Oakland University, Physics, USA

This report is on magneto-electric (ME) effects in core-shell nanofibers of hexagonal ferrites and ferroelectrics. Such fiber composites are of interest since the large uniaxial or planar anisotropy field in the hexaferrites is expected to result in strong ME response in the absence of a bias magnetic field and will have the potential for use in magnetic sensors and energy harvesting applications. Core-shell fibers of hexagonal ferrites and ferroelectric PZT or barium titanate (BTO) were synthesized by electrospinning [1,2]. The fibers of PZT and BTO with SrM, Ni<sub>2</sub>Y, Zn<sub>2</sub>Y, Co<sub>2</sub>W and Zn<sub>2</sub>W were found to be free of impurity phases and the core-shell structure was confirmed by electron and scanning probe microscopy. The coaxial fibers showed good ferroelectric polarization. The magnetization, however, was much smaller than that for bulk hexaferrites. Magneto-electric (ME) coupling strength was characterized by measuring the magnetic field H induced polarization and ME voltage coefficient (MEVC) for films of coaxial fibers. In SrM-PZT/BTO fibers the remnant polarization decreased by as much as 20% with the application of H. Among the fibers with Y-type, films with Zn<sub>2</sub>Y showed a higher MEVC than films with Ni<sub>2</sub>Y. The highest MEVC of 20.3 mV/cm Oe was measured for Co<sub>2</sub>W-PZT fibers. The fibers studied here are of interest for use in magnetic sensors and high-frequency device applications.

## FMAs Poster Session

Room: Star Bay 1/2

5:30 PM

### (FMAs-P047-2022) Anomalous dielectric response of Pb<sub>0.60</sub>Ca<sub>0.40</sub>TiO<sub>3</sub> under different poling conditions

C. P. Moreira<sup>\*2</sup>; F. P. Milton<sup>2</sup>; F. R. Estrada<sup>1</sup>; D. Garcia<sup>2</sup>

1. National Research Center on Energy and Materials (CNPEM), Brazil
2. Federal University of Sao Carlos, Brazil

Investigations on the structure-property relationships of the Pb<sub>1-x</sub>Ca<sub>x</sub>TiO<sub>3</sub> system have been carried out as an effort to contribute to the establishment of its yet undetermined phase diagram. In this work, the dielectric and piezoelectric characteristics of Pb<sub>0.60</sub>Ca<sub>0.40</sub>TiO<sub>3</sub> ceramics were evaluated under different poling conditions. The overall characterization was made on conventionally sintered ceramic discs with relative apparent density >95%. After cutting and polishing the samples, silver electrodes were deposited on both faces and the electric DC poling process was performed at same temperature (70-75°C) but varying time and strength of the electric field. Thermal depoling was performed between measurements and next poling step. Electric hysteresis loops were measured using a modified Sawyer-Tower circuit and the dielectric/piezoelectric properties were determined by impedance spectroscopy analysis. The results showed markedly increase of the dielectric losses for the poled samples. Since the situation is reversible independently of the poling conditions, such result is not due to the physical degradation of the samples. Therefore, also considering results from the ferroelectric and piezoelectric characterization analyses, the discussions and conclusions are based on a possible phase transition induced by electric field.

### (FMAs-P048-2022) High Purity [In, Ta] Dipolar Pair Substituted BaTiO<sub>3</sub> Ceramics

E. K. Merkey<sup>1</sup>; I. Chedzoy<sup>1</sup>; N. Betancur-Granados<sup>1</sup>; K. Ning<sup>\*1</sup>; J. I. Tobón<sup>2</sup>; O. J. Restrepo<sup>2</sup>; H. Shulman<sup>1</sup>; W. A. Schulze<sup>1</sup>; S. Tidrow<sup>1</sup>

1. Alfred University, New York State College of Ceramics, School of Engineering, USA
2. Universidad Nacional de Colombia, Materials and Minerals Department, Colombia

The fabrication of [In, Ta] dipole pair substituted BaTiO<sub>3</sub> ceramics has been performed using high purity precursor powders in order to investigate the dipole pair concentration dependent dielectric behavior. The dielectric permittivity shows the evolution from ferroelectric to diffuse phase transition and to relaxor like behavior, as the dipolar pair concentration increases. Microstructure, resistivity, and optical band gap are also studied in order to understand this unique dielectric properties, including not being a strict classic relaxor. Further, modeling efforts are anticipated to provide an improved understanding of these unique properties.

### (FMAs-P049-2022) Influence of the point-defects and microstructural characteristics on the physical properties of KNbO<sub>3</sub>-based ferroelectric ceramics

M. Cristina Oliveira Silva<sup>1</sup>; A. Carvalho da Silva<sup>1</sup>; M. Aurélio de Oliveira<sup>3</sup>; Y. Mendez González<sup>2</sup>; A. Ferreira Gomes do Monte<sup>1</sup>; J. M'Peko<sup>4</sup>; A. Carlos Fernandes<sup>4</sup>; J. de los Santos Guerra<sup>\*1</sup>

1. Federal University of Uberlandia, Institute of Physics, Brazil
2. Universidad de la Habana, Facultad de Física, Cuba
3. Universidade do Estado de Minas Gerais, Brazil
4. Uniiversity of Sao Paulo, Sao Carlos Physics Institute, Brazil

KNbO<sub>3</sub>-based ferroelectric materials have been in the last years much more closely investigated because of many interesting physical properties that make them actually suitable for designing multifunctional electronic components. This is the case of the (1-x)KNbO<sub>3</sub>-xBaNi<sub>1/2</sub>Nb<sub>1/2</sub>O<sub>3-δ</sub> (KBNN) solid-solutions, which have received special attention for practical applications, including for high-performance photovoltaic devices. In this work, KBNN ceramics were produced via conventional solid-state sintering, followed by a comprehensible study of their (micro)structural, electrical and optical properties. The processed data are analyzed and discussed in terms of the effect from structural oxygen-vacancy defects in such materials, together with that from the grain size on the specific case of the observed electrical response. Overall, the results suggest these materials to be a good alternative of perovskite-structured semiconducting ferroelectric oxides for solar cell applications. ACKNOWLEDGMENTS: The authors thank to CNPq (303447/2019-2), FAPEMIG (00661-16 and APQ-02875-18) and CAPES (Finance Code 001) Brazilian agencies for the financial support.

### (FMAs-P050-2022) A- and B-sites co-doped PLZT system for energy-storage application: A systematic study on physical properties

A. Carvalho da Silva<sup>1</sup>; M. Aurélio de Oliveira<sup>2</sup>; Y. Mendez González<sup>2</sup>; R. Guo<sup>4</sup>; A. S. Bhalla<sup>4</sup>; J. de los Santos Guerra<sup>\*1</sup>

1. Federal University of Uberlandia, Institute of Physics, Brazil
2. Universidade do Estado de Minas Gerais, Brazil
3. Universidad de la Habana, Facultad de Física - IMRE, Cuba
4. University of Texas, San Antonio, USA

Dielectric materials with high energy-storage density have attracted the attention of the scientific community over the recent years viewing their integration in several technological applications, such as power generation and high-power pulse devices. In this way, capacitors with high-power density and fast charge/discharge time have led to a rising interest in the investigation of ceramic materials. In this work, the physical properties of PLZT-based ferroelectric system, synthesized via conventional solid-state sintering

method, have been investigated. In particular, the structural, micro-structural and (di)electrical properties were analyzed considering co-doping achievement at both A- and B-sites. The results suggest these materials to be excellent candidates for practical applications. ACKNOWLEDGMENTS: The authors thank to CNPq (303447/2019-2), FAPEMIG (PPM-00661-16 and APQ-02875-18) and CAPES (Finance Code 001) for the financial support.

**(FMAs-P051-2022) Effect of temperature and pressure on dielectric properties of nanocomposite between porous clay heterostructure (BC-PCH) and PLA/PBAT blends**

S. Chotiradsirikun<sup>\*1</sup>; R. Guo<sup>2</sup>; A. S. Bhalla<sup>3</sup>; H. Manuspiya<sup>1</sup>

1. The Petroleum and Petrochemical college, Polymer Science, Thailand
2. The University of Texas at San Antonio, Department of Electrical and Computer Engineering, USA
3. University of Texas, San Antonio, USA

New type of dielectric material with excellent dielectric behaviour was reported in this study. The nanocomposite films between compatibilized PLA/PBAT blends and porous clay heterostructure from mixed surfactant system (BC-PCH) were fabricated using melt-mixing process as a dielectric material. The effects of PBAT, compatibilizer, and BC-PCH loading on dielectric properties were investigated at the temperature ranging from -50 °C to 120 °C at 10<sup>4</sup> Hz with LCR meter interfaced with a temperature controller. The results revealed that the dielectric constant increased with increasing temperature due to the  $\alpha$ -relaxation of main chain segments. Moreover, when BC-PCH was introduced, the dielectric constant of all components remained constant under a wide range of temperature. In addition, the disordered ( $\alpha'$ ) to ordered ( $\alpha$ ) phase transition was found in all samples except for neat PBAT. The effect of pressure on dielectric properties was analyzed by using MTS Acument 3 electrodynamic test system with LCR meter. The results demonstrated the change in charge density with the increase in applied pressure leading to change in capacitance and, as a result, the dielectric constant. Consequently, this dielectric material represented some sensing and monitoring properties that can be used as dielectric sensor

**(FMAs-P052-2022) Figures of merit of PLZT ferroelectric ceramics for practical applications**

J. de los Santos Guerra<sup>\*1</sup>; A. Peláiz Barranco<sup>2</sup>; F. Calderón Piñar<sup>2</sup>; A. Carlos Iglesias Jaime<sup>3</sup>

1. Federal University of Uberlandia, Institute of Physics, Brazil
2. University of Havana, Faculty of Physics, Cuba
3. Universidad Tecnológica de La Habana José A. Echeverría, Departamento de Física, Cuba

Dielectric, pyroelectric and structural properties were investigated in PZT-based ceramics for a composition close to the morphotropic phase boundary, as a function of the lanthanum content. Ceramic samples were prepared via the standard solid-state reaction sintering method. Two compositions were synthesized and studied following the  $\text{PbZr}_{0.53}\text{Ti}_{0.47}\text{O}_3 + x$  mole% La nominal composition (labeled as PLZT-25 and PLZT-50, respectively), where  $x = 2.5$  and 5.0. The structural characterization revealed the presence of both tetragonal and rhombohedral phases, showing a decrease in the tetragonality with the increase of the lanthanum content. The obtained low pores concentration microstructure, confirmed by the scanning electron microscopy, and the observed decrease in the stability of the ferroelectric phase (in favor of the paraelectric one) have been discussed in light of the solubility of the doping cation into the studied PZT perovskite structure. The figures of merit, such as current response ( $F_i$ ), voltage response ( $F_v$ ) and detectivity response ( $F_D$ ) of the as-prepared PLZT samples were also investigated in a wide temperature interval. The lower lanthanum content composition exhibited the best properties for practical applications, such as higher pyroelectric coefficient, lower dielectric losses, higher figures of merit and a relative smaller dielectric permittivity at room

temperature. ACKNOWLEDGMENTS: The authors thank to CNPq (303447/2019-2), FAPEMIG (PPM-00661-16 and APQ-02875-18) and CAPES (Finance Code 001) for the financial support.

**(FMAs-P053-2022) Studies on Microwave Processed (1-x)  $\text{PbZr}_{0.65}\text{Ti}_{0.35}\text{O}_3 - x\text{Ni}_{0.8}\text{Zn}_{0.2}\text{Fe}_2\text{O}_4$  Magnetolectric Composites**

C. Prakash<sup>\*1</sup> - **WITHDRAWN**

1. Maharaja Agrasen Institute of Technology, Applied Sciences, India

Composites of ferroelectric and ferrimagnetic materials are finding applications in a variety of systems. Here, we are reporting studies on composites with compositional formula  $(1-x)\text{PbZr}_{0.65}\text{Ti}_{0.35}\text{O}_3 - x\text{Ni}_{0.8}\text{Zn}_{0.2}\text{Fe}_2\text{O}_4$  ( $x = 0, 0.020$  and  $0.025$ ). The sample powders were prepared by conventional solid state reaction method. The reacted powders were uniaxially pressed and sintered by using microwave technique due to its unique characteristics such as rapid heating of the material, less thermal energy losses, fine microstructure, takes less time, and hence reduction in PbO loss. Sintered pellets were studied for their structural, dielectric, ferroelectric, and ferro-magnetic properties. The presence of two phases (ferroelectric and ferrite) was confirmed by X-ray diffraction analysis. Dielectric properties were measured as a function of temperature and frequency. To study ferroelectric and ferromagnetic properties, P-E and M-H hysteresis loops were recorded, respectively. Microwave processing results in improved dielectric loss and better ferroelectric properties.

**(FMAs-P054-2022) Structural, Ferroelectric Properties of  $\text{Ba}_{0.90}\text{Sr}_{0.10}\text{Ti}_{1-3x/4}\text{M}_x\text{O}_3$  ( $\text{M} = \text{Fe}^{3+}, \text{Cr}^{3+}$ ) Ceramics**

R. Choudhary<sup>\*1</sup>; P. Kumar<sup>1</sup>; S. Sachdev<sup>1</sup>; C. Prakash<sup>2</sup>

1. DIT University, Department of Physics, School of Physical Sciences, India
2. Maharaja Agrasen Institute of Technology, Applied Sciences, India

Polycrystalline ceramics with compositional formula  $\text{Ba}_{0.90}\text{Sr}_{0.10}\text{Ti}_{1-3x/4}\text{M}_x\text{O}_3$  ( $\text{M} = \text{Fe}^{3+}, \text{Cr}^{3+}$ ) with  $x = 0, 0.005, 0.010$  were prepared by the solid-state reaction method. The samples were sintered at 1300°C for 4 hours. The sintered samples were subjected to X-ray diffraction (XRD) analysis for phase confirmation. The dielectric constant and tangent loss was measured as a function of frequency for all the samples. PE hysteresis loops were recorded for all the samples at room temperature. The variation of remanent polarization ' $P_r$ ' and coercive field ' $E_c$ ' was studied as a function of electric field and substitution content. The effect of substitution of transition metal ions  $\text{Fe}^{3+}$  and  $\text{Cr}^{3+}$  on structural and ferroelectric properties was investigated and analysed.

**(FMAs-P055-2022) Conductivity mechanism and analysis of impedance spectroscopy of barium titanate ceramics synthesized by mechanochemical method**

S. Swain<sup>\*1</sup>; P. Kumar<sup>1</sup>; D. Nanda<sup>1</sup>; R. Sahu<sup>1</sup>; A. Parida<sup>1</sup>

1. National Institute of Technology, Rourkela, Physics & Astronomy, India

Barium titanate/BT is a promising lead-free ferroelectric material with a perovskite structure. In the present study, temperature-dependent impedance spectroscopy of BT is investigated which was synthesized by the mechanochemical method. AC conductivity study indicated an increase in conduction with the increase of frequency as well as temperature. The activation energy was calculated from the Arrhenius plot. Impedance and modulus analysis revealed overall grain and grain boundary effects with temperatures ranging from 200°C to 450°C. From the Cole-Cole plots, decreased radii and displaced centers of semicircles from the real axis of impedance with the increase of temperature suggested a non-Debye type relaxation mechanism.



## (FMAs-P056-2022) Comparative Study of CCTO Ceramics Synthesized by Normal and High Energy Ball Milling

A. Parida\*<sup>1</sup>; S. Swain<sup>1</sup>; R. Sahu<sup>1</sup>; P. Kumar<sup>1</sup>

1. National Institute of Technology, Rourkela, Physics & Astronomy, India

The sintering of a system depends on particle size, shape, and agglomeration of starting precursors. Particle size is also a major criterion as it determines the activation energy and hence the grain growth of ceramics. In the present study, polycrystalline  $\text{CaCu}_2\text{Ti}_4\text{O}_{12}$  (CCTO) ceramics were synthesized by two different processes as normal ball milling/NBM and high energy ball milling/HEBM assisted solid-state reaction route. The effect of particle size of CCTO on different characterization was investigated for both NBM and HEBM. NBM was performed for 24 hours taking acetone and zirconia balls as grinding medium, whereas HEBM was performed for 5 hours with 300rpm taking zirconia balls as grinding medium. XRD results confirmed the formation of a single-phase with the cubic structure of the CCTO phase. Various characterization techniques were used to study structural, microstructural, dielectric, FTIR, and Raman spectroscopy properties.

## (FMAs-P057-2022) Study of Structural and Electrical Properties of Lead-free Bulk $0.80(\text{Ba}_{0.92}\text{Ca}_{0.08}\text{Ti}_{0.92}\text{Sn}_{0.08}\text{O}_3)$ - $0.20\text{NiFe}_2\text{O}_4$ Composite System - **WITHDRAWN**

B. Kar\*<sup>1</sup>; S. Panigrahi<sup>1</sup>; P. Kumar<sup>1</sup>

1. National Institute of Technology, Physics & Astronomy, India

In the present work,  $0.80(\text{Ba}_{0.92}\text{Ca}_{0.08}\text{Ti}_{0.92}\text{Sn}_{0.08}\text{O}_3)$ - $0.20\text{NiFe}_2\text{O}_4$  compositesceramics were synthesized by conventional ball milling assisted solid-state reaction route. The calcination temperature for ferroelectric and ferromagnetic phases formation was optimized to be  $1200^\circ\text{C}$  for 3 hrs and  $1075^\circ\text{C}$  for 5 hrs, respectively. The composite system was sintered at  $1275^\circ\text{C}$  for 3 hrs. X-ray diffraction (XRD) was performed for phase examination of the synthesized composites. Rietveld's analysis confirmed pure phase formation for individual phases and composite systems. SEM study showed good phase connectivity between ferroelectric and ferromagnetic phases in the composite. Substitution of  $\text{Ca}^{2+}$  and  $\text{Sn}^{4+}$  ions at  $\text{Ba}^{2+}$  and  $\text{Ti}^{4+}$  sites modified the phase boundary of the pure  $\text{BaTiO}_3$  system. From the dielectric study, it was found that the whole effect of doping shifted the ferroelectric-paraelectric phase transition temperature towards the lower temperature side as compared to the pure  $\text{BaTiO}_3$  system. From the polarization vs. electric field hysteresis loop study, a lossy PE loop was observed due to the presence of a ferromagnetic phase. Further, the microstructural electric transport properties of this system have been carried by the complex impedance spectroscopic (CIS) technique.

## (FMAs-P058-2022) Influence of Graphene Oxide on the Dielectric Properties of Polyvinylidene Difluoride

R. Pandey\*<sup>1</sup>; N. Singhal<sup>1</sup>; P. Kumar<sup>2</sup>; A. Mehta<sup>3</sup>; C. Prakash<sup>3</sup>

1. DIT University, Chemistry, India
2. DIT University, Physics, India
3. Maharaja Agrasen Institute of Technology, Applied Sciences, India
4. DIT University, Physics, India

Graphene oxide 'GO' reinforced polyvinylidene difluoride (PVDF) polymer composites were prepared by solution casting method. PVDF to GO ratio was selected as 100:0, 90:10, 80:20, 70:30, 60:40, 50:50 and 60:40. The phase confirmation of the prepared thick films was done by using X-ray diffraction technique. Temperature dependent dielectric constant and tangent loss 'tan $\delta$ ' was measured for all the samples at different frequencies (1, 10, 100, 1000 kHz). Electrical conductivity ' $\sigma_{ac}$ ' was determined using measured values of dielectric constant and tan $\delta$ . The influence of the reinforced material 'GO' on the dielectric properties and electrical conductivity of PVDF as matrix was investigated and discussed in the present work.

## (FMAs-P059-2022) Effect of Ultrasonication on Nucleation of $\gamma$ -Phase, Dielectric and Ferroelectric properties in PVDF-HFP/ Metal-Organic Framework composite films

S. Paramee\*<sup>1</sup>; S. Charoensuk<sup>1</sup>; R. Guo<sup>2</sup>; A. S. Bhalla<sup>2</sup>; H. Manuspiya<sup>3</sup>

1. The Petroleum and Petrochemical College, Chulalongkorn University, Thailand
2. University of Texas, San Antonio, USA
3. Center of Excellence on Petrochemical and Materials Technology, Chulalongkorn University, Thailand

The self-polarization of PVDF-HFP has been investigated via ultrasonication to improve electroactive phase ( $\gamma$ -Phase) by simple process and without applying external electrical poling or mechanical stretching. Poly(vinylidene fluoride-co-hexafluoropropylene) (PVDF-HFP) polymer base composites with metal-organic frameworks (MOFs), imidazolium magnesium formate (HImMg) as fillers, was fabricated via solution casting method by two different production routes, i.e. with and without ultrasonication. The transformation of  $\alpha$ -phase to  $\gamma$ -phase in PVDF-HFP was determined by X-ray diffraction and Fourier transform infrared spectroscopy. The ultrasonication time at 60 min assists the fabrication of pure PVDF-HFP films with the highest fraction  $\gamma$ -phase ca. 85%. Whereas the ultrasonication and addition of fillers samples increased up to 95%  $\gamma$ -phase. Additionally, shifting of FT-IR vibration modes of  $-\text{CF}_2-$  in PVDF-HFP from the interfacial interaction between positively charged imidazolium groups of HImMg and negatively charge  $-\text{CF}_2$  dipoles of PVDF-HFP by formation of hydrogen bonding was observed. As a result, ultrasonication process and addition of fillers are very effective for preparation of PVDF-HFP films and influences the dielectric and the ferroelectric properties since the induced  $\gamma$ -phase are dramatically affected.

## (FMAs-P060-2022) Multi-composite Stacked Transducers for Energy Harvesting

B. Gamboa\*<sup>1</sup>; R. Guo<sup>1</sup>; A. S. Bhalla<sup>2</sup>

1. University of Texas, San Antonio, USA
2. University of Texas, San Antonio, USA

Compressive and tensile stresses can provide limitless energy in piezoelectric transducers. Optimization of transducer design for applications require engineered composites. Stacked 1:3 composites under compression offer increased energy harvesting capabilities while maintaining mechanical stability. Emphasis on low frequency applications is addressed in this study as high frequency applications typically desire cantilever and other piezoelectric energy harvesting designs. Numerous composite constructs are evaluated for output power versus input mechanical excitation. Additional interest is addressed based on mechanical longevity, output power as a function of volume percent, output power versus force/pressure, and different geometric configurations. Engineering guidelines have been established to design stacked composite structures for low frequency energy harvesting applications.

## (FMAs-P061-2022) Hot uniaxial forging and magnetoelectric characterization of 50PZN-PT/50CFO particulate composites from powders synthesized by one-step Pechini method

A. V. Rodrigues\*<sup>1</sup>; C. P. Castro<sup>1</sup>; F. P. Milton<sup>1</sup>; C. P. Perdomo<sup>1</sup>; R. H. kiminami<sup>1</sup>; W. Santa-Rosa<sup>1</sup>; D. Garcia<sup>1</sup>

1. Federal University of Sao Carlos, Physics, Brazil

Ceramic powders were prepared by one-step Pechini method, which ensured the co-synthesis of the  $0.90[\text{Pb}(\text{Zn}_{1/3}\text{Nb}_{2/3})\text{O}_3]$ - $0.10(\text{PbTiO}_3)$  perovskite ferroelectric phase and the inverted spinel  $\text{CoFe}_2\text{O}_4$  phase. The composite powders, at 50/50 molar ratio, were cold pressed into cylinder form (10mm high and 10mm in diameter) and hot uniaxially forged at  $1200^\circ\text{C}/2\text{h}/5\text{MPa}$  in an  $\text{O}_2$  atmosphere. X-ray diffraction analysis and scanning electron microscopy showed, respectively, that the ceramic bodies retained the original phases and were highly dense, but electrical measurements resulted in relatively

high dc electrical conductivity. For piezoelectric activation of the ferroelectric phase and consequent magnetoelectric (ME) characterization, samples were electrically poled using a dynamic method. Unipolar square voltage pulses were applied at 10Hz, during 15 to 90 minutes, at room temperature. The determination of the magnetoelectric coefficient (dE/dH) was made by measuring the induced electric field from a DC magnetic field superimposed on an AC magnetic field (max 20Oe, 1kHz). It practically doubled as the poling electric field increased from 1 to 2kV/mm for all poling times and showed a maximum within 60 minutes of poling regardless the amplitude of the applied electric field, reaching  $\sim 2,5\text{mV/cmOe}$  and  $\sim 5\text{mV/cmOe}$ , respectively.

#### (FMAs-P062-2022) Remarkably method of synthesis of single-phase and highly resistive BiFeO<sub>3</sub> compound

H. N. Machado\*<sup>1</sup>; L. F. Cótica<sup>1</sup>; G. S. Dias<sup>1</sup>; I. A. Santos<sup>2</sup>

1. State University of Maringa, Department of Physics, Brazil
2. State University of Maringa, Physics, Brazil

Materials which exhibit the coexistence of more than one ferroic order are multiferroics. Between them are found magnetoelectric materials. Magnetoelectric effect consists in the coexistence and coupling of the (anti)ferroelectric and (anti)ferromagnetic orders. BiFeO<sub>3</sub> is the only compound that presents magnetoelectric ordering at room temperature ( $T_C = 830\text{ }^\circ\text{C}$  and  $T_N = 370\text{ }^\circ\text{C}$ ). Despite its many potentialities, the synthesis of BiFeO<sub>3</sub> presents some difficulties as the formation of secondary phases and oxygen vacancies, influencing the magnetic and electrical properties. Thus, solutions have been proposed to correct these problems, as site engineering, synthesis route and oxygen treatment. The high energy ball milling and fast firing has been efficient in suppressing the formation of spurious phases. In contrast, the high conductivity in BiFeO<sub>3</sub> ceramics is related to oxygen vacancies. In order to suppress these vacancies, thermal treatment in a positive oxygen atmosphere has been used. In this work Bi<sub>2</sub>O<sub>3</sub> and Fe<sub>2</sub>O<sub>3</sub> powders were homogenized, high-energy ball milled in air, fast fired at 875 °C and quenched at room temperature. The resulting samples were submitted to XRD analysis and then to thermal annealing at different periods of time in positive oxygen pressure. The dielectric and resistivity measurements point to an expressive influence of oxygen treatment in the conductivity of BiFeO<sub>3</sub>.

#### (FMAs-P063-2022) Structure-properties correlations in BiFeO<sub>3</sub> ceramics obtained via cryo-milling

H. N. Machado\*<sup>1</sup>; G. S. Dias<sup>1</sup>; I. A. Santos<sup>1</sup>; L. F. Cótica<sup>1</sup>

1. State University of Maringa, Department of Physics, Brazil

Multiferroics (such as magnetoelectrics) exhibit the coexistence of more than one ferroic order. BiFeO<sub>3</sub> is an auspicious magnetoelectric (coexistence and coupling of the (anti)ferroelectric and (anti)ferromagnetic orders) because is the only one which presents magnetoelectric ordering at room temperature ( $T_C = 830\text{ }^\circ\text{C}$  and  $T_N = 370\text{ }^\circ\text{C}$ ). Particularly, the antiferromagnetic properties are originated by super exchange interaction of iron atoms located at B site of the material's structure (rhombohedral distorted perovskite). The resulting short-range G-type antiferromagnetic ordering is modeled by a cycloidal structure in which the macroscopic magnetization is canceled. Though, it has been reported the influence of cryo-milling process on magnetic properties of multiferroic BiFeO<sub>3</sub>. In this work, Bi<sub>2</sub>O<sub>3</sub> and Fe<sub>2</sub>O<sub>3</sub> precursor were high-energy ball milled in air, fast fired at 875 °C, quenched at room temperature and submitted to cryo-milling (approx. 100 K), using six different chrome steel balls sizes (from 0.1109 to 4.1103 g/ball). Samples aliquots were taken every 15 minutes. Vibrating sample magnetometry (VSM), X-ray diffraction (XRD) and scanning electron microscopy (SEM) analysis were performed. The correlation between energy transferred during the cryo-milling process, structural changes, and consequent improvements in ferroic properties have been established and will be discussed in detail.

#### (FMAs-P064-2022) Extreme conditions route for sintering BiFeO<sub>3</sub> based ceramics

R. C. Oliveira\*<sup>1</sup>; G. S. Dias<sup>2</sup>; I. A. Santos<sup>3</sup>; J. A. Eiras<sup>4</sup>; E. a. Volnistem<sup>1</sup>; D. Garcia<sup>4</sup>

1. State University of Maringá, PFI, Brazil
2. State University of Maringa, Department of Physics, Brazil
3. State University of Maringa, Physics, Brazil
4. Federal University of São Carlos, GMF, Brazil

The bismuth ferrite (BFO) is a magnetoelectric multiferroic material with a rhomboedrally distorted perovskite structure (R3c) and presents ferroelectric and antiferromagnetic (G-type) orders at room temperature, it's one of the very few single phased magnetoelectric material at room temperature. It exhibits an antiferromagnetic-paramagnetic phase transition at 643 K and a ferroelectric-paraelectric phase transition at 1103 K. The synthesis of pure phase BFO ceramics present several challenges, such as the easily formation of undesired phases and high conductivity. The BFO has great potential for multifunctional device application and the fine tuning of its proprieties via its sintering route is an important study. The ionic substitution of the bismuth is one-step in overcome these challenges, that when combined with and appropriate synthesis route can tune the desired proprieties. In this work, single phased BFO and La, Nd, Sc and Er doped powders were obtained by an extreme conditions route consisting of HEBM followed by fast firing sintering, quenching to room temperature and cryomilling (HEBM bellow 170 K), this powder was then used to synthesizes bulk ceramics by spark plasma sintering and then the samples were reoxidized. The samples obtained proved to be single phased and presented great densification, whereas the results point out a promising extreme condition synthesis route for BFO polycrystalline ceramics.

#### (FMAs-P065-2022) Cobalt Ferrite-Barium Titanate Core-Shell Nanoparticles for Biomedical Applications

S. Hossain\*<sup>1</sup>; R. Guo<sup>1</sup>; A. S. Bhalla<sup>1</sup>

1. The University of Texas at San Antonio, Electrical Engineering, USA

This presentation focuses on the applications of smart magnetoelectric core-shell nanoparticles with emphasis on Cobalt Ferrite-Barium Titanate. Smart magneto-electric materials such as Cobalt Ferrite-Barium Titanate core-shell nanoparticles have been synthesized for targeted mapping of biological cells and to explore their potential applications in biomedicine and chemotherapeutic areas. The magnetostrictive nature of cobalt ferrite can generate corresponding strain from the externally applied magnetic field and the coupled barium titanate shell can simultaneously translate the generated acoustic waves to electric pulses. The synthesized structures in the vitro studies have shown that the movement of core-shell particles, in the 50 to 80 nm in size range, can be controlled by the externally applied rotating magnetic field of 40 to 60 Oe, (contingent to the corresponding frequency magnitude from 60 Hz to 1kHz) to target the specific biological cell. Nanoparticles of ferrites have also shown potential applications in understanding the hypothermia. In the case of applied magnetic field of kHz to 1MHz range, the localized heating in the cell nucleus is accounted to the magnetic energy losses (due to the oscillating applied field). FEA has been carried out to verify such hypothesis. The required temperature rises in the nucleus to induce magnetic hypothermia is approximately 42°C. It is also noticed that the size and synthesis procedure of core-shell nanoparticles do influence their optical absorption properties. The shift in the absorption peak is directly correlated with both the size and composition of the core-shell. Thus it is critical to understand this feature and to expand further such applications in the biomedicine and other diagnostic areas. In vivo studies have been performed to analyze the hypothesis.

## (FMAs-P066-2022) Structural, ferroelectric and magnetic properties of single phase epitaxial $(1-x)\text{Pb}(\text{Zr},\text{Ti})\text{O}_3-x\text{Pb}(\text{Fe},\text{Nb})\text{O}_3$ thin films

L. Imhoff<sup>1</sup>; S. Barolin<sup>1</sup>; M. Rengifo<sup>2</sup>; J. Caicedo Roque<sup>3</sup>; J. Santiso<sup>3</sup>; M. Aguirre<sup>2</sup>; M. Stachiotti<sup>1</sup>

1. IFIR-UNR-CONICET, Argentina
2. INMA-UNIZAR, Spain
3. ICN2, Spain

Many works have been carried out in the last years exploring the multiferroicity of perovskite oxides, identifying and designing materials that present both ferroelectric and ferromagnetic behavior. Among these, the incorporation of magnetic  $\text{Fe}^{3+}$  cations into the widely known ferroelectric  $\text{Pb}(\text{Zr},\text{Ti})\text{O}_3$  proved to be a successful strategy for the development of multiferroic compounds in both bulk and thin film form. In a recently published work, promising results of polycrystalline  $(1-x)\text{Pb}(\text{Zr}_{0.52}\text{Ti}_{0.48})\text{O}_3-x\text{Pb}(\text{Fe}_{0.5}\text{Nb}_{0.5})\text{O}_3$  ( $0 < x < 0.5$ ) thin films fabricated by a practical sol-gel method were shown. The films present both excellent ferroelectric and weak ferromagnetic behavior at room temperature for  $x > 0.3$  compositions. In this work,  $(1-x)\text{Pb}(\text{Zr}_{0.52}\text{Ti}_{0.48})\text{O}_3-x\text{Pb}(\text{Fe}_{0.5}\text{Nb}_{0.5})\text{O}_3$  ( $x=0.4, 0.5$ ) films were grown onto 100-oriented  $\text{SrTiO}_3$  substrates by PLD. The films present epitaxial growth with excellent crystalline quality and no signs of secondary phases. In addition, both ferroelectric and weak ferromagnetic loops were measured at room temperature. Finally, a comparison with the polycrystalline samples was made, providing a deeper understanding on the properties and possibilities of applications of this material into functional devices.

## (FMAs-P067-2022) Structural, electric and magnetic characterization of $\text{Pb}(\text{Fe},\text{Nb})\text{O}_3$ thin films fabricated by a practical sol-gel route

L. Imhoff<sup>1</sup>; S. Barolin<sup>1</sup>; N. Pellegrini<sup>1</sup>; M. Aguirre<sup>2</sup>; M. Stachiotti<sup>1</sup>

1. IFIR-UNR-CONICET, Argentina
2. INMA-UNIZAR, Spain

In this work,  $\text{Pb}(\text{Fe}_{0.5}\text{Nb}_{0.5})\text{O}_3$  (PFN) thin films were fabricated by a modified sol-gel route based on the use of acetoin (3-Hydroxy 2-butanone) as chelating agent. This route offers the advantages of a simple and rapid solution synthesis, and proved to be appropriate for the fabrication of excellent-quality  $(1-x)\text{Pb}(\text{Zr},\text{Ti})\text{O}_3-x\text{Pb}(\text{Fe},\text{Nb})\text{O}_3$  perovskite films in different compositions. In this case, the  $\text{Pb}(\text{Fe}_{0.5}\text{Nb}_{0.5})\text{O}_3$  precursor solution was deposited onto platinumized silicon substrates Pt/Ti/SiO<sub>2</sub>/Si by spin-coating. Rapid thermal annealing was applied at two different temperatures, 650 and 700 °C. The resulting PFN films were found to be dense, free of cracks and well adhered to the substrate. XRD structural characterization showed presence of a majoritarian perovskite phase. Dielectric characterization was performed as a function of frequency, obtaining relative permittivity values of ~1000 at 1 kHz. Low dielectric losses (~0.04) were measured for the whole range of applied frequencies. Ferroelectric properties were tested at 50 Hz and 1 kHz, and magnetic measurements determined a weak ferromagnetic behavior of the samples.

## (FMAs-P068-2022) Raman investigations of pressure induced phase transitions in La doped $\text{BiFeO}_3$ - $\text{PbTiO}_3$ polycrystals

L. Macková<sup>1</sup>; E. A. Volnistem<sup>1</sup>; F. L. Hegeto<sup>1</sup>; H. D. Deróide<sup>1</sup>; O. A. Protzek<sup>1</sup>; A. M. Farias<sup>3</sup>; R. F. Muniz<sup>4</sup>; V. F. Freitas<sup>2</sup>; G. S. Dias<sup>1</sup>; A. M. Neto<sup>1</sup>; I. A. Santos<sup>1</sup>

1. State University of Maringá, Department of Physics, Brazil
2. Universidade Estadual do Centro-Oeste - Unicentro, Physics, Brazil
3. Universidade Tecnológica Federal do Paraná, Campus Guarapuava, Brazil
4. State University of Maringá, Department of Science, Brazil

$(1-x)\text{BiFeO}_{3-x}\text{-PbTiO}_3$  (BF-PT) solid solutions are multiferroic materials that exhibit enhanced ferroelectric, piezoelectric and magnetic properties when compared to pure  $\text{BiFeO}_3$  (BFO) or

$\text{PbTiO}_3$  (PT) compounds. In addition, the possibility of tuning structural symmetries by stoichiometric control or external or chemical pressure permits obtaining a morphotropic phase boundary (MPB). In fact, it is known that with the increase of the PT content there is a structural phase transition (from rhombohedral, R3c, to tetragonal, P4mm) along with the emergence of an MPB for some specific concentrations. La doping can also affect the structural transitions of the BFPT system, changing the stoichiometric concentrations for the existence of the MPB. In this sense, the study of structural transitions for the La doped BFPT solid solutions under extreme conditions (high pressure) is important for understanding the origin and the pressure effects on the BFPT physical properties. In this contribution, Raman spectroscopic investigations under high pressures were conducted in  $(0.6)(\text{Bi}_{0.97}\text{La}_{0.03})\text{FeO}_3 - (0.4)\text{PbTiO}_3$  powders. It was observed the coexistence of R3c and P4mm symmetries, characterized by 7 characteristic active Raman bands, for pressures ranging from 1.6 GPa to 6 GPa, and the emergence of an unidentified structural phase transition for pressures higher than 6 GPa.

## (FMAs-P069-2022) Variation of infrared absorption and Raman spectra of mullite-type $\text{Bi}_2(\text{Fe}_x\text{Ga}_{1-x})_4\text{O}_9$

L. Macková<sup>1</sup>; R. T. Santiago<sup>1</sup>; K. L. da Silva<sup>1</sup>; M. Fabian<sup>2</sup>; L. F. Cótica<sup>1</sup>; I. A. Santos<sup>1</sup>

1. State University of Maringá, Department of Physics, Brazil
2. Slovak Academy of Sciences, Institute of Geotechnics, Slovakia

The polycrystal mullite-type  $\text{Bi}_2(\text{Fe}_x\text{Ga}_{1-x})_4\text{O}_9$  ( $0 \leq x \leq 1$ ) oxides were prepared by mechano-chemical-thermal synthesis and were investigated by X-ray diffraction (XRD), Fourier transform infrared (FTIR) and Raman spectroscopies. XRD diffractograms show the samples are single phase with orthorhombic structure and space group Pbam (No.55). In similarity with other mullite systems, IR bands 850-400  $\text{cm}^{-1}$  and Raman bands 750-300  $\text{cm}^{-1}$  are attributed to stretching and bending vibrations of the tetrahedral and octahedral site coordinates. It has been observed a shift in the peak positions towards lower wavenumber in FTIR and Raman spectroscopies with increasing of iron content. High-energy IR modes showed only a presence of Ga-O-Ga and Ga-O-Fe/Fe-O-Ga stretching vibrations for  $x < 0.5$ . For Raman band 5 it can be observed not so deeply linearly shifting for  $x < 0.5$  with comparison to Raman band 1. These results are in the good concordance with the results given by the Rietveld refinement and Mössbauer spectroscopy, which confirm the preference of the  $\text{Fe}^{3+}$  ions to the octahedral site for the solutions  $x < 0.5$ .

## (FMAs-P070-2022) Low temperature ferroelectric Berry phase in the $\text{Eu}_{0.5}\text{Bi}_{0.5}\text{FeO}_3$ ferromagnetic semiconductor

J. Roa-Rojas<sup>1</sup>; J. A. Jairo Roa-Rojas<sup>2</sup>; C. E. Deluque Toro<sup>3</sup>; A. V. Gil Rebaza<sup>4</sup>; D. A. Landínez Téllez<sup>1</sup>

1. Universidad Nacional de Colombia, Physics, Colombia
2. Grupo de Física de Nuevos Materiales, Universidad Nacional de Colombia, Physics, Colombia
3. Grupo de Nuevos Materiales, Universidad del Magdalena, Ingeniería, Colombia
4. Universidad Nacional de La Plata, Physics, Argentina

The low temperature biferric nature of  $\text{Eu}_{0.5}\text{Bi}_{0.5}\text{FeO}_3$  perovskite was reported from pyroelectric and thermo-stimulated current measurements. In the present work a theoretical study of the structural, magnetic, electronic and ferroelectric properties of this material is performed. Energy minimization processes for three types of cation distributions, different rotation angles, octahedral tilt, and several types of magnetic ordering suggest that a G-type antiferromagnetic is the most energetically favorable in the ground state. Calculation of electronic structure is performed by considering that the exchange and correlation mechanisms are described by the generalized gradient approach with potential corrections and spin polarization. The ferroelectric feature is analyzed by determining the ferroelectric polarization from the Berry phase calculation with results that are

consistent with the experimental reports. Material exhibits a biferroic behavior at low temperatures, since the Berry phase introduces hybridizations between the 3d-Fe and 2p-O states that favor the appearance of Dzyaloshinskii-Moriya interactions, which facilitate the appearance of ferroelectricity coexisting with weak ferromagnetism. The study of thermodynamic properties in the presence and absence of the Berry phase by the Debye quasi-harmonic model reveals the occurrence of a ferroelectric transition at  $T=112.5$  K.

#### (FMAs-P071-2022) Microstructural and dielectric properties of (1-x)BaTiO<sub>3</sub>-(x)CoFe<sub>2</sub>O<sub>4</sub> fibers grown by LHPG technique

A. L. Oliveira<sup>\*2</sup>; F. P. Milton<sup>2</sup>; D. Fukano Viana<sup>2</sup>; M. R. Andreeta<sup>1</sup>; D. Garcia<sup>2</sup>

1. Federal University of Sao Carlos, Department of Materials Engineering, Brazil
2. Federal University of Sao Carlos, Physics Department, Brazil

Fibers of the (1-x)BaTiO<sub>3</sub>-(x)CoFe<sub>2</sub>O<sub>4</sub> magnetoelectric system with  $x = 0.2$  and  $0.3$  were grown by unidirectional solidification using the Laser-Heated Pedestal Growth (LHPG) technique. The pedestal samples were ceramic rods prepared by solid state reaction method and the seed was a SrTiO<sub>3</sub> single crystal. XRD analysis confirmed the tetragonal perovskite phase of the barium titanate and the inverted spinel phase of the cobalt ferrite as majority phases. SEM analysis of parallel and perpendicular surfaces respect to growth direction revealed formation of lamellar structures of both phases (Chinese script) and twins of barium titanate. The twin concentration varies by the distance from the center of the sample and cut direction. The twins also decrease in number and size from  $x=0.2$  to  $x=0.3$ , indicating the latter one is closer to the eutectic composition of the system. Based on the EBSD analysis and from expected growth habit of barium titanate twins, 001 and 110 planes are preferred along growth direction. Such different degree of crystallographic texture and microstructural heterogeneity rises strong differences on the electric and dielectric properties of each cut between compositions. Moreover, the lamellar structure contributes to the percolation path of the magnetic (semiconductor) phase being dielectric losses much higher for the quasi-eutectic composition.

#### (FMAs-P072-2022) Structural and microstructural characterizations of Ta modified AgNbO<sub>3</sub> ferroelectric thin films

Y. Mendez González<sup>2</sup>; F. Agulló-Rueda<sup>3</sup>; J. de los Santos Guerra<sup>\*1</sup>; A. Fernández García<sup>4</sup>; V. Torres Costa<sup>4</sup>; M. Manso Silván<sup>4</sup>

1. Federal University of Uberlandia, Institute of Physics, Brazil
2. Universidad de la Habana, Facultad de Física - IMRE, Cuba
3. Instituto de Ciencia de Materiales de Madrid (ICMM), Spain
4. Universidad Autónoma de Madrid, Departamento de Física Aplicada and Instituto de Ciencia de Materiales Nicolás Cabrera, Spain

Lead-free Ag(Nb<sub>0.80</sub>Ta<sub>0.20</sub>)O<sub>3</sub> thin films were synthesized via a chemical solution deposition process by spin-coating technique. The effect of two different heat-treatment methods on the structural and microstructural properties has been systematically investigated. The XRD and Raman results revealed that a majority orthorhombic perovskite structure was successfully obtained for the film crystallized from a conventional heat-treatment cycle. Secondary phases based on Ag<sub>8</sub>(Nb,Ta)<sub>26</sub>O<sub>69</sub>, Ag<sub>2</sub>(Nb,Ta)<sub>8</sub>O<sub>21</sub>, Ag<sub>2</sub>(Nb,Ta)<sub>4</sub>O<sub>11</sub> and metallic Ag were detected by XRD measurements for the rapid heat-treatment crystallized film. The microstructure is not noticeably influenced by the crystallized method, revealing a dense and smooth surface with metallic silver defects for studied samples. ACKNOWLEDGMENTS: The authors thank to CNPq (303447/2019-2), FAPEMIG (00661-16 and APQ-02875-18) and CAPES (Finance Code 001) Brazilian agencies for the financial. Dr. Mendez-González acknowledges the financial support by Fundación Carolina from Spain.

#### (FMAs-P073-2022) Temperature and electric field effects on erbium PL emissions using PLMN-PT ferroelectric ceramics as host materials - **WITHDRAWN**

G. I. Correr<sup>\*1</sup>; F. P. Milton<sup>1</sup>; F. A. Badillo<sup>2</sup>; D. Garcia<sup>1</sup>; M. P. de Godoy<sup>1</sup>

1. Federal University of Sao Carlos, Physics Department, Brazil
2. University of Antioquia, Colombia

Relaxor ferroelectric materials present distinct electric characteristics at critical temperatures, e.g., at freezing temperature feature a peculiar electric induced birefringence. However, despite their technological importance, the optical emission behavior of rare earth doped relaxor ferroelectrics at critical temperatures is not well known. In this work, we investigated the temperature and applied electric field effects in the optical response of the 0.87PLMN-0.13PT (lanthanum modified lead magnesium niobate – lead titanate) relaxor ferroelectric ceramic doped with 1% weight of erbium (III) oxide (Er<sub>2</sub>O<sub>3</sub>). The erbium ions exhibit two electronic transitions  $^4S_{3/2} \rightarrow ^4I_{15/2}$  and  $^2H_{11/2} \rightarrow ^4I_{15/2}$  under resonant excitation (442nm) in a photoluminescence setup, that split into 4 and 2 sublevels, respectively. The results from different in-situ electric field configurations (550 V/cm maximum) indicated a dependence on the dynamics of polar nanoregions to the anomalous behavior, while various combinations of temperature and electric field highlight the influence of the polar state on observed rare earth emission anomalies, showing also an energy shift of the emissions to lower energies.

#### (FMAs-P074-2022) Structural and Optical Properties of BiFeO<sub>3</sub> Thin Films

E. A. Ching<sup>\*1</sup>; H. S. Miranda<sup>1</sup>; E. De Obaldía<sup>2</sup>

1. Universidad Tecnológica de Panamá, Natural Science, Panama
2. Universidad Tecnológica de Panamá, VIPE, Panama

Thin films of BiFeO<sub>3</sub> were prepared at 550°C annealing temperature on glass and aluminum substrates by spin-coating technique. Bismuth acetate and iron nitrate were utilized as precursors materials, while ethylene glycol was used as solvent. Structural measurements by XRD indicate crystallization phase in the samples. Transmittance and reflectance spectra, from 190 to 25000 nm (UV-Visible-infrared), were collected and they are fitted using the Lorentz classical dispersion model of the complex dielectric function to obtain additional optical properties, such as: complex refraction index, absorption coefficient, electrical conductivity, etc. These results will be presented and discussed. In addition, first principles calculation using Density Functional theory (DFT) of crystallized BiFeO<sub>3</sub> is performed to observe the structural and optical properties. These theoretical results will be compared with those obtained experimentally.

#### (FMAs-P075-2022) Optical and energy storage properties of TeO<sub>2</sub>-based ferroelectric glass-ceramics

R. Cruvinel de Oliveira<sup>1</sup>; A. Almeida Silva<sup>2</sup>; N. Oliveira Dantas<sup>2</sup>; J. de los Santos Guerra<sup>\*3</sup>

1. Instituto Federal Goiano, Brazil
2. Universidade Federal de Alagoas, Instituto de Física, Brazil
3. Federal University of Uberlandia, Institute of Physics, Brazil

Glass-ceramic materials have been a subject of intensive studies over the last years. In particular, ferroelectric glass-ceramics are promising composites combining both high dielectric permittivity and dielectric breakdown strength due to the pore-free nature of the residual glass. These characteristics allow them to be applied in a new generation of technological devices. Glass-ceramics of xBaO-xTiO<sub>2</sub>-(100-2x)TeO<sub>2</sub> (BTT) ternary system were prepared through a melt-quenching method and the crystallization kinetics was investigated for different compositions (xBTT). The crystalline structure evolution was investigated considering both thermal treatment and annealing time. Structural changes, analyzed from optical absorption (OA) measurements, confirmed the formation of ferroelectric nanocrystals (FeNCs) consisting in BaTiO<sub>3</sub> tetragonal phase.

The room temperature energy-storage performance of these BT glass-ceramics, as assessed using P-E hysteresis loops, shows to be dependent on the composition  $x$ . Results confirmed excellent energy storage density with a very high energy efficiency, revealing the obtained ferroelectric glass-ceramics to be promising materials for use in nano-technology applications as high energy storage density dielectrics. **ACKNOWLEDGMENTS:** The authors thank to CNPq (303447/2019-2), FAPEMIG (PPM-00661-16 and APQ-02875-18) and CAPES (Finance Code 001) for the financial support.

### (FMAs-P076-2022) Study of the physical properties of $\text{BaTi}_{1-x}\text{Sn}_x\text{O}_3$ ferroelectric ceramics for practical applications

R. Guilherme Flávio Dornelas<sup>\*1</sup>; A. Carvalho da Silva<sup>1</sup>; J. Eduardo García García<sup>2</sup>; J. de los Santos Guerra<sup>1</sup>

1. Federal University of Uberlandia, Institute of Physics, Brazil
2. Universitat Politècnica de Catalunya, Department of Physics, Spain

The demand for the production of clean energy has been increasing over the last years due to the various climate changes, which are strongly afflicting the world. Therefore, it is necessary to implement new and alternative energy sources that contribute for the environment preservation. That is the case, for instance, of novel energy-storage devices, which could contribute for the current demand of clean energies. In fact, most of the system used nowadays are those lead-based materials, which are strongly pollutant and contribute for the environment contamination. In this way, the interest in the development and study of lead-free materials has become a real priority in the scientific community. The objective of the present work is to synthesize and investigate the physical properties of lead-free ferroelectric systems based on  $\text{BaTiO}_3$  (BT) with technological interest. In particular, the structural and (di)electric properties have been investigated as a function of the Sn cation content, used as a doping element in the BT hosting crystalline structure. The phase transition characteristics have been also analyzed in a wide temperature and frequency interval. **ACKNOWLEDGMENTS:** The authors thank to CNPq (303447/2019-2), FAPEMIG (PPM-00661-16 and APQ-02875-18) and CAPES (Finance Code 001) Brazilian agencies for the financial support. The financial support of the PGC2018-099158-B-I00 project (Spanish Government) is also gratefully acknowledged.

### (FMAs-P077-2022) Structural and microstructural behavior of PLT:ER ferroelectric system

L. F. Davila Espinosa<sup>\*1</sup>; A. Herrera Carrillo<sup>1</sup>; F. A. Londoño Badillo<sup>1</sup>; H. A. Colorado L.<sup>2</sup>; F. P. Uribe<sup>1</sup>

1. Universidad de Antioquia, ciencias exactas y naturales, Colombia
2. Universidad de Antioquia, Colombia

In this work were calcined and densified samples of the lanthanum modified lead titanate system ( $\text{Pb}(1-32x)\text{LaX}_2\text{TiO}_3$ ) con  $x=0.21$ , PLT21, undoped and doped in weight with rare earths: Samarium, Ytterbium and Erbium. Samarium 1.0%; PLT:Sm, Samarium 1.0% and Iterbium at 0.5%; PLT:Sm:Yb, Samarium 1.0% and Erbium at 1.0%; PLT:Sm:Er. The powders were obtained by mixture of oxides method. Structural and microstructural characterizations were carried out both in the powders and in the ceramic systems, observing the influence of the incorporation of the rare earths in the perovskite-type structure, with the variation of the lattice parameters. The formation of agglomerates was observed in the powders. The ceramics presented high density values and a uniform microstructure. with the objective of determining the influence of rare earths on the material and its multifunctional potential, electrical and photoluminescence measurements will be carried out.

### (FMAs-P078-2022) Dielectric properties of BCZT ceramics prepared by combustion synthesis and spark plasma sintering

C. F. Villaquiran Raigoza<sup>\*1</sup>; M. E. Figueroa Arteaga<sup>1</sup>; D. Garcia<sup>2</sup>; F. Zabotto<sup>2</sup>; F. P. Milton<sup>2</sup>

1. Universidad del Cauca, Física, Colombia
2. Universidade Federal de Sao Carlos, Física, Brazil

Powders of the system  $(1-x)\text{Ba}(\text{Zr}_{0.2}\text{Ti}_{0.8})\text{O}_3-x(\text{Ba}_{0.7}\text{Ca}_{0.3})\text{TiO}_3$ , with  $x=0.40, 0.50, 0.60$  were prepared through self-propagating high temperature synthesis. The exothermic reactions were ignited at  $\sim 600^\circ\text{C}$ , with  $\text{Ba}(\text{NO}_3)_2$ ,  $\text{Zr}[\text{O}(\text{CH}_2)_3\text{CH}_3]_4$ ,  $\text{CaCO}_3$  and  $\text{C}_{16}\text{H}_{36}\text{O}_4\text{Ti}$  as starting reagents and glycine/urea as fuel. The resulting material showed particle agglomerates with non-uniform shape and size distribution ( $\sim 70$ - $200$  nm) and perovskite as predominant phase. After high energy ball milling, the powders were densified by spark plasma sintering (SPS) at  $1300^\circ\text{C}/15$  min and 50 MPa, and the resulting samples were investigated for structural, microstructural and dielectric properties. XRD analysis revealed one single phase with perovskite structure. Confocal laser scanning microscopy showed highly dense microstructures of  $\sim 1.5$ - $3$  mm grain size, with apparent density decreasing as  $x$  increased. Impedance spectroscopy from 150 up to 400K (after thermal annealing of the samples at  $1000^\circ\text{C}/6$ h in air), revealed anomalies in the temperature dependence of the real and imaginary parts of the electric permittivity typical of ferroelectric phase transitions. Such results indicate that the combined use of combustion synthesis and SPS techniques can be a powerful protocol to produce dense, fine grained lead-free ferroelectric ceramics at relatively low temperatures.

### (FMAs-P079-2022) Edge dislocation density in cryo-milled $\text{BiFeO}_3$ nanoparticles: Estimation approaches

E. A. Volnistem<sup>\*1</sup>; R. C. Oliveira<sup>1</sup>; V. F. Freitas<sup>2</sup>; G. S. Dias<sup>1</sup>; L. F. Cótica<sup>1</sup>; I. A. Santos<sup>1</sup>

1. State University of Maringá, Department of Physics, Brazil
2. Universidade Estadual do Centro-Oeste - Unicentro, Physics, Brazil

Symmetry breaking caused by edge a dislocations can result in the enhancement of magnetic, optical and electronic properties in some multiferroics.  $\text{BiFeO}_3$  is a perovskite structured ( $\text{ABO}_3$ ) multiferroic magnetoelectric material that presents simultaneous ferroelectric and antiferromagnetic ordering at room temperature, making this prototype phase a great candidate for electronic applications. Recently, the cryo-milling technique has been applied to the synthesis of  $\text{BiFeO}_3$  nanoparticles with different and controlled internal strain levels and enhanced magnetic properties. In this sense, the estimation of dislocation density is indispensable to correlate the defects induced by the synthesis method and the novel or enhanced properties associated with this defects. In fact, it is well known that dislocations cause line broadening and peak asymmetry in XRD patterns particularly for polycrystalline materials. However, there is a lack in literature of such analysis regarding multiferroic materials. In this study, three different methods (Variance method, modified Williamson-Hall and Stephens model) were applied to estimate the dislocation density in cryo-milled  $\text{BiFeO}_3$  nanoparticles. The differences between them are discussed in detail and the dislocation density was correlated with the micro-strain level and the observed changes in the magnetic, optic and local electric properties.

### (FMAs-P080-2022) Characterization of a- $\text{Ba}_{1-x}\text{Fe}_x\text{TiO}_3$ Thin films Prepared by Sol-Gel Technique

G. Pitti<sup>1</sup>; A. Watson<sup>1</sup>; E. De Obaldía<sup>1</sup>; E. A. Ching<sup>\*1</sup>

1. Universidad Tecnológica de Panamá, Natural Science, Panamá

Thin films of a- $\text{Ba}_{1-x}\text{Fe}_x\text{TiO}_3$  (with  $x=0, 0.01, 0.05$  and  $0.1$ ) on glass substrate were prepared by sol-gel technique at  $500^\circ\text{C}$  for 6 hours using barium acetate and titanium isopropoxide as precursors materials and ethylene glycol and triethanolamine as solvent and chelating agent, respectively. The samples were characterized structural, morphological, optical, and elemental by XRD, SEM,

UV-Visible and XPS, respectively. Transmittance and reflectance spectra, from 190 to 110 nm, were collected and they are fitted using Lorentz model. Thus, it was possible obtain different optical properties, such as: complex dielectric function, complex refraction index, absorption coefficient, electrical conductivity, etc. These results will be presented and discussed. In addition, Molecular Dynamics (MD) and first principles calculation using Density Functional theory (DFT) of tetragonal  $\text{Ba}_{1-x}\text{Fe}_x\text{TiO}_3$  are performed to observe the iron effect on the structure and the optical properties. These theoretical results will be compared with those obtained experimentally.

#### (FMAs-P081-2022) A Phenomenological Model for the Magnetodielectric Effect in Multiferroics

R. A. Carvalho<sup>\*1</sup>; F. L. Zabotto<sup>1</sup>

1. Federal University of Sao Carlos, Brazil

In this work, a phenomenological expression for the nonlinear dielectric permittivity dependence on magnetic field i.e., Magnetodielectric Effect, is modeled after multiferroic materials. The desired expression is derived using well-established results in multiferroics field – dielectric dependence on electric polarization, thermodynamic constitutive equations and magnetomechanical effects – and correctly predicts the experimental behavior reported in the literature. Simulations with the expression showed an intrinsic correlation of the spontaneous polarization state of the sample and the measured curves. The model is validated for KNN/CFO and KNN/NFO multiferroic bulk samples.

#### (FMAs-P082-2022) Scope of Samarium content on optical and structural properties of KNN-based ceramics - *WITHDRAWN*

S. A. Zabala<sup>\*1</sup>; F. A. Badillo<sup>1</sup>; A. E. Isaza<sup>2</sup>

1. Universidad de Antioquia, Institute Physic, Colombia

2. Universidad de Antioquia, chemistry institute, Colombia

The study of KNN-based ceramics continues to be a milestone in advanced materials research, with a special focus on multifunctional applications. In this work, the physical, structural, microstructural and spectral properties as a function of samarium concentration for the  $(\text{K,Na})_{0.9-3x}\text{Ca}_{0.1}\text{Li}_{0.2}\text{Sm}_x\text{NbO}_3$  ( $x=0.005, 0.01, 0.015$ ) system (KNN–CaLi–xSm) manufactured by the solid state reaction method are presented and analyzed. Regarding the physical properties, an increase in porosity was found (evidenced with micrographs and a decrease in density) as a function of the increase in the concentration of  $\text{Sm}^{+3}$  it is estimated that it is the product of the structural vacancies of the sites A for perovskite. The structural analyzes show preservation of the morphotropic phase contour typical of KNN-based systems, such as a Tetrahedral (T) and Orthorhombic (O) phase codomain in different rare earth ion contents with a higher T phase content for  $x=10$ . Structural changes are presented in powders calcined at different temperatures guided by DTA-TG results, allowing the compositional and Thermal stability analysis of the system, showing a lower total decomposition temperature with  $x=0.1$  at 770°C. Finally, the spectral analyzes reveal the polychrome nature with the introduction of the rare earth ion in the structure of the lead-free KNN-based study system.

#### (FMAs-P083-2022) Influence of Mn and Cu on the Multiferroic Properties of co-doped $\text{BiFeO}_3$ Thin Films

H. S. Miranda<sup>\*1</sup>; E. De Obaldia<sup>1</sup>; A. Watson<sup>1</sup>; E. A. Ching<sup>1</sup>

1. Universidad Tecnológica de Panamá, Ciencias Naturales, Panama

An Mn and Cu co-doping  $\text{BiFeO}_3$  thin film was fabricated on FTO/glass substrate by sol-gel method with a sequential layer deposition process. The raw materials used in the starting solution were, bismuth nitrate pentahydrate ( $\text{Bi}(\text{NO}_3)_3 \cdot 5\text{H}_2\text{O}$ ), iron(III) nitrate nonahydrate ( $\text{Fe}(\text{NO}_3)_3 \cdot 9\text{H}_2\text{O}$ ), Manganese (II) acetate tetrahydrate ( $\text{C}_4\text{H}_6\text{MnO}_4 \cdot 4\text{H}_2\text{O}$ ) and copper (II) acetate monohydrate ( $(\text{CH}_3\text{COO})_2\text{Cu} \cdot \text{H}_2\text{O}$ ) were used as dopants. All of these previous reagents were mixed together using ethylene glycol ( $\text{HOCH}_2\text{CH}_2\text{OH}$ ) as solvent. The atomic ratio used was  $\text{BiFe}_{0.94}\text{Mn}_{0.04}\text{Cu}_{0.02}\text{O}_3$  and

5 mol% of excess of bismuth was employed to compensate its volatility during high-temperature annealing. The structural, morphological, optical properties and the charge transport mechanisms of the sample were studied using X-rays Diffraction (XRD), Scanning Electron Microscopy (SEM), UV-visible Spectroscopy, and Impedance Spectroscopy, respectively. The transmittance spectrum was fitted, on 190 to 1100 nm optical range, using the classical dispersion theory of Drude-Lorentz in order to approximate interest optical parameters, such as the complex dielectric function, the complex refractive index, the absorption coefficient, the electrical conductivity, etc. The chemical composition and the ferroelectric properties were studied by X-ray Photoelectron Spectroscopy (XPS) and ferroelectricity measures through Sawyer-Tower circuit configuration, respectively. Finally, the first principles calculation was performed using the density functional theory (DFT) to observe the co-doping effect of Mn and Cu on the  $\text{BiFe}_{0.94}\text{Mn}_{0.04}\text{Cu}_{0.02}\text{O}_3$  physical properties. These theoretical results will be compared with those obtained experimentally.

#### (FMAs-P084-2022) Effect of the rare-earth doping on the structural phase transitions in $\text{AgNbO}_3$ ceramics

T. Hathenher Toledo Rosa<sup>\*1</sup>; A. Carvalho da Silva<sup>1</sup>; Y. Mendez González<sup>2</sup>;

R. Guo<sup>3</sup>; A. S. Bhalla<sup>3</sup>; J. de los Santos Guerra<sup>1</sup>

1. Federal University of Uberlandia, Institute of Physics, Brazil

2. Institute of Science and Technology of Material, University of Havana, Cuba, NANOMAT, Cuba

3. University of Texas, San Antonio, USA

Ferroelectric materials have played a crucial role in modern electronic devices because of their interesting physical properties. Their relatively high spontaneous polarization, very high dielectric permittivity and excellent piezoelectric response make possible their use in numerous applications, such as non-volatile memories, capacitors, transducers, and others. Another very interesting class of materials with peculiar characteristics in their electrical response are the so-called antiferroelectrics. They have revealed as promising candidates for application in energy storage devices due to their relatively high energy density associated with the large maximum polarization, small remnant polarization and relatively high break-down electric field. Between them,  $\text{AgNbO}_3$ -based materials emerged as potential candidates to develop lead-free energy storage devices and the next-generation of piezoelectrics, thus replacing the well-known lead zirconate titanate (PZT). The aim of the present work is to provide a systematic study of the phase transition characteristics, considering both structural and the dielectric response over a wide temperature range. In particular, the influence of the lanthanum doping on the physical properties has been taken into account in  $\text{Ag}_{1-3x}\text{La}_x\text{NbO}_3$  ceramics. ACKNOWLEDGMENTS: The authors thank to CNPq (303447/2019-2), FAPEMIG (PPM-00661-16 and APQ-02875-18) and CAPES (Finance Code 001) for the financial support.

#### (FMAs-P085-2022) Synthesis, structural and optical characterizations of PVDF-based lead-free ceramic composites

E. Alexandre Falcão<sup>1</sup>; A. Carvalho da Silva<sup>2</sup>; Y. Mendez González<sup>3</sup>; R. Guo<sup>4</sup>;

A. S. Bhalla<sup>4</sup>; J. de los Santos Guerra<sup>\*2</sup>

1. Universidade Federal da Grande Dourados, Faculdade de Ciências Exatas e Tecnologia, Brazil

2. Federal University of Uberlandia, Institute of Physics, Brazil

3. Universidad de la Habana, Facultad de Física - IMRE, Cuba

4. University of Texas, San Antonio, USA

Poly(vinylidene fluoride) (PVDF) is a ferroelectric polymer (FP) with wide application in many technological areas, such as electro-mechanical and electro-thermal transducers, sensors, and bio-medicine. Although PVDF presents the best electroactive properties compared to other FP, these properties are lower than the observed in ceramics. However, many researchers centered their efforts on the called hybrid materials (polymer/ceramic) in the last years, which are very interesting from a technological point of view. In

this way, the present work aims the investigation of the structural and optical properties of PVDF-based composites considering three different ceramic compounds ( $\text{BaTiO}_3$ ,  $\text{BaFe}_{12}\text{O}_{19}$ , and  $\text{SrFe}_{12}\text{O}_{19}$ ). The studied samples were characterized by X-ray diffraction and FT-IR and the relative percentage of the b phase was obtained. Results confirmed the successful incorporation of dopants in the polymeric matrix. From UV-Vis measurements, it was observed a change in the bandgap energy caused by the ceramic addition. The experimental results revealed that the PVDF/ $\text{BaTiO}_3$ , PVDF/ $\text{BaFe}_{12}\text{O}_{19}$ , and PVDF/ $\text{SrFe}_{12}\text{O}_{19}$  composites are potential candidates for electro-electronic applications. The authors thank Fundect, CNPq (483683/2010-8, 208232/2014-1 and 303447/2019-2), FAPEMIG (PPM-00661-16 and APQ-02875-18), FINEP (04.13.0448.00/2013) and CAPES (Finance Code 001) for the financial support.

### (FMAs-P086-2022) Synthesis and characterization of $\text{Cu}_2\text{O}$ nanoparticle-embedded PZT thin films

M. Di Marco<sup>\*1</sup>; M. Roldán<sup>1</sup>; M. Santiago<sup>1</sup>; M. Stachiotti<sup>1</sup>

1. Instituto de Física de Rosario (IFIR), CONICET-UNR, Argentina

In this work, we develop a strategy for the incorporation of cuprous oxide nanoparticles into a  $\text{PbZr}_{0.52}\text{Ti}_{0.48}\text{O}_3$  (PZT) thin films. The  $\text{Cu}_2\text{O}$  nanoparticles were synthesized by a colloidal chemistry approach, using ascorbic acid as a reducing agent and polyvinylpyrrolidone as a surfactant. Cubic-shaped nanoparticles with an edge length of  $\sim 160\text{nm}$  were obtained, and a bandgap of  $\sim 2.1\text{eV}$  was determined from optical measurements. PZT thin films were fabricated by a chemical solution deposition method, using acetoin as a chelating agent. The  $\text{Cu}_2\text{O}$  nanoparticles were incorporated into the PZT matrix by the spin coating deposition of the colloidal suspension between PZT layers of  $\sim 80\text{ nm}$  thickness. Uniform and dense films were successfully fabricated on Pt substrates. The XRD analysis showed a single-phase perovskite structure. The samples exhibited good dielectric properties and well-saturated ferroelectric hysteresis loops at 50 Hz. We showed that the ferroelectric properties of 3-layer PZT thin films are not strongly affected by the incorporation of the  $\text{Cu}_2\text{O}$  nanoparticles. The direct bandgap of the thin films was slightly red-shifted by the incorporation of the nanoparticles, from 3.8eV to 3.6eV. In addition, a small absorption was found at the energy  $\sim 2.2\text{eV}$ , consistent with the bandgap measured for the synthesized cuprous oxide nanoparticles.

### (FMAs-P087-2022) Optical and electrical characterization of sol-gel synthesized PZT thin films on FTO glass substrates

M. Di Marco<sup>\*1</sup>; L. Imhoff<sup>1</sup>; M. Roldán<sup>1</sup>; M. Stachiotti<sup>1</sup>

1. Instituto de Física de Rosario (IFIR), CONICET-UNR, Argentina

In this work, lead zirconate titanate (PZT) thin films were fabricated onto transparent conductive substrates to investigate optical and electric properties. The precursor solution of  $\text{PbZr}_{0.52}\text{Ti}_{0.48}\text{O}_3$  was obtained by a modified sol-gel process based on the use of acetoin as a chelating agent, and then deposited onto fluorine-doped tin oxide (FTO) coated aluminoborosilicate glass substrates, by spin-coating. Both conventional furnace annealing (CFA) and rapid thermal annealing (RTA) were investigated to determine the optimum conditions for the fabrication of good-quality films, at temperatures ranging from 550C to 650C. Crack-free films with a single-phase perovskite structure were successfully fabricated. The measured direct bandgap of the PZT coatings was about 3.7eV and showed a slight increase with the increment of the annealing temperature. Preliminary results suggest that RTA at 650C is preferable to enhance the structural and electric properties of the material.

### (FMAs-P088-2022) Improvement of dielectric properties of bioactive glasses through thermal treatment - **WITHDRAWN**

A. Nascimento<sup>\*1</sup>; E. a. Volnistem<sup>1</sup>; W. R. Weinand<sup>1</sup>; F. Pedrochi<sup>2</sup>; I. A. Santos<sup>1</sup>; F. Sato<sup>1</sup>

1. State University of Maringa, Departmente of Physics, Brazil

2. Federal University of Maranhão, Departmente of Physics, Brazil

Electrical stimulation of bioactive compounds has been presented as an interesting alternative for applications of biomaterials as scaffolds targeting bone regeneration presenting growth of apatite layer. Bioactive glasses (BG) have been considered as a great alternative to be applied as scaffolds for bone repair due to its biocompatibility, bioactivity and biofunctionality. However, dielectric properties of bioactive glasses, such as low resistivity, is a drawback regarding the application of electrical fields for the enhancement of the apatite layer growth. In this sense, heat treatment arises as a possible method for the formation of ceramic phases in bioactive glasses, improving its dielectric properties. In this work,  $60\text{B}_2\text{O}_3\text{-}8\text{CaO-}4\text{P}_2\text{O}_5\text{-}18\text{Na}_2\text{O-}10\text{CaF}_2$  bioactive glass was thermally treated at 518, 634, 773, 810 e 900 °C resulting in the formation of ceramic phases which improved its dielectric properties. Structural (XRD), chemical (EDX mapping) and dielectric characterizations (Impedance Spectroscopy), revealed the formation of  $\text{CaNaB}_3\text{O}_9$ ,  $\text{CaNa}_3\text{B}_5\text{O}_{10}$  and  $\text{Ca}_5(\text{PO}_4)_3\text{F}$  (between 634 and 810 °C) and  $\text{CaB}_2\text{O}_4$ ,  $\text{Ca}_5(\text{PO}_4)_3\text{F}$  e  $\text{NaO}_2$  (at 900 °C). The enhancement of the dielectric properties was correlated with the presence of ceramic phases formed through thermal treatment. Such improvements can enlighten the synthesis and application of bioactive glass ceramics for electrical field stimulated bone repair.

### (FMAs-P089-2022) Investigation of the structural characteristics in $\text{PbTiO}_3$ ferroelectric thin films

M. Aparecido dos Santos Mariano<sup>\*1</sup>; A. De Giovanni Rodrigues<sup>2</sup>; Y. Mendez González<sup>2</sup>; E. Carvalho de Lima<sup>3</sup>; J. de los Santos Guerra<sup>1</sup>

1. Federal University of Uberlândia, Institute of Physics, Brazil

2. Federal University of São Carlos, Physics Department, Brazil

3. Institute of Science and Technology of Material, University of Havana, Cuba, NANOMAT, Cuba

4. Federal University of Tocantins, Brazil

Ferroelectric materials have been studied over the last several decades due to their exceptional physical properties, which make them promissory for several applications, such as pyroelectric sensors, non-volatile memories, electro-optical devices, capacitors, etc. Between them, lead titanate ( $\text{PbTiO}_3$ , PT), which has a tetragonal perovskite structure (P4mm), has been considered a promising material for infrared detector applications (in both thin films and ceramic forms) and, therefore, it has been up today under the interest of many research from the scientific community. In fact, recent advances in the synthesis methods for obtaining PT based materials have promoted very interesting and intriguing phenomena in their micro(structural) properties, which still remains not fully understood. In this context, this work aims the investigation of the structural properties of  $\text{PbTiO}_3$  thin films, studied through X-ray diffraction and Raman spectroscopy techniques. In particular, the influence of the synthesis parameters, such as pyrolysis temperature, has been considered. ACKNOWLEDGMENTS: The authors thank to CNPq (303447/2019-2), FAPEMIG (PPM-00661-16 and APQ-02875-18) and CAPES (Finance Code 001) for the financial support.

**(FMAs-P090-2022) Oxygen vacancy ordering structure and modulated anomalous magnetic properties in cobaltate thin films**Y. Chen<sup>\*1</sup>; C. Chen<sup>2</sup>; J. Ma<sup>1</sup>

1. Tsinghua University, School of Materials Science and Engineering, China
2. University of Texas, San Antonio, USA

Oxygen vacancy concentration and configurations have a direct effect on the crystal structure and are strongly coupled with the magnetic, electronic, and transport properties of transition metal oxides, leading to versatile applications. We investigated  $\text{Y}_3\text{SrCo}_4\text{O}_{10.5+\delta}$  thin films on a LSAT (001) substrate prepared via pulsed laser deposition. The oxygen vacancy was controlled using in-situ high temperature X-ray diffraction and the structure was simultaneously characterized during annealing process. Transition electron microscopy reveals different oxygen vacancy ordering structures in the as-deposited and post-annealed films. The as-deposited films are less-ordered with the oxygen vacancy planes mainly perpendicular to the heterointerface in some small regions below critical thickness while the oxygen vacancy ordering in post-annealed samples are more ordered and homogeneous with the planes parallel to the heterointerface below critical thickness. Magnetic characterization indicates that the post-annealed films exhibit a long-range ferromagnetic ground state with very large coercive field, and the hysteresis loop shows an anomalous giant vertical shift upon field cooling. These results manifest that the magnetic property is closely correlated with the oxygen ordering domains and thus provide an effective method to manipulate multifunctionality in transition metal oxides.

**(FMAs-P091-2022) Enhanced insulating behaviors in  $(\text{PrCoO}_3)_n/(\text{CaCoO}_{2.5})_n$  Superlattices**J. Xiaomin<sup>\*1</sup>; C. Chen<sup>2</sup>; J. Ma<sup>1</sup>

1. Tsinghua University, School of Materials Science and Engineering, China
2. University of Texas, San Antonio, USA

Double ordered perovskite cobaltates ( $\text{AA}'\text{Co}_2\text{O}_{5+\delta}$ ) have received tremendous attention due to their fast oxygen transport kinetics and novel electromagnetic properties. Here, we report that  $(\text{PrCoO}_3)_n/(\text{CaCoO}_{2.5})_n$  superlattice films are successfully fabricated to artificially manipulate designable an A-site ordered structure. Although all the superlattices exhibit insulating behaviors irrespective of the periodicity  $n$ , the transport properties do not change monotonically with  $n$ . As  $n$  decreases from 40 to 2, the resistivities decrease with  $n$ . However, superlattice with  $n=1$  shows the largest resistivity with 3 orders of magnitude at room temperature more than that in the  $n=2$  SL. It is interesting to note that the  $n=1$  SL also shows a ferromagnetic transition at a critical temperature  $T_C$  of  $\sim 70$  K. The parent compounds,  $\text{PrCoO}_3$  and  $\text{CaCoO}_{2.5}$ , show no apparent ferromagnetic transition, indicating the breaking of the time-reversal symmetry at  $\text{PrCoO}_3/\text{CaCoO}_{2.5}$  interfaces. The electronic and magnetic transport properties of the  $n=1$  SL are significantly different from the  $\text{PrCaCo}_2\text{O}_{5+\delta}$  thin films, although they have the same chemical composition. Our results provide an important information to design and fabricate the ordered superstructure with unique electronic and magnetic transport properties.

**(FMAs-P092-2022) Study of the electrocaloric response in lanthanum doped  $(\text{Bi}_{0.5}\text{Na}_{0.5})_{0.92}\text{Ba}_{0.08}\text{TiO}_3$  lead-free ceramics**Y. Mendez González<sup>2</sup>; A. Peláiz Barranco<sup>2</sup>; J. de los Santos Guerra<sup>\*1</sup>

1. Federal University of Uberlandia, Institute of Physics, Brazil
2. Universidad de la Habana, Facultad de Física, Cuba

The electrocaloric effect of  $(\text{Bi}_{0.5}\text{Na}_{0.5})_{0.92}\text{Ba}_{0.08-3x/2}\text{La}_x\text{TiO}_3$  lead-free ceramics, with  $x = 0, 0.01, 0.02$  and  $0.03$  (labeled as BNLBT- $x$ ), were investigated by the indirect method. An enhanced ECE response was achieved for the  $(\text{Bi}_{0.5}\text{Na}_{0.5})_{0.92}\text{Ba}_{0.05}\text{La}_{0.02}\text{TiO}_3$  composition at  $80^\circ\text{C}$ , with an adiabatic temperature change ( $\Delta T$ ) of  $2.70^\circ\text{C}$  and an electrocaloric strength ( $\Delta T/\Delta E$ ) of  $0.54\text{ K mm kV}^{-1}$ . Both parameters were obtained under a relatively low applied electric field of  $50\text{ kV/cm}$ . For this material, a maximum entropy change ( $\Delta S$ )

was also obtained ( $\sim 3.06\text{ J kg}^{-1}\text{ K}^{-1}$ ) under the same conditions. These results are higher than the reported in the current literature for lead-free materials, suggesting this system as a potential candidate for practical electrocaloric device applications. ACKNOWLEDGMENTS: The authors thank to CNPq (303447/2019-2), FAPEMIG (00661-16 and APQ-02875-18) and CAPES (Finance Code 001) Brazilian agencies for the financial support and the ICTP, Trieste-Italy, for financial support of Latin-American Network of Ferroelectric Materials (NET-43, currently NT-02). MSc. Mendez-González acknowledges the partial financial support by the ICTP-CLAF agreement AF-13.

**(FMAs-P093-2022) High entropy perovskite: An ultra-low thermal conductivity thermoelectric material**R. Banerjee<sup>\*1</sup>; T. Maiti<sup>1</sup>

1. IIT Kanpur, MSE, India

Though high entropy alloys are being investigated since 2004 due to their cocktail effects, leading to exciting novel properties, high entropy oxides (HEO) or perovskites (HEP) have not been examined until 2015. Though few reports have been published on batteries, hydrogen storage or magnetic properties, for the very first time we are reporting any high entropy oxide thermoelectric properties. We have prepared  $\text{Sr}(\text{TiFeNbMoCr})\text{O}_3$  HEP by solid state reaction route. Detailed thermodynamics calculation and Rietveld analysis with excellent fitting ( $\chi^2 = 1.75$ ) is done in designing the calcination temperature of this material and in determining Pm-3m symmetry of the material having a lattice parameter of  $3.94\text{ \AA}$  respectively. A dense microstructure having average grain size of  $0.85\text{ }\mu\text{m}$  is seen in FESEM with all the elements distributed throughout the scan area by EDXS studies. XRF analysis confirms that the constituent elements present in our sample is same to that of theoretical formula of HEP and XPS analysis helps to understand us all the B site cations present in our system have multiple oxidation state. The lowest Lphonon among all the  $\text{SrTiO}_3$  based material causing ultra-low thermal conductivity of  $0.7\text{ W/m-K}$  at  $1100\text{ K}$  is achieved. Lattice thermal conductivity is fitted by Debye Callaway Model to find out that the presence of 5 or more cations causes anharmonicity leading to higher order phonon scattering. This low thermal conductivity opens up a new avenue for enhancing the thermoelectric properties at high temperature of thermoelectric materials.

**(FMAs-P094-2022) Reinforcement of MXene in perovskite oxides for thermoelectric power generation**P. Dixit<sup>\*1</sup>; T. Maiti<sup>1</sup>

1. IIT Kanpur, Materials Science and Engineering, India

Thermoelectric materials have shown great potential for generating electricity from the waste heat. Fabrication of nanocomposites has been proven to be a robust way of enhancing the energy conversion efficiency of thermoelectric materials. In the present work we have used MXene, a new generation 2D material to synthesize the nanocomposites with oxides.  $\text{Ti}_3\text{C}_2\text{T}_x$  MXene has been synthesized by selective etching of Al from  $\text{Ti}_3\text{AlC}_2$  MAX phase using a low-cost processing technique. Nanosized layered sheets of MXene have been incorporated as inclusions in the matrix of  $\text{SrTi}_{0.85}\text{Nb}_{0.15}\text{O}_3$  oxides by Spark Plasma Sintering (SPS) method. Thermoelectric properties such as Seebeck coefficient, electrical conductivity and thermal conductivity of these novel nanocomposites have been measured in the temperature range from  $323\text{ K}$  to  $921\text{ K}$ . Introduction of MXene has shown significant improvement in the thermoelectric power factor (PF) and figure of merit (ZT) of  $\text{SrTi}_{0.85}\text{Nb}_{0.15}\text{O}_3$  based nanocomposites. Further, transport properties of these composites have been analyzed in correlation with XRD, SEM, XPS and Raman Spectra.



## (FMAs-P095-2022) High performance ( $ZT > 1$ ) n-type oxide thermoelectric composites from earth abundant materials

S. S. Jana<sup>\*1</sup>; M. Acharya<sup>1</sup>; T. Maiti<sup>2</sup>

1. IIT Kanpur, Material Science and Engineering, India
2. IIT Kanpur, Dept. of Materials Science & Engineering, India

Oxide based thermoelectrics are always advantageous over conventional chalcogenides in the context of being environmentally benign, less costly, high temperature stable. Unfortunately, they suffer from poor thermoelectric performance ( $ZT < 1$ ) which pull them back from their commercialization. We report  $ZT > 1$  in composite of 15 mol% Nb doped SrTiO<sub>3</sub> (STN) with simple natural graphite (G). It is interesting to observe that addition of graphite forms a conductive network in STN matrix which enhances the weighted mobility by 21 times resulting in remarkable augmentation in electrical conductivity. To illustrate the electron transport mechanism, we have put forward the idea of Anderson localization of electrons in pristine STN and their delocalization from localized state after graphite incorporation. Furthermore, the increase in total thermal conductivity has been restrained as lattice contribution of it is suppressed by enhanced Umklapp scattering after graphite addition especially at elevated temperature. As a result, maximum  $ZT$  of 1.42 has been obtained for STN+0.5wt% G composite which is 15 times larger compared to pristine STN. This ground breaking  $ZT$  value by n-type oxide remained unattainable till now. We have reported a strategy to design composite of rare earth free thermoelectric oxide with natural graphite for high temperature thermoelectric power generation.

## (FMAs-P096-2022) Monitoring the ferroelectric phase transition of barium titanate ceramics via impulse excitation

W. Pabst<sup>\*1</sup>; E. Gregorova<sup>1</sup>; P. Simonova<sup>1</sup>

1. University of Chemistry and Technology, Prague, Department of Glass and Ceramics, Czechia

It is well known that the ferroelectric phase transition of barium titanate ceramics is accompanied by an elastic anomaly near the Curie temperature. However, monitoring this anomaly in the temperature dependence of elastic moduli via impulse excitation is relatively unusual. In this contribution we show that impulse excitation is a suitable technique to determine the temperature dependence of Young's modulus and thus to monitor the ferroelectric phase transition of barium titanate ceramics. By measurement with a resonant frequency and damping analyzer from room temperature to 250 °C and back, it is found that even in unpoled barium titanate ceramics there is a strong elastic anomaly with a sharp minimum (at 120 °C during heating and 110 °C during cooling), below and above which Young's modulus adopts values of 40–50 GPa and up to 90 GPa, respectively. Concomitantly with these changes in Young's modulus, the damping (inverse quality factor) changes from values of order 0.01 below to values less than 0.001 above the phase transition temperature. While damping for ceramics with crystallites in the tetragonal low-temperature phase exhibits significant scatter, this scatter is absent for the cubic high-temperature phase. For Young's modulus both the absolute values and the hysteresis of the phase transition temperature between heating and cooling are completely reproducible.

## (FMAs-P097-2022) Evaluation of a macroscopic statistical model for the bias electric field dependence of the diffuse phase transition of relaxor ceramics

E. C. Lima<sup>\*3</sup>; J. de los Santos Guerra<sup>2</sup>; E. B. Araujo<sup>1</sup>

1. São Paulo State University, Physics and Chemistry, Brazil
2. Federal University of Uberlandia, Institute of Physics, Brazil
3. Federal University of Tocantins, Physics, Brazil

Relaxors are a unique class of materials in which dielectric permittivity depends on the frequency of the applied electric field. Ceramics of relaxor Pb(Mg<sub>1/3</sub>Nb<sub>2/3</sub>)O<sub>3</sub> were prepared, and dielectric properties experimentally studied as a function of frequency, temperature, and

magnitude of dc bias. It was found that the dependence of dielectric permittivity on temperature can be well described in a wide temperature range, typically between 100K and 400K, by a macroscopic statistical model. Using this phenomenological model and PMN ceramics as an example, we revisit the dependence of dielectric permittivity with temperature with the bias field superposition, analyzing their diffuse phase transition behaviors and providing a complete description of the temperature and field range. The frequency dependence of the temperature of maximum permittivity follows the Vogel-Fulcher relationship. The results were discussed in terms of the different contributions to dielectric permittivity with the different dc bias field conditions.

## (FMAs-P098-2022) Designing High Entropy Perovskite (Na<sub>0.2</sub>Bi<sub>0.2</sub>Ba<sub>0.2</sub>Sr<sub>0.2</sub>Ca<sub>0.2</sub>)TiO<sub>3</sub> for lead free Relaxor Ferroelectrics

S. S. Jana<sup>\*1</sup>; V. P. Singh<sup>3</sup>; A. Dwivedi<sup>3</sup>; T. Maiti<sup>2</sup>

1. IIT Kanpur, Dept. Material Science and Engineering, India
2. IIT Kanpur, Dept. of Materials Science & Engineering, India
3. IIT BHU, Department of Ceramic Engineering, India

Relaxor ferroelectric is an integral part of modern electronics such as capacitors, actuators, optoelectronic device etc. Enormous efforts have been devoted for years to replace lead based conventional relaxor ferroelectrics (such as (PMN), PbZn<sub>1/3</sub>Nb<sub>2/3</sub>O<sub>3</sub> (PZN)) by lead free novel perovskites which can match their performance. We have adopted a novel approach to design lead free relaxor ferroelectric by synthesizing high entropy perovskite oxides (HEP). In the present work, single phase (Na<sub>0.2</sub>Bi<sub>0.2</sub>Ba<sub>0.2</sub>Sr<sub>0.2</sub>Ca<sub>0.2</sub>)TiO<sub>3</sub> has been synthesized through solid state route. The phase stability at elevated temperature has been studied through high temperature XRD. A broader peak of permittivity and loss tangent near 650 K have been observed at different frequencies from 1 kHz to 1000 kHz. The observed frequency dispersion of dielectric constant is clear indication of relaxor behavior. Further, narrowing down of the P-E loop at higher temperature also suggests relaxor behavior. It is quite fascinating to observe that the ferroelectric behavior of the HEP is retained from cryogenic temperature to about 400 K although none of the constituting titanates except BaTiO<sub>3</sub> exhibits ferroelectricity. Other characterisation techniques such as XPS, FESEM have also been carried out for better understanding in structure property relations.

## (FMAs-P100-2022) Ab initio study of samarium doped barium titanate

A. Aslla Quispe<sup>\*1</sup>; G. Cruz Yupanqui<sup>2</sup>; R. Hiroki Miwa<sup>3</sup>; J. de los Santos Guerra<sup>3</sup>

1. Universidad Nacional Intercultural de Quillabamba, Peru
2. Universidad Nacional Tecnológica de Lima Sur, Peru
3. Federal University of Uberlandia, Institute of Physics, Brazil

We used density functional theory with spin polarization to investigate multifunctional properties of A-site trivalent Sm-doped BaTiO<sub>3</sub>, the self-consistent calculation results was used to analyze ferromagnetic and dielectric properties, the spontaneous electric polarization is calculate under the King-Smith and Vanderbilt theory, 1s core-hole absorbing atom was used to calculate the XANES spectra, the TDDFT theory was used to study optical properties. The Hubbard correction was considered over f rare earth electrons. The results for x=0.125 Sm concentration show dielectric with a narrow energy band gap, ferroelectric with higher spontaneous polarization than the tetragonal BaTiO<sub>3</sub>, and ferromagnetic properties with 5.89 Bohr mag/cell induced mainly by Sm presence. The authors would like to thank to FAPEMIG, CAPES and CNPq Brazilian agencies for financial support.

Wednesday, July 27, 2022

## PACC4: Bioceramics and Biocomposites

### **Bioceramics and Biocomposites**

Room: Millennium (Level B)

Session Chair: Franz Weber, University of Zurich

**8:30 AM**

#### **(PACC-S4-001-2022) Biologically Derived Architectures for Next Generation Advanced Materials (Invited)**

D. Kisailus\*<sup>1</sup>

1. University of California at Irvine, Materials Science and Engineering, USA

There is an increasing need for the development of multifunctional lightweight materials that are strong, tough, and reconfigurable. Natural systems have evolved efficient strategies, exemplified in the biological tissues of numerous animal and plant species, to synthesize and construct composites from a limited selection of available starting materials that often exhibit exceptional mechanical properties that are similar, and frequently superior to, mechanical properties exhibited by many engineering materials. These biological systems have accomplished this feat by establishing controlled synthesis and hierarchical assembly of nano- to micro-scaled building blocks that are integrated into macroscale structures. However, Nature goes one step further, often producing materials with that display multi-functionality in order to provide organisms with a unique ecological advantage to ensure survival. In this work, we investigate a variety of organisms that have taken advantage of hundreds of millions of years of evolutionary changes to derive structures, which are not only strong and tough, but also demonstrate the ability to articulate as well as display multifunctional features dependent on the underlying organic-inorganic components. We discuss the mechanical properties and functionality stemming from these hierarchical features as well as how they are formed.

**9:00 AM**

#### **(PACC-S4-002-2022) Bioactive glass based scaffolds incorporating phytotherapeutics for bone regeneration (Invited)**

A. R. Boccaccini\*<sup>1</sup>

1. University of Erlangen-Nuremberg, Institute of Biomaterials, Germany

Extensive research is being done on producing three-dimensional scaffolds for bone tissue regeneration with special focus on the repair of critical bone defects. Scaffolds based on bioactive glasses (BGs) are promising for bone tissue engineering due to their ability to bond to bone. Additionally, BGs stimulate new tissue formation via the activation of gene expression modulated by the release of ions during BG degradation. The use of traditional herbal medicine in combination with BGs is gaining attention to obtain multifunctional platforms, for example able to stimulate the regeneration of tissue and simultaneously prevent bacterial infection. In this study, BG scaffolds were produced via the foam replica technique and dip-coated with polymer solutions containing biologically active compounds such as Manuka honey or icariin. The bioactivity, mechanical properties, release behavior and antibacterial effect of coated and non-coated scaffolds were investigated. Interestingly, scaffolds coated with plant derived bioactive compounds exhibited a superior antibacterial effect against *S. aureus* compared to the other tested scaffolds, this antibacterial effect was dependent on concentration. Furthermore, there was no effect of the coating on the osteoconductive behavior of the scaffolds, suggesting the potential use of such coatings on BG scaffolds for bone tissue engineering applications.

**9:30 AM**

#### **(PACC-S4-003-2022) Unforeseen molecular mechanisms govern the formation, stabilization, and additive-incorporation behavior of amorphous calcium carbonate: Implications for biomineralization and biomaterial design (Invited)**

S. E. Wolf\*<sup>1</sup>

1. Friedrich-Alexander-University Erlangen-Neurnberg, Department of Materials Science and Engineering, Chair of Glass and Ceramics, Germany

Transient amorphous calcium carbonate (ACC) is crucial in various biomineralization processes. Some additives of small-molecular feature a disproportionately high impact on ACC formation incomensurable with classical concepts weight and thus take an elusive role in biogenic, geologic, and industrial calcification processes. Therefore, we looked closely at potent small-molecular-weight additives that strongly impact calcium carbonate formation and ACC stabilization. We find that only those additives show a behavior aberrant from classical concepts if they actively interact with so-called prenucleation clusters in solution, i.e., spontaneously forming carbonate calcium complexes. Recently, calcium carbonate and especially ACC received attention for its potential use as a biomaterial and drug-delivery system; for these undertakings, our findings are significant as they highlight the molecular machinery governing ACC composition. Our results demonstrate that ACC forms via aggregation of PNCs and that its formation is highly susceptible only to additives that specifically interact with PNCs. Our results reveal molecular mechanisms that operate beyond established mechanistic conceptions, motivating a re-assessment of the role of small molecules in biomineralization and biomaterials design.

**10:20 AM**

#### **(PACC-S4-004-2022) Micro and nanoarchitecture of 3D printed ceramic scaffolds for osteoconduction and bone augmentation (Invited)**

F. E. Weber\*<sup>1</sup>

1. University Zurich, Center for Medical Dentistry/oral Biotechnology & Bioengineering, Switzerland

Osteoconduction is a key phenomenon in the healing of bone defects and bone augmentation is needed for the placement of dental implants. The questions we wanted to answer was: is the best micro- and nanoarchitecture for osteoconduction and bone augmentation the same? For the production of scaffolds, we applied a lithography-based additive manufacturing system. As in vivo test model, we used a calvarial defect and a bone augmentation model in rabbits. The histomorphometric analysis showed that bone formation was significantly increased with pores between 0.7-1.2 mm in diameter. Best microarchitecture for osteoconduction and bone augmentation are different. Moreover, microporosity appeared to be a strong driver of osteoconduction and influenced osteoclastic degradation for tri-calcium phosphate based scaffolds. For hydroxyapatite based scaffolds, however, microporosity appears to influence osteoconductivity to a lesser extent. In essence, additive manufacturing enables to generate libraries of microarchitectures to search for the most osteoconductive microarchitecture for orthopaedics and the ideal microarchitecture for bone augmentation purposes. Moreover, additive manufacturing appears as a promising tool for the production of personalized bone tissue engineering scaffolds to be used in cranio-maxillofacial surgery, dentistry, and orthopaedics.

**10:50 AM - WITHDRAWN**

### **(PACC-S4-005-2022) Hydroxyapatite-graphene coatings produced by axial suspension plasma spraying**

N. Markocsan<sup>\*1</sup>; G. Manivasagam<sup>2</sup>

1. University West, Dept. of Engineering Science, Sweden
2. VIT University, India

Axial suspension plasma spraying (ASPS) is an emerging coating technology that uses as feedstock a suspension of very finer powders (nano- to submicrometric particle size) and demonstrated promising results for biocompatible coatings. This work highlights the influence of incorporated graphene nano platelets (GNPs) on behavior of ASPS hydroxyapatite (HAP) coatings. HAP coatings with varying GNP contents (0, 0.5, 2 and 5 wt. %) were produced and investigated. Characterization of the ASPS HAP + GNP coatings was carried out using SEM, EDS, Confocal Raman, White light interferometry, and contact angle measurements. Mechanical properties such as hardness, roughness, adhesion strength and porosity were also evaluated along with fretting wear performance. Additionally, the biocompatibility of HAP + GNP coatings was evaluated via cytotoxicity testing and visualization of cell adhesion using SEM and Laser Scanning Microscopy. The addition of GNP enhanced the tribocorrosion resistance properties. In gene expression studies, a 2% GNP content upregulated RunX2 gene and down-regulated pluripotent gene NANOG and SOX2, implying this composition to be a much-suited candidate among the rest for bioactive orthopaedic coatings.

**11:10 AM**

### **(PACC-S4-006-2022) In-vitro biological effect of dissolution products from silicate bioactive glasses**

M. Arango-Ospina<sup>\*1</sup>; A. R. Boccacini<sup>1</sup>

1. University of Erlangen-Nuremberg, Institute of Biomaterials, Germany

Silicate-based bioactive glasses (BGs) have been studied in the context of bone tissue engineering due to their ability to react with the biological environment and bond to hard tissue. The bioactive behavior of BGs is typically characterized by the formation of a hydroxycarbonate apatite layer on the surface of the material, as well as by the release of ionic dissolution products during the degradation process. This aspect plays an important role at a cellular level to stimulate the formation of new tissue. The incorporation of metallic ions is a convenient approach to enhance the intrinsic properties of BGs and obtain materials with multiple biological functionalities, for example with antibacterial, angiogenic and osteogenic properties. In this study silicate-based BGs were produced via the melt-quench route based on the 45S5 BG composition, and the incorporation of metallic ions such as zinc, strontium and boron was investigated. The bioactive behavior of the BGs was studied in simulated body fluid and characterized with FTIR, SEM and XRD. The biological effect of BGs was determined by analyzing the viability and differentiation of pre-osteoblast cells (MC3T3-E1), as well as the release of vascular endothelial growth factor (VEGF) as a potential indicator of angiogenesis. The antibacterial effect of BGs was studied using *E. coli* bacteria. The results suggest the potential application of ion-doped BGs for bone regeneration with Sr-doped BGs showing superior biological properties compared to other BGs.

**11:30 AM**

### **(PACC-S4-007-2022) Additive Manufacturing of Materials of Polymers and Polymer-Ceramic Hybrid Materials for Medical Applications (Invited)**

R. Narayan<sup>\*1</sup>

1. North Carolina State University, USA

This presentation will consider several laser-based additive manufacturing techniques for processing microstructured and nanostructured materials for use in next generation medical devices. For example, a 3D printing approach known as two photon

polymerization was used for selective polymerization of photo-sensitive polymer and polymer-ceramic hybrid material resins. Polymerization of solid features with microscale and nanoscale features is attainable since the two photon absorption process possesses a nonlinear relationship with the incident light intensity. We have used two photon polymerization process several types of medically-relevant structures with microscale and nanoscale features from photosensitive polymers and polymer-ceramic hybrid materials. For example, we used two photon polymerization to manufacture small-scale devices known as microneedles. We have demonstrated the use of these devices for transdermal delivery of pharmacologic agents and transdermal sampling of body fluids. We have also used two photon polymerization to manufacture many types of tissue engineering scaffolds. The in vitro testing, in vivo testing, and clinical translation of two photon polymerization-manufactured structures will be described.

## **PACC5: Advances in Cements, Geopolymers, and Structural Clay Construction Materials**

### **Geopolymers and Structural Clay Construction**

#### **Materials**

Room: Venetian (Level B)

Session Chairs: Natalia Betancur-Granados, Corporación Universitaria Minuto de Dios; Henry Colorado L., Universidad de Antioquia

**8:30 AM**

#### **(PACC-S5-001-2022) Use of construction and demolition waste for developing geopolymer cements (Invited)**

A. Cardoza<sup>\*1</sup>; H. A. Colorado L.<sup>1</sup>

1. Universidad de Antioquia, Colombia

In the present investigation, a geopolymer cement was developed with construction and demolition waste in aqueous solution with sodium hydroxide and sodium silicate as activators. The main goal is to produce a solution that reduces pollution related to the construction and demolition wastes at Colombia. Diverse sample formulations were manufactured, and compressive strength, density, scanning electron microscopy, and x-ray diffraction characterization tests were included in this research in order to understand the structure-property relations of the developed formulations.

**9:00 AM**

#### **(PACC-S5-002-2022) Thermal behavior of geopolymers for new catalytic applications (Invited)**

R. V. Eleuterio<sup>\*1</sup>; F. T. Albino<sup>1</sup>; L. Simão<sup>1</sup>; L. Senff<sup>1</sup>; D. Hotza<sup>1</sup>

1. Federal University of Santa Catarina, Brazil

Aluminosilicate inorganic polymers (geopolymers) may be used as catalytic supports due to their chemical and thermal stability and relative high specific surface area. In this work, metakaolin-based geopolymers were 3D-printed and used as catalyst support of nickel as an active phase for applications at high temperatures. Direct Ink Writing of pastes with proper rheology, high buildability, and shape retention enabled the production of scaffold-like structures of total porosity close to 70 vol%. The impregnation of the structures with nickel-nitrate was preceded and followed by calcination at 800 °C to remove combined water and possible impurities and to assess the behavior of the new catalyst when subjected to high temperatures. The amounts of salt (nickel nitrate hexahydrate) were known considering the relationship among the metal amount required (20 wt.%), the mass of the catalytic support to be impregnated, and the molar masses of salt (g/mol) and metal (g/mol). Nickel was successfully impregnated to the sample's surface with 10 to 15 wt% of metal. Thermogravimetric and structural characterization of the resulting catalyst showed stability after exposure to

high temperature, confirmed with image and elemental analysis via SEM and EDS. The results suggest that Ni-impregnated 3D-printed geopolymeric structures may be adequate to use as catalysts up to 800 °C.

**9:30 AM**

**(PACC-S5-003-2022) Manufacture of alkali-activated cements from agro-industrial waste (Invited)**

N. Betancur-Granados<sup>\*1</sup>; D. Gonzalez<sup>2</sup>; F. F. Franco Aguirre<sup>2</sup>; I. Taborda Llano<sup>2</sup>; J. J. Pérez Molina<sup>2</sup>; M. J. Florez Tirado<sup>2</sup>; N. Zapata Perez<sup>2</sup>; P. A. Giraldo Gamboa<sup>2</sup>; S. Restrepo Lopez<sup>2</sup>; J. Durango Duarte<sup>1</sup>; A. A. Hoyos Montilla<sup>2</sup>

1. Corporación Universitaria Minuto de Dios - UNIMINUTO, Faculty of engineering, Colombia
2. Universidad Nacional de Colombia, School of architecture, Colombia

Within sustainable construction, the reduction of the environmental impact by the construction industry is sought, through the efficient and conscious use of available resources, prioritizing the recycling of raw materials and the comprehensive planning of buildings from their design. The production of alkali-activated cements allows the incorporation of alternative raw materials, in a production process with lower energy demand and environmental impact. Considering the above, this project has as its purpose the analysis of agro-industrial and industrial residues that can be incorporated in the production of alkali-activated cements. With this, it carried out the identification of agro-industrial waste with the potential to be used as raw materials in the production of alkali-activated cement, closing the life cycle of different waste by generating a circular economy through a cement with characteristics superior to or equal to cement.

**10:20 AM**

**(PACC-S5-004-2022) Potential for industrialization of belite nanoparticles manufactured by aerosol pyrolysis compared to other synthesis methods (Invited)**

D. Gil Velasquez<sup>\*1</sup>; J. J. Pérez Molina<sup>1</sup>; J. I. Tobón<sup>2</sup>; O. J. Restrepo<sup>2</sup>; N. Betancur Granados<sup>3</sup>

1. Universidad Nacional de Colombia, Architecture, Colombia
2. Universidad Nacional de Colombia, Department of minerals and materials, Colombia
3. Corporación universitaria minuto de dios UNIMINUTO, Department of Basic Sciences, Colombia

Conventional method to obtain Portland cement clinker represents two major disadvantages: long thermal treatment and elevated temperatures of synthesis, both of which cause high emissions of CO<sub>2</sub> to the atmosphere. This leads to efforts to hydraulically stabilize the active forms of calcium silicates and to develop new cementitious materials with alite and belite particles with good hydraulic reactivity properties without problems of resistance at early age and a reduction in CO<sub>2</sub> emissions at the atmosphere. A proven way to achieve this is through the application of new nanoparticle synthesis technologies, which would allow reductions in energy consumption, calcium demand and CO<sub>2</sub> emissions. The aim of this work was review alternative methods for the synthesis of dicalcium silicates to produce ecofriendly cementitious materials at high rate with less demand of calcium oxide and energy. This research presents a comparison between experimental results by the production of belite through Flame Spray Pyrolysis (FSP), with a collection of the state of the art in the development of cements with belite nanoparticles obtained other alternative synthesis methods as Pechini, Sol-gel, Hydrothermal and Self-propagating in search of possibilities of mass production of cements with belite nanoparticles with lower demand for calcium oxide and energy. The study concludes that alternative methods such as flame spray pyrolysis appear to be promising for the mass production of elements, but the proof of these alternative methods in the high production of nanoparticles of belite cement is still a lack of knowledge.

**PACC8: Novel, Green, and Strategic Processing and Manufacturing Technologies**

**Novel, Green, and Strategic Processing IV**

Room: Bellagio (Level B)

Session Chair: Ralf Riedel, TU Darmstadt, Germany

**8:30 AM**

**(PACC-S8-020-2022) High Voltage Pulsed Discharge for selective separation at the multi-materials interface (Invited)**

C. Tokoro<sup>\*1</sup>

1. Waseda University, Japan

Nowadays, separation technology is indispensable to reuse/recycle multi-materials after disposal. Recycling technologies consist of physical separation followed by chemical separation. In general, physical separation is low energy but its separation efficiency of it is not so high. Chemical separation is the opposite. Therefore, the best combination of them is necessary to achieve a low energy recycling process with high separation efficiency. Also, technological innovation is required to improve the physical separation efficiency. In this presentation, a novel physical separation technology using high-voltage pulsed discharge is introduced. By controlling the voltage, current, and pulse waveforms, this technology achieves a selective separation at the interface of the multi-materials due to heat and shock waves generated by plasma on the discharge path. For example, it is effective for the separation of foil and particles of the positive electrode material in a lithium-ion battery, the separation of metal wires and resin from the cell sheet in a solar panel, the separation between bonded metal materials by adhesive, and the peeling of a coated metal layer. Separation by the high-voltage pulsed discharge is instantaneous by a huge electric power with a small amount of energy.

**9:00 AM**

**(PACC-S8-021-2022) Sustainable Recovery, Reprocessing and Reuse of Rare-Earth Magnets in Circular Economy**

M. Zakotnik<sup>\*1</sup>

1. Urban Mining Company, USA

Neodymium iron boron (NdFeB) based magnets have high magnetic properties and energy density, and thus are the material of choice for a wide variety of renewable and industrial applications. NdFeB magnets were recognized as critical and yet are largely discarded within urban mines globally; examples of end of life discarded products include, hard disk drives, electric motors, MRIs, wind turbines, electronics, etc. Urban Mining Company has a setup a novel process whereby this urban mine can be tapped to recover rare earths from end of life materials. This recovery process has now been operational for 4 years and is operating on an industrial scale. Until recently, USA and developing countries of the Americas were fully dependent on international supplies of these critical rare earth NdFeB-based magnets. The Urban Mining Companies magnet-to-magnet recycling approach, setup in America can deliver high quality engineered NdFeB magnets from end-of-use waste NdFeB feedstock material. This process also substantially lowers the rate of critical materials (Dy, Tb, Nd, Pr, Co) consumed in the production of rare earth NdFeB-type products. Reprocessed NdFeB magnets can sustainably fit in a circular economy thus competing by performance with NdFeB magnets that were manufactured using virgin elemental feedstock material.

9:20 AM

### (PACC-S8-022-2022) Recycling Wastes Into Clay Brick Manufacturing

G. Wie-Addo<sup>\*1</sup>; A. H. Jones<sup>1</sup>; S. Palmer<sup>2</sup>; J. Renshaw<sup>2</sup>; P. A. Bingham<sup>1</sup>

1. Sheffield Hallam University, Materials and Engineering Research Institute, United Kingdom
2. Wienerberger Ltd., United Kingdom

A modified body composition for brick masonry ceramics was prepared mixing clay with 4wt% additives and fired at 950°C and 1040°C. The relevance of this study is to maintain brick quality and reduce fuel use in heavy clay brick manufacture using recycled waste streams. Technological properties of fired ceramics were examined by nine characterization techniques. Properties of fired clay are compared with the reformulated fired body composition. Results reveal that additives promote development of new phases. Industrial wastes ceramics are less porous compared with the ceramics produced using only clays. The additives react with pyrites in clay during sintering producing whitish stains on ceramic surface after firing. This effect is slightly greater than for ceramics produced from clay alone. Boiling water absorption for the ceramics produced using waste derived additives are lower than colemanite and for the base material. Results obtained from <sup>57</sup>Fe Mössbauer spectroscopy reveal that iron is present in all samples, predominantly as Fe<sup>3+</sup> as hematite (Fe<sub>2</sub>O<sub>3</sub>) except for the unfired clay which had Fe<sup>2+</sup> as well. Differences in Fe<sup>3+</sup> partitioning and site populations between samples is consistent with observed differences in XRD patterns and can be related to colour differences of the fired ceramics. Results support raw material substitution for more sustainable and flexible product colour range for heavy clay ceramic manufacture.

9:40 AM

### (PACC-S8-023-2022) Green Synthesis of Materials Via Reaction of Metal Oxides with Aqueous Reagents (Invited)

A. Apblett<sup>\*1</sup>

1. Oklahoma State University, USA

Ceramic materials are often prepared from the reaction of their component oxides at high temperature, a process that typically involves several cycles of grinding, pressing, and firing. Materials chemists have shown that solution-based routes such as sol-gel, co-precipitation, and the Pechini method are faster and require lower temperatures. The reaction of metal oxides with an aqueous salt of another metal is a hybrid method that can have significant advantages for synthesis of bimetallic metal oxides. For example, the reaction of lanthanum oxide with aqueous vanadyl sulfate provides a simple pathway to LaVO<sub>4</sub> or VO(OH)<sub>2</sub> depending on stoichiometry. A similar reaction can be used to derivatize the surface of alumina catalyst support pellets to produce catalytic materials. Reaction of MoO<sub>3</sub> with aqueous metal salts can be used to produce a myriad of lanthanide, actinide, transition metal, and main group molybdates. Indeed, these reactions can be used to remove heavy metals and uranium from contaminated waters. Replacement of MoO<sub>3</sub> in these reactions by tungstic acid, H<sub>2</sub>WO<sub>4</sub>, provides low-temperature routes to metal tungstates. Examples of these reactions will be provided and the potential for these reactions will be discussed including a recent method for direct preparation of a trimetallic oxide, Na<sub>2</sub>Fe(MoO<sub>4</sub>), a promising battery electrode material.

10:30 AM

### (PACC-S8-024-2022) Design of insulating ceramic foams for high temperature applications (Invited)

V. R. Salvini<sup>\*1</sup>

1. UFSCar, Materials Engineering, Brazil

The main reason of applying insulating foams ceramics as high temperature equipment linings are related to energy costs and environmental concerns. From the emission point of view, most of high temperature equipment operates in the infrared wavelength range

(0.7µm to 100µm), where the thermal transmission by radiation is the major mechanism for the total effective thermal conductivity. This information is fundamental to design the composition and the microstructure of insulating ceramic materials. Considering the infrared wavelengths, a good thermal insulating material must be able to reduce the intensity of radiation emitted within the temperature range of interest. There are two ways to reach this target: by adding substances which absorb partially the radiation in the wavelength range of interest and/or by generating micropores to scatter the heat radiation. Design of insulating ceramic foams is presented focusing on applications, such as at hot face furnace linings operating at 1700°C and as ladle linings for direct contact with liquid metals. The foam ceramics compositions, as well as their microstructures were specially designed for each application.

11:00 AM

### (PACC-S8-025-2022) Nb<sub>2</sub>O<sub>5</sub> containing alumina foams for high temperature applications

V. R. Salvini<sup>\*1</sup>; M. F. Santos<sup>2</sup>; E. França<sup>3</sup>; R. A. Mesquita<sup>3</sup>; M. Stuart<sup>4</sup>; V. C. Pandolfelli<sup>1</sup>

1. UFSCar, Materials Engineering, Brazil
2. RED Lab, Brazil
3. CBMM, Brazil
4. St3 Consultoria, Brazil

High temperature industrial equipment and processes operate in the IR infrared wavelength range ( $\lambda=100\mu\text{m}$  to  $0.7\mu\text{m}$ ) and consume high amount of energy. Technological innovation to reduce heat loss, the consumption and energy costs of these processes and equipment include the use of thermal insulating ceramic alumina foams. A good thermal insulating ceramic material should be able to reduce the intensity of the radiation emitted within the IR temperature range. Literature data indicate the existence of an ideal pore diameter range of  $0.5\mu\text{m}$  to  $3.0\mu\text{m}$  that minimizes thermal conductivity in the range between 1000°C and 1700°C. In this work, it was found that the thermal insulation efficiency of high Al<sub>2</sub>O<sub>3</sub> foams can be increased by adding 1wt% Nb<sub>2</sub>O<sub>5</sub> to their compositions. The thermal conductivity and the compressive strength of these materials are respectively 0.8W/mK and 23MPa (91% Al<sub>2</sub>O<sub>3</sub> foam) and 0.4W/mK and 5MPa (98% Al<sub>2</sub>O<sub>3</sub> foam). Thermal and energetic analysis of Fe-Nb alloy ladle lined with these ceramic foams as backup layer revealed gains in the temperature of the metal bath, lower temperature on the shell and reduced thermal gradient at the refractory working face.

11:20 AM

### (PACC-S8-026-2022) Novel Processing of Porous Ceramics for Unidirectional Porous Structures

T. Ohji<sup>\*1</sup>; M. Fukushima<sup>2</sup>

1. National Institute of Advanced Industrial Science and Technology (AIST), Japan
2. National Institute of Advanced Industrial Science and Technology (AIST), Japan

Porous ceramics are now being used for various applications from diesel particulate filters (DPF) and coal gasification gas filters to separation membrane supports, and a number of innovative processing routes have been developed for critical control of porous structures. This paper first gives an overview on the recent progresses of porous ceramics, mainly macro-porous ceramics whose pore size is larger than 50 nm. The representative processes of making macro-porous ceramics are classified into four categories including “partial sintering”, “sacrificial fugitives”, “replica templates”, and “direct foaming”, and some examples of the innovative techniques in these categories are addressed. Then, focus is placed on freeze-dry processing where water or liquid are used as fugitive materials and pores are formed by the sublimation of ice crystals unidirectionally grown from them. As one of the latest achievements on this technique, we will report thermal insulators

prepared by a gelation-freezing method using platelet particles and discuss the effects of the platelets on the mechanical properties and thermal conductivities. The addition of the platelets could reduce the shrinkage during sintering and enhance the thermal stability and compressive strength. We will also discuss the relationship between the orientation degree and the properties.

## **PACC10: Ceramics for Sustainable Agriculture**

### **Soil Management**

Room: Vitri (Level M)

Session Chair: Mrityunjay Singh, Ohio Aerospace

#### **8:30 AM**

#### **(PACC-S10-008-2022) Ceramics for Capture of Plant Nutrients and Their Subsequent Use as a Slow Release Fertilizer (Invited)**

A. Apblett<sup>\*1</sup>; C. Kelley<sup>1</sup>; R. Rahman<sup>1</sup>; P. Kitzel<sup>1</sup>; N. materer<sup>1</sup>; E. Kadossov<sup>2</sup>; S. Shaikh<sup>2</sup>

1. Oklahoma State University, USA

2. XploSafe, LLC, USA

Nutrient pollution is a costly problem with widespread negative health and ecological effects. Similarly, build-up of nutrients in aquaria water leads to algal growth and toxicity to aquatic organisms and fish. An ideal solution to these problems is capturing such nutrients in a form that is amenable to application as a fertilizer, thus turning a pollutant into a valuable resource. We have developed magnesium aluminum oxide and magnesium iron oxide ceramics from calcining a layered double hydroxide that are good adsorbents for both phosphate and nitrate. These materials can capture plant nutrients from contaminated water and can then be utilized as time release fertilizer. The possibility of using this low-cost material as a soil additive to prevent fertilizer runoff will also be discussed.

#### **9:00 AM**

#### **(PACC-S10-009-2022) Utilization of porous ceramics for plant growth materials**

M. Fukushima<sup>\*1</sup>; T. Ohji<sup>1</sup>

1. National Institute of Advanced Industrial Science and Technology (AIST), Japan

Highly porous ceramic balls with porosity ranging from 70 to 90% were prepared through gelation-freezing route. The objective of this research is to produce ceramic plant growth material. The soil-less growing media used in agriculture and horticulture are used to provide oxygen and water to the roots at simultaneously sufficient levels. Porous ceramics prepared have been attempted to the use of for plant cultivation and soilless culture. The process and applications will be discussed, in terms of porosity.

#### **9:20 AM**

#### **(PACC-S10-010-2022) An Overview of Biomass as a Potential Source for Designing Functional Materials**

S. Gupta<sup>\*1</sup>

1. University of North Dakota, Mechanical Engineering, USA

Biomass is an underutilized resource which can be used for manufacturing functional materials for agricultural and other related applications. In this presentation, I present current progress on the usage of biomass for developing functional materials. The presentation will be divided into different sections. In part-A, I will summarize some of the recent progress in designing ceramics from biomass. During part-B, I will present current progress in advanced polymeric materials biomass. Detailed microstructure and characterization analysis will be presented. It is expected that these technologies can be commercialized.

#### **9:40 AM**

#### **(PACC-S10-011-2022) Natural fibers and ceramic wastes in composites and soils**

H. A. Colorado L.<sup>\*1</sup>

1. Universidad de Antioquia, Colombia

This research presents several cases involving ceramic wastes and natural fibers in soils, construction materials and composites. Ceramic materials are by weight the most manufactured materials worldwide, which includes ceramics such as soils, concrete, and clays. Moreover, from organic and inorganic solid wastes can be obtained fibers and ceramic particles than can be added as a reinforcement or as a functional material acting as a fertilizer, pozzolanic material, or other function. Therefore, the use of natural fibers is very beneficial for the environment because not only is a biodegradable material, but also because these can have a waste origin and thus, its use, also contributes to a less pollute environment. Similarly, the use of ceramic wastes in agriculture can be a very competitive solution also with environmental benefits. This presentation explores the progress of using these materials in Colombia.

## **PACC12: Special Symposium: Ceramics and Materials Education in the Americas**

### **Education**

Room: Revolution (Level B)

Session Chairs: Sylvia Johnson, NASA-Ames Research Center (ret.);

#### **8:30 AM**

#### **(PACC-S12-001-2022) An interdisciplinary experience of teaching Materials Science at the Universidad de Antioquia (Invited)**

H. A. Colorado L.<sup>\*1</sup>

1. Universidad de Antioquia, Colombia

This research present results regarding the interdisciplinary experience in the teaching of materials courses at the University of Antioquia for undergraduate and graduate students of engineering. Case studies of project based-learning are presented with a solutions for the local community. Another case involving the University Museum in collaboration with the Engineering School is presented, involving arts, biology and engineering, and evaluated not only with people of different ages and education, but also with children and people not related to the University. The teaching and didactics at the University level is discussed, and the main strengths, challenges and limitations for both the University and the Country are analyzed as well in terms of the relation University, Industry, Government and Community.

#### **8:50 AM**

#### **(PACC-S12-002-2022) Ceramics and Materials Education in Brazil (Invited)**

E. N. Muccillo<sup>\*1</sup>

1. Energy and Nuclear Research Institute, Brazil

Brazil has nowadays, in several state and federal universities, different types of courses in the area of ceramics and materials science and engineering. However, there are significant differences in these courses. These differences, as well as the evolution of the courses to the present day along with technician training and development of technological courses, will be presented. The motivating agents for changes in the teaching of materials science and technology will also be analyzed. Finally, suggestions for optimization in local education in ceramics and materials science and engineering will be considered.

**9:10 AM**

**(PACC-S12-003-2022) Ceramic Education in Japan (Invited)**

T. Ohji\*<sup>1</sup>

1. National Institute of Advanced Industrial Science and Technology (AIST), Japan

This paper will first give an overview of education activities made by the Ceramic Society of Japan (CerSJ). CerSJ has been organizing the Ceramics Education Program for Beginners (CEPRO), where a seminar made by university professors or high-class industry engineers is being held 7 times a year, all in Tokyo area. One seminar contains 3 classes (80 min./class) and the number of participants of each class is approximately 100. CEPRO focuses on education for students and young professionals who do not learn or have not done technically ceramic materials in schools including universities. (CEPRO is financially supported by the Ceramic and Glass Industry Foundation (CGIF).) CerSJ has also been organizing annually the High-School Education Forum, which is a half-day forum on ceramic unique experiments for high school education. The forum is designed principally for high-school teachers who can make similar experiments in their own classes or education events. Currently high schools and universities of Japan are strongly encouraged to organize science education events to attract and interest regional pupils and students in science. CerSJ has also been financially supporting such science education events related to ceramics throughout the country. The paper also will introduce education activities made in high-school and other academic institutes of Japan and others.

**9:30 AM**

**(PACC-S12-004-2022) Ceramic Engineering Education at Missouri University of Science and Technology (Invited)**

D. Lipke\*<sup>1</sup>; G. Hilmas<sup>1</sup>

1. Missouri University of Science & Technology, Materials Science & Engineering, USA

Since 1922 the Missouri University of Science and Technology (Missouri S&T, formerly University of Missouri - Rolla, originally Missouri School of Mines and Metallurgy) has offered undergraduate and graduate degrees in Ceramic Engineering. As one of only two degree-awarding departments in the United States specialized in the discipline, the program trains future leaders in foundational principles and practical applications of ceramic materials in the classroom, in hands-on laboratories, through a robust internship and co-operative education program, and via internationally recognized sponsored research activities. This presentation will highlight the evolution of the program at Missouri S&T from inception to modern day, and will include perspectives on curricular trends, opportunities for collaboration, growth, and outreach, and challenges facing higher education and the discipline.

**9:50 AM**

**(PACC-S12-005-2022) Considerations of a BS in Ceramic Engineering at Colorado School of Mines (Invited)**

I. Reimanis\*<sup>1</sup>; G. L. Brennecke<sup>2</sup>; B. Gorman<sup>1</sup>; A. Rockett<sup>1</sup>; V. E. Stevanovic<sup>1</sup>

1. Colorado School of Mines, USA
2. Colorado School of Mines, USA

The Colorado School of Mines is an R1 US research university with about 5500 undergraduates and 1500 graduate students. The Metallurgical and Materials Engineering (MME) Department at Mines currently offers one bachelor of science program for about 50 undergraduates per year. The current MME BS degree is ultimately derived from the extractive metallurgy curriculum that Mines offered nearly 150 years ago. About 30 years ago Mines hired faculty with expertise in ceramics to enhance relationships with local industry and leverage the existing strengths in extractive metallurgy and materials processing to develop curricula in ceramics. Today, both ceramics and metals are in the core mission of MME. This presentation describes efforts in the last few years to create a BS

degree in ceramic engineering at Mines. It will include details on the industrial needs for such a program, the specific curricular adaptations, and challenges/opportunities associated with the department culture.

**10:30 AM**

**(PACC-S12-006-2022) An alternative to traditional doctorate in USA: The Pasteur Partners PhD (P3) track (Invited)**

H. Jain\*<sup>1</sup>; V. Dierolf<sup>2</sup>; A. Jagota<sup>1</sup>; H. L. Columba<sup>1</sup>

1. Lehigh University, USA
2. Lehigh University, Physics, USA

We describe a new model of doctoral training, which is in contrast to traditional curiosity-driven research, and is especially valuable to those who wish to see the impact of their doctoral dissertation in real life within a reasonable timeframe. It provides graduate training through active partnership with companies that are familiar with potential applications and the needs of the society at large. Its features include: 1. The student is actively involved in defining the scope of her/his dissertation. P<sub>3</sub> starts with a pre-program summer internship at a company to get the 'big picture' of the problem of interest through discussions with industry researchers. 2. With a broad perspective of research problem, the student selects appropriate courses in consultation with the academic adviser. Overall, each scholar's program is personalized with co-advisers from both the university and a partner company. 3. A one to two semester company residency is required to ensure use-inspired, industrial perspective as well as the rigor of a doctoral degree. 4. In addition to meeting Departmental requirements, the student is required to take modular, graduate-level professional development courses, co-taught by faculty and industry researchers. P3 is developed with support from NSF's Innovation in Graduate Education program.

**10:50 AM**

**(PACC-S12-007-2022) North American Summer School on Photonic Materials (NASSPM): An experiment on incorporating laboratory experience in short courses (Invited)**

H. Jain\*<sup>1</sup>; K. Richardson<sup>2</sup>; Y. Messaddeq<sup>3</sup>

1. Lehigh University, International Materials Institute for New Functionality in Glass, USA
2. University of Central Florida, CREOL, USA
3. Université Laval, Optic-Photonic Pavillion, Canada

NSF's Int'l Materials Institute for New Functionality in Glass pioneered the concept of weeklong international school, which brought together subject experts from various countries to teach glass science and engineering to young researchers. The goal was to attract bright young scientists to glass research, introduce them to the latest scientific and technological advancements, while building an international community with lasting professional friendships. The idea was significantly expanded in the form of ICG Summer School, which has been held annually since 2009 at University of Montpellier. The success of this School has been emulated by a similar school in Wuhan, China since 2015. These forums have served to teach formation, structure, and properties of glass to graduate students/postdocs from all over the world. Although they have offered exposure to cutting edge topics of glass science and engineering, they lacked hands-on lab experience. This gap was filled by NASSPM held at Laval U., which focused on optics and photonic materials. It was highly successful based on feedback from 80 students from 12 countries, and its impact on students' subsequent research. In this presentation, we describe the challenges and benefits of this mode of advanced training of graduate level workforce in materials research.

11:10 AM

**(PACC-S12-008-2022) Discovering, Designing, Making, and Manufacturing Materials to 2040 (Invited)**G. Gaustad\*<sup>1</sup>; S. Tidrow<sup>2</sup>

1. NYS College of Ceramics, Alfred University, Inamori School of Engineering, USA
2. Alfred University, USA

A large number of recent studies focus on the workforce of the future. These reports show startling data when it comes to what our current and future engineering graduates will be doing out in the workforce. The World Economic Forum predicts that 70 million jobs will be displaced by global shifts, with 133 million new jobs being created. McKinsey Global Institute found that while 50% of work can be automated, less than 10% of jobs can be automated over 90%. A theme throughout all of these studies is the need for today's engineering students to have agility to work among different disciplines, understand automation and how to work well with it, have significant digital literacy and at least some computer science and programming expertise, and be comfortable working with large sets of data (Forum 2018, Stubbings and Williams 2018, Lund, Manyika et al. 2019). This presentation will share how the Inamori School of Engineering at Alfred University is updating our curriculum to prepare engineering graduates for this future while at the same time celebrating and staying true to our rich history and focus on ceramics and glass materials.

**Ferroelectrics Meeting of Americas****Applications of Ferroics**

Room: Mirage (Level B)

Session Chair: Steven Tidrow, Alfred University

8:30 AM

**(FMAs-043-2022) Defect Engineered Complex Oxide Thin Films with Anomalous Multifunctionalities (Invited)**C. Chen\*<sup>1</sup>

1. University of Texas San Antonio, Physics, USA

Complex oxides have showed various important physical properties such as tunable dielectric and unusual magnetic properties as well as various quantum phenomena. These extraordinary phenomena are highly dependent upon the degrees of the freedom of the charge distribution, spin and orbital status, and the lattice structures.  $\text{LnBaCo}_2\text{O}_{5+d}$  ( $\text{LnBCO}$ ,  $\text{Ln}$ = rare transition metal elements) systems exhibit various unique physical properties not only due to the presence of A-site disordered and A-site ordered structures, but also the degree of ordered oxygen vacancy structures. These defect engineered structures induce the formation of various double perovskite structures and the strong couplings of multifunctionalities from ferroelectricity to ferromagnetism and optic/magnetolectric response as well as various anomalous quantum phenomena in a single phase double perovskite thin films. More exact to say, defect engineered double perovskite  $\text{LnBCO}$  system is an only magic oxide system with a single phase oxide compound, two types of ionic charge carriers, three different atomic structures, and four field co-tuned multifunctionality system! These findings open a new avenue for material genetic design and synthesis by tailoring the atomic defect structures to facilitate the strong correlated multifunctionalities for quantum materials design, energy harvest system, and novel device development.

9:00 AM - **WITHDRAWN****(FMAs-044-2022) Novel Processing of Advanced Functional Materials (Invited)**C. Prakash\*<sup>1</sup>

1. Maharaja Agrasen Institute of Technology, Applied Sciences, India

Materials that have functionality are attributed to functional materials. Their physical, electrical, and chemical properties are sensitive to a change in environmental parameters such as temperature, pressure, humidity, electric field, magnetic field, etc. They form an essential component of any smart system. Ferroelectrics are an important class of materials whose functionality is exploited to make a number of devices for a variety of applications. These materials are used in various applications ranging from smart and intelligent sensors to sophisticated defence systems. Most of the practical applications are based on bulk ceramics. Material can be tailored to get desired characteristics to meet specific requirements by molecular engineering. Though the material properties are predominantly governed by composition, processing methodology plays an important role to control material performance. Microwave processing and mechanical alloying of materials are novel techniques to get material with improved properties. These are cheaper, faster, and environment friendly. Here, some examples of improvement of material properties by employing these techniques are discussed. The materials studied are barium titanate, modified PZT, lithium ferrites, and magnetolectric composites. All the materials show significant improvement in the properties by using these novel processing techniques in addition to saving time and energy.

9:20 AM

**(FMAs-045-2022) Review on Piezoelectric Footwear Power Generators**B. Zhao<sup>1</sup>; B. Poster<sup>1</sup>; A. Hatfield<sup>1</sup>; F. Qian<sup>3</sup>; L. Zuo<sup>2</sup>; T. Xu\*<sup>1</sup>

1. Old Dominion University, Mechanical and Aerospace Engineering, USA
2. Virginia Tech, Mechanical Engineering, USA
3. Penn State Behrend, Department of Mechanical Engineering Technology, USA

In the last couple of decades, the rapid development of lower-power wearable electronics, health monitoring systems, and implantable medical electronics have driven numerous interests in studying piezoelectric footwear power generators (PFPGs) for a sustainable power supply. This endeavor conducts a comprehensive review on the piezoelectric footwear generators reported in the literature and summarizes the characteristics of those PFPGs. Various piezoelectric footwear power generators will be introduced, compared, and categorized in terms of the piezoelectric materials used, the transduction configurations and mechanism, excitation sources, power generation performance, and intrusiveness, etc. The advantages and disadvantages of the existing piezoelectric footwear power generators and the research methods are then discussed and summarized. Finally, the future perspectives of piezoelectric footwear power generation and its applications are explored.

9:40 AM

**(FMAs-046-2022) Enhanced Photocatalytic Degradation Activity of Cryomilled  $\text{BiFeO}_3$ - $\text{Fe}_3\text{O}_4$  Nanocomposites**V. S. Silva<sup>1</sup>; E. A. Volnistem<sup>1</sup>; L. F. Cótica<sup>1</sup>; I. A. Santos<sup>1</sup>; G. S. Dias\*<sup>1</sup>

1. State University of Maringa, Department of Physics, Brazil

One of the biggest environmental problems resulting from industries is the water contamination. In this sense, several techniques have been studied to promote the water decontamination and photocatalysis has attracted great attention due its great potential. In this topic Bismuth Ferrite (BFO) has obtained notoriety mainly due to its low bandgap (~2.1 eV), which allows the use of the visible light in the degradation process. However, the long-time required for the degradation of methylene blue (MB) by BFO (~350 min) prevent its industrial application. Furthermore, the fast



electron-hole recombination time reduce its degradation efficiency. The BFO coupling with magnetics particles shows up as a solution due to promoted electron drainage and the use of magnetic field for the catalyst recovering. In this study, BFO nanoparticles were synthesized by fast-firing sintering followed by cryo-milling while BFO-Fe<sub>3</sub>O<sub>4</sub> nanocomposites were mechanically coupled in a planetary ball mill. UV-Vis analyses revealed that the BFO-Fe<sub>3</sub>O<sub>4</sub> composite accelerated up to 30 min the degradation time of MB. KFM Microscopy showed a more homogeneous potential distribution and an increase of composite surface potential while SEM microscopy analyses proved the coupling of magnetic particles on the BFO surface. These facts are straight associated to degradation time decrease of MB, and will be discussed in detail.

### 10:20 AM

#### (FMAs-047-2022) Multifunctional epitaxial LaBaCo<sub>2</sub>O<sub>5.5+δ</sub> and PrBaCo<sub>2</sub>O<sub>5.5+δ</sub> thin films: A systematic microstructure and interface investigation (Invited)

J. Jiang<sup>\*1</sup>; C. Chen<sup>2</sup>; E. I. Meletis<sup>1</sup>

1. University of Texas, Arlington, Materials Science and Engineering, USA
2. University of Texas, San Antonio, Department of Physics and Astronomy, USA

Epitaxial LaBaCo<sub>2</sub>O<sub>5.5+δ</sub> films present a variety of novel properties, such as hard ferromagnetic with a magnetoresistance effect value ~24%, semiconductor behavior at T < 300 K, giant magnetoresistances (19% at 40 K), highly directional-dependent metal-insulator transition, extraordinary sensitivity to reducing-oxidizing environment. Epitaxial PrBaCo<sub>2</sub>O<sub>5.5+δ</sub> films have a polarization resistance of 0.109 W cm<sup>2</sup> at 597 °C in air and an ultrafast surface exchange coefficient (0.006 cm/s at 598 °C) with low activation energy (0.77 eV). They can be an excellent cathode material for intermediate-temperature solid oxide fuel cells. Such numerous unique properties in LaBaCo<sub>2</sub>O<sub>5.5+δ</sub> and PrBaCo<sub>2</sub>O<sub>5.5+δ</sub> films were achieved by growing them epitaxially on various single-crystal substrates SrTiO<sub>3</sub>, LaAlO<sub>3</sub>, MgO and NdGaO<sub>3</sub> using PLD with different conditions and post-deposition processes. In this work, we present a systematic microstructure and interface structure investigation of these films using HRTEM and diffraction analysis. Major findings including (i) self-assembled 3-dimensional nano cube structures with a size of 2 to 10 nm; (ii) spontaneous formed triple-layered structure with different phases and lattice misfit strains; (iii) gradient film structures induced by interface strain layers, (iv) effect of film thicknesses and substrate miscut will be reported.

### 10:50 AM

#### (FMAs-048-2022) Fundamental Issues related to Characterization of Electrocaloric Effect

F. Najmi<sup>1</sup>; Z. Cheng<sup>\*1</sup>

1. Auburn University, Materials Engineering, USA

Electrocaloric effect (ECE) can be used to change the temperature of a material by applying electric field. Due to the advantages of ECE-based heat pumps over vapor compression based heat pumps, various designs of ECE-based heat pumps have been introduced, in which the ECE of an electrocaloric material (ECM) is the key parameter. Both indirect and direct methods have been used to characterize the ECE. In the direct methods, the change in the temperature of an ECM is measured when the electric field applied on the ECM is changed. In the indirect methods, the polarization response of an ECM under an electric field is measured at different temperatures and, then, the temperature dependence of the polarization of the ECM under the electric field is used to determine the ECE. It has been reported by different groups that there is a big, even giant, difference in the coefficients of the ECE obtained by the direct and indirect methods. In this talk, the fundamental issues related to the difference between the direct and indirect methods are discussed first using phenomenological theory. Based on the dielectric, mechanical, and thermal properties of the ECM reported,

it is concluded that there are two critical issues that have not been considered in the current study and play an important role on the characterization of the ECM.

### 11:10 AM

#### (FMAs-049-2022) Role of Defect and Power Dissipation on Ferroelectric Memristive Switching

P. Roy<sup>\*2</sup>; D. Zhang<sup>1</sup>; S. Kunwar<sup>1</sup>; J. MacManus-Driscoll<sup>3</sup>; H. Wang<sup>4</sup>; Q. Jia<sup>2</sup>; A. Chen<sup>1</sup>

1. Los Alamos National Lab, USA
2. University at Buffalo, Materials Design and Innovation, USA
3. University of Cambridge, Dept. of Materials Science, United Kingdom
4. Purdue University, School of Materials Engineering, USA

Advancement of information technology requires low power, high speed, and large capacity non-volatile memory. Memristors have potential applications for not only information storage but also neuromorphic computation. Memristive devices have been mostly focused on the use of binary oxides as the resistive switching materials. On the other hand, polarization assisted memristive devices based on ternary ferroelectric oxides are attracting more attention due to their unique switching properties. However, the underlying switching mechanisms and the current-voltage rotation direction are still not fully understood yet. By comparing stoichiometric BaTiO<sub>3</sub>, BiFeO<sub>3</sub> and Bi<sub>1-x</sub>FeO<sub>3-δ</sub> ferroelectric memristors with different cation stoichiometry, we found that off-stoichiometry-induced traps can play a critical role in controlling the ferroelectric memristive switching behavior. Ferroelectrics with slight off-stoichiometry show greatly enhanced switching properties, and here the switching on/off ratio is mainly determined by the trap energy levels and concentrations. The rotation direction of current-voltage hysteresis loop is directly affected by the defects, which can be controlled by synthesis and power dissipation. These findings provide insight in understanding the role of defects in ferroelectric memristors and offer guidance to design ferroelectric memristors with enhanced performance.

### 11:30 AM

#### (FMAs-050-2022) BiFeO<sub>3</sub>-Based Ferroelectric Perovskites: Potential for Multifunctional Photovoltaic Applications

V. F. Freitas<sup>\*1</sup>; E. A. Astrath<sup>2</sup>; L. C. Dias<sup>1</sup>; M. Mazur<sup>1</sup>; T. G. Bonadio<sup>1</sup>; D. M. Silva<sup>3</sup>; G. S. Dias<sup>4</sup>; L. F. Cótica<sup>4</sup>; I. A. Santos<sup>5</sup>

1. Universidade Estadual do Centro-Oeste - Unicentro, Physics, Brazil
2. Federal Institute of Paraná, Campus Paranavai, Brazil
3. State university of Maringá, Physics, Brazil
4. State University of Maringá, Department of Physics, Brazil
5. State University of Maringá, Physics, Brazil

The multifunctional multiferroic BiFeO<sub>3</sub> and 0.6BiFeO<sub>3</sub>-0.4PbTiO<sub>3</sub> (BFPT) thin films are presented as an interesting alternative for multifunctional photovoltaic applications. These films were used as active layers in a heterostructured photovoltaic arrangement and its good electrical responses to white light illumination to prove their photovoltaic behavior. Electron-hole pair recombination control mechanisms have been associated with ferroelectric domain walls and a qualitative conceptual model of this mechanism was developed to try to understand it. Known multifunctional properties of these compounds, such as ferroelectricity, piezoelectricity, weak and antiferromagnetism, magnetoelectric coupling, among others, have been speculated to be associated with their recently investigated photovoltaic property for multifunctional and multipurpose applications in smart devices. The chemically and structurally stability of these compounds at high temperatures, as the thermal stability of the magnetic and ferroelectric properties, gives them good reliability to work under difficult operating conditions, such as sunlight radiation. Nanostructured single-phased thin films were processed and their electric, dielectric, structural, optics and photovoltaic properties were characterized in this work and the results indicate high potential to photovoltaic applications.

**11:50 AM - WITHDRAWN****(FMAs-051-2022) Electrocaloric effect in  $(\text{Na}_{0.5}\text{Bi}_{0.5})\text{TiO}_3$  -  $\text{BaTiO}_3$  -  $\text{Bi}(\text{Mg}_{0.5}\text{Ti}_{0.5})\text{O}_3$  relaxor ceramics**V. V. Shvartsman<sup>\*1</sup>; S. M. Fathabad<sup>1</sup>; D. C. Lupascu<sup>3</sup>; E. Politova<sup>2</sup>

1. University of Duisburg-Essen, Institute for Materials Science, Germany
2. Semenov Federal Research Center for Chemical Physics, Russian Academy of Sciences, Russian Federation
3. University of Duisburg-Essen, Institute for Materials Science, Germany

Colling technology based on the electrocaloric effect (ECE) has generated considerable interest as an environmentally-friendly alternative to classical gas-compression based refrigerators and air-conditioners. The electrocaloric effect consists in a change in the lattice entropy (temperature), which compensates for the variation in polar entropy caused by an external electric field. Therefore, materials with inherent polar disorder, such as relaxor ferroelectrics, are considered promising for achieving large values of the ECE. In this work, we report on direct and indirect measurements of the electrocaloric effect in  $(y-1)[x\text{BaTiO}_3 - (1-x)(\text{Na}_{0.5}\text{Bi}_{0.5})\text{TiO}_3] - y\text{Bi}(\text{Mg}_{0.5}\text{Ti}_{0.5})\text{O}_3$  (BT-NBT-BMT),  $x = 0.5, 0.1, 0.2$ , and  $y = 0, 0.1, 0.2$ . Ceramic samples were prepared using the solid-state synthesis method. The effect of the BMT additive on the ferroelectric and electrocaloric properties has been studied. We have found that the addition of BMT in NBT-BT compositions promotes antiferroelectric relaxor behavior characterized by double slim hysteresis loops. The polarization hysteresis loops measured at different temperatures were used to indirectly estimate the ECE based on the Maxwell relation. Direct investigation of the electrocaloric effect was conducted using a quasi-adiabatic calorimeter. The effect of the crossover from ferroelectric to antiferroelectric relaxor behavior on the ECE is discussed.

**Ferroics and Multiferroics II**

Room: Star Bay 3 (Level B)

Session Chair: Hathaikarn Manuspiya, Chulalongkorn University

**8:30 AM****(FMAs-056-2022) Investigations on PZT-PFN - A Room Temperature Nanoscale Multiferroic Prepared by PLD Technique (Invited)**R. Katiyar<sup>\*1</sup>; K. Mishra<sup>1</sup>

1. University of Puerto Rico, USA

Highly (001) oriented  $0.7\text{Pb}(\text{Zr}_{0.52}\text{Ti}_{0.48})\text{O}_3$ - $0.3\text{Pb}(\text{Fe}_{0.5}\text{Nb}_{0.5})\text{O}_3$  (0.7PZT-0.3PFN) multiferroic thin films were deposited on LSMO buffer layer on LSAT (001) substrate in oxygen atmosphere employing pulse laser deposition technique. The 0.7PZT-0.3PFN films were found to grow in a tetragonal phase with orientation along (001) plane as evident from the x-ray diffractometry analysis. The temperature dependent dielectric measurements (80-750 K) on the metal-ferroelectric-metal heterostructure capacitors in the frequency range of  $10^2$ - $10^6$  Hz exhibited a diffused dielectric maximum of  $\sim 2200$  over a wide range of temperature from 400-700 K. The well saturated slim polarization hysteresis loop of the thin film capacitors suggests nano-scale ferroelectric ordering (relaxor type) in these films. The ferroelectric-piezoelectric nature of the films was confirmed from a strong domain switching response revealed from PFM studies. A saturated magnetization loop utilizing PPMS was observed. The magnetization studies involving zero field cool and field cool magnetization curves down to 4 K indicated an irreversible magnetic ordering in these films. human body to measure glucose level in Direct evidence of robust magneto-electric coupling in thin films was obtained from the magneto-electric studies (M-E coefficient) at room temperature. These results suggest that our films are magnetoelectric multiferroic at room temperature.

**9:00 AM****(FMAs-053-2022) Enhanced Thermoelectric Performance in La And Nb Co-doped  $\text{SrTiO}_3$  Composite Using Graphite as a Momentum Booster**S. S. Jana<sup>\*1</sup>; T. Maiti<sup>2</sup>

1. IIT Kanpur, Material Science and Engineering, India
2. IIT Kanpur, Dept. of Materials Science & Engineering, India

Thermoelectric power generation from waste heat energy is evolving as one of the promising renewable energy sources in this current era of energy and environmental challenges. Thermoelectric generator (TEG) has capability of converting heat energy into electricity without any carbon foot print. However, implication of thermoelectric device is limited by their poor performance as well as poor temperature stability. In our work, we have fabricated graphite composite with La and Nb co-doped  $\text{SrTiO}_3$  (LSTN). Graphite acts as a momentum booster in LSTN matrix causing an order of magnitude increase in weighted mobility which otherwise suffers from Anderson localization of electrons. Accordingly, more than 6 times increment in power factor is found after graphite incorporation. Lattice thermal conductivity in graphite composite is simultaneously suppressed due to enhanced level of Umklapp scattering as confirmed by Debye-Callaway fitting. As a result, maximum ZT of 0.68 has been obtained in LSTN+G composite at 980K which is around 423% larger value than that of pristine LSTN. Finally, we have also constructed a 4-legged TEG device in uni-leg configuration where we have achieved milli-watt (2.5 mW) level of power output. This remarkable power output is unattainable up until now in the context of oxide thermoelectrics.

**9:20 AM****(FMAs-054-2022) Revisiting the origin of defects and their relationship to the electrical properties of  $\text{BiFeO}_3$  thin films**E. B. Araujo<sup>\*1</sup>. **WITHDRAWN**

1. São Paulo State University, Physics and Chemistry, Brazil

The bismuth ferrite ( $\text{BiFeO}_3$ ) is a canonical multiferroic characterized by a coexistence of the antiferromagnetic ( $T_N \sim 643$  K) and ferroelectric ( $T_C = 1103$  K) phases at room temperature and by superior ferroelectric properties with a giant remanent polarization. The  $\text{BiFeO}_3$  has been considered in the past years a promising material for the next generation of microelectronic devices such as ferroelectric random-access memory, multistate memories, and others. Unfortunately, a large leakage current often observed in  $\text{BiFeO}_3$  thin films has been a significant obstacle limiting their practical applications. Controversies on its conductivity mechanisms and different results reported in the literature suggest an intrinsic relationship with difficulties of preparing single phase  $\text{BiFeO}_3$ , independently of the method for the synthesis. In practice, obtaining monophasic  $\text{BiFeO}_3$  free from chemical defects proved to be a challenging job. In my talk, I will revisit the origin of defects in  $\text{BiFeO}_3$  thin films prepared by the chemical solution route, the possible influence of secondary phases, non-stoichiometry, and its implications on their leakage current densities. Finally, the origin of different results observed in the literature will also be discussed and compared with recent results of  $\text{BiFeO}_3$  thin films.

9:40 AM

## (FMAs-055-2022) Apatite Growth Induced by Electric Field in Bioferroelectric PVDF/BCP composite

T. G. Bonadio<sup>\*1</sup>; J. M. Rosso<sup>2</sup>; G. B. Souza<sup>2</sup>; L. M. Silva<sup>2</sup>; D. M. Silva<sup>2</sup>; V. F. Freitas<sup>1</sup>; W. R. Weinand<sup>2</sup>; I. A. Santos<sup>2</sup>

1. Midwestern Parana State University, Brazil
2. State University of Maringa, Physics, Brazil

The discovery of new biological effects related to endogenous and external electric currents and fields in tissue regeneration has been helping to understand the physical mechanisms that govern the behavior of the living organism. In fact, the possibility of using external stimuli to accelerate bone regeneration processes, for example, has inspired the development of some "fourth generation biomaterials" capable of mimicking electrical properties and micro-environments in living tissues. In this work, we use an external alternating electric field to stimulate bonelike apatite formation on a bioferroelectric composite of PVDF and biphasic calcium phosphate (BCP). The PVDF/BCP composite was immersed in a simulated body fluid with and without the presence of an alternating electric field. The composite surface after immersion was evaluated by ATR/FTIR, XRD and SEM. The results have shown that the apatite was formed in both samples (with and without the electric field) but the apatite formation occur in less time with the application of the electric field. In conclusion, the observations of this work have shown that PVDF/BCP composite is a promising candidate for bone replacements and the synthetic bone growth can be accelerated by an alternating electric field. The authors would like to thank Fundação Araucária for their financial support in participating in this event.

10:20 AM

## (FMAs-057-2022) Review on Piezoelectric Ultrasonic Motors (2015-2020) and Perspectives from Industry 4.0 (Invited)

T. Xu<sup>\*1</sup>

1. Old Dominion University, Mechanical and Aerospace Engineering, USA

This paper gives a comprehensive review on piezoelectric ultrasonic motors (USM) developments during recently 5 years (2015-2020). First the review paper will provide the following summaries: i) the summary of number of publications in each research areas of USM in the years of 2015-2020; ii) the summary of number of publications per year on USM from 2015 to 2020; iii) the summary of USM publication numbers of author's country and region distribution; and iv) the summary of USM publication numbers in the top ten journals. Secondly, the paper will discuss the basic principles of USMs and the piezoelectric ceramic materials are used on various USMs. Thirdly, the paper will highlight the most advantages and disadvantages of new designs. Finally, this paper will discuss the current contributions of USMs on Industry 4.0 and the perspectives from the industry 4.0 for USMs future developments.

10:40 AM

## (FMAs-058-2022) Structural and magnetic properties of BiFeO<sub>3</sub> doped ceramics sintered under extreme conditions

R. C. Oliveira<sup>\*1</sup>; G. S. Dias<sup>2</sup>; I. A. Santos<sup>3</sup>; M. Melo<sup>2</sup>; E. a. Volnistem<sup>1</sup>; S. J. Süllo<sup>4</sup>; F. J. Littest<sup>4</sup>; D. J. Baabe<sup>5</sup>

1. State University of Maringá, PFI, Brazil
2. State University of Maringa, Department of Physics, Brazil
3. State University of Maringa, Physics, Brazil
4. Technische Universität Braunschweig, Institut für Physik der Kondensierten Materie, Germany
5. TU Braunschweig, Institut für Anorganische und Analytische Chemie, Germany

At room temperature, the BiFeO<sub>3</sub> (BFO), is a type-G antiferromagnetic material with a cycloidal spin structure. To enhance the magnetic properties one can disturb this cycloidal structure by a couple of means, e.g. by promoting nano-structuration to sizes smaller than the cycloid correlation length (~64 nm), by introducing

defects in the lattice, by atomic substitution or most probably by a combination of these. By producing La doped BFO ceramics by non-thermodynamically stable routes, such as cryo-milling and spark plasma sintering it is possible to obtain dense and phase-pure ceramics with improved magnetic and dielectric properties. In this work we produced pure and La, Er, Nd and Sc doped BFO ceramics and performed its structural, by XRD and Mössbauer spectroscopy, and magnetic characterizations. We intend to correlate the changes of its magnetic properties with its structural ones in a threefold manner, i) being the introduction of high values of micro-strain, generated by the atomic substitution and the synthesis route, ii) the second one being the breakage/suppression of the cycloidal structure, and iii) due to the magnetic character of the doping atom.

11:00 AM

## (FMAs-059-2022) Improving the photocatalytic degradation of organic dyes by the formation of BiFeO<sub>3</sub>/Fe<sub>2</sub>O<sub>3</sub> nanointerfaces

G. S. Dias<sup>\*1</sup>; E. a. Volnistem<sup>1</sup>; R. D. Bini<sup>1</sup>; D. M. Silva<sup>1</sup>; J. M. Rosso<sup>1</sup>; L. F. Cótica<sup>1</sup>; I. A. Santos<sup>1</sup>

1. State University of Maringa, Department of Physics, Brazil

Tons of different types of organic textile dyes are discarded annually in water bodies, harming aquatic life. In this sense, many methods, such as bioremediation and physical-chemical approaches, have been studied to detoxify wastewaters. Among them, heterogeneous photocatalysis solid materials has been used in the oxidation of contaminants by transducing light energy into electrical and chemical ones. In this context, synthesis of efficient catalysts is necessary since the demand of fast effluent treatments has been intensifying. The photo-active properties of BiFeO<sub>3</sub> (BFO) have been investigated for solar cells, water splitting and photocatalysts applications. Its ferroelectric properties, which reduce the recombination of electron-holes, allied to its band gap (~2.1eV), make BFO an excellent candidate for visible light-driven photocatalysis. In addition, composites make it possible to tune the band gap and the Fermi level at interfaces, facilitating the charge separation, preventing its recombination. In this sense, we proposed the synthesis of magnetic recoverable BFO/Fe O nanocomposites via high energy ball milling. The modification of the band structure and the work function under visible light was confirmed by KFM microscopy characterizations and the photocatalytic tests presented an expressive reduction of time degradation. The results will be discussed in detail.

11:20 AM

## (FMAs-060-2022) Processing of zinc oxide using a reactive inkjet printing technique

S. Garnsey<sup>\*1</sup>; A. S. Bhalla<sup>1</sup>; R. Guo<sup>1</sup>

1. University of Texas, San Antonio, USA

Zinc Oxide (ZnO) is a material with decades of investigation and use in coatings, biochemistry, and electronics. In the 1950s, ZnO was found to exhibit a piezoelectric effect among other favorable optoelectronic properties (wide bandgap semiconducting behavior, optical transparency, and photoluminescence) and has since been used as a piezoelectric element in conventional electronics. The rise of additive manufacturing and printed electronics has seen increased interest in ZnO as a versatile feed material for 3D-printed electronics. If realized, zinc oxide could play an important role as a multi-functional electronic material whose properties can be tuned via in-situ processing conditions to achieve desirable behavior. Within this study, a ZnO precursor, Zinc Acetylacetonate Dihydrate, is formulated into an inkjet-printable ink using a methodology based around Hansen Solubility Parameter (HSP). Processing conditions of the printed film such as ink film thickness, UV and IR radiation, and substrate heating are investigated to yield in-situ morphological control. Characterization of print film morphological, electromechanical, and dielectric properties is conducted. This work has been supported by the U.S. Office of Naval Research grant.

Thursday, July 28, 2022

## Ferroelectrics Meeting of Americas

### Design, Synthesis and Fabrication

Room: Star Bay 3 (Level B)

Session Chair: Tanmoy Maiti, IIT Kanpur

8:30 AM

#### (FMAs-061-2022) Tailoring the electromechanical coupling in stretchable inorganic thin-film electronics (Invited)

Y. Lin<sup>\*1</sup>

1. University of Electronic Science and Technology of China, School of Materials and Energy, China

Flexible and stretchable electronics play an increasingly important role in the emerging electronic field since they can keep stable and durable with large deformation thus expand the applications. Especially, flexible and stretchable inorganic thin-film electronics have attracted lots of attention due to the excellent electrical/optical performance of inorganic functional materials. However, stable strategy to render flexibility while maintaining excellent performance of inorganic thin films is the most demanding and challenging both for academic and industrial communities. Electromechanical coupling is believed to be one of the key factors to achieve flexible and stretchable electronics with desired performance. In this report, we will present our research on how to achieve flexible and stretchable devices based on inorganic materials such as inorganic ferroelectrics, semiconductors and other oxide thin films. Manipulation of the electromechanical coupling in these flexible and stretchable inorganic thin film devices will be demonstrated via the design of materials, geometric structures and interface coupling.

9:00 AM

#### (FMAs-062-2022) Fabrication and evaluation of 3D printed strain gauge sensor

W. Dipon<sup>\*1</sup>; S. Garnsey<sup>1</sup>; A. S. Bhalla<sup>1</sup>; R. Guo<sup>1</sup>

1. University of Texas at San Antonio, Electrical and Computer Engineering, USA

The prevailing use of Internet-of-Things (IoT) and sensing technologies have facilitated advanced research on the fabrication of sensors for various applications. As the demand for sensor technology continues to rise, there is also an increased need for fabrication methods that are inexpensive and fit-for-use. Most conventional fabrication methods are not adaptive to rapid design and materials change. Strain gauge sensors play a vital role in monitoring subtle mechanical deformations in rigid bodies. Additive manufacturing techniques can be utilized to easily prototype sensors that fit the application's specific geometric and material needs. Also, modifications of design in terms of both shape and substrate can be implemented and tested using rapid prototyping. Within this study, the performance of inkjet printed meandering-line strain gauge sensors is investigated. A custom-designed prototype setup for stress sensing under an MTS Acumen 3 electrodynamic testing platform was used to characterize and validate the functionality of the fabricated sensors. A design of experiments (DoE) was developed wherein the parameters of line width, thickness, and shape were varied and their impact on performance is analyzed. Finite-element modeling in COMSOL is used to validate the obtained results. This work has been supported by grants from the U.S. Department of Energy and U.S. Office of Naval Research.

9:20 AM

#### (FMAs-063-2022) Edge dislocation in BiFeO<sub>3</sub> nanoparticles: Magnetism and Mossbauer effects

E. a. Volnistem<sup>\*1</sup>; R. C. Oliveira<sup>1</sup>; G. S. Dias<sup>2</sup>; M. Melo<sup>1</sup>; L. F. Cótica<sup>1</sup>; F. J. Littest<sup>4</sup>; S. J. Süllow<sup>4</sup>; D. J. Baabe<sup>5</sup>; I. A. Santos<sup>3</sup>

1. State University of Maringá, Department of Physics, Brazil
2. State University of Maringá, Department of Physics, Brazil
3. State University of Maringá, Physics, Brazil
4. TU Braunschweig, Institut für Physik der Kondensierten Materie, Germany
5. TU Braunschweig, Institut für Anorganische und Analytische Chemie, Germany

Bismuth ferrite (BFO) is a perovskite structured multiferroic magnetoelectric material (ABO<sub>3</sub>) that, due to its simultaneous ferroelectric and antiferromagnetic ordering at room temperature, is one of the most promising potential candidates for applications in electronics. Edge dislocations, can affect functional properties in many multifunctional materials. In this study, we applied the cryomilling (CM) to obtain BFO nanoparticles for the controlled introduction of dislocation density besides controlling its crystallite size. Structural analysis estimated the average crystallite size is reduced from 106 to 23 nm and the dislocation density reaches  $1.7 \times 10^{13} \text{ cm}^{-2}$ , revealing that the CM promotes both the nanostructuring of the samples accompanied by the introduction of atomic defects such as edge dislocations. Such results were correlated with those obtained by magnetic measurements (VSM, FC-ZFC and Mossbauer spectroscopy). A change on the magnetic hysteresis loops from a ferromagnetic-like behavior to a coexistent weak-ferromagnetic besides superparamagnetic contribution were verified. Mossbauer results revealed the superparamagnetism from tiny particles and suggest a strongly distorted structure caused by the strain. The correlation between the decrease in crystallite sizes and the increase of dislocation density, besides possible mechanisms involved in these changes are discussed in detail.

9:40 AM

#### (FMAs-064-2022) Fabrication of a pressure sensor using inkjet printed metal-organic frameworks and interdigitated electrodes

M. Duong<sup>\*1</sup>; A. S. Bhalla<sup>1</sup>; R. Guo<sup>1</sup>

1. The University of Texas at San Antonio, USA

Metal-organic frameworks (MOFs) have emerged as a class of promising materials since its discovery in the 1990s. The synthetic material has generated much interest and has a broad array of applications including sensing, drug delivery, and catalysis due to their tunable structure, polymeric composition, porosity, functionality, and biocompatibility. MOF UiO-66 (Hf) has been researched more closely due to its extraordinary properties and superior stability as well as its exhibited piezoelectric and ferroelectric responses. The advancement of additive manufacturing technology and printed electronics has facilitated various experimental approaches in the ongoing study of MOFs. While the integration of 3D printed technology for MOFs is relatively new, there have been studies accomplished such as a stretchable in situ grown MOF hydrogel composite using MOF HKUST-1 by direct ink writing and thin films using MOF-525 by inkjet deposition. For this study, a MOF UiO-66 (Hf) functional ink and interdigitated electrodes fabricated through inkjet deposition are examined to develop a flexible, biocompatible sensor. This study aims to evaluate the piezoelectric and ferroelectric properties of the MOF material, as well as enhanced sensitivity and detection by incorporating interdigitated electrode technology. This work has been supported by the Office of Naval Research grant, US.

**10:20 AM**

**(FMAs-065-2022) Multi-ferritic CFO/BTO Core-shell Nanocomposite Films fabricated via Inkjet Printing for Wireless Sensing Applications**

P. Flynn<sup>\*1</sup>; R. Guo<sup>1</sup>; A. S. Bhalla<sup>1</sup>

1. The University of Texas at San Antonio, USA

Multi-ferritic materials exhibit more than one primary ferroic properties in the same phase. These materials show promise for applications in sensors, actuators, switches, memory devices as well as medical diagnostics, therapeutics, and drug delivery. Inkjet printing is a direct-write deposition technology capable of fabricating structures under ambient conditions without masking, etching, etc. In this work, multi-ferritic films of core-shell cobalt ferrite/barium titanate nanoparticles are fabricated via inkjet printing. The development of stable ink formulations and ideal processing parameters is explored. Printed films are characterized by x-ray diffraction, optical, scanning electron, and atomic force microscopy. The dielectric and magneto-electric properties are also evaluated. Applications of these films for wireless sensing and communication are discussed.

**10:40 AM**

**(FMAs-066-2022) Smart Tooth to Measure Glucose Level for Diabetic Patient Using Piezoelectric**

J. Parsi<sup>\*1</sup>; N. Namakforoosh<sup>1</sup>; P. Morton<sup>1</sup>; A. S. Bhalla<sup>1</sup>; C. Qian<sup>1</sup>; R. Guo<sup>1</sup>

1. University of Texas, San Antonio, ECE Dept., USA

There have been many decades of search to utilize some external part of the human body to measure glucose level in a non-invasive painless way for diabetic patients. The utilized methods are human epithelial by means of interstitial fluid, human cornea of eyes, oral cavity and saliva and to a lesser extent human sweat. We have explored human molar tooth more specifically the pulp of the molar tooth to measure glucose levels. In this approach we used both piezoelectric and photodiode sensors using Near Infrared light in the photoacoustic and optical techniques respectively to characterize glucose levels. We show here that utilizing these sensors in a flexible circuitry in a crown seated on top of the tooth, it is possible to quantify glucose concentrations in blood. We have demonstrated using distilled water, different concentrations of glucose in the water, milk and bovine blood that glucose concentrations can be possibly measured with predicably higher accuracy.

# Author Index

\* Denotes Presenter

<b>A</b>	
A Jiménez, J. . . . .	19
Abdul Rajak, M. . . . .	24
Achary, S. N. . . . .	8
Acharya, M. . . . .	58
Acosta, C.* . . . .	36
Aepuru, R. . . . .	17, 19
Aepuru, R.* . . . .	19
Affatigato, M. . . . .	25
Aguirre, I.* . . . .	44
Aguirre, M. . . . .	52
Agulló-Rueda, F. . . . .	53
Aitken, B. . . . .	37
Akiyama, T. . . . .	31
Albino, F. T. . . . .	60
Alexandre Falcão, E. . . . .	55
Almeida Silva, A. . . . .	53
Ambrosi, A. . . . .	42
Anayee, M. . . . .	10
Andreeta, M. R. . . . .	53
Anthony, V. . . . .	38
Antonelli, E. . . . .	19
Aparecido dos Santos Mariano, M.* . . . .	56
Apblett, A.* . . . .	62, 63
Aqueveque, P. . . . .	19
Arango-Ospina, M.* . . . .	60
Araujo, E. B. . . . .	36, 58
Araujo, E. B.* . . . .	67
Aredes, R. G.* . . . .	19
Arnold, B. R. . . . .	34, 47
Arshad, S. E. . . . .	24
Arunachalam, A.* . . . .	38
Aslla Quispe, A.* . . . .	58
Astrath, E. A. . . . .	66
Auciello, O. . . . .	27
Aurélio de Oliveira, M. . . . .	48
<b>B</b>	
B, K. . . . .	19
B, V. . . . .	27
Baabe, D. J. . . . .	68, 69
Badillo, F. A. . . . .	53, 55
Bailin, C. L.* . . . .	33
Balazsi, C. . . . .	8, 26
Balazsi, C.* . . . .	40
Balazsi, K. . . . .	26, 40
Balázsi, K. . . . .	8
Balderson, L. . . . .	42
Balmori, H.* . . . .	29
Banerjee, R.* . . . .	57
Barolin, S. . . . .	52
Barua, R.* . . . .	42
Basler, G. . . . .	38
Baudin, C.* . . . .	11
Bedolla-Valdez, Z. . . . .	21
Ben Zine, H. R. . . . .	26
Benavides, V. . . . .	32
Benavidez, E.* . . . .	11, 12
Bergmann, F.* . . . .	9
Bernard, S.* . . . .	14
Beron, F. . . . .	19
Betancur Granados, N. . . . .	61
Betancur-Granados, N. . . . .	23, 48
Betancur-Granados, N.* . . . .	23, 45, 61
Bhalla, A. S. . . . .	15, 36, 47, 48, 49, 50, 51, 55, 68, 69, 70
Bhattarai, M.* . . . .	46
Bingham, P. A. . . . .	62
Bini, R. D. . . . .	68
Bisulca, C. . . . .	31, 33
Bisulca, C.* . . . .	33
<b>C</b>	
Boccaccini, A. R. . . . .	60
Boccaccini, A. R.* . . . .	59
Boiko, V. . . . .	13
Bolaños Rivera, J. O. . . . .	25
Bonadio, T. G. . . . .	20, 66
Bonadio, T. G.* . . . .	68
Bonini, R. P. . . . .	47
Bordia, R. . . . .	22, 29, 39, 40
Borja-Urby, R. . . . .	28
Boschilia, R. J. . . . .	19
Bosworth, B. . . . .	9
Boussard-Pledel, C. . . . .	25
Bram, M.* . . . .	29
Brandaleze, E. . . . .	12
Braun, M.* . . . .	7
Brazhkin, V.* . . . .	10
Brennecka, G. L. . . . .	64
Burato, J. . . . .	20
Bureau, B. . . . .	25
Butt, D. P.* . . . .	7
<b>C</b>	
C Denardin, J. . . . .	19
Cabrera, M. . . . .	21
Cai, R. . . . .	41
Caicedo Roque, J. . . . .	52
Calderón Piñar, F. . . . .	49
Calvo, W. A. . . . .	24
Camacho Montes, H. . . . .	23
Camacho Montes, H.* . . . .	22, 39
Camerucci, M. A. . . . .	25
Cardoza, A.* . . . .	60
Carlos Hernandes, A. . . . .	48
Carlos Iglesias Jaime, A. . . . .	49
Carvajal Contreras, D. R.* . . . .	32
Carvalho da Silva, A. . . . .	48, 54, 55
Carvalho de Lima, E. . . . .	56
Carvalho, R. A.* . . . .	55
Castillo, I. W. . . . .	45
Castro, C. P. . . . .	50
Castro, M. . . . .	17
Castro, R.* . . . .	10
Catellani, I. B. . . . .	15
Catellani, I. B.* . . . .	20
Cavallieri, F. . . . .	17
Cebulski, J. . . . .	25
Cedillo-González, E. I. . . . .	25
Celierer, S. . . . .	30
Certuche Arenas, C. S. . . . .	25
Cesarino, V. . . . .	14
Chaney, H. . . . .	9
Charoensuk, S. . . . .	50
Chedzoy, I. . . . .	45, 48
Chen, A. . . . .	66
Chen, A.* . . . .	46
Chen, C. . . . .	57, 66
Chen, C.* . . . .	65
Chen, V. J. . . . .	32
Chen, X.* . . . .	45
Chen, Y. . . . .	27
Chen, Y.* . . . .	57
Cheng, Z.* . . . .	35, 66
Chica, E. . . . .	18
Ching, E. A. . . . .	55
Ching, E. A.* . . . .	53, 54
Cho, Y.* . . . .	9
Choa, F. . . . .	34, 47
Chodisetti, S.* . . . .	27
Choi, H. . . . .	41
Chotiradsirikun, S.* . . . .	49
Choudhary, R.* . . . .	49
<b>D</b>	
Colorado L., H. A. . . . .	17, 18, 38, 54, 60
Colorado L., H. A.* . . . .	63
Colsmann, A. . . . .	7
Columba, H. L. . . . .	64
Conceição, C. . . . .	29
Conner, R. L. . . . .	13
Contreras, D. . . . .	32
Correa, M. . . . .	37
Correr, G. I.* . . . .	53
Cótica, L. F. . . . .	16, 20, 51, 52, 54, 65, 66, 68, 69
Cótica, L. F.* . . . .	15
Cristina Oliveira Silva, M. . . . .	48
Cruvinel de Oliveira, R. . . . .	53
Cruz Yupanqui, G. . . . .	58
Cullum, B. . . . .	34, 47
<b>D</b>	
da Silva, K. L. . . . .	52
Dahon, N. . . . .	24
Dai, Z. . . . .	13
Das, S. . . . .	9
Davenport, P. . . . .	38
Davila Espinosa, L. F.* . . . .	54
De Armas, Y. . . . .	21
De Giovanni Rodrigues, A. . . . .	56
de Godoy, M. P. . . . .	53
de los Santos Guerra, J. . . . .	36, 54, 55, 56, 58
de los Santos Guerra, J.* . . . .	48, 49, 53, 55, 57
De Noni Junior, A. . . . .	29
De Obaldía, E. . . . .	53, 54, 55
De Obaldía, E.* . . . .	27
Delgado Salido, A. . . . .	22
Delgado, J. C.* . . . .	21
Deluque Toro, C. E. . . . .	20, 21, 26, 52
Deróide, H. d. . . . .	52
Dey, M. . . . .	41
Dey, M.* . . . .	42
Dey, S.* . . . .	37
Di Luccio, M. . . . .	42
Di Marco, M.* . . . .	56
Dias, G. S. . . . .	15, 20, 51, 52, 54, 66, 68, 69
Dias, G. S.* . . . .	65, 68
Dias, L. C. . . . .	66
Dierolf, V. . . . .	37, 64
Difeo, M. C.* . . . .	17
Dipon, W.* . . . .	69
Dixit, P.* . . . .	57
Dulanto, J. . . . .	44
Duong, M.* . . . .	69
Durango Duarte, J. . . . .	61
Dutra Zanotto, E.* . . . .	7
Dwivedi, A. . . . .	58
<b>E</b>	
Eduardo García García, J. . . . .	54
Eiras, J. A. . . . .	16, 47, 51
Eiras, J. A.* . . . .	36
Eleuterio, R. V.* . . . .	60
Elnobi, S. . . . .	31
Espinosa Almeyda, Y. . . . .	39
Espinoza Ochoa, I. M. . . . .	22, 23, 39
Espinoza Ochoa, I. M.* . . . .	22
Estrada Contreras, V. . . . .	26
Estrada, F. R. . . . .	48
Estrada, F. R.* . . . .	16
<b>F</b>	
Fabian, M. . . . .	52
Fahrenheitz, W. . . . .	38
Fajardo, S. . . . .	32
Farias, A. M. . . . .	52

# Author Index

Fathabad, S. M. ....	67	Gupta, S. ....	26, 41, 42	Ji, W. ....	41
Fernández García, A. ....	53	Gupta, S.* ....	63	Jia, Q. ....	66
Ferraris, M. ....	27	Gutiérrez-Campos, D. ....	12	Jiang, J.* ....	66
Ferreira Gomes do Monte, A. ....	48	Gutiérrez-Campos, D. ....	25	Jones, A. H. ....	62
Ferreira, E.* ....	14	Gutiérrez-Campos, D.* ....	24		
Figgemeier, E. ....	30	Guzman-Verri, G. G.* ....	15		
Figueroa Arteaga, M. E. ....	54			<b>K</b>	
Finsterbusch, M. ....	27, 30	<b>H</b>		K. ....	34, 46
Fiore, S. ....	28	Habrioux, A. ....	30	Kadossov, E. ....	63
Fiorilli, S.* ....	28	Hagerstrom, A. ....	9	Kaghazchi, P. ....	37
Fleming, H. ....	33	Haghipour, N. ....	32	Kaou, M. H.* ....	26
Florez Tirado, M. J. ....	61	Haines, L. ....	33	Kar, B.* ....	50
Flynn, P.* ....	70	Hasegawa, M. ....	9	Katiyar, R. ....	8, 37, 46
França, E. ....	62	Hasegawa, T. ....	14	Katiyar, R.* ....	45, 67
Franco Aguirre, F. F. ....	61	Hatfield, A. ....	65	Kawano, N.* ....	13
Freitas, V. F. ....	20, 52, 54, 68	Hathenher Toledo Rosa, T.* ....	55	Kelley, C. ....	63
Freitas, V. F.* ....	16, 66	Hayashi, Y.* ....	31	Kelly, L. R. ....	47
Fu, Z. ....	14, 41	He, Q.* ....	29	Kim, B. ....	40
Fuentes-Cobas, L. ....	28	Hegeüs, N.* ....	8	Kiminami, R. H. ....	50
Fuentes, J. ....	21	Hegeto, F. L. ....	52	Kindelmann, M. ....	29
Fukano Viana, D. ....	53	Held, T. ....	38	King, L. ....	33
Fukushima, M. ....	41, 62	Hemrick, J. G. ....	12	Kisailus, D.* ....	59
Fukushima, M.* ....	63	Hendriks, L. ....	32	Kita, K. ....	41
Furuya, Y.* ....	9	Henkin, J.* ....	43	Kitanaka, Y. ....	15
		Herrera Carrillo, A. ....	54	Kitzel, P. ....	63
<b>G</b>		Herrera-Perez, G. M. ....	23	Kondo, N. ....	41
G. Villora, E. ....	31	Herrera-Perez, G. M.* ....	28	Kovalenko, O.* ....	35
Galindo, R. R.* ....	32	Hilmas, G. ....	38, 64	Kumar, P. ....	35, 46, 49, 50
Galliano, P. G. ....	24	Hinterstein, M. ....	7	Kumar, P.* ....	34
Gamboa, B.* ....	50	Hiroki Miwa, R. ....	58	Kunwar, S. ....	66
García Reyes, A. ....	22	Hmok, H. ....	21	Kuo, L.* ....	37
García, D. ....	16, 48, 50, 51, 53, 54	Hmok, H.* ....	21	Kurosawa, S.* ....	13
García, D. E. ....	29	Hoffmann, M. ....	7	Kutnjak, Z. ....	35
Garnsey, S. ....	69	Holden, A. ....	32		
Garnsey, S.* ....	68	Homberger, E. ....	33	<b>L</b>	
Gass, S. E. ....	24	Hossain, S.* ....	51	Ladonis, A. ....	10
Gaustad, G.* ....	65	Hosseini-Toudeshki, H. ....	28	Lagorio, Y. ....	11
Geetha, D. ....	9	Hotta, M. ....	41	Lakusta, M. ....	38
Geng, X. ....	40	Hotza, D. ....	39, 42, 60	Lam, T. ....	43
Geng, X.* ....	40	Hotza, D.* ....	29, 39	Lambert, J. B. ....	33
German, R. M. ....	39	Hoyos Montilla, A. A. ....	23, 61	Landínez Téllez, D. A. ....	20, 21, 26, 52
Gibbs, F. ....	17	Hreniak, D.* ....	13	Lapteva, A. M. ....	27
Gil Rebaza, A. V. ....	52	Hu, Y. ....	12	Lartundo, L. ....	22
Gil Rebaza, A. V.* ....	20	Huerta, E. H.* ....	32	Laura, L. ....	32
Gil Velasquez, D. ....	23	Huertas Pulido, L. ....	21	Leu, M. ....	38
Gil Velasquez, D.* ....	61	Hung Hung, Y. X.* ....	25	Li, D. ....	40
Giraldo Gamboa, P. A. ....	61			Li, J. ....	13, 40
Giraldo, C. H. ....	38	<b>I</b>		Li, Q. ....	29, 42
Gogotsi, Y.* ....	10	Ihrig, M.* ....	27	Liang, C. H. ....	15
Goldsbey, J. C.* ....	8	Iizuka, F.* ....	43	Lima, E. C.* ....	58
Golovchak, R. ....	25	Imhoff, L. ....	56	Lin, H.* ....	7
Gonçalves, A. M. ....	36	Imhoff, L.* ....	52	Lin, W. ....	31
Gonzalez, D. ....	23, 61	Iñáñez, J. G.* ....	43	Lin, Y. ....	37
Gorman, B. ....	64	Instan, A. A. ....	8	Lin, Y.* ....	69
Goski, D.* ....	11	Irassar, E. F. ....	12	Lipke, D.* ....	38, 64
Gracia Pinilla, M. ....	19	Isaza, A. E. ....	55	Littest, F. J. ....	68, 69
Gracia Reyes, A. ....	39	Iwamoto, Y. ....	30	Littlewood, P. ....	15, 16
Gracia-Pinilla, M. ....	17			Littlewood, P.* ....	7
Graczyk-Zajac, M. ....	30	<b>J</b>		Liu, C.* ....	12
Graeve, O. A. ....	11	Jackson, M. D.* ....	31	Liu, Y. ....	48
Graeve, O. A.* ....	28	Jacobsohn, L. G.* ....	13	Liu, Z. ....	14
Gregorova, E. ....	24, 29, 58	Jagota, A. ....	64	Lokanathan, M.* ....	17
Gregorova, E.* ....	24	Jain, H. ....	37	Londoño Badillo, F. A. ....	54
Grier, S. ....	38	Jain, H.* ....	64	Lopez-Bezanilla, A.* ....	16
Gualdi, A. J. ....	47	Jairo Roa-Rojas, J. A. ....	52	López-Juárez, R. ....	21
Gugar, N. ....	46	Jana, S. S.* ....	58, 67	López-Noda, R. ....	21
Gugar, N.* ....	35	Janssen, R. ....	39	Lopez, M. ....	32
Guilherme Flávio Dornelas, R.* ....	54	Jape, S. ....	38	Lowers, H. ....	43
Guillon, O. ....	18, 27, 29, 37	Jaramillo Palacio, J. ....	21	Loya Caraveo, H. M. ....	22
Guo, R. ....	15, 36, 47, 48, 49, 50, 51, 55, 68, 69, 70	Jaramillo, J. ....	32	Lu, K. ....	9
Guo, W. ....	29	Jesse, S. ....	37	Lu, K.* ....	10, 41
				Lupascu, D. C. ....	67

M	N	
M'Peko, J. . . . .	Najmi, F. . . . .	Placeres-Jiménez, R. . . . .
Ma, J. . . . .	Nakajima, T. . . . .	Plateau, T. . . . .
Ma, Q. . . . .	Nakamura, F. . . . .	Plaza, C. . . . .
Ma, Z. . . . .	Nakauchi, D. . . . .	Politova, E. . . . .
Maček Krzmann, M. . . . .	Nalandhiran, P.* . . . .	Portelles, J. . . . .
Machado, H. N.* . . . .	Namakforoosh, N. . . . .	Posada Henao, O. F.* . . . .
Machado, R. . . . .	Nanda, D. . . . .	Poster, B. . . . .
Mackenzie, G. . . . .	Narayan, R.* . . . .	Pradhan, D. K.* . . . .
Macková, L.* . . . .	Nascimento, A.* . . . .	Prakash, C. . . . .
MacManus-Driscoll, J. . . . .	Nejatpour, M.* . . . .	Prakash, C.* . . . .
Madrazo, B. M. . . . .	Neto, A. M. . . . .	Priya, S.* . . . .
Mahapatra, M.* . . . .	Neto, J. R. . . . .	Prokhorenko, O.* . . . .
Mahlovanji, B. . . . .	Neto, A.* . . . .	Protzek, O. A. . . . .
Maiti, S.* . . . .	Ning, K. . . . .	Pylypko, S. . . . .
Maiti, T. . . . .	Ning, K.* . . . .	
Maiti, T.* . . . .	Nino, J. C.* . . . .	<b>Q</b>
Majhi, M. . . . .	Nishihora, R. . . . .	Qian, C. . . . .
Mallmann, M. . . . .	Nolan, D. . . . .	Qian, F. . . . .
Mandal, K. . . . .	Nomoto, J. . . . .	
Mandal, K.* . . . .	Noyes, M. . . . .	<b>R</b>
Mangalaraja, R. V. . . . .	Nudd, S.* . . . .	Ragulya, A. . . . .
Manivasagam, G. . . . .	Nur, K. . . . .	Rahman, R. . . . .
Manso Silván, M. . . . .		Ramajo, L. . . . .
Manuspiya, H. . . . .	<b>O</b>	Ramesh, R. . . . .
Manuspiya, H.* . . . .	Ohji, T. . . . .	Ramirez-Rico, J.* . . . .
Manzani, D. . . . .	Ohji, T.* . . . .	Rao, P. . . . .
Manzani, D.* . . . .	Olevsky, E. . . . .	Raymond, O. . . . .
Markocsan, N.* . . . .	Olevsky, E.* . . . .	Rebellón, H.* . . . .
Marksz, E. . . . .	Oliveira Dantas, N. . . . .	Rednam, U. . . . .
Mars, E. M.* . . . .	Oliveira, A. L.* . . . .	Reedy, C. L.* . . . .
Marth, T. . . . .	Oliveira, J. . . . .	Reimanis, I.* . . . .
Martínez-Aguilar, E.* . . . .	Oliveira, O. G. . . . .	Ren, L. . . . .
Materer, N. . . . .	Oliveira, O. G.* . . . .	Rendon, J.* . . . .
Mathur, S.* . . . .	Oliveira, R. C. . . . .	Rengifo, M. . . . .
Mayo, C. J.* . . . .	Oliveira, R. C.* . . . .	Renshaw, J. . . . .
Mazur, M. . . . .	Olivera Castillo, A. F.* . . . .	Resio, L. C.* . . . .
McAnany, S. . . . .	Olmos, B. . . . .	Restrepo Lopez, S. . . . .
McGath, M. K.* . . . .	Olmos, B.* . . . .	Restrepo Tobón, S.* . . . .
McPherson, S. . . . .	Olugbade, E. . . . .	Restrepo, O. J. . . . .
Mehta, A. . . . .	Orloff, N. . . . .	Reyes-Montero, A. . . . .
Mehta, A.* . . . .	Ornelas-Gutierrez, C. . . . .	Reyes-Rojas, A. . . . .
Meletis, E. I. . . . .	Osada, M.* . . . .	Riapanitra, A. . . . .
Melo, M. . . . .	Ozeki, S. . . . .	Richardson, K. . . . .
Mendez González, Y. . . . .		Riedel, R.* . . . .
Mercy, C. . . . .	<b>P</b>	Roa-Rojas, J. . . . .
Merkey, E. K. . . . .	Pabst, W. . . . .	Roa-Rojas, J.* . . . .
Mesquita, R. A. . . . .	Pabst, W.* . . . .	Rockett, A. . . . .
Messaddeq, Y. . . . .	Palmer, S. . . . .	Rodas-Lima, E. . . . .
Michaelis, A.* . . . .	Pandey, R.* . . . .	Rodrigues, A. V.* . . . .
Milton, F. P. . . . .	Pandolfelli, V. C. . . . .	Roldán, M. . . . .
Miranda, H. S. . . . .	Panigrahi, S. . . . .	Rosas, B. Y.* . . . .
Miranda, H. S.* . . . .	Panneer Selvam, S. . . . .	Rosso, J. M. . . . .
Mishra, K. . . . .	Paraguay-Delgado, F. . . . .	Rosso, J. M.* . . . .
Mishra, K. K. . . . .	Paramee, S.* . . . .	Roy, P.* . . . .
Mishra, T. . . . .	Parida, A. . . . .	Rubio-Marcos, F. . . . .
Misture, S. T.* . . . .	Parida, A.* . . . .	Rubio, T. I. . . . .
Moliné, M. N. . . . .	Park, C. . . . .	Ruiz, Y. L. . . . .
Montes, L. H. . . . .	Park, J. . . . .	
Morais Ferreira, R. . . . .	Parsi, J.* . . . .	<b>S</b>
Moreira, C. P.* . . . .	Pedrochi, F. . . . .	Sabah, J. . . . .
Morel Escobar, M. . . . .	Peláiz Barranco, A. . . . .	Sachdev, S. . . . .
Morell, G. . . . .	Peláiz Barranco, A. . . . .	Saffirio, S. . . . .
Moreno Aldana, L. C. . . . .	Pellegrini, N. . . . .	Sahu, R. . . . .
Moreno Gobbi, A. . . . .	Pellegrino, V. . . . .	Saladino, M. . . . .
Morita, K. . . . .	Pellegrino, V.* . . . .	Salazar González, W.* . . . .
Morton, P. . . . .	Peng, F. . . . .	Salazar, L. C.* . . . .
Muccillo, E. N.* . . . .	Peng, F.* . . . .	Salgado-Ceballos, C.* . . . .
Muccillo, R.* . . . .	Perdomo, C. P. . . . .	Salvini, V. R.* . . . .
Mujib, S.* . . . .	Pérez Molina, J. J. . . . .	Salvo, M. . . . .
Mulinari, J.* . . . .	Pérez Molina, J. J.* . . . .	Sandino del Busto, J. W. . . . .
Muniz, R. F. . . . .	Perin, G. . . . .	Sandoval, M. L. . . . .
Muñoz Pulido, K.* . . . .	Pilgrim, S. M. . . . .	Santa-Rosa, W. . . . .
	Pitti, G. . . . .	Santarelli, M. . . . .

\*Denotes Presenter



# Author Index

Santiago-Blay, J. A. ....	33	Swain, S.* .....	49	Wang, H.* .....	14
Santiago, M. ....	56	Swamy, A. ....	17	Wang, W. ....	14, 29, 41
Santiago, R. T. ....	52			Wang, W.* .....	41
Santiso, J. ....	52	<b>T</b>		Watson, A. ....	54, 55
Santos, G. M. ....	20	Taborda Llano, I. ....	23, 61	Watts, J. ....	38
Santos, I. A. ....	15, 16, 20, 51, 52, 54, 56, 65, 66, 68, 69	Talou, M. H. ....	25	Wauters, V.* .....	44
Santos, I. A.* .....	47	Tanemura, M.* .....	31	Weber, F. E.* .....	59
Santos, M. F. ....	62	Tang, J. ....	40	Weinand, W. R. ....	56, 68
Sarkar, S. ....	40	Teixeira, M. H.* .....	39	Wie-Addo, G.* .....	62
Sato, F. ....	56	Téllez Arias, M. G.* .....	22	Wiff, J.* .....	15
Saxena, A.* .....	35	Tellez-Jurado, L. ....	29	Wolf, S. E.* .....	59
Schiavi, I. ....	28	Terrés, E. ....	22	Wu, J.* .....	35
Schulze, W. A. ....	17, 45, 48	Thandapani, P.* .....	19		
Senff, L. ....	60	Thangaraj, P.* .....	19	<b>X</b>	
Shaikh, S. ....	63	Thirumurugan, A.* .....	18	Xiao, H. ....	40
Shaji, S. ....	17	Tian, T. ....	41	Xiaomin, J.* .....	57
Sharma, S. ....	9, 31	Tidrow, S. ....	16, 17, 34, 36, 45, 48, 65	Xu, T.* .....	45, 65, 68
Sharma, S.* .....	9	Tidrow, S.* .....	36		
Sharma, V. ....	42	Tietz, F. ....	18	<b>Y</b>	
Sheridan, B. ....	40	Timme, N. ....	38	Yaakob, Y. ....	31
Shi, Y. ....	40	Tobón, J. I. ....	23, 45, 48, 61	Yamaguchi, I. ....	15
Shimamura, K.* .....	31	Tokoro, C.* .....	61	Yamaji, A. ....	13
Shpotyuk, O. ....	25	Tomba Martínez, A. G. ....	12, 24	Yanagida, T. ....	13
Shpotyuk, Y.* .....	25	Tong, J. ....	40	Yang, A.* .....	18
Shulman, H. ....	17, 45, 48	Torres Costa, V. ....	53	Yang, Y. ....	31
Shvartsman, V. V.* .....	67	Torresani, E. ....	11, 39	Yang, Y.* .....	27
Siligardi, C. ....	25	Trachenko, K.* .....	24	Ye, R. ....	18
Silva, D. M. ....	20, 66, 68	Trippy, M.* .....	15	Ye, R.* .....	30
Silva, L. M. ....	68	Tsuchiya, T.* .....	15	Ye, Y. ....	12
Silva, V. S. ....	65	Tu, B. ....	14	Yin, S.* .....	14
Simão, L. ....	60			Young, B. D.* .....	47
Simonova, P. ....	29, 58	<b>U</b>		Yuan, D. ....	31
Singh, G. ....	18, 37	Udayabhaskar, R. ....	17	Yusop, M. ....	31
Singh, N. B.* .....	34, 47	Ujji, H. ....	13	Yusslee, E. F.* .....	24
Singh, R. N.* .....	34	Uribe, F. P. ....	54		
Singh, V. P. ....	58	Uzawa, Y. ....	15	<b>Z</b>	
Singh, V.* .....	20			Zabala, S. A.* .....	55
Singhal, N. ....	50	<b>V</b>		Zabotto, F. ....	54
Siqueiros, J. ....	9, 21	Vacchi, M.* .....	25	Zabotto, F. L. ....	19, 55
Škapin, S. ....	35	Vakharia, V.* .....	11	Zabotto, F. L.* .....	47
Smeacetto, F. ....	28	Vaschalde, L. ....	31	Zakotnik, M.* .....	61
Smeacetto, F.* .....	27	Vasudevan, R. ....	37	Zapata Perez, N. ....	61
Smith, G. D.* .....	32	Veenhuizen, K. J.* .....	37	Zarazua, L. ....	29
Sofowora, E. ....	42	Vega Siverio, A. ....	39	Zhang, D. ....	66
Somani, N.* .....	46	Vega Siverio, A.* .....	23	Zhang, H. ....	14
Sone, H. ....	13	Velásquez, X. A.* .....	26	Zhang, J.* .....	42
Souza, G. B. ....	68	Vengust, D. ....	35	Zhang, L. ....	11
Spreitzer, M. ....	35, 46	Vennu, D. ....	19	Zhao, B. ....	45, 65
Srinivasan, G.* .....	48	Vicenzi, E. P.* .....	43	Zhao, H. ....	42
Stachiotti, M. ....	52, 56	Villaquiran Raigoza, C. F.* .....	54	Zhitomirsky, I.* .....	30
Stefanski, M. ....	13	Villar Gonzalez, E. ....	20	Zhou, Y. ....	12
Stevanovic, V. E. ....	64	Viswanathan, M. ....	8, 19, 38	Ziamahmoodi, N. ....	42
Stuart, M. ....	62	Volnistem, E. A. ....	47, 51, 52, 56, 65, 68	Zong, X. ....	14
Su, C. H. ....	34, 47	Volnistem, E. A.* .....	54, 69	Zuluaga-Gomez, C. C.* .....	37
Süllow, S. J. ....	68, 69			Zuo, L. ....	65
Suvorov, D.* .....	46	<b>W</b>			
Suzuki, T. S.* .....	40	Wagner, S. ....	7		
Swain, S. ....	50	Wang, A. ....	41		
		Wang, H. ....	41, 66		